Univerzita Karlova
Přírodovědecká fakulta

Ústav pro životní prostředí

Studijní program: Environmentální vědy

Mgr. Lenka Čermáková

Charakterizace a eliminace obtížně odstranitelných látek při úpravě vody

Characterisation and elimination of compounds difficult to remove during water treatment

Disertační práce

Školitel: doc. RNDr. Martin Pivokonský, Ph.D.

Praha, 2020

PROHLÁŠENÍ

Prohlašuji, že jsem závěrečnou práci zpracovala samostatně a že jsem uvedla všechny použité informační zdroje a literaturu. Tato práce ani její podstatná část nebyla předložena k získání jiného nebo stejného titulu.

DECLARATION

I declare that I have prepared this thesis individually, using only the information sources and literature cited. This thesis or its substantial part has not been submitted for the award of the same or any other academic degree.

Praha, 22. června 2020

Lenka Čermáková

FINANČNÍ PODPORA

Výzkum, jehož výsledky jsou prezentovány v disertační práci, byl financován Grantovou agenturou České republiky v rámci projektů GA18-14445S a GA18-05007S.

Disertační práce byla vypracována ve spolupráci s Ústavem pro hydrodynamiku Akademie věd České republiky, v. v. i.

ŠKOLITEL

doc. RNDr. Martin Pivokonský, Ph.D.
Ústav pro hydrodynamiku Akademie věd České republiky, v. v. i.

PODĚKOVÁNÍ

Velice děkuji Martinu Pivokonskému za skvělé vedení, ochotu, pomoc a podporu během celého Ph.D. studia. Můj dík patří i všem mým kolegům a kolegyním z Ústavu pro hydrodynamiku AV ČR, v. v. i., bez nichž jako týmu by nikdy takový výzkum nebyl možný. V neposlední řadě děkuji také své rodině a přátelům za podporu, a to nejen v průběhu doktorského, ale celého vysokoškolského studia.

SEZNAM PUBLIKACÍ

Disertační práce je založena na výsledcích prezentovaných v následujících 9 publikacích:

Publikace 1

Načeradská, J., Novotná, K., Čermáková, L., Cajthaml, T., Pivokonský, M., 2019. Investigation of non-proteinaceous algal organic matter: Optimizing coagulation performance and identification of removal mechanisms. *Journal of Environmental Sciences* 79, 25-34.

Lenka Čermáková se podílela na experimentální práci a na přípravě manuskriptu.

Publikace 2

Barešová, M., Načeradská, J., Novotná, K., Čermáková, L., Pivokonský, M., 2020. The impact of preozonation on coagulation of cellular organic matter produced by *Microcystis aeruginosa* and its toxin degradation. *Journal of Environmental Sciences* 98, 124-133.

Lenka Čermáková se podílela na zpracování dat a na přípravě manuskriptu.

Publikace 3

Filipenská, M., Vašatová, P., Pivokonská, L., Čermáková, L., Gonzalez-Torres, A., Henderson, R.K., Načeradská, J., Pivokonský, M., 2019. Influence of COM-peptides/proteins on the properties of flocs formed at different shear rates. *Journal of Environmental Sciences* 80, 116-127.

Lenka Čermáková se podílela na vyhodnocování dat a na přípravě podkladů a manuskriptu.

Publikace 4

Čermáková, L., Kopecká, I., Pivokonský, M., Pivokonská, L., Janda, V., 2017. Removal of cyanobacterial amino acids in water treatment by activated carbon adsorption. *Separation and Purification Technology* 173, 330-338.

Lenka Čermáková se podílela na experimentální práci, vyhodnocování dat a na přípravě podkladů a manuskriptu.

Publikace 5

Čermáková, L., Fialová, K., Kopecká, I., Barešová, M., Pivokonský, M. Investigating adsorption of model low-MW AOM components onto different types of activated carbon – influence of temperature and pH value. *Environmental Technology* – v recenzním řízení.

Lenka Čermáková se podílela na experimentální práci, vyhodnocování dat a na přípravě podkladů a manuskriptu.

Publikace 6

Čermáková, L., Pivokonská, L., Kopecká, I., Pivokonský, M., Janda, V., 2015. Adsorpce peptidů produkovaných fytoplanktonem na aktivním uhlí. *Chemické listy* 109, 176-179.

Lenka Čermáková se podílela na experimentální práci, vyhodnocování dat a na přípravě podkladů a manuskriptu.

Publikace 7

Čermáková, L., Pivokonská, L., Kopecká, I., Pivokonský, M., Janda, V., 2016. Vliv aminokyselin produkovaných fytoplanktonem na úpravu vody a jejich adsorpce na aktivním uhlí. *Chemické listy* 110, 418-423.

Lenka Čermáková se podílela na experimentální práci, vyhodnocování dat a na přípravě podkladů a manuskriptu.

Publikace 8

Pivokonský, M., Čermáková, L., Novotná, K., Peer, P., Cajthaml, T., Janda, V., 2018. Occurrence of microplastics in raw and treated drinking water. *Science of the Total Environment* 643, 1644-1651.

Lenka Čermáková se podílela na experimentální práci, vyhodnocování dat a na přípravě podkladů a manuskriptu.

Publikace 9

Novotná, K., Čermáková, L., Pivokonská, L., Cajthaml, T., Pivokonský, M., 2019. Microplastics in drinking water treatment – Current knowledge and research needs. *Science of the Total Environment* 667, 730-740.

Lenka Čermáková se podílela na přípravě podkladů a manuskriptu.

PROHLÁŠENÍ O SPOLUPRÁCI NA ODBORNÝCH PUBLIKACÍCH

Jménem dalších spoluautorů prohlašuji, že se Mgr. Lenka Čermáková významně podílela na vzniku výše uvedených publikací. Rozsah jejího podílu je uveden u jednotlivých prací.

DECLARATION OF COOPERATION ON SCIENTIFIC PUBLICATIONS

On behalf of the other co-authors, I declare that Mgr. Lenka Čermáková contributed significantly to the preparation of the aforementioned publications. The extent of her participation in the individual papers is indicated in the List of publications.

Praha, 22. června 2020

doc. RNDr. Martin Pivokonský, Ph.D.

ABSTRAKT

Disertační práce se zabývá charakterizací organických látek produkovaných fytoplanktonem (AOM – Algal Organic Matter), které patří k obtížně odstranitelným látkám při úpravě vody, a na základě charakteru AOM pak posuzuje různé metody jejich eliminace, např. koagulaci, oxidaci s následnou koagulací a adsorpci na aktivním uhlí. Zvláštní důraz je přitom kladen na zjištění optimálních podmínek daných procesů a na popis při nich se uplatňujících mechanismů a interakcí. V rámci druhé skupiny z hlediska úpravy vody problematických látek, antropogenních mikropolutantů, se disertační práce zabývá vysoce aktuální problematikou výskytu mikroplastů ve vodě.

Bylo zjištěno, že účinnost odstranění jednotlivých složek AOM se zásadně liší v závislosti na použité eliminační metodě. Velmi se různí i identifikované optimální podmínky jednotlivých metod a především pak mechanismy, které se při odstranění cílových látek uplatňují. Neproteinová složka AOM se konvenční koagulací i za optimalizovaných podmínek (pH 6,6-7,5 pro koagulační činidlo síran hlinitý a pH 7,5-9,0 pro polyaluminium chlorid) odstraňuje s velmi nízkou účinností (max. 25 %), přičemž hlavní příčinou je vysoký obsah obtížně koagulovatelných nízkomolekulárních látek. Jako dominantní se zde uplatňuje mechanismus adsorpce na hydratované oxidy hliníku. Dále výsledky ukazují, že použití předoxidace ozónem nevede ke zvýšení koagulační účinnosti AOM, ale naopak k jejímu poklesu, a to z důvodu rozkladu vysokomolekulárních látek na látky nízkomolekulární, které koagulaci nepodléhají. Tento vliv se pak významněji projevuje při použití hlinitého koagulačního činidla v porovnání se železitým. Pozitivní účinek má naopak předoxidace prostřednictvím ozónu na degradaci cyanotoxinů. V rámci výzkumu vlivu AOM na koagulaci ostatních příměsí bylo zjištěno, že AOM zásadně ovlivňují charakter vznikajících agregátů, především pak jejich velikost, kompaktnost a velikostní distribuci. Koagulací neodstranitelné nízkomolekulární látky lze efektivně odstranit adsorpcí na aktivním uhlí. Účinnost adsorpce je však výrazně ovlivněna charakterem adsorbované látky a použitého aktivního uhlí. Liší se také dle aplikovaného pH, teploty a iontové síly roztoku. Tyto faktory ovlivňující proces adsorpce se pak projevují v závislosti na mechanismech a interakcích uplatňujících se mezi adsorbentem a adsorbátem.

V rámci disertační práce se také podařilo v surové i pitné vodě prokázat přítomnost mikroplastů, a to v řádech stovek, respektive tisíců částic na litr, přičemž dominovala velikostní frakce 1-10 μm. Z hlediska tvaru převládaly částice

nepravidelného tvaru (fragmenty) a z materiálů převažovaly polyetylén tereftalát, polypropylén a polyetylén.

ABSTRACT

The Ph.D. thesis deals with the characterization of algal organic matter (AOM), which is difficult to remove in water treatment, and on the basis of AOM character, various methods for its elimination, e.g. coagulation, oxidation with subsequent coagulation and adsorption onto activated carbon are assesed. Special emphasis is placed on identifying the optimal conditions of the processes and on describing the mechanisms and interactions involved. In terms of anthropogenic micropollutants, the thesis deals with the highly topical issue of the occurrence of microplastics in water.

It was found that the removal efficiency of the individual AOM components varies substantially depending on the elimination method used. The identified optimum conditions of individual methods and especially the mechanisms that apply to the removal of target substances varied widely. The non-proteinaceous fraction of AOM was removed with very low efficiency (max. 25%) by conventional coagulation even under optimized conditions (pH 6.6-7.5 for aluminium sulfate as the coagulating agent and pH 7.5-9.0 for polyaluminium chloride) and it was given by the high content of low molecular weight (LMW) substances that are difficult to coagulate. The dominant coagulation mechanism was adsorption onto aluminium hydroxide precipitates. Furthermore, the results showed that the using of ozone pre-oxidation did not lead to an increase in the coagulation efficiency of AOM, but rather to a decrease due to the decomposition of high molecular weight compounds into LMW compounds that are difficult to coagulate. This effect was more pronounced when an aluminium aid was used compared to a ferric coagulant. On the other hand, ozone pre-oxidation had a positive effect on cyanotoxin degradation. Further, it was found that AOM significantly influenced the character of aggregates, especially their size, compactness and size distribution. LMW AOM that is difficult to coagulate can be effectively removed by adsorption on activated carbon. However, the adsorption efficiency is strongly influenced by the nature of the adsorbate and of the activated carbon used. It also differs according to the applied pH, temperature and ionic strength of the solution. These factors affecting the adsorption process then manifest themselves in dependence on the mechanisms and interactions between adsorbent and adsorbate.

The Ph.D. also proved the presence of microplastics in raw and drinking water in the order of hundreds or thousands of particles per litre, the size fraction of 1-10 μm dominated. In terms of shape, irregularly shaped particles (fragments) predominated and

the materials predominantly included polyethylene terephthalate, polypropylene and polyethylene.

OBSAH

SEZNAM SYMBOLŮ A ZKRATEK

AOM	organické látky produkované fytoplanktonem (Algal Organic Matter)
AMK	aminokyselina
AU/GAU/PAU	aktivní uhlí/granulované aktivní uhlí/práškové aktivní uhlí
COM	celulární organické látky (Celullar Organic Matter)
Da/kDa	Dalton/kilodalton (jednotka molární hmotnosti)
DBPs	vedlejší produkty desinfekce vody (Disinfection By-Products)
DOC	rozpuštěný organický uhlík (Dissolved Organic Carbon)
DOM	rozpuštěné organické látky (Dissolved Organic Matter)
EOM	extracelulární organické látky (Extracellular Organic Matter)
HAA	halogenderiváty kyseliny octové (haloacetic acids)
IS	iontová síla
MPs	mikroplasty
MC-RR	mikrocystin RR (-R = arginin)
MH	molekulová hmotnost
NOM	přírodní organické látky (Natural Organic Matter)
PACl	polyaluminum chlorid
PFCs	perfluorované organické látky (Perfluorinated Organic Compounds)
pH [-]	záporně vzatý dekadický logaritmus aktivity oxoniových kationtů
pH_{NBN} [-]	pH nulového bodu náboje (pH_{PZC} – pH Point of Zero Charge)
p*I* [-]	izoelektrický bod
POPs	perzistentní organické látky (Persistent Organic Pollutants)
PTC	polytitanium tetrachloride
THM	trihalogenmetany (trihalomethanes)

1 ÚVOD

Povrchové vody určené jako zdroje surové vody pro výrobu vody pitné jsou v současné době velmi zatíženy probíhající klimatickou změnou a stále narůstající chemizací životního prostředí. Kvalita vody klesá a velmi rychle se mění charakteristické zastoupení látek ve vodě obsažených. Kdysi dominantní huminové látky vznikající rozkladem alochtonní organické hmoty dnes na mnoha lokalitách ustupují svým podílem autochtonním organickým látkám produkovaným sinicemi a řasami, tzv. AOM – Algal Organic Matter (Pivokonský a kol., 2016). Masivní rozvoj fytoplanktonu je způsoben zvyšujícím se množstvím živin, především dusíku a fosforu, ve vodním prostředí, který je navíc podpořen nárůstem průměrných teplot vody a prodlužováním vegetační sezóny v důsledku postupující klimatické změny. Rozvoj planktonních fotosyntetizujících mikroorganismů, především sinic, v letním a podzimním období vede ke značné produkci nejen jejich vlastních buněk, ale hlavně AOM, které velmi negativně ovlivňují celý proces úpravy vody. Z praxe jsou popsány i případy, kdy tyto látky způsobily úplný kolaps úpravny vody (Henderson a kol., 2008a; Zhang a kol., 2010). Bylo popsáno, že AOM obsažené v surové vodě 1) negativně ovlivňují průběh koagulace/flokulace (Pivokonský a kol., 2006, 2012, 2014, 2016; Šafaříková a kol., 2013); 2) snižují účinnost terciálního stupně úpravy vody – způsobují zanášení membránových filtrů, inhibují adsorpci mikropolutantů na aktivním uhlí (Her a kol., 2004; Amy a kol., 2008; Hnaťuková a kol., 2011; Qu a kol., 2012a; Zhang a kol., 2013a,b); 3) negativně ovlivňují organoleptické vlastnosti vody – především chuť a zápach (Froese a kol., 1999; Harada, 2004; Freuze a kol., 2005; Ozawa a kol., 2005; Dyble a kol., 2008; Dixon a kol., 2010; Zhang a kol., 2010; Li a kol., 2012); 4) obsahují řadu toxických sloučenin – sinicové toxiny (Carmichael, 1992; Sivonen a Jones, 1999; Dixon a kol., 2010); 5) jsou prekursory pro tvorbu karcinogenních a mutagenních vedlejších produktů desinfekce při hygienickém zabezpečování konečného produktu (pitné vody) chlorovanými činidly (Nguyen a kol., 2005; Kim a Yu, 2005; Hong a kol., 2009; Huang a kol., 2009; Fang a kol., 2010; Li a kol., 2012). Z uvedeného výčtu vlivu AOM na procesy úpravy vody je patrné, že tyto látky představují pro současné technologie úpravy vody značné riziko a výzkum zaměřený na jejich odstranění a potlačení jejich negativního vlivu na produkci pitné vody z povrchových zdrojů je dnes jedním z celosvětově nejdiskutovanějších odborných témat v oblasti úpravy vody (Pivokonský a kol., 2016). V této souvislosti je

však také třeba zmínit, že některé práce prokázaly, a to především u vysokomolekulární proteinové složky AOM, také pozitivní vliv na koagulaci huminových látek (Pivokonský a kol., 2015) a buněk sinic (Barešová a kol., 2017).

AOM přitom pro současný výzkum nepředstavují jedinou výzvu. Značný a zvětšující se problém způsobuje narůstající míra výskytu antropogenních mikropolutantů, např. pesticidy, persistentní organické sloučeniny (POPs – Persistent Organic Pollutants), perfluorované organické látky (PFCs – Perfluorinated Organic Compounds), zbytky léčiv, hormonů, ale také částice mikroplastů. Tyto látky nacházíme ve zdrojích surové vody stále častěji a pravděpodobně to nebude jen z důvodu neustálého rozvoje moderních analytických metod, které tyto látky umožňují detekovat ve stále nižších koncentracích, ale kvůli jejich narůstající produkci. Přestože se mikropolutanty vyskytují ve vodě mnohdy v nízkých koncentracích, mohou představovat reálné riziko pro lidské zdraví (Kim a Zoh, 2016; Yang a kol., 2017; Grandjean, 2018). Nutné je brát v úvahu také možnost jejich negativního synergického působení. Vzhledem ke svému charakteru (nízká koncentrace, malá molekulová hmotnost, hydrofilní charakter) jsou tyto látky konvenční koagulací/flokulací téměř neodstranitelné a některé z nich nelze eliminovat, nebo jen s velmi malou účinností, ani terciálním stupněm úpravy založeném na adsorpci na aktivním uhlí (Szajdzinska-Pietek a Gebicki, 2000; Hölzer a kol., 2009; Shivakoti a kol., 2010; Deblonde a kol., 2011; Takagi a kol., 2011; Eschauzier a kol., 2012; Xiao a kol., 2013; Luo a kol., 2014; Rahman a kol., 2014; Kim a Zoh, 2016).

Zatímco v minulosti se technologie úpravy vody potýkala především s odstraňováním znečišťujících příměsí, jako jsou huminové látky, jílovité částice (hlinitokřemičitany), případně ionty, např. Fe^{3+}, Mn^{2+} nebo NO_3^+, dnes je nutné pozornost obrátit právě ke dvěma výše zmiňovaným skupinám – AOM a mikropolutantům, a to nejen v oblasti výzkumu, ale v návaznosti také v technologické praxi.

2 ORGANICKÉ LÁTKY VE VODĚ

Přirozenou součástí všech typů povrchových vod jsou přírodní organické látky – NOM (Natural Organic Matter). Jedná se složitou směs organických látek lišících se původem a charakterem, strukturou, velikostí a molekulovou hmotností (Newcombe a Drikas, 1997; Henderson a kol., 2008a,b; Matilainen a kol., 2011; Pivokonský a kol., 2016). Z hlediska původu je rozlišujeme na látky allochtonní, které se do vody dostávají z okolního prostředí a jsou zastoupeny především huminovými kyselinami a fulvokyselinami, a na látky autochtonní vznikající ve vodě samotné a představují je zejména látky produkované fytoplanktonem, tzv. AOM (Algal Organic Matter) (Leloup a kol., 2013; Pivokonský a kol., 2016). Uvedené látky jsou ve vodách obsaženy v různých koncentracích a jejich přítomnost ve zdrojích sloužících pro pitné účely zcela zásadně ovlivňuje celý proces úpravy pitné vody (Pivokonský a kol., 2016).

2.1 ORGANICKÉ LÁTKY PRODUKOVANÉ FYTOPLANKTONEM (AOM)

Organické látky produkované fytoplanktonem představují významnou složku NOM. Vznikají činností různých druhů fytoplanktonu, jako jsou sinice (*Cyanobacteria*), řasy (*Chlorophyta*), rozsivky (*Diatomeae*), obrněnky (*Dinophyta*) a skrytěnky (*Cryptophyceae*) (Paerl a kol., 2001). Během života fytoplanktonu se jeho metabolickou činností do vody uvolňují tzv. extracelulární organické látky (EOM – Extracellular Organic Matter). Koncentrace EOM mohou být značné a v laboratorních podmínkách při kultivaci různých druhů fytoplanktonu (sinice, řasy a rozsivky) se pohybují mezi cca 20-60 mg/l (měřeno jako koncentrace rozpuštěného organického uhlíku – DOC; DOC – Dissolved Organic Matter) při počtu buněk řádově 10^5-10^7 na 1 mililitr (Pivokonský a kol., 2006, 2014). Po odumření fytoplanktonu a buněčné lyzi se do vody uvolňují tzv. celulární organické látky (COM – Cellular Organnic Matter) (Nguyen a kol., 2005; Pivokonský a kol., 2006; Zhang a kol., 2010). Jejich koncentrace mohou dosáhnout značných hodnot a právě tyto látky mnohdy představují pro technologie úpravy vody největší problém (Pivokonský a kol., 2016). Přestože je výskyt AOM v důsledku rozvoje vodního květu obvykle v našich podmínkách považován za sezónní, je dnes vzhledem k probíhající klimatické změně a eutrofizaci tato složka NOM ve vodách přítomna celosezónně (Pivokonský a kol., 2019). Zastoupení AOM v povrchových vodách mírného pásma stoupá a v některých zdrojích představuje dominantní podíl NOM (Pivokonský a kol., 2016, 2019).

2.1.1 Složení AOM

AOM jsou složitou směsí různých druhů organických sloučenin, jako jsou proteiny, peptidy, aminokyseliny, mono-, di-, oligo- a polysacharidy, lipidy, mastné kyseliny, nukleové kyseliny, aminosacharidy, lipopolysacharidy, aldehydy a další (Bertocchi a kol., 1990; Myklestad, 1995; Paerl a kol., 2001; Her a kol., 2004; Nguyen a kol., 2005; Pivokonský a kol., 2006, 2014; Huang a kol., 2007b; Henderson a kol., 2008a; Markou a kol., 2012; Laurens a kol., 2014; Villacorte a kol., 2015). Obsahují také řadu toxinů, např. hepatotoxický microcystin, nodularin, cylindrospermopsin nebo neurotoxický anatoxin a saxitoxin (Carmichael, 1992; Dixon a kol., 2010; Pearson a kol., 2016). Mnoha studiemi bylo prokázáno, že charakter, chemické složení a množství AOM uvolňovaných do vody se mění v závislosti na druhu, stáří a růstové fázi fytoplanktonu (Hoyer a kol., 1985; Pivokonský a kol., 2006, 2014; Henderson a kol., 2008a; Leloup a kol., 2013). V laboratorních podmínkách byly identifikovány čtyři růstové fáze – lagová (klidová) fáze, exponenciální, stacionární a fáze odumírání (Pivokonský a kol., 2006, 2014; Barešová a kol., 2017). Během exponenciální fáze převažuje v AOM podíl extracelulárních organických látek. V průběhu stacionární fáze začínají dominovat COM a během fáze odumírání tvoří COM již téměř 100 % AOM (Pivokonský a kol., 2006, 2014; Henderson a kol., 2008a; Barešová a kol., 2017). Průběh produkce AOM, jejich složení a množství je ovlivňováno také řadou faktorů prostředí, jako je doba a intenzita slunečního záření, teplota, hodnota pH a iontové síly vody, množství dostupných živin nebo přítomnost toxinů (van der Westhuizen a Eloff, 1985; Myklestad, 1995; Pivokonský a kol., 2006, 2014; Huang a kol., 2007b; Li a kol., 2012).

2.1.2 Vlastnosti AOM ve vztahu k úpravě pitné vody

Charakterizací a složením AOM se zabývala řada studií (Hoyer a kol., 1985; Nguyen a kol., 2005; Pivokonský a kol., 2006; 2014; Henderson a kol., 2008a; Fang a kol., 2010; Huang a kol., 2012; Li a kol., 2012; Leloup a kol., 2013). Zkoumáno bylo především zastoupení peptidů/proteinů a sacharidů/polysacharidů, distribuce molekulových hmotností, povrchový náboj, poměr hydrofilní a hydrofobní složky (Pivokonský a kol., 2006, 2009b, 2014; Henderson a kol., 2008a, Barešová a kol., 2017). Uvedené vlastnosti ovlivňují mechanismy a interakce mezi: i) molekulami AOM; ii) AOM a koagulačním činidlem; iii) AOM a ostatními znečišťujícími

příměsemi; iv) AOM a povrchem aktivního uhlí či jiného sorpčního materiálu užívaného v procesu úpravy vody; v) AOM a desinfekčním činidlem (Pivokonský a kol., 2016)

Obsah peptidů/proteinů, sacharidů/polysacharidů

Chemické složení AOM je druhově specifické a mění se se stářím fytoplanktonu. (Pivokonský a kol., 2006, 2014). Obsah peptidů/proteinů se obvykle pohybuje mezi cca 12-70 % z celkového množství AOM právě v závislosti na druhu a růstové fázi kultury. Obecně literatura uvádí, že u sinic představují peptidy/proteiny 40-70 %, u zelených řas 12-50 % a u rozsivek 50 % AOM (Whyte, 1987; Brown, 1991; Chronakis, 2001; Pivokonský a kol., 2006, 2014). Zároveň je podíl peptidové/proteinové složky výrazně vyšší v COM než v EOM. Obsahem peptidů/proteinů v EOM/COM různých druhů fytoplanktonu (sinice *Microcystis aeruginosa* a *Anabaena flos-aquae*, rozsivka *Fragilaria crotonensis* a zelené řasy *Chlamydonomas geitleri* a *Scenedesmus quadricauda*) se ve svých pracích zabýval Pivokonský a kol. (2006, 2009b, 2012, 2014). Během kultivace uvedených organismů došlo v EOM k postupnému nárůstu množství peptidů/proteinů. Nejvyšší podíl proteinové složky (až 47 %) byl zjištěn ve stacionární fázi růstu u obou druhů sinic. Naopak nejnižší množství peptidů/proteinů (max. 28 %) obsahovaly EOM zelených řas (Pivokonský a kol., 2006, 2014). V případě COM dosahovaly peptidy/proteiny nejvyššího podílu u sinice *M. aeruginosa*, a to téměř 70 % (Pivokonský a kol., 2006, 2009b, 2012, 2014. O něco méně pak byly peptidy/proteiny zastoupeny v COM *F. crotonensis* (53 %) (Pivokonský a kol., 2014) a *A. flos-aquae* (51 %) (Pivokonský a kol., 2006). U zelených řas *C. geitleri* a *S. quadricauda* činil podíl peptidů/proteinů v COM 33 %, resp. 29 % (Pivokonský a kol., 2006; 2014). Dusíkaté látky jsou kromě peptidů/proteinů v AOM zastoupené také ve formě aminokyselin (AMK). Společně s peptidy/proteiny tvoří dominantní složku dusíkaté frakce AOM. Zdrojem aminokyselin je metabolická činnost fytoplanktonu a degradace jejich buněk (Thurman, 1985; Scully a kol., 1988; Jugnia kol., 2006; Pivokonský a kol., 2006, 2014; Hong a kol., 2009; Fang a kol., 2010). Koncentrace peptidů/proteinů společně s AMK dosahuje v povrchových vodách v závislosti na biologické aktivitě koncentrace až několika mg/l. Koncentrace volných aminokyselin se pak pohybuje v rozmezí 50-1000 μg/l (Thurman, 1985; Hureiki a kol., 1994; Hong a kol., 2009). Nejčastěji se v AOM vyskytují volné AMK glycin, kyselina glutamová,

alanin, kyselina asparagová, leucin, serin (Thurman, 1985; Hong a kol., 2009). V COM jsou nejvíce zastoupeny arginin, lysin a glycin (Fang a kol., 2010).

Druhou významnou složkou AOM jsou sacharidy/polysacharidy (Lewin, 1956; Myklestad, 1974, 1995; Laurens a kol., 2014; Villacorte a kol., 2015). Stejně jako v případě peptidů/proteinů závisí jejich obsah na druhu organismu a mění se v průběhu jeho růstu (Myklestad, 1974; Maksimova a kol., 2004; Laurens a kol., 2014; Pivokonský a kol., 2014). Například Myklestad (1995) ve své studii stanovil podíl extracelulárních sacharidů/polysacharidů u dvou druhů řas *Chaetoceros affinis* a *Chaetoceros curvisetus* až 80-90 %. Ve své pozdější studii (Myklestad, 1995) pak naměřil cca 50% podíl sacharidů/polysacharidů u zelených řas *Chlorella* sp. a *Scenedesmus* sp. Nižší množství sacharidů/polysacharidů, a to 25 % u *Chlamydomonas mexicana* a 20-40 % u *Chlorella pyrenoidosa*, bylo zjištěno ve studiích Lewin (1956) a Maksimova a kol. (2004), respektive. V AOM polysacharidech jsou nejčastěji zastoupeny arabinóza, fukóza, galaktóza, manóza, ramnóza, ribóza a xylóza (Lewin, 1956; Fogg, 1971; Hellebust, 1974; Bertochi a kol., 1990; Nicolaus a kol., 1999; Huang a kol., 2007b; Markou a kol., 2012). Významnou složku polysacharidů tvoří také uronové kyseliny a aminosacharidy (Bertochi a kol., 1990; Nicolaus a kol., 1999).

Podíl proteinové vs. neproteinové složky AOM je pro úpravu vody velmi zásadní. Důvodem je, že tyto jednotlivé složky AOM mají velice odlišné vlastnosti, které jsou pro účinnost jejich odstranění zcela zásadní. Peptidy/proteiny jsou obvykle koagulací odstranitelné snadněji, což je dáno především hodnotou jejich celkového náboje, který umožňuje interakce s opačně nabitým koagulačním činidlem (Pivokonský a kol., 2012, 2015, 2016). V neproteinové složce jsou naopak velmi hojně zastoupeny látky nenabité nebo jen s velmi malým celkovým nábojem, např. různé polysacharidy tvořené molekulami uronových kyselin, a k interakcím s koagulačním činidlem tak dochází jen v omezené míře a účinnost jejich odstranění je nízká (Berndhard a kol., 1985; Hoyer a kol., 1985).

Distribuce molekulových hmotností

Organické látky produkované fytoplanktonem obsahují sloučeniny s širokým rozsahem molekulových hmotností (MH) od několika stovek daltonů (Da) do stovek kilodaltonů (kDa) a jejich distribuce molekulových hmotností je značně širší než v případě huminových látek (Pivokonský a kol., 2006, 2014; Henderson a kol., 2008a;

Fang a kol., 2010; Li a kol., 2012; Wang a kol., 2013; Zhang a kol., 2013a). Nízkomolekulární frakce (< 10 kDa) zahrnuje peptidy, aminokyseliny, mono-, di- a oligosacharidy, aminy, aminosacharidy a aldehydy (Nguyen a kol., 2005; Huang a kol., 2007b). Mezi AOM se střední molekulovou hmotností (10-100 kDa) patří např. polypeptidy, jako jsou enzymy a jejich stavební sloučeniny (Pivokonský a kol., 2014). K vysokomolekulárním AOM s molekulovou hmotností > 100 kDa se řadí především biopolymery, jako jsou proteiny a polysacharidy, které jsou významnou složkou AOM (Lewin, 1956; Chrost a Faust, 1983; Hoyer a kol., 1985; Myklestad, 1995; Maksimova a kol., 2004; Henderson a kol., 2008a; Qu a kol., 2012b; Pivokonský a kol., 2014). Například u *M. aeruginosa* činil obsah peptidů/proteinů > 100 kDa v EOM a COM 25 %, resp. 22 %. Neproteinová složka EOM a COM, kam lze zařadit polysacharidy, pak obsahovala pro druhy *C. geitleri*, *F. crotonensis* a *M. aeruginosa* 20-27 %, resp. 22-35 % sloučenin s MH > 100 kDa (Pivokonský a kol., 2014). Neméně významnou složkou z hlediska zastoupení je nízkomolekulární frakce. Dokonce i látky s MH < 1 kDa mohou být velmi početné. Například ve studii Henderson a kol. (2008a) činil podíl těchto sloučenin u *C. vulgaris* 30 %, u *M. aeruginosa* 38 %, u *Melosira* sp. 53 % a u *Asterionella formosa* dokonce 81 % z celkových AOM. Distribuce molekulových hmotností přitom není specifická jen druhově, ale mění se také se stářím kultury a je odlišná v EOM a COM (Myklestad, 1995; Henderson a kol., 2008a; Pivokonský a kol., 2006, 2014). Pro většinu studovaných druhů fytoplanktonu (*A. flos-aque*, *C. geitleri*, *F. crotonensis*, *M. aeruginosa*, *S. quadricauda*) platí, že COM mají mnohem širší distribuci MH v porovnání s EOM. Rozdíly v distribuci MH byly také pozorovány u EOM z exponenciální a stacionární fáze (Pivokonský a kol., 2006, 2014).

Velikost molekul, respektive molekulová hmotnost, hraje při odstraňování organických látek při úpravě vody zásadní roli. S vysokou účinností se odstraňují především vysokomolekulární látky (MW < 10 kDa), zatímco látky s nízkou molekulovou hmotností jsou koagulací odstranitelné jen obtížně (MW = 10-3 kDa) nebo prakticky vůbec (MW < 3 kDa) (Pivokonský a kol., 2009a,b). Zastoupení vysokomolekulárních a nízkomolekulárních látek tvořících AOM tak rozhoduje o účinnosti celého procesu úpravy vody. Podíl vysokomolekulárních látek vůči látkám nízkomolekulárním je dán především druhem a růstovou fází mikroorganismu (Henderson a kol., 2008a; Pivokonský a kol., 2006, 2014, 2016).

Povrchový náboj

Povrchový náboj je z hlediska úpravy vody zcela zásadní charakteristikou AOM (Pivokonský a kol., 2012; 2015; 2016; Hnaťuková a kol., 2011; Šafaříková a kol., 2013; Kopecká a kol., 2014; Barešová a kol., 2017; Načaradská a kol., 2017). Náboj AOM je dán charakterem a množstvím funkčních skupin a také hodnotou pH roztoku, která ovlivňuje jejich disociaci (Creighton, 1993). Zjistilo se, že AOM mají v širokém rozsahu pH záporný náboj (Bernhardt a kol., 1985, 1986; Bernhardt a Clasen, 1991; Henderson a kol., 2008a). Ten je způsoben přítomností kyselých funkčních skupin, jako jsou –COOH, –OH, –SH (Creighton, 1993). Velikost a charakter náboje AOM jsou závislé na druhu organismu a stáří jeho kultury (Bernhardt a kol., 1985; Paralkar a Edzwald, 1996; Henderson a kol., 2008a). Například, velikost náboje EOM *M. aeruginosa* klesla z 0,2 meq na 1 g DOC v exponenciální fázi na 0,1 meq na 1 g DOC ve stacionární fázi. Naopak v případě zelené řasy *Chlorella vulgaris* velikost náboje přechodem z exponenciální fáze do stacionární vzrostla z 0,9 meq na 1 g DOC na 3,2 meq na 1 g DOC (Henderson a kol., 2008a). V souvislosti s obsahem různých funkčních skupin mají různé složky AOM odlišné nábojové charakteristiky. Např. COM peptidy/proteiny sinice *M. aeruginosa* vykazují vzhledem k hodnotě izoelektrického bodu mezi 4,8-8,1 při hodnotách pH úpravy vody záporný náboj (Pivokonský a kol., 2012; Šafaříková a kol., 2013). Naopak neproteinová složka obsahuje sloučeniny s nízkým počtem karboxylových skupin nebo neionizovatelnými skupinami, a nese tedy v porovnání s proteinovou složkou celkově nižší náboj (Hoyer a kol., 1985). Peptidy/proteiny mohou vzhledem ke svému amfoternímu charakteru a přítomnosti funkčních skupin, např. $–NH_3^+$, $=NH_2^+$ nést i kladný náboj, a to v kyselé oblasti pH (Creighton, 1993).

Vzhledem k tomu, že koagulace znečišťujících příměsí probíhá především na základě elektrostatických interakcí, je povrchový náboj znečišťujících příměsí i koagulačního činidla zcela zásadní veličinou ovlivňující celou účinnost procesu úpravy vody. S ohledem na skutečnost, že jeho velikost je dána vedle množství ionizovatelných funčních skupin na povrchu příměsí i činidla především hodnotou pH, je zcela nezbytné provádět koagulaci v optimálních hodnotách tohoto ukazatele (Pivokonský a kol., 2012; 2015, 2016; Šafaříková a kol., 2013; Kopecká a kol., 2014; Barešová a kol., 2017; Načaradská a kol., 2017).

3 ODSTRAŇOVÁNÍ ORGANICKÝCH LÁTEK PŘI ÚPRAVĚ VODY

Při využívání povrchových vod jako zdrojů pro výrobu pitné vody je nutné maximální možné odstranění organických látek. Jejich zbytkové koncentrace totiž způsobují řadu nežádoucích problémů:

i. jsou prekursory tvorby vedlejších produktů desinfekce vody (DBPs – Disinfection By-Products), především trihalogenmetanů (THM) a halogenderivátů kyseliny octové (HAA), při hygienickém zabezpečování vyrobené vody činidly na bázi chlóru (Nguyen a kol., 2005; Kim a Yu, 2005; Hong a kol., 2009; Huang a kol., 2009; Fang a kol., 2010; Li a kol., 2012; Pivokonský a kol., 2016),
ii. negativně ovlivňují organoleptické vlastnosti vody, především chuť a zápach (Froese a kol., 1999; Freuze a kol., 2005; Dixon a kol., 2010; Zhang a kol., 2010; Li a kol., 2012),
iii. zvyšují spotřebu desinfekčních činidel (Hureiki a kol., 1994),
iv. jako zdroj biodegradabilního uhlíku představují živný substrát pro rozvoj nežádoucích mikroorganismů v distribuční síti (Gagnon a kol., 2000).

Běžný proces úpravy vody zahrnuje několik technologických kroků. Konvenční úprava vody je založená na koagulaci následované sedimentací/flotací nebo přímou pískovou filtrací. Toto klasické technologické schéma může být doplněno moderními technologiemi, jako je adsorpce na aktivním uhlí nebo membránová filtrace. Stále častěji je pro eliminaci NOM také využíváno oxidačních metod, jako je ozonizace, UV záření, oxidace manganistanem draselným, chlorem, pomocí K_2FeO_4 (potassium ferrate), atd. (Xie a kol., 2016). Přítomnost AOM, jako specifické složky NOM, v surové vodě navíc celý proces úpravy vody velmi znesnadňuje a tyto látky představují pro jednotlivé technologické kroky značné zatížení. AOM:

i. způsobují poruchy koagulace buněk mikroorganismů a ostatních znečišťujících příměsí, zákalotvorných částic – hlinitokřemičitanů, huminových látek (Bernhardt a kol., 1985; Pivokonský a kol., 2006, 2012; Takaara a kol., 2007; Henderson a kol., 2010; Ma a kol., 2012b; Vandamme a kol., 2012; Garzon-Sanabria a kol., 2013; Šafaříková a kol., 2013; Wang a kol., 2013; Barešová a kol., 2017),

ii. tvoří rozpuštěné komplexní sloučeniny s koagulačním činidlem Fe/Al, čímž inhibují průběh koagulace a zvyšují spotřebu koagulačního činidla (Pivokonský a kol., 2012, 2015, 2016),
iii. způsobují zanášení membránových filtrů (Her a kol., 2004; Amy a kol., 2008; Hnaťuková a kol., 2011; Qu a kol., 2012a,b; Zhang a kol., 2013a,b),
iv. inhibují proces adsorpce mikropolutantů na aktivním uhlí (Hnaťuková a kol., 2011; Pivokonský a kol., 2016),
v. zvyšují spotřebu koagulačních, desinfekčních, případně oxidačních činidel (Henderson a kol., 2010; Edzwald a Haarhoff, 2011; Ma a kol., 2012a,b; Pivokonský a kol., 2012; Šafaříková a kol., 2013; Wang a kol., 2013; Načeradská a kol., 2017).

3.1 KOAGULACE AOM

Konvenční metodou pro odstraňování nežádoucích látek z vody je koagulace. Tento proces je založený na destabilizaci ve vodě přítomných příměsí pomocí produktů hydrolýzy kovů (Al/Fe) obsažených v koagulačních činidlech, nejčastěji v síranu hlinitém či železitém. Přidáním činidel do surové vody dochází k tvorbě agregátů a jejich následné separaci pomocí sedimentace nebo flotace a/nebo pískové filtrace. Podmínky, které vedou k uvedenému procesu, jsou velmi specifické a liší se v závislosti na mnoha faktorech. Zásadní roli hraje hodnota pH. Ta ovlivňuje disociaci funkčních skupin ve struktuře AOM a stupeň hydrolýzy koagulačního činidla, tedy nábojové poměry v systému. V závislosti na převažující formě koagulačního činidla probíhá koagulace různými mechanismy, z nichž v případě AOM je nejčastější nábojová neutralizace a adsorpce, a závisí na mnoha faktorech, především na hodnotě pH, kyselinové neutralizační kapacitě a teplotě vody, ale např. na iontové síle roztoku nebo přítomnosti ostatních ve vodě obsažených znečišťujících příměsí (jílovité minerály, huminové látky, buňky řas a sinic atd.) a jejich vzájemných interakcích (Bernhardt a kol., 1985, 1986; Creighton, 1993; Paralkar a Edzwald, 1996; Šafaříková a kol., 2013; Pivokonský a kol., 2009a,b, 2015; Barešová a kol., 2017; Načeradská a kol., 2017).

Při úpravě povrchové vody s obsahem sinic a řas je zcela zásadní odstranění buněk fytoplanktonu i s jejich celulárním obsahem, tedy bez jejich poškození (Chow a kol., 1998, 1999; Briley a Knappe, 2002; Pietsch a kol., 2002). Koagulaci buněk sinic a řas se doposud věnovala celá řada studií a ve většině případů nepředstavuje tento

proces závažnější problém (Henderson a kol., 2008b, 2010; Ghernaout a kol., 2010; Edzwald and Haarhoff, 2011). Ne vždy je však provedení koagulace bez uvolněného buněčného obsahu možné, a to především vzhledem ke dvěma zásadním skutečnostem. Povrchové vody běžně vedle buněk obsahují i značné množství rozpuštěných AOM ve formě produktů metabolické činnosti (EOM) nebo jako výsledek odumírání fytoplanktonu a lyze buněk (COM) (Pivokonský a kol., 2006, 2014; Vandamme a kol., 2012; Wu a kol., 2012). Kromě toho mohou být AOM do vody uvolněny i během procesu úpravy vlivem mechanického nebo chemického poškození buněk, např. při různých oxidačních procesech (Ma a Liu, 2002; Henderson a kol., 2008a; Ma a kol., 2012a,b). Koagulací buněk v přítomnosti AOM (EOM/COM) se zabývala celá řada studií (Bernhardt a Clasen, 1991, Ma a Liu, 2002; Plummer a Edzwald, 2002; Henderson a kol., 2008a, 2010; Ma a kol., 2012b; Vandamme a kol., 2012; Wu a kol., 2012; Zhang a kol., 2012; Garzon-Sanabria a kol., 2013; Wang a kol., 2013). Bylo zjištěno, že v přítomnosti EOM probíhá koagulace s nižší účinností a jsou potřebné vyšší dávky koagulačního činidla (Henderson a kol., 2010; Vandamme a kol., 2012; Wu a kol., 2012; Garzon-Sanabria a kol., 2013). Na druhou stranu, v některých případech mohou mít EOM/COM, a to především ty s vysokou molekulovou hmotností, pozitivní vliv na průběh koagulace. V případě použití předoxidačních metod mohou vysokomolekulární EOM/COM působit jako pomocné koagulační činidlo a tím zvyšovat účinnost koagulace samotných buněk (Ma a Liu, 2002; Henderson a kol., 2010; Ma a kol., 2012a; Wang a kol., 2013). Pozitivní vliv měly COM i na koagulaci buněk pikosinice *Merismopedia tenuissima* (Barešová a kol., 2017).

Existují i studie, které se zabývaly vlivem AOM na koagulaci dalších znečišťujících příměsí a látek obsažených ve vodě (Bernhardt a kol., 1985, 1986; Šafaříková a kol., 2013, Pivokonský a kol., 2015). Ze studií Bernhardt a kol. (1985, 1986) a Šafaříková a kol. (2013) vyplývá, že AOM mohou působit jako pomocné činidlo při koagulaci anorganických hlinitokřemičitanů, které nesou v širokém rozmezí pH záporný náboj (např. kaolin). Ve studii Šafaříková a kol. (2013) AOM proteinového charakteru přispěly vzhledem ke svému amfoternímu charakteru ke koagulaci záporně nabitých kaolinových částic, a to v rozmezí hodnot pH 4-4,5, kdy peptidy/proteiny nesou i částečný kladný náboj díky přítomnosti $–NH_3^+$ skupin. Dochází tedy k elektrostatickým interakcím mezi záporně nabitými funkčními skupinami peptidů/proteinů a kladně nabitými Fe-hydroxopolymery (koagulačním činidlem) a zároveň mezi kladně nabitými skupinami peptidů/proteinů a kaolinovými částicemi

nesoucími záporný náboj. Pozitivní vliv v podobě snížení dávky koagulačního činidla měla proteinová složka COM sinice *M. aeruginosa* i na koagulaci huminových látek (Pivokonský a kol., 2015).

Ke konci vegetační sezóny je však rozvoj vodního květu na ústupu a podíl buněk fytoplanktonu vůči látkám jimi produkovaným, především COM, klesá. Odumíráním fytoplanktonu a lyzí buněk se do vody uvolňuje značné množství COM, které jsou následně vlivem podzimní mixe rozptýleny do celého vodního sloupce. Z tohoto důvodu je nutné zabývat se i koagulací těchto látek. V porovnání s odstraňováním buněk však koagulaci AOM taková pozornost doposud věnována nebyla (Bernhardt a kol., 1985, 1986, 1991; Widrig a kol., 1996; Pivokonský a kol., 2009a,b, 2012, 2015; Henderson a kol., 2010; Šafaříková a kol., 2013; Barešová kol., 2017; Načeradská a kol., 2017; Tang a kol., 2017). Z uvedených studií přitom vyplývá, že účinnost koagulace AOM je významně nižší než v případě koagulace buněk. Například ve studii Henderson a kol. (2010) bylo u koagulace EOM čtyř druhů fytoplanktonu (*M. aeruginosa*, *Chlorella vulgaris*, *Adterionella formosa* a *Melosira* sp.) při použití hlinitého koagulačního činidla dosaženo účinnosti 46-71 %, zatímco buňky těchto organismů byly odstraněny s účinností 94-99 %. Také studie Tang a kol. (2017) prokázala nižší míru odstranění EOM *M. aeruginosa* (< 40 %) v porovnání s buňkami uvedeného organismu (> 90 %). I v případě koagulace buněk a COM sinice *Merismopedia tenuissima* dosahovala účinnost koagulace buněk vyšších hodnot (až 99 %) než u COM (43-53 %) (Barešová a kol., 2017).

Jak již bylo řečeno výše, účinnost odstranění nežádoucích látek z vody koagulací je silně závislá na hodnotě pH. Mnoha studiemi bylo zjištěno, že koagulace AOM probíhá účinněji v kyselé oblasti pH (4,5-6,5), kde negativně nabité funkční skupiny AOM elektrostaticky interagují s pozitivně nabitými hydrolytickými produkty koagulačního činidla (Fe/Al), a tím dochází k jejich destabilizaci nábojovou neutralizací a následné koagulaci (Widrig a kol., 1996; Pivokonský a kol., 2009a,b, 2012, 2015; Šafaříková a kol., 2013; Barešová a kol., 2017; Načeradská a kol., 2017). Například ve studii Widrig a kol. (1996) zjistili, že účinnost odstranění EOM tří druhů mikroorganismů (*M. aeruginosa*, *Scenedesmus quadricauda* a *Dictiosphaericum pulchellum*) koagulací pomocí Fe a Al činidla dosahovala při pH 5 pro jednotlivé druhy 20-50 %, zatímco při pH 8 činila pouze 5-10 %. Stejně tak koagulace COM sinice *M. tenuissima* probíhala nejúčinněji v rozmezí hodnot pH 5-6,5 (Barešová a kol., 2017). Ve studii Pivokonský a kol. (2009a) pak dosahovala nejvyšší účinnosti koagulace COM

sinice *M. aeruginosa* při použití síranu železitého (50 %) a hlinitého (40 %) při pH 4,5-6,5. Avšak nejnižší zbytkové koncentrace činidel, které je nutné brát také v úvahu, byly zjištěny při pH 6-6,5 v případě Fe a při pH 6,5-7 při použití Al činidla.

Obecně je většina prací zabývajících se koagulací organických látek produkovaných fytoplanktonem zaměřena na koagulaci peptidové/proteinové složky, případně na AOM (COM/EOM) jako celku (Bernhardt a kol., 1985, 1991; Pivokonský a kol., 2009a,b, 2012, 2015, 2016; Šafaříková a kol., 2013; Barešová a kol., 2017; Načeradská a kol., 2017). Bylo zjištěno, že např. peptidová/proteinová složka COM sinice *M. aeruginosa* se v případě použití železitého koagulačního činidla nejúčinněji odstraňuje v rozmezí pH 4-6, a to mechanismem nábojové neutralizace mezi negativně nabitými skupinami ve struktuře peptidů/proteinů a produkty hydrolýzy Fe činidla nesoucími kladný náboj. Při vyšším pH 6-8 pak dochází ke koagulaci adsorpcí peptidů/proteinů na hydrolytické produkty činidla a velmi důležitou roli při tom hraje poměr COM/Fe. Uvedený proces se totiž objevuje pouze při nízkém poměru COM/Fe $< 0,33$. Pokud je tento poměr překročen, tedy COM/Fe $> 0,33$, dochází ke sterické stabilizaci hydrolyzovaných částic koagulačního činidla vrstvou peptidů/proteinů a koagulace neprobíhá. Navíc bylo zjištěno, že při pH = 6,2 dochází k tvorbě rozpustných komplexních sloučenin, tzv. Fe-peptidových/proteinových komplexů, které brání účinné koagulaci (Pivokonský a kol., 2012). Koagulace těchto látek prostřednictvím hlinitého činidla probíhá nejúčinněji při trochu vyšším pH (5-6,5) a i v tomto případě se cca při pH 7 objevují rozpustné komplexy Al činidla s peptidy/proteiny (Pivokonský a kol., 2015).

V rámci studie Pivokonský a kol. (2009a) však bylo zjištěno, že účinnost koagulace COM úzce souvisí také s tím, zda je se jedná o peptidovou/proteinovou či neproteinovou složku. Zatímco peptidová/proteinová složka se při použití Fe a Al činidla odstraňovala se 74%, resp. 50% účinností, koagulace neproteinové složky dosahovala účinnosti pouze 12 %, resp. 22 %. Vyšší účinnosti koagulace proteinů (75 %, resp. 69 %) než sacharidů (30 %, resp. 40 %) pomocí chloridu hlinitého a PACl (polyaluminium chlorid) bylo dosaženo i ve studii Cui a kol. (2016). Práce, které by se zabývaly koagulací samotné neproteinové složky a vysvětlovaly mechanismy či objasňovaly důvod, proč při jejím odstraňování dochází k mnohem nižší účinnosti než v případě proteinů, však úplně chybí.

Z hlediska charakteru AOM hraje velmi důležitou roli při koagulaci také jejich hydrofobicita/hydrofilicita a molekulová hmotnost. Mnoha studiemi bylo prokázáno, že

hydrofilní látky jsou v porovnání s hydrofobními mnohem hůře koagulovatelné (Edzwald, 1993; Ghernaout a kol., 2010; Henderson a kol., 2010; Ma a kol., 2012a). Z řady studií přitom vyplývá skutečnost, že AOM jsou ze své podstaty spíše hydrofilní povahy (Edzwald, 1993; Pivokonský a kol., 2006, 2009a, 2012, 2014, 2015; Henderson a kol., 2008b, 2010; Ghernaout a kol., 2010; Ma a kol., 2012a), přičemž podíl hydrofilní frakce dosahuje v závislosti na druhu organismu 54-90 % (Her a kol., 2004; Henderson a kol., 2008a; Li a kol., 2012; Pivokonský a kol., 2014; Barešova a kol., 2017; Goslan a kol., 2017). Nízká účinnost koagulace AOM může být zapříčiněna právě jejich hydrofilním charakterem (Pivokonský a kol., 2016). Další možnou příčinou poměrně nízké odstranitelnosti AOM může být vysoké zastoupení látek s nízkou molekulovou hmotností (< 10 kDa). Zatímco vysokomolekulární látky jsou koagulací odstranitelné poměrně snadno a je dosahováno vysokých účinností, nízkomolekulární frakce koagulaci téměř nepodléhá, a tvoří tak v upravené vodě často vysoké koncentrace zbytkových organických látek (Pivokonský a kol., 2009a, 2012, 2015; Henderson a kol., 2010; Barešová a kol., 2017, Načeradská a kol., 2017). Např. ve studii Henderson a kol. (2010) činilo zastoupení nízkomolekulárních látek (< 1 kDa) v EOM tří organismů (*Chlorella vulgaris*, *M. aeruginosa*, *Asterionella formosa*) 30 %, 38 % a 81 %, resp., přičemž účinnost jejich odstranění dosahovala 71 %, 55 %, resp. 46 %. Nízkou účinnost odstranění nízkomolekulární složky prokázaly také další studie (Cheng a Chi, 2003; de Figuereido a kol., 2004; Ma a kol., 2012a; Pivokonský a kol., 2012, 2015; Sillanpää a kol., 2018). Vzhledem ke skutečnosti, že koagulace není pro některé druhy látek (viz výše) dostatečně účinná a zbytkové koncentrace organických látek přinášejí řadu problémů (viz kapitola 3), je nutné do procesu úpravy vody zařadit další technologické kroky a metody, které mají potenciál i takové látky eliminovat. Vhodné a v současné době již hojněji k tomuto účelu využívané jsou adsorpce na aktivním uhlí (Hnaťuková a kol., 2001; Kopecká a kol., 2014) nebo membránová filtrace (Teixeira a Rosa, 2005; Dixon a kol., 2010), které budou detailněji popsány níže v kapitole 3.4. Poměrně značná pozornost je v poslední době v oblasti výzkumu úpravy vody věnována také oxidačním metodám zařazovaných v různých stupních procesu, a to s očekáváním, že při optimalizovaném procesu by mohlo dojít k přeměně vlastností nežádoucích organických látek na ty pro proces úpravy vody vhodnější, nebo teoreticky k oxidaci látek až na vodu a oxid uhličitý. V případě předoxidace by tak pak teoreticky mohly být koncentrace organických látek sníženy ještě před konvenční koagulací.

3.2 PŘEDOXIDAČNÍ METODY

Pro zvýšení účinnosti koagulace jsou v současné době často aplikovány předoxidační metody prostřednictvím užití různých oxidačních činidel, jako je chlor, oxid chloričitý, manganistan draselný, ozon nebo ozon v kombinaci s peroxidem vodíku (Sukenik a kol., 1987; Paralkar a Edzwald, 1996; Petruševski a kol., 1996; Widrig a kol., 1996; Ma a Liu, 2002; Plummer a Edzwald, 2002; Chen a Yeh, 2005; Chen a kol., 2009; Ma a kol., 2012a,b; Coral a kol., 2013; Pranowo a kol., 2013; Wang a kol., 2013; Xie a kol., 2013; Qi a kol., 2016, Xie a kol., 2016; Načeradská a kol., 2017; Wen a kol., 2017). Použití předoxidace může mít na koagulaci pozitivní vliv různými způsoby. V případě koagulace buněk vede působení oxidačního činidla k jejich inaktivaci a také ke změnám struktur organických látek tvořících jejich povrch – buněčnou membránu. To usnadní jejich destabilizaci, poté koagulaci a následně i separaci např. sedimentací. Vliv předoxidace ozonem a manganistanem draselným na koagulaci suspenze buněk sinice *Microcystis aeruginosa* pomocí síranu hlinitého byl studován v práci Xie a kol. (2016). Bylo zjištěno, že obě oxidační činidla v závislosti na dávce zvýšila účinnost koagulace buněk o 15-25 %. Podobně i ve studii Chen a kol. (2009) došlo při předoxidaci pomocí O_3 a $KMnO_4$ ke zvýšení účinnosti koagulace a následné sedimentace buněk zelené řasy *Chodatella* sp., a to z 84 % na 93 % (O_3) a 98 % ($KMnO_4$). Při oxidaci buněk může také dojít k částečnému uvolnění obsahu buněk, především vysokomolekulárních COM, které následně mohou působit jako pomocné koagulační činidlo a zvýšit účinnost koagulace samotných buněk (Pranowo a kol., 2013; Wang a kol., 2013, Wen a kol., 2017). Studie Wang a kol. (2013) prokázala, že použití předoxidace pomocí manganistanu draselného o nízké dávce 2 mg/l při koagulaci buněk *M. aeruginosa* vede k uvolnění látek s MH > 200 kDa, které následně společně s koagulačním činidlem PACl prostřednictvím tvorby polymerních můstků zvyšují účinnost koagulace. V případě použití manganistanu draselného jako předoxidačního činidla může být nárůst účinnosti koagulace/flokulace buněk mikroorganismů způsoben také vznikem částic MnO_2, které na svém povrchu umožňují jejich sorpci (Petruševski a kol., 1996; Chen a Yeh, 2005; Chen a kol., 2005; Xie a kol., 2016).

U rozpuštěných AOM způsobuje oxidace nárůst množství karboxylových skupin ve struktuře jejich molekul, které obecně zvyšují účinnost koagulace (Bose a Reckhow, 2007; Chen a Yeh, 2005; Načeradská a kol., 2017). V některých případech, zejména při

použití ozonu a při delší době oxidace, může také docházet k poklesu koncentrace AOM přeměnou organického uhlíku až na oxid uhličitý (Hoyer a kol., 1987; Ma a Liu, 2002; Pranowo a kol., 2013; Wang a kol., 2013). Vše přitom závisí nejen na dávce a typu použitého oxidačního činidla, ale také na druhu a růstové fázi fytoplanktonu, které ovlivňují složení AOM (Hoyer a kol., 1987; Widrig a kol., 1996; Ma a Liu, 2002; Plummer a Edzwald, 2002; Coral a kol., 2013).

Vedle výše uvedených studií popisujících pozitivní vliv předoxidace na koagulaci/flokulaci buněk mikroorganismů, existuje i řada studií s opačným výsledkem. Bylo prokázáno, že působením oxidačního činidla, především jeho vysokých koncentrací, na buňky může dojít k jejich lyzi a uvolnění jejich obsahu, např. látek negativně ovlivňujících organoleptické vlastnosti vody a toxinů, do upravované vody. (Hoyer a kol., 1987; Paralkar a Edzwald, 1996; Henderson a kol., 2008b; Ma a kol., 2012a; Coral a kol., 2013; Pranowo a kol., 2013; Wang a kol., 2013; Xie a kol., 2013). Nutné je také brát v úvahu, že při použití oxidačních činidel na bázi chloru a ozonu, hrozí riziko vzniku nežádoucích vedlejších produktů desinfekce (Henderson a kol., 2008b; Coral a kol., 2013; Xie a kol., 2013). Xie a kol. (2013) zkoumali chloraci jako hygienické zabezpečení vody po úpravě koagulací s předoxidací dvěma různými činidly – ozonem a manganistanem draselným. Zatímco při použití ozonu došlo k poškození buněk, vylití jejich obsahu (COM) a zvýšení podílu nízkomolekulární složky a tím i k velké míře vzniku vedlejších produktů desinfekce při následné chloraci, při aplikaci manganistanu draselného k zásadnímu poškození buněk nedošlo, a produkce DBPs tak byla značně nižší. Předoxidace pomocí manganistanu draselného tak může být vzhledem k možnému riziku tvorby DBPs v porovnání s ostatními činidly vhodnější (Xie a kol., 2016). Na druhou stranu však při použití jeho nadměrných dávek může dojít k nežádoucímu nárůstu koncentrace zbytkového Mn, barvy, zákalu či nakonec také k poškození odstraňovaných buněk (Qui a kol., 2016; Xie a kol., 2016).

V porovnání s pracemi zabývajícími se vlivem předoxidace na koagulaci buněk či buněk v přítomnosti EOM, studií zaměřených na vliv předoxidace na samotné rozpuštěné AOM a jejich koagulaci existuje jen velmi málo (Hoyer a kol., 1987; Paralkar a Edzwald, 1996; Widrig a kol., 1996; Načeradská a kol., 2017). Bylo zjištěno, že oxidace AOM může způsobit jejich degradaci a štěpení na látky s nízkými molekulovými hmotnostmi, které jsou koagulací odstranitelné s velmi nízkou účinností (viz kapitola 3.1) (Hoyer a kol., 1987; Paralkar a Edzwald, 1996; Henderson a kol., 2008b; Ma a kol., 2012a; Coral a kol., 2013; Pranowo a kol., 2013; Wang a kol., 2013;

Xie a kol., 2013; Wei a kol., 2016; Wen a kol., 2017). Například ve studii Paralkar a Edzwald (1996) zjistili, že ozonizace EOM zelených řas *Chlorella vulgaris* a *Scenedesmus quadricauda* a rozsivky *Cyclotella* sp. způsobila pokles podílu vysokomolekulárních látek a látek se střední molekulovou hmotností a značně navýšila množství nízkomolekulárních látek. Koncentrace DOC přitom nijak neklesla (Paralkar a Edzwald, 1996). Také ve studii Widrig a kol. (1996) došlo předozonizací k degradaci makromolekulárních proteinů a mastných kyselin na menší molekuly. A i v tomto případě došlo jen k velmi zanedbatelnému poklesu DOC, a to o 0-3 % (Widrig a kol. (1996). Hoyer a kol. (1987) ve své studii posuzovali pokles DOC během ozonizace EOM tří druhů organismů *Fragilaria* sp., *Pseudanabaena* sp. a *Dictyosphaerium* sp. při dávkách ozonu 0,5-1,0 mg O_3 na 1 mg DOC (s počátečním DOC 20-40 mg/l) s tím, že ozon byl kontinuálně probubláván do roztoků EOM a koncentrace ozonu se tak časem zvýšila. Ke snížení DOC vlivem ozonizace ale v průběhu 0-20 min, a to již dávka ozonu činila 74-86 mg/l, prakticky nedošlo. Až při době ozonizace delší než 30 min došlo ke snížení koncentrace DOC, a to o 5,4-18 % v závislosti na druhu organismu a době aplikace O_3. Takové dávky ozonu však nejsou při úpravě pitné vody vůbec použitelné a bylo prokázáno, že i dávky, které byly několikrát nižší, způsobují nežádoucí destrukci buněk řas, které jsou běžně přítomny v surové vodě spolu s EOM (Fan a kol., 2013; Xie a kol., 2013). Velmi pozitivní účinky předoxidace pomocí $KMnO_4$ byly pozorovány při koagulaci peptidové/proteinové složky COM sinice *M. aeruginosa* prostřednictvím železitého koagulačního činidla (Načeradská a kol., 2017). Došlo nejen ke zvýšení koagulační účinnosti (o 5-12 %), ale také ke snížení potřebné dávky koagulačního činidla, k rozšíření optima pH koagulace (z pH 4,3-6,0 na 4,6-7,3), k eliminaci tvorby Fe-peptidových/proteinových komplexů a k efektivnímu odstranění toxického mikrocystinu (Načeradská a kol., 2017).

I mnoha jinými pracemi bylo prokázáno, že předoxidace může velmi účinně eliminovat cyanotoxiny (Rositano a kol., 1998; Al Momani a kol., 2008; Ohio AWWA & Ohio EPA, 2015; Health Canada, 2017). Např. ve studii Rositano a kol. (1998) došlo vlivem oxidace ozonem při pH < 7,5 k odstranění veškerého mikrocystinu-RR (MC-RR). Některé studie však uvádí, že v přítomnosti jiných organických sloučenin může dojít k inhibici degradace toxinů (Rositano a kol., 1998, 2001; Miao a Tao, 2009). Například ve studii Miao a Tao (2009) došlo při zvýšení koncentrace DOC huminových kyselin z 1 na 4 mg/l k nárůstu zbytkových koncentrací MC-RR z přibližně 10 % na 30 %. Ve stejné studii byl také pozorován pokles míry rozkladu MC-RR v přítomnosti

supernatantu z řas (20 % zbytkový MC-RR ve srovnání s úplnou degradací toxinu ve vzorcích bez řas). K podobným zjištěním došli i ve studii Rositano a kol. (1998), kdy ozonizace samotných mikrocystinů byla velice účinná, avšak v přítomnosti EOM sinice *M. aeruginosa* docházelo ke konkurenčním reakcím mezi ozonem, toxiny a EOM, což ovlivnilo účinnost oxidace. Degradaci toxinů v přítomnosti AOM by tedy měla být věnována větší pozornost.

3.3 VLIV AOM NA STRUKTURU AGREGÁTŮ

Celková účinnost procesu úpravy vody je vedle účinnosti destabilizace (koagulace) znečišťujících příměsí dána také účinností agregace (flokulace) již destabilizovaných částic a následně účinností separace (sedimentace, flotace, filtrace) v předchozích krocích vytvořených vločkovitých agregátů (Pivokonský a kol., 2011). Účinnost separace je přitom závislá na vlastnostech vytvořených agregátů (vloček), především pak na jejich velikosti, struktuře, tvaru, pevnosti a sedimentační rychlosti (Pivokonský a kol., 2011; Bubáková a kol., 2013). Různé druhy separace vyžadují pro účinný průběh agregáty různých vlastností (Bubáková a kol., 2011). Pro jednostupňovou separaci sestávající pouze z filtrace jsou vhodné malé a husté agregáty do velikosti 50-60 μm (Ngo a kol., 1995; Pivokonský a kol., 2011; Bubáková a Pivokonský, 2012). Názory na vlastnosti agregátů odpovídající separaci suspenze flotací se různí. Dle studií Edzwald (1995, 2010) by se velikostní distribuce flotací separovaných částic měla pohybovat v rozmezí 10-30 μm, resp. 25-50 μm a agregáty by měly být pevné. Naopak Vlaški a kol. (1997) ve své studii uvádějí, že i velké agregáty (> 50 μm), když vznikají při velmi pomalém gradientu rychlosti (G = 10 s^{-1}), mají nízkou hustotu, a jsou tedy vhodné pro separaci flotací. Sedimentace pak vyžaduje pevné agregáty o velikosti > 100 μm, které mají vysokou sedimentační rychlost (Edzwald, 1995; Bubáková a kol., 2011).

Vlastnosti agregátů jsou obecně ovlivněny několika parametry, především složením a koncentrací odstraňované znečišťující příměsi, typem a dávkou koagulačního činidla, gradientem rychlosti a dobou míchání (Pivokonský a kol., 2011). Práce, které by se zabývaly vlivem samotných AOM na strukturu agregátů, jsou velice ojedinělé. Existuje však několik studií, které se zaměřily na výzkum vlivu buněk na strukturu a tvorbu agregátů (Henderson a kol., 2006; Pivokonský a kol., 2009a,b; Gonzalez-Torres a kol., 2014, 2017; Vandamme a kol., 2014; Jiao a kol., 2015; Chekli

a kol., 2017). Uvedenými studiemi bylo prokázáno, že charakter vytvořených agregátů AOM závisí na typu a dávce koagulačního činidla a velmi silně na hodnotě pH. Například Chekli a kol. (2017) ve své studii zkoumali proces odstraňování AOM rozsivky *Chaetoceros muelleri* pomocí $TiCl_4$ a PTC (polytitanium tetrachloride) v porovnání s konvenčním činidlem $FeCl_3$ a zjistili, že při použití $TiCl_4$ a PTC je účinnost odstranění vyšší a dochází k tvorbě větších, pevnějších a kompaktnějších agregátů než v případě $FeCl_3$. Gonzalez-Torres a kol. (2014) posuzovali vlastnosti agregátů buněk a AOM sinice *Micrycystis aeruginosa* vytvořených koagulací $Al_2(SO_4)_3$ a $FeCl_3$ při pH 6 a 7. Ukázalo se, že železité agregáty jsou větší než ty tvořené hlinitým koagulačním činidlem, a to bez ohledu na dávku a koagulační pH. V rámci jednoho typu koagulačního činidla se přitom s jeho rostoucí dávkou velikost vloček zvětšovala. Při posuzování jedné dávky jednoho činidla pak hrálo ve velikosti vloček velmi významnou roli i pH. Při pH 7 vznikaly větší vločky než při pH 6. Pevnost vloček pak byla dána velikostí dávky koagulačního činidla, nikoli jeho typem, a s rostoucí dávkou se zvyšovala. Nejpevnější agregáty vznikaly při koagulaci pomocí železitého činidla při pH 6 (Gonzalez-Torres a kol., 2014).

Ostatní výše zmíněné práce se zabývaly vlivem AOM na vlastnosti vloček tvořenými jílovitými minerály nebo buňkami. Avšak vzhledem k tomu, že jednotlivé studie se velmi liší v aplikovaných podmínkách použitých experimentů (různé/nespecifikované rychlosti gradientu, různé dávky koagulačního činidla, různé složení a koncentrace AOM), je nemožné vzájemné porovnání jejich zjištění či vyvozování významnějších souhrnných závěrů. Obecně lze pouze říci, že přítomnost AOM v surové vodě ovlivňuje velikost vloček tvořených koagulací ostatních znečišťujících příměsí. Například Vandamme a kol. (2014) koagulovali buňky řasy *Chlorella vulgaris* samotné a v přítomnosti AOM pomocí hlinitého činidla, chitosanu a kationtového škrobu a zjistili, že agregáty s AOM jsou větší a v případě chitosanu až desetinásobně. Ve studii Henderson a kol. (2006) zkoumali vlastnosti agregátů tvořených koagulací buněk *C. vulgaris* v přítomnosti EOM a vloček z anorganických částic (kaolin) a NOM (huminové látky). Zjistili, že vločky buněk řasy a jejích EOM jsou v porovnání s těmi z ostatních znečišťujících příměsí větší a méně pevné. Ale vzhledem k tomu, že koagulace samotných buněk provedena nebyla, není možné příspěvek EOM na velikosti tvořených agregátů jednoznačně určit (Henderson a kol., 2006). Studie Pivokonský a kol. (2009b) pak uvádí, že velikost agregátů je také ovlivněna koncentrací koagulované příměsi. Zjistili, že s klesající koncentrací COM

M. aeruginosa klesá i velikost tvořených vloček. Vliv původu a složení AOM na vlastnosti agregátů studovali ve své práci také Gonzalez-Torres a kol. (2017). Ti koagulovali buňky a EOM řasy *C. vulgaris* a sinice *M. aeruginosa* pomocí hlinitého koagulačního činidla vzniklé agregáty charakterizovali pomocí FTIR (Fourier Transform infrared). Bylo zjištěno, že vločky *M. aeruginosa* byly měřitelně menší, jednotnější a pevnější než ty *C. vulgaris*, což bylo přisuzováno hlavně rozdílnému složení a koncentraci AOM jednotlivých druhů (Gonzalez-Torres a kol., 2017).

Z uvedených informací jednoznačně vyplývá, že vliv AOM na strukturu a vlastnosti agregátů v závislosti na podmínkách koagulace nebyl doposud spolehlivě objasněn a že je v této oblasti nutný další výzkum. Charakter a struktura agregátů vytvořených při koagulaci je totiž zcela zásadní pro jejich následnou separaci, a tedy celkovou účinnost procesu úpravy vody.

3.4 ADSORPCE AOM NA AKTIVNÍM UHLÍ

Adsorpce na aktivním uhlí (AU) je hojně využívána metoda k eliminaci obtížně odstranitelných nežádoucích organických látek přírodního i antropogenního charakteru (Bjelopavlic a kol., 1999; Moreno-Castilla, 2004; Bond a kol., 2011; Ho a kol., 2011; Zhang a kol., 2011a; Delgado a kol., 2012). Řada studií prokázána, že konvenční koagulací není možné odstranit veškeré organické látky a zejména ty nízkomolekulární pak představují v upravené vodě zbytkové koncentrace organických látek, které jsou příčinou řady problému (viz kapitola 3) (Pivokonský a kol., 2012; Šafaříková a kol., 2013). V praxi je nejčastěji adsorpce používána ve spojení s koagulací a pískovou filtrací, přičemž aktivní uhlí je aplikováno buď ve fázi koagulace jako práškové (PAU), nebo častěji za pískovou filtrací ve formě granulované (GAU). Práškové AU je obvykle dávkováno do vody současně s koagulačním činidlem a jeho použití je většinou spojeno s přechodným zhoršením kvality vody. Kontinuální používání PAU se na úpravnách nepředpokládá. Po použití se totiž PAU nijak nerecykluje, z upravované vody je odstraněno při separaci suspenze, nejčastěji při pískové filtraci, a stává se tak součástí kalové vody z praní filtrů. Granulované aktivní uhlí tvoří náplň atmosférických nebo tlakových filtrů a jeho aplikace bývá většinou zařazena za pískovou filtraci a před konečný krok úpravy, hygienické zabezpečení upravené vody. Velmi často je před GAU pro zvýšení účinnosti adsorpce a eliminaci mikropolutantů zařazována ještě oxidace ozónem (Chu a kol., 2012; Oloibiri a kol., 2015; Rozas a kol., 2017; Huang a kol.,

2018; Guillossou a kol., 2020). Aktivní uhlí v granulované formě lze regenerovat, nejčastěji teplotně či působením vodní páry (Newcombe, 2006).

Převážná většina studií zaměřených na odstraňování organických látek prostřednictvím adsorpce na aktivním uhlí se zabývá huminovými látkami či obecně rozpuštěnými organickými látkami (DOM – Dissolved Organic Matter; > 0,45 μm) (Schreiber a kol., 2005; Matilainen a kol., 2006; Gur-Reznik a kol., 2008; Wei a kol., 2008; Kristiana a kol., 2011; Velten a kol., 2011; Matsui a kol., 2012; Gibert a kol., 2013). Studie zaměřené na adsorpci samotných sinicových a řasových produktů (AOM) jsou doposud velmi ojedinělé a to přesto, že by zařazení adsorpce do procesu úpravy vody odstranění AOM výrazně napomohlo (Henderson a kol., 2008b; Hnaťuková a kol., 2011; Zhang a kol., 2011a,b; Kopecká a kol., 2014). Bylo zjištěno, že COM peptidy *M. aeruginosa* < 10 kDa jsou adsorpcí velice dobře odstranitelné a že velký vliv na účinnost adsorpce má druh GAU a hodnota pH a iontové síly roztoku. Nejvyšší účinnosti odstranění bylo dosaženo na GAU Picabiol 12x40 při pH 5 a vyšší iontové síle (0,3 M NaCl). Nejvyšší účinnosti adsorpce COM *M. aeruginosa* v kyselé oblasti pH bylo dosaženo i ve studii Hnaťuková a kol. (2011). Konkrétně byla míra adsorpce při hodnotě pH 5 dvakrát větší než při pH 8,5. Vysoká účinnost adsorpce COM peptidů byla vysvětlena tvorbou vodíkových můstků mezi protonovanými funkčními skupinami peptidů a skupinami na povrchu aktivního uhlí. Při pH 8,5 se naopak projevily odpudivé elektrostatické síly mezi záporně nabitými skupinami COM peptidů i GAU. Zároveň bylo v rámci této studie prokázáno, že zbytkové organické látky mohou inhibovat adsorpci ostatních mikropolutantů, pro které je většinou technologický krok adsorpce na AU na úpravnách vody zařazen. Vysoká afinita COM peptidů k povrchu AU způsobila výrazné snížení účinnosti adsorpce dvou herbicidů, terbuthylazinu a alachloru, a to přitom ještě ve větší míře při pH 5 než při pH 8,5, což koresponduje s vysokou účinností adsorpce COM peptidů právě při pH 5 (Hnaťuková a kol., 2011). Na snížení kapacity AU pro uvedené pesticidy se nejvíce podílely COM peptidy o MH 700-1700 Da. Peptidy s MH nad 2300 Da pak sice nekompetitovaly s herbicidy při adsorpci ve vnitřní struktuře AU, ale na druhou stranu způsobily blokaci transportních pórů při vstupu látek do této vnitřní struktury AU (Hnaťuková a kol., 2011). Přímou kompetici by bylo pravděpodobně možné pozorovat při odstraňování mikropolutantů, jako jsou pesticidy, i z vody s obsahem dalších významných nízkomolekulárních AOM, a to aminokyselin. Molekulové hmotnosti aminokyselin se pohybují v nižších stovkách Da stejně jako např. molekulové hmotnosti dvou výše uvedených herbicidů terbuthylazinu

a alachloru. Ačkoli jsou jednoduché i kombinované aminokyseliny významnou složkou AOM, jejich adsorpcí v souvislosti s procesem úpravy vody se doposud nezabývala žádná studie. Existují pouze práce zabývající se jejich adsorpcí pro aplikace v potravinářství, medicíně, biochemii nebo geochemii. V této souvislosti byla posuzována jejich adsorpce na hydroxyapatitu (Kresak a kol., 1976), kaolinitu (Ikhsan a kol., 2004), montmorillonitu (Parbhakar a kol., 2007), polymerech (Liu a kol., 2007), zeolitech (Titus a kol., 2003), modifikovaném oxidu křemičitém (O'Connor a kol., 2006; Goscianska a kol., 2013, 2014) a aktivním uhlí (Vinu a kol., 2006). Z uvedených studií vyplývá, že adsorpční účinnost aminokyselin je z hlediska jejich struktury ovlivněna především molekulovou hmotností, velikostí a geometrií molekuly, rozpustností, polaritou a charakterem funkčních skupin postranního řetězce (Pászti a Guczi, 2009; Goscianska a kol., 2013; Greiner a kol., 2014). Na adsorpci mají kromě struktury a charakteru adsorbátu stejně jako v případě peptidů vliv také povaha adsorbentu a vlastnosti roztoku. Mezi nejvýznamnější charakteristiky roztoku, které ovlivňují proces adsorpce AMK a určují jeho průběh, patří hodnota pH, iontová síla (IS), teplota a počáteční koncentrace adsorbátu (Tentorio a Canova, 1989; Titus a kol., 2003; Ikhsan a kol., 2004; Vinu a kol., 2006; O'Connor a kol., 2006; Liu a kol., 2007; Gao a kol., 2008; Elsellami a kol., 2010; Clark a kol., 2012; Greiner a kol., 2014). Kombinace těchto faktorů pak určuje charakter a mechanismy adsorpce, z nichž za dominantní jsou považovány elektrostatické interakce (O'Connor a kol., 2006), hydrofobní interakce (Vinu a kol., 2006; Clark a kol., 2012) a vodíkové můstky (Ikhsan a kol., 2004).

Některé studie se zabývají použitím aktivního uhlí pro odstraňování AOM v kombinaci s dalšími technikami úpravy vody, nejčastěji s membránovou filtrací. Například Zhang a kol. (2011b) studovali vliv přídavku práškového aktivního uhlí na proces ultrafiltrace (UF) vody s obsahem AOM. Zjistili, že samotnou ultrafiltrací je možné dosáhnout téměř 100% odstranění buněk mikroorganismů (konkrétně buněk sinice *M. aeruginosa*), avšak pro samotné AOM je ultrafiltrace velmi neúčinná. Míra odstranění AOM se zvýšila až po přídavku PAC, a to o 10,9 ± 1,7 % DOC. Navíc u nízkomolekulárních mikrocystinů došlo vlivem PAC k navýšení účinnosti jejich odstranění až o 40,8 ± 4,2 %. Srovnatelných výsledků bylo dosaženo i ve studii Campinas a Rosa (2010), kde posuzovali účinnost kombinace PAU a UF pro odstraňování různých druhů organických látek. Zjistili, že použitím PAU došlo ke zvýšení účinnosti odstranění AOM (EOM + COM) *M. aeruginosa* z 35 na 55 %, což

bylo srovnatelné s účinností eliminace taninů (tannic acids) a huminových kyselin. Použití práškového aktivního uhlí navíc eliminovalo zanášení membránového filtru a výrazně prodloužilo filtrační cyklus. Odstraňování buněk sinic, toxinů a AOM dvou druhů sinic *Anabaena circinalis* a *Microcystis flos-aquae* prostřednictvím komplexního procesu koagulace–PAU–UF se ve své práci zabývali Dixon a kol. (2011). V případě *A. circinalis* se účinnost odstranění AOM zvedla z 35 % při použití samotné UF na 69 %, resp. 71 % při zařazení koagulace a koagulace s následnou adsorpcí na PAU. V případě *M. flos-aquae* dosáhla účinnost odstranění DOC max. 65 % při použití všech kombinací procesů. Kromě ultrafiltrace se v kombinaci s PAC používá i mikrofiltrace. Bylo prokázáno, že využitím těchto dvou technik lze dosáhnout vysoké účinnosti odstranění buněk i látek způsobujících nežádoucí zápach vody (geosmin) (Matsushita a kol., 2008). Existuje i několik studií, které se zaměřují na použití adsorpce na aktivním uhlí při odstraňování sinicových toxinů, především mikrocystinů a saxitoxinů (Pendleton a kol., 2001; Huang a kol., 2007b; Campinas a Rosa, 2010; Dixon a kol., 2011; Ho a kol., 2011).

3.4.1 Faktory ovlivňující adsorpci AOM na aktivním uhlí

Účinnost adsorpce organických látek na aktivním uhlí je ovlivněna celou řadou faktorů. Důležitou roli hrají nejen vlastnosti adsorbentu – aktivního uhlí, jako je velikostní distribuce pórů nebo obsah funkčních skupin vázaných na povrchu, ale zásadní je i charakter sorbované látky (molekulová hmotnost, náboj, charakter a množství funkčních skupin, rozpustnost) a především pak vlastnosti roztoku, zejména hodnota pH, teplota a iontová síla (Moreno-Castilla, 2004; Campinas a Rosa, 2006; Newcombe, 2006).

Charakter aktivního uhlí

Účinnost adsorpce organické látky na AU je z hlediska vlastností adsorbentu dána hodnotou specifického povrchu, charakterem a množstvím funkčních skupin na povrchu AU a také velikostní distribucí pórů (Bjelopavlic a kol., 1999; Pelekani a Snoyeink, 1999; Ebie a kol., 2001; Li a kol., 2003a,b; Destgheib a kol., 2004; Newcombe, 2006; Hnaťuková a kol., 2011; Kopecká a kol., 2014). Hodnota specifického povrchu řídí účinnost adsorpce především antropogenních polutantů a nízkomolekulárních NOM, jako jsou např. fulvokyseliny (Newcombe, 2006). Míra adsorpce AOM je však pravděpodobně dána spíše velikostní distribucí pórů AU (Li a kol., 2003a,b). Bylo

prokázáno, že v případě AOM se molekuly přednostně zachycují, tedy sorbují, v pórech velikostně jim odpovídajících. Důvodem je pak pravděpodobně uplatnění většího počtu kontaktních bodů mezi velikostně si odpovídajícími molekulami AOM a aktivními místy na povrchu a ve vnitřní struktuře AU (Hnaťuková a kol., 2011; Kopecká a kol., 2014). Vzhledem k molekulové hmotnosti AOM peptidů, která se pohybuje v rozmezí několika set až tisíc Da (Pivokonský a kol., 2012, 2014), uplatňují se při jejich adsorpci především mezopóry (d > 2 nm) a mikropóry (d = 0,8-2 nm) (Destgheib a kol., 2004). V rámci studie Hnaťuková a kol. (2011) byla nejúčinnější adsorpce zjištěna pro AOM peptidy s molekulovou hmotností pod 2 kDa. Naopak peptidy s MH > 2 kDa významně snížily účinnost adsorpce blokací vstupních (transportních) pórů AU. I další studie prokázala vyšší účinnost adsorpce u AOM s nízkou molekulovou hmotností (< 4,5 kDa) (Kopecká a kol., 2014). Tedy, jestliže je velikost pórů dostatečná pro vstup nízkomolekulárních AOM i těch s vyšší molekulovou hmotností, je míra adsorpce těchto látek řízena přímou kompeticí o adsorpční místa (Pelekani a Snoyeink, 1999; Ebie a kol., 2001). Pokud jsou však póry velikostně vhodné pouze pro adsorpci látek s nízkou MH a nedostatečně velké pro látky s vyšší molekulovou hmotností, blokují tyto látky vnitřní strukturu AU s mikropoŕy svou adsorpcí na povrchu AU nebo v makro- a mezopórech. Míra této blokace (nepřímé kompetice) je pak dána dávkou AU a poměrem množství nízkomolekulárních látek a látek s vyšší MH (Pelekani a Snoyeink, 1999; Ebie a kol., 2001). Z hlediska vlastností AU má pak na účinnost adsorpce kromě velikostní distribuce velký vliv především charakter a množství funkčních skupin na jeho povrchu, které v závislosti na pH určují celkový náboj AU a ten ovlivňuje při adsorpci se uplatňující mechanismy a interakce (více viz kapitola 3.4.2).

Charakter adsorbátu (AOM)

Z hlediska vlastností sorbovaných látek má na účinnost adsorpce zásadní vliv molekulová hmotnost, respektive velikost molekul, a charakter funkčních skupin zastoupených v jejich molekulách (Newcombe a kol., 1997; Ebie a kol., 2001; Kilduff a Karanfil, 2002; Kim a Yu, 2005; Dixon a kol., 2011; Hnaťuková a kol., 2011; Zhang a kol., 2011a,b; Kopecká a kol., 2014). Mnoha studiemi bylo prokázáno, že účinnost adsorpce souvisí především s distribucí molekulových hmotností adsorbátu (Newcombe a kol., 1997; Ebie a kol., 2001; Kilduff a Karanfil, 2002). Obecně lze říci, že účinnost adsorpce se zvyšuje s klesající molekulovou hmotností sorbované látky (Newcombe

a kol., 1997; Kim a Yu, 2005; Hnaťuková a kol., 2011; Zhang a kol., 2011a,b; Kopecká a kol., 2014). Například ve studii Zhang a kol. (2011b) došlo přidáním práškového AU do vody upravované ultrafiltrací ke zvýšení účinnosti odstranění nízkomolekulárních mikrocystinů (MH cca 1 kDa), zatímco koncentrace vysokomolekulárních proteinů a polysacharidů (AOM sinice *M. aeruginosa*) se nesnížila. Také v rámci studie Dixon a kol. (2011) bylo při zařazení PAU ke koagulaci a ultrafiltraci dosaženo vyšší účinnosti odstranění AOM sinice *Anabaena circinalis*, a to především v rozmezí molekulových hmotností 1500-3000 Da. Adsorpcí nízkomolekulárních COM peptidů sinice *M. aeruginosa* pod 10 kDa se zabývali ve své studii i Kopecká a kol. (2014). Bylo zjištěno, že peptidy s MH = 1,0-4,5 kDa byly adsorbovány s vyšší účinností než peptidy s molekulovou hmotností 8,3 a 9,5 kDa. Podobně i ve studii Hnaťuková a kol. (2011) byly přednostně sorbovány COM peptidy stejného druhu sinice s molekulovými hmotnostmi v rozmezí 700-1700 Da, které navíc inhibovaly adsorpci dvou zkoumaných herbicidů, terbuthylazinu a alachloru. Stejných poznatků bylo dosaženo i ve studiích zaměřených na adsorpci NOM, kde vysoká účinnost adsorpce nízkomolekulární složky výrazně snížila účinnost odstranění organických polutantů (Newcombe a kol., 1997; Zhang a kol., 2011a). Kromě molekulové hmotnosti má na účinnost adsorpce zásadní vliv i konformace molekul, která je určována především experimentálními podmínkami a souvisí s celkovým nábojem sorbovaných molekul. Je-li množství záporného a kladného náboje, respektive počet záporně a kladně nabitých funkčních skupin v molekule, vyrovnané, nedochází tak k významnému uplatňování mezimolekulárních odpudivých sil a molekuly mají tendenci zaujímat kompaktnější tvar. To pak následně usnadňuje jejich vstup do vnitřní struktury AU (Huang a kol., 2007a; Goscianska a kol., 2013, 2014; Kopecká a kol., 2014). Podobně jako u AU má pak i v případě adsorbentu množství a charakter funkčních skupin zásadní vliv na uplatňující se interakce, a tím i na účinnost adsorpce.

Charakter roztoku

Při adsorpci hrají významnou roli vlastnosti roztoku, respektive jeho chemismus, především hodnota pH a iontové síly a teplota (Newcombe a Drikas, 1997; Bjelopavlic a kol., 1999; Moreno-Castilla, 2004; Bansal a Goyal, 2005; Campinas a Rosa, 2006; Knappe, 2006; Hnaťuková a kol., 2011; Kopecká a kol., 2014). Hodnota pH ovlivňuje disociaci funkčních skupin jak na povrchu aktivního uhlí, tak ve struktuře molekul sorbovaných látek. V závislosti na hodnotě pH převládají v molekulách AOM kladně (–

NH_3^+, $=NH_2^+$), nebo záporně ($–COO^-$, $–O^-$) nabité funkční skupiny (Šafaříková a kol., 2013). Obdobně pH ovlivňuje také charakter (protonizaci/deprotonizaci) funkčních skupin na povrchu aktivního uhlí. V případě, že je pH roztoku nižší než pH_{NBN} (pH nulového bodu náboje), je celkový náboj AU kladný. Pokud je naopak pH roztoku vyšší než pH_{NBN}, nese AU celkový záporný náboj (Moreno-Castilla, 2004; Bansal a Goyal, 2005; Knappe, 2006). Uvedené funkční skupiny ve struktuře molekul AOM a na povrchu AU, ať už v deprotonizovaném či protonizovaném stavu, se pak během adsorpce účastní různých typů interakcí (elektrostatické, hydrofobní, vodíkové vazby), a tím zásadním způsobem ovlivňují účinnost celého procesu (Newcombe a Drikas, 1997; Bjelopavlic a kol., 1999; Moreno-Castilla, 2004; Knappe, 2006; Hnaťuková a kol., 2011; Kopecká a kol., 2014). Obecně z literatury vyplývá, že účinnost adsorpce AOM roste s klesající hodnotou pH roztoku (Hnaťuková a kol., 2011; Kopecká a kol., 2014). Například, ve studii Hnaťuková a kol. (2011) dosahovala adsorpce COM peptidů sinice *M. aeruginosa* vyšší účinnosti při pH 5 než při pH 8,5. Stejně tak ve studii Kopecká a kol. (2014) došlo k účinnější adsorpci COM peptidů stejného druhu sinice v kyselé oblasti pH (při pH 5) než v neutrální (pH 7) a zásadité oblasti pH (pH 8). Prostřednictvím změny míry a charakteru při adsorpci se uplatňujících interakcí mezi adsorbentem a adsorbátem účinnost adsorpce ovlivňuje také iontová síla (IS) roztoku. Má vliv především na elektrostatické interakce a ten se mění v závislosti na typu AU a pH roztoku. Obecně dochází při nárůstu iontové síly roztoku k potlačení odpudivých elektrostatických interakcí, což vede ke zvýšení účinnosti adsorpce (Newcombe a Drikas, 1997; Bjelopavlic a kol., 1999; Moreno-Castilla, 2004; Campinas a Rosa, 2006). Záleží však i na koncentraci adsorbátu. V případě, že je koncentrace látek sorbovaných na povrchu AU nízká a mezi účastníky adsorpce převládají přitažlivé síly, účinnost adsorpce vlivem zvýšení iontové síly poklesne. Ionty soli přitažlivé síly oslabí, čímž se míra adsorpce sníží. Pokud však převládají při nízké koncentraci látek sorbovaných na povrchu AU interakce odpudivé, ionty přidané soli mohou tyto interakce částečně odstínit a míru adsorpce tím zvýšit. Jestliže je koncentrace sorbovaných látek na povrchu AU vyšší, dostanou se molekuly se stejným nábojem do přílišné blízkosti a začnou mezi nimi působit odpudivé síly. Při adsorpci se pak mohou projevit i interakce neelektrostatické povahy. I za těchto podmínek však může vlivem zvýšení iontové síly roztoku dojít k ostínění odpudivých elektrostatických sil a tím k nárůstu účinnosti adsorpce (Newcombe a Drikas, 1997; Bjelopavlic a kol., 1999). Vliv iontové síly roztoku na adsorpci je přitom úzce spojen s hodnotou pH roztoku, která

určuje protonizaci/deprotonizaci funkčních skupin adsorbentu a adsorbátu, a tím tedy i možnost projevu pozitivního i negativního účinku iontové síly (Kopecká a kol., 2014). Vzhledem k převážně záporně nabitým AOM vede v případě použití AU s nízkým pH_{NBN} zvýšení iontové síly k nárůstu účinnosti adsorpce vlivem odstínění odpudivých sil mezi shodně nabitými funkčními skupinami AU a AOM téměř v celém rozsahu pH. Naopak při aplikaci AU s vyšším pH_{NBN} se může vliv zvýšení iontové síly při různých hodnotách pH projevovat různě v závislosti na nábojových poměrech v celém systému (Kopecká a kol., 2014). Značný vliv na účinnost adsorpce může mít i teplota roztoku (Moreno-Castilla, 2004; Schreiber a kol., 2005). Teplota roztoku může mít vliv na kinetickou energii či Brownův pohyb sorbovaných částic, na viskozitu roztoku a rozpustnost sorbované látky a může se na účinnosti adsorpce projevit pozitivně i negativně (Amend a Helgeson, 1997; Terzyk a kol., 2003; Rabe a kol., 2011; Liu a kol., 2013). Obecně se předpokládá, že adsorpce je ze své podstaty procesem exotermním, tedy účinnost procesu roste s klesající teplotou (Moreno-Castilla, 2004). Avšak některé práce naopak uvádějí rostoucí míru adsorpce organických látek s klesající teplotou roztoku (Schreiber a kol, 2005; Tan a kol., 2009). To může souviset s rolí rozpouštědla (v tomto případě vody) v tomto procesu, kdy u některých organických látek musí nejdříve dojít k porušení jeho vazeb s molekulami sorbované látky tak, aby mohlo dojít k jejich sorpci na AU. Toto porušení vazeb mezi rozpouštědlem a adsorbátem přitom může vyžadovat energii dodanou např. v podobě zvýšení teploty roztoku (Liu a kol., 2007; Anastopoulos a Kyzas, 2016). Přestože tedy může mít teplota roztoku na účinnost adsorpce AOM vliv, neexistuje doposud žádná práce, která by se této problematice věnovala.

3.4.2 Mechanismy adsorpce AOM na aktivním uhlí

Adsorpce organických látek na aktivním uhlí je komplikovaný proces ovlivněný mnoha faktory, jejichž projev následně určuje adsorpční mechanismy a interakce uplatňující se mezi adsorbentem a sorbovanou látkou (Newcombe a Drikas, 1997; Bjelopavlic a kol., 1999; Moreno-Castilla, 2004; Hnaťuková a kol., 2011; Kopecká a kol., 2014). Bylo prokázáno, že dominantním mechanismem adsorpce AOM jsou elektrostatické (přitažlivé a odpudivé) a hydrofobní interakce a vodíkové vazby, přičemž se tyto jednotlivé typy interakcí projevují v silné závislosti na hodnotě pH a iontové síly (IS) roztoku (Newcombe a Drikas, 1997; Bjelopavlic a kol., 1999; Hnaťuková a kol., 2011; Kopecká a kol., 2014). Hodnota pH roztoku určuje stupeň

disociace funkčních skupin ve struktuře molekul adsorbátu a na povrchu AU a tím projev uvedených interakcí (Hnaťuková a kol., 2011; Kopecká a kol., 2014). Iontová síla roztoku pak projev těchto sil zesiluje či oslabuje (Newcombe a Drikas, 1997; Bjelopavlic a kol., 1999; Moreno-Castilla, 2004; Kopecká a kol., 2014). Studie Hnaťuková a kol. (2011) zabývající se adsorpcí COM peptidů *M. aeruginosa* < 10 kDa při pH 5 a pH 8,5 na dvou druzích komerčně dostupných druhů GAU zjistila, že vyšší účinnosti bylo dosaženo při pH 5 a důvodem bylo uplatnění přitažlivých elektrostatických sil mezi pozitivně nabitými funkčními skupinami COM peptidů a negativně nabitými skupinami na povrchu AU. Naopak při pH 8,5 byly již COM peptidy nabity převážně záporně a oba druhy GAU také nesly již velký záporný náboj, což způsobilo silné elektrostatické odpuzování a tím nízkou míru adsorpce. Navíc při pH 5 docházelo mezi účastníky adsorpce také k tvorbě vodíkových vazeb (Hnaťuková a kol., 2011). Elektrostatické interakce a vodíkové vazby byly označeny za dominantní při adsorpci COM peptidů < 10 kDa na GAU i v práci Kopecká a kol. (2014), kdy vlivem přitažlivých elektrostatických sil mezi opačně nabitými účastníky adsorpce a také vodíkových vazeb bylo dosaženo vyšší účinnosti opět při pH 5 v porovnání s pH 7 a 8. Při pH 5 se projevily silné přitažlivé elektrostatické síly mezi pozitivně nabitými skupinami $=NH_2^+$, α-NH_3^+, ε-NH_3^+ a negativně nabitými skupinami na povrchu AU, především $–COO^-$ a $–S^-$. S rostoucím pH se postupně zvětšoval negativní náboj COM peptidů i GAU vlivem disociace stále většího počtu skupin $–COO^-$ a $–S^-$, čímž se začaly projevovat odpudivé elektrostatické interakce. Zároveň se při adsorpci COM peptidů vzhledem k přítomnosti skupin –OH, které mají disociační konstantu až v poměrně vysokých hodnotách pH (pH > 9), uplatnily také vodíkové vazby (Kopecká a kol., 2014). Oba výše diskutované typy interakcí jsou považovány za dominantní i při adsorpci jiných nízkomolekulárních AOM, např. aminokyselin (Tentorio a Canova, 1989; Ikhsan a kol., 2004; O'Connor a kol., 2006; Vinu a kol., 2006; Gao a kol., 2008; Clark a kol., 2012; Greiner a kol., 2014) nebo nízkomolekulárních NOM a mikrocystinů (Campinas a Rosa, 2006). Vlivem přitažlivých elektrostatických sil došlo na různých druzích sorbentů např. k účinné adsorpci aminokyselin histidinu (Vinu a kol., 2006), lysinu (O'Connor a kol., 2006), argininu (Gao a kol., 2008) nebo fenylalaninu (Clark a kol., 2012). Naopak odpudivé elektrostatické interakce znemožnily např. adsorpci kyseliny asparagové a glutamové (Tentorio a Canova, 1989; Ikhsan a kol., 2004; Gao a kol., 2008; Greiner a kol., 2014). Kromě elektrostatických sil a vodíkových vazeb se při adsorpci organických látek mohou uplatňovat také hydrofobní interakce a π-π

interakce (Moreno-Castilla, 2004). V případě hydrofobních sil se jedná spíš o efekt, vlastnost celého systému, než o interakci mezi dvěma partnery v pravém slova smyslu. Pokud je molekula látky nebo některá její část hydrofobní povahy, snaží se omezit styk s molekulami vody vazbou na hydrofobní povrch AU (Moreno-Castilla, 2004). Otázka přispění hydrofobních interakcí k adsorpci na povrch AU však zůstává v současné době nedořešena. Existují totiž práce, které prokázaly hydrofilní charakter povrchu aktivního uhlí (Schrader, 1975; Ashraf a kol., 2013). Jako dominantní se hydrofobní interakce projevují při adsorpci malých molekul, např. aminokyselin s nepolárním řetězcem (Titus a kol., 2003; Clark a kol., 2012), a to především při takových experimentálních podmínkách, které neumožňují projev elektrostatických sil, např. při pH roztoku, kdy nedochází k disociaci karboxylových skupin (Clark a kol., 2012; Kodíček a Karpenko, 2013). Interakce prostřednictvím sdílení π-elektronů pak byly popsány např. při adsorpci antropogenních organických polutantů, pesticidů (Hnaťuková a kol., 2011). Podle Yoon a kol. (1999) má zásadní vliv na dominanci některého z výše uvedených typů interakcí chemismus povrchu adsorbentu. Obsahuje-li hydrofobní povrch adsorbentu malé množství silně či slabě kyselých funkčních skupin, je adsorpce řízena hydrofobními silami. Pokud je však na povrchu adsorbentu navázáno velké množství těchto skupin, jsou v případě přítomnosti slabě kyselých skupin hlavním mechanismem adsorpce vodíkové vazby a elektrostatické interakce ji řídí v případě přítomnosti silně kyselých funkčních skupin (Yoon a kol., 1999).

Projev přitažlivých nebo odpudivých elektrostatických interakcí může být posílen nebo zeslaben přidáním elektrolytu do roztoku, tedy zvýšením iontové síly (IS) roztoku (Newcombe a Drikas, 1997; Bjelopavlic a kol., 1999; Moreno-Castilla, 2004; Newcombe, 2006; Kopecká a kol., 2014). V případě, že mezi účastníky adsorpce převládají odpudivé elektrostatické interakce, může dojít vlivem přídavku elektrolytu k jejich odstínění a tím ke zvýšení účinnosti adsorpce. Pokud jsou však adsorbent a adsorbát nabity opačně a působí mezi nimi elektrostatické přitažlivé interakce, přídavek soli (elektrolytu) tyto síly oslabí a účinnost adsorpce poklesne (Newcombe a Drikas, 1997; Bjelopavlic a kol., 1999). Vliv nárůstu iontové síly roztoku (z 0 M NaCl na 0,3 M NaCl) na adsorpci COM peptidů na dvou druzích GAU byl posuzován například ve studii Kopecká a kol. (2014). Studie potvrdila vliv iontové síly na účinnost adsorpce, a to v závislosti na druhu použitého GAU (tedy pravděpodobně na pH_{NBN} GAU). V případě GAU Picabiol 12x40 vedla zvýšení iontové síly k nárůstu účinnosti adsorpce při všech sledovaných hodnotách pH (pH 5, 7, 8), a to v důsledku odstínění

elektrostatických odpudivých sil mezi záporně nabitý skupinami v systému. Při adsorpci na GAU Filtrasorb TL 830 došlo k nárůstu účinnosti adsorpce vlivem oslabení elektrostatických repulzí pouze při pH 5 a 8. Při pH 7 přídavek elektrolytu oslabil přitažlivé elektrostatické interakce a účinnost adsorpce se snížila. Pozitivní účinek na účinnost adsorpce po přidání elektrolytu do systému byl pozorován i při posuzování adsorpce NOM huminového charakteru (Bjelopavlic a kol., 1999). Další studie Newcombe a Drikas (1997) zkoumala adsorpci NOM (500–3000 Da) na dva druhy AU při vysoké a nízké iontové síle roztoku v rozmezí hodnot pH 3-9. Bylo zjištěno, že při vysokém adsorbovaném množství NOM způsobilo zvýšení IS nárůst účinnosti adsorpce při všech hodnotách pH. Tento nárůst účinnosti byl přitom výraznější při vyšším pH, kdy odpudivé interakce působily intenzivněji. Některé studie rovněž potvrdily, že vyšší IS vede k vyšší účinnosti absorpce dané látky v důsledku změn jejích chemických a strukturálních vlastností. Zejména ve vyšších adsorbovaných množstvích, když jsou molekuly látky v těsné blízkosti, může být intramolekulární odpuzování mezi funkčními skupinami sníženo přidáním elektrolytu a následným smrštěním molekuly a usnadněním adsorpce (Newcombe a Drikas, 1997; Campinas a Rosa, 2006). Negativně se naopak zvýšení iontové síly projevilo při adsorpci kyseliny třís lové (tannin, použita jako modelová látka NOM) na PAU. Nárůst IS z 2,5 mM KCl na 10 mM KCI způsobil pokles míry adsorpce vlivem oslabení přitažlivých elektrostatických sil. Ke snížení míry adsorpce vlivem zvýšení IS může dojít také v případě, že adsorpce probíhá v podmínkách, především při hodnotě pH blízké izoelektrickému bodu sorbované látky. Tehdy se u adsorbátu předpokládá vyrovnané množství pozitivního a negativního náboje, což způsobí, že molekuly jsou vlivem silných intermolekulárních sil v kompaktní formě a lépe prostupují do vnitřní struktury AU. Přídavkem elektrolytu ale dojde ke změnám v poměru nábojů a tím k oslabení těchto sil a poklesu účinnosti adsorpce. Uvedený jev se pravděpodobně projevil i v případě poklesu adsorpce COM peptidů na Filtrasorb TL 830 při pH 7 ve studii Kopecká a kol. (2014), kdy experimentální podmínky, tedy hodnota roztoku, téměř odpovídaly izoelektrickému bodu COM peptidů (pI = 7,1) (Kopecká a kol., 2014). Nejvyšší účinnost adsorpce při pH blízkém izoelektrickému bodu (experimentální pH 5,6; pI_{Phe} = 5,48) byla zjištěna i při posuzování adsorpce aminokyseliny fenylalanin (*Phe*) ve studiích Goscianska a kol. (2013 a 2014), kde autoři toto vysvětlují právě kompaktností molekul fenylalaninu při daných podmínkách. S ohledem na molekulovou hmotnost a strukturu molekuly této aminokyseliny je však takové vysvětlení spíše méně pravděpodobné.

V oblasti p*I* sice reálně ke smrštění molekuly docházet může, avšak u takto malé molekuly jako je *Phe* bude mít pravděpodobně zanedbatelný vliv.

4 MIKROPOLUTANTY

Spolu s organickými látkami produkovanými fytoplanktonem představují výzvu pro současný výzkum v oblasti úpravy vody také antropogenní mikropolutanty (Luo a kol., 2014; Barbosa a kol., 2016; Kim a Zoh, 2016; Yang a kol., 2017). Jedná se především o pesticidy, persistentní organické látky, zbytky hormonů a léčiv, produkty osobní péče a v poslední době se do popředí dostává problematika perfluorovaných organických látek a mikroplastů (Heberer, 2002; Luo a kol., 2014; Rahman a kol., 2014; Eerkes-Medrano a kol., 2015; Koelmans a kol., 2015; Yang a kol., 2017; Di a Wang, 2018; Grandjean, 2018). V rámci disertační práce byla pozornost věnována problematice mikroplastů a jejich výskytu ve zdrojích vody a vodě pitné.

4.1 MIKROPLASTY

Stále narůstající výroba a následná spotřeba plastů dnes významně motivuje výzkum zaměřovat se na přítomnost a akumulaci těchto materiálů v různých složkách životního prostředí. Pozornost je přitom častěji, než pouhým okem viditelným plastovým fragmentům, věnována mnohem menším částicím v mikrometrových řádech, tzv. mikroplastům. Pojmem mikroplasty (MPs) jsou definovány plastové částice menší než 5 mm (Andrary, 2011; Eerkes-Medrano a kol., 2015; Koelmans a kol., 2015), přičemž dolní velikostní hranice nebyla jednotně stanovena a většinou se ve studiích odvíjí od použité metody odběru vzorků (Eerkes-Medrano a kol., 2015; Mason a kol., 2016; Su a kol., 2016; Di a Wang, 2018). Velmi často se hlavně při odběru vzorků v mořích a jezerech používají sítě o velikosti ok 333 μm. Mnoho autorů však uvádí, že podíl částic menších než 333 μm může být značný (Andrary, 2011; Eerkes-Medrano a kol., 2015; Su a kol., 2016; Anderson a kol., 2017). Do životního prostředí se mikroplasty dostávají přímou cestou jako součást spotřebních výrobků (např. v kosmetice a čisticích prostředcích) nebo sekundárně rozpadem či rozkladem větších předmětů. V případě vodních ekosystémů to jsou zejména rozklad plastového odpadu a odpadní vody vypouštěné z čistíren odpadních vod, kde je významným zdrojem mikroplastů především uvolňování syntetických vláken během praní prádla (Browne

a kol., 2011). Konvenční čistírny odpadních vod jsou přitom schopné odstranit pouze určitý podíl mikroplastů a značné množství (stovky až tisíce částic na 1 m^3 odpadní vody), zejména nižších velikostních frakcí, tak čistírenská technologie nepostihne (Mason a kol., 2016; Mintenig a kol., 2017). Přestože ekologický dopad mikroplastů zatím není uspokojivě objasněn, jsou mikroplasty považovány za významné polutanty s možným vlivem na lidské zdraví. Mají velký potenciál vázat na sebe škodlivé perzistentní chemické látky a vzhledem ke své velikosti být pohlcovány biotou, čímž může docházet i k jejich přenosu mezi trofickými úrovněmi a následné bioakumulaci (Andrary, 2011; Eerkes-Medrano a kol., 2015).

V rámci vodního prostředí se doposud většina studií věnovala detekci a kvantifikaci plastových částic v oceánech, mořích a sedimentech (Cole a kol., 2011; Auta a kol., 2017). Méně prací se pak zabývalo výskytem mikroplastů ve sladkovodních útvarech, jako jsou přehradní nádrže, jezera či řeky (Dris a kol., 2015; Su a kol., 2016; Anderson a kol., 2017; Leslie a kol., 2017; Di a Wang, 2018). Metody zjišťování jejich přítomnosti i způsoby odběrů vzorků se však mezi jednotlivými studiemi značně liší a konkrétní výsledky jsou jen obtížně porovnatelné. Obecně lze říci, že byly v povrchových vodách nalezeny a identifikovány mikroplastové částice různých velikostí, tvarů (vlákna, film, pěna, fragmenty, pelety, kuličky) a původem z různých druhů materiálů (např. akryl, polyamid, polyester, polyethylen, polypropylen, polystyren atd.) (Eerkes-Medrano a kol., 2015; Mason a kol., 2016; Su a kol., 2016; Anderson a kol., 2017; Leslie a kol., 2017; Di a Wang, 2018). Studiemi, ve kterých byla použita metoda odběru vzorků sítěmi z vodní hladiny a vrstvy těsně pod hladinou (většinou do hloubky 1 m), se počet mikroplastů pohyboval v rozmezí $1 \cdot 10^3$-$68 \cdot 10^5$ částic na km^2 (Free a kol., 2014; Su a kol., 2016; Anderson a kol., 2017). Více studií pak zjišťovalo počet mikroplastů v odebraném a analyzovaném objemu vzorku vody a výsledek vyjadřuje jako počet částic na litr (Su a kol., 2016; Leslie a kol.., 2017; Di a Wang, 2018). Například ve vodní nádrži Tři soutěsky v Číně se počet mikroplastů ve velikostním rozsahu 48 μm – 5 mm pohyboval v rozmezí 1,6 až 12,6 částic na litr v závislosti na odběrovém místě. Nejvíce jich přitom bylo menších než 0,5 mm, a to 31,2-74,4 % z celkového počtu, opět v závislosti na místě odběru (Di a Wang, 2018). V jezeře Taihu (Čína) pak činil počet mikroplastů > 5 μm 3,4-25,8 částic na litr (v závislosti na odběrovém místě). Nejvíce početnou byla přitom velikostní kategorie 100-1000 μm (Su a kol., 2016). Ve studii Leslie a kol. (2017), kde zjišťovali počet mikroplastů v amsterdamských kanálech, zjistili ve velikostním rozmezí přibližně

10 μm – 5 mm přítomnost 48 až 187 částic na litr. Studie, které by se zabývaly zjišťováním přítomnosti mikroplastů ve zdrojích surové vody pro výrobu vody pitné nebo v pitné vodě samotné však doposud chybí. Dvě práce se pak věnují obsahu mikroplastových částic ve vodě balené (Oßmann a kol., 2018; Schymanski a kol., 2018). Ve studii Schymanski a kol. (2018) nalezli ve vodě balené v různých druzích obalových materiálů až 118 ± 88 mikroplastových částic na litr > 5 μm. Oßmann a kol. (2018) pak naměřili počet mikroplastů od velikosti 1 μm až 6292 ± 10 521 částic na litr.

5 MOTIVACE A CÍLE PRÁCE

Zvyšující se míra eutrofizace, probíhající klimatická změna a narůstající chemizace životního prostředí představují v současné době velké zatížení pro kvalitu povrchových zdrojů vody a tím pro úpravu vody na vodu pitnou (Henderson a kol., 2008a; Zhang a kol., 2010; Pivokonský a kol., 2016). Kvalita surové (povrchové) vody, tedy složení látek v ní obsažených, se významně mění. V rámci přírodních organických látek (NOM) výrazně narůstá podíl látek produkovaných fytoplanktonem (AOM) a na významu nabývají i antropogenní polutanty, především pak jejich variabilita (Kim a Zoh, 2016; Yang a kol., 2017; Grandjean, 2018; Pivokonský a kol., 2019). Technologie založená na koagulaci/flokulaci a následné jedno nebo dvoustupňové separaci, na které je založený běžný proces úpravy vody, již pro některé druhy látek přírodního i antropogenního původu není dostatečně účinná (Szajdzinska-Pietek a Gebicki, 2000; Hölzer a kol., 2009; Shivakoti a kol., 2010; Deblonde a kol., 2011; Takagi a kol., 2011; Eschauzier a kol., 2012; Xiao a kol., 2013; Luo a kol., 2014; Rahman a kol., 2014; Kim a Zoh, 2016; Pivokonský a kol., 2016). Tato technologie je vhodná především pro látky vysokomolekulární, např. pro proteiny a polysacharidy produkované fytoplanktonem nebo pro huminové látky a hlinitokřemičitany (Pivokonský a kol., 2006, 2009a,b, 2012, 2015, 2016; Šafaříková a kol., 2013; Barešová a kol., 2017). Látky s malou molekulovou hmotností, mezi které se řadí sinicemi a řasami produkované peptidy, aminokyseliny, sacharidy a mikropolutanty, jako jsou pesticidy či mikroplasty, jsou koagulací/flokulací odstranitelné jen velmi obtížně či téměř vůbec (Pivokonský a kol., 2012, 2016). Z tohoto důvodu je nutný výzkum a vývoj dalších metod, které by současnou technologii úpravy vody doplnily a umožnily odstranění i uvedených problematických látek. Jen v takovém případě bude možné držet kvalitu upravené vody na požadované vysoké úrovni a eliminovat rizika spojená např. s tvorbou vedlejších produktů desinfekce vody při hygienickém zabezpečování upravené vody činidly na bázi chlóru či ozónu, jejichž prekursory jsou právě zbytkové organické látky. Nezbytnou součástí takového výzkumu pak musí být i charakterizace takových látek, tedy detailní popis jejich vlastností a zejména těch zásadních ve vztahu k metodám jejich odstraňování. Jedině tak je možné vyvinout nové účinné technologie, které budou schopné problematické látky eliminovat.

Doposud se výzkum v oblasti úpravy vody v rámci AOM zabýval odstraňováním především buněk sinic a řas, a to zejména koagulací/flokulací a také zvýšením její

účinnosti v kombinaci s oxidačními metodami (ozonizace, oxidace pomocí $KMnO_4$, ClO_2, Cl_2). Bylo zjištěno, že koagulace/flokulace je pro odstraňování buněk vhodná a její účinnost lze za určitých podmínek zvýšit použitím oxidačních metod (Henderson a kol., 2008b, 2010; Ghernaout a kol., 2010; Edzwald a Haarhoff, 2011). Méně často byl však výzkum zaměřen na odstraňování produktů fytoplanktonu – AOM (EOM/COM). V rámci koagulace/flokulace byla za optimalizovaných podmínek prokázána vysoká účinnost odstranění vysokomolekulárních AOM proteinového původu, přičemž posouzení účinnosti koagulace/flokulace AOM neproteinového charakteru či zhodnocení vlivu užití oxidačních metod bylo doposud opomíjeno (Pivokonský a kol., 2006, 2009a,b, 2012, 2015, 2016; Šafaříková a kol., 2013; Barešová a kol., 2017; Načaradská a kol., 2017). Z hlediska optimalizace koagulace/flokulace pak téměř chybí výzkum v oblasti vlivu AOM na strukturu agregátů. Poměrně malá pozornost pak byla věnována i eliminaci nízkomolekulárních látek, u kterých byla prokázána téměř nulová účinnost odstranění konvenční koagulací/flokulací (Pivokonský a kol., 2012, 2016). V rámci mikropolutantů je pak v současné době hojně diskutováno téma mikroplastů, jejichž přítomnost se doposud podařilo prokázat v povrchových vodách, zdrojích pitné vody i ve vodách balených (Anderson a kol., 2017; Cole a kol., 2011; Koelmans a kol., 2015; Mason a kol., 2016; Mintenig a kol., 2017; Oβmann a kol., 2018; Schymanski a kol., 2018; Di a Wang, 2018). Výskyt mikroplastů ve vodě pitné však doposud zjišťován nebyl.

Cílem předkládané disertační práce je charakterizace obtížně odstranitelných látek při úpravě vody a posouzení různých metod pro jejich odstranění. Konkrétní cíle jsou:

- zhodnotit účinnost koagulace neproteinové složky AOM za optimalizovaných podmínek a popsat probíhající interakce a mechanismy (Publikace 1),
- posoudit možnost využití předoxidace prostřednictvím ozónu pro zvýšení účinnosti odstranění AOM (Publikace 2),
- popsat vliv AOM na strukturu agregátů tvořených při koagulaci/flokulaci hydrolyzujícími hlinitými a železitými koagulačními činidly v přítomnosti znečišťujících příměsí – hlinitokřemičitanů reprezentovaných kaolinem (Publikace 3),

- zhodnotit účinnost eliminace AOM adsorpcí na aktivním uhlí, popsat probíhající interakce a mechanismy a objasnit vliv faktorů (hodnota pH, iontová síla a teplota roztoku) adsorpci ovlivňujících (Publikace 4, 5, 6 a 7),
- potvrdit/vyvrátit přítomnost mikroplastů v surové a upravené vodě a shrnout dosavadní poznatky o výskytu tohoto druhu polutantu v povrchových a balených vodách a ve vodě pitné (Publikace 8 a 9).

Dosažené výsledky jsou uvedeny v následujících devíti publikacích, které tvoří stěžejní část předkládané disertační práce.

PUBLIKACE 1

Investigation of non-proteinaceous algal organic matter: Optimizing coagulation performance and identification of removal mechanisms

Jana Načeradská, Kateřina Novotná, **Lenka Čermáková**, Tomáš Cajthaml a Martin Pivokonský

Journal of Environmental Sciences 79 (2019) 25-34
DOI 10.1016/j.jes.2018.09.024

Available online at www.sciencedirect.com

ScienceDirect

www.elsevier.com/locate/jes

JES JOURNAL OF ENVIRONMENTAL SCIENCES

www.jesc.ac.cn

Investigating the coagulation of non-proteinaceous algal organic matter: Optimizing coagulation performance and identification of removal mechanisms

Jana Naceradska[1], *Katerina Novotna*[1], *Lenka Cermakova*[1], *Tomas Cajthaml*[2], *Martin Pivokonsky*[1,*]

1. *Institute of Hydrodynamics of the Czech Academy of Sciences, Pod Patankou 5, 166 12 Prague 6, Czech Republic*
2. *Institute of Microbiology of the Czech Academy of Sciences, Videnska 1083, 142 20 Prague 4, Czech Republic*

ARTICLE INFO

Article history:
Received 15 August 2018
Revised 25 September 2018
Accepted 25 September 2018
Available online 5 October 2018

Keywords:
Algal organic matter
Chlorella vulgaris
Coagulation
Flocculation
Non-proteinaceous matter
Water treatment

ABSTRACT

The removal of algal organic matter (AOM) is a growing concern for the water treatment industry worldwide. The current study investigates coagulation of non-proteinaceous AOM (AOM after protein separation), which has been minimally explored compared with proteinaceous fractions. Jar tests with either aluminum sulphate (alum) or polyaluminium chloride (PACl) were performed at doses of 0.2–3.0 mg Al per 1 mg of dissolved organic carbon in the pH range 3.0–10.5. Additionally, non-proteinaceous matter was characterized in terms of charge, molecular weight and carbohydrate content to assess the treatability of its different fractions. Results showed that only up to 25% of non-proteinaceous AOM can be removed by coagulation under optimized conditions. The optimal coagulation pH (6.6–8.0 for alum and 7.5–9.0 for PACl) and low surface charge of the removed fraction indicated that the prevailing coagulation mechanism was adsorption of non-proteinaceous matter onto aluminum hydroxide precipitates. The lowest residual Al concentrations were achieved in very narrow pH ranges, especially in the case of PACl. High-molecular weight saccharide-like organics were amenable to coagulation compared to low-molecular weight (<3 kDa) substances. Their high content in non-proteinaceous matter (about 67%) was the reason for its low removal. Comparison with our previous studies implies that proteinaceous and non-proteinaceous matter is coagulated under different conditions due to the employment of diverse coagulation mechanisms. The study suggests that further research should focus on the removal of low-molecular weight AOM, reluctant to coagulate, with other treatment processes to minimize its detrimental effect on water safety.

* *Corresponding author.*
E-mail: pivo@ih.cas.cz (Martin Pivokonsky).

https://doi.org/10.1016/j.jes.2018.09.024
1001-0742/

Introduction

The presence of seasonal algal blooms in drinking water sources creates serious challenges in drinking water production. Water quality can be severely impacted by the release of algal organic matter (AOM), which reacts with disinfectants to form potentially harmful disinfection by-products (DBPs, Goslan et al., 2017). AOM is released during the growth of algae due to metabolic processes as extracellular organic matter (EOM) or during cell lysis as cellular organic matter (COM) and comprises a wide range of compounds, with polysaccharides, proteins, lipids, and small molecules being the main components (Henderson et al., 2008; Pivokonsky et at., 2014; Villacorte et al., 2015).

Coagulation/flocculation is one of the most widely applied techniques of AOM treatment in drinking water production. The complexity of AOM composition complicates the understanding of coagulation pathways and consequently, AOM removal. Therefore, efforts have been made to divide AOM according to its properties and coagulate the separate fractions (Liu et al., 2018; Pivokonsky et al., 2012, 2015). In recent years, attention has been paid to the coagulation of the proteinaceous fraction of the COM of cyanobacterium *Microcystis aeruginosa* (Pivokonsky et al., 2009, 2015). These studies ascertained that peptides/proteins of *M. aeruginosa* were removed by coagulation at acidic pH values with efficiencies of 60%–85% by both ferric and aluminum coagulants. They also demonstrated that peptides/proteins may inhibit coagulation by the formation of complexes with coagulant metals, but this can be avoided by consistent optimization of the coagulation pH value (Pivokonsky et al., 2009, 2015). By contrast, little work has been done on the coagulation of non-proteinaceous AOM. Pivokonsky et al. (2009), who coagulated the COM of *M. aeruginosa* by either ferric or aluminum sulphate, demonstrated higher removal efficiencies for proteinaceous (74% and 50%, respectively) than non-proteinaceous compounds (12% and 22%, respectively). Higher removal efficiencies for proteins (75% and 69%, respectively) than saccharides (30% and 40%, respectively) were also achieved by Cui et al. (2016), who coagulated effluent organic matter from a wastewater treatment plant by either aluminum chloride ($AlCl_3$) or polyaluminium chloride (PACl). Aluminum chloride was, therefore, better for protein removal, while PACl was more effective in polysaccharide removal. Slightly higher COM removal for PACl than $AlCl_3$ was observed by Liu et al. (2018), who investigated the coagulation of COM produced by *M. aeruginosa* together with kaolin particles. Since these studies indicated that non-proteinaceous COM is generally disinclined to coagulate, attention should be paid to the limits of coagulation of non-proteinaceous COM and also the character of compounds not removed by coagulation. The properties of residual compounds will impact the setup of subsequent treatment technologies.

On the basis of these considerations, this study aims to systematically investigate the coagulation of non-proteinaceousCOM of green alga *Chlorella vulgaris*. The study focuses on COM, as these compounds present most of organic matter during the algal bloom decay and are known to disturb coagulation (Pivokonsky et al., 2016). The study quantifies the removal of non-proteinaceous COM after the consistent optimization of coagulation conditions and identifies the coagulation pathways. Special attention is paid to the influence of the pH value on coagulation because it governs the form of coagulants as well as the surface charge of coagulated impurities and thus coagulation mechanisms. In order to better understand the coagulation pathways and properties of residual organics after coagulation, characterization of non-proteinaceous COM before and after coagulation was performed. Two types of coagulants, traditional aluminum sulphate (alum) and polymeric coagulant polyaluminium chloride (PACl), were compared in this study as they have demonstrated diverse Al species distribution, coagulation mechanisms and efficiency. Finally, the coagulation of proteinaceous COM (investigated in our previous studies) and non-proteinaceous COM was compared in terms of efficiency, coagulation mechanisms and the character of residual organics. The outcomes may be of practical value in enhancing the removal of AOM and controlling its adverse effects on water quality.

1. Materials and methods

1.1. Cultivation of Chlorella vulgaris

Chlorella vulgaris was chosen for this study since it is a cosmopolitan bloom-forming alga, the COM of which contains large portion of non-proteinaceous compounds (Henderson et al., 2008; Safi et al., 2014). An inoculum of *Chlorella vulgaris* (strain CCALA 256) was obtained from Centre Algatech of the Institute of Microbiology, CAS, Czech Republic. The culture was grown in a photobioreactor in glass tubes situated in a water bath (30 °C) under continuous illumination with incident light intensity 100 μE m^{-2} sec^{1} (PAR sensor QSL-2101, Biospherical instruments Inc., USA) and feeding of air enriched with 2% CO_2 (V/V) at 15 L/hr per tube. Each tube contained 300 mL of mineral medium, having the initial composition (mg/L): 1100 $(NH_2)_2CO$, 238 KH_2PO_4, 204 $MgSO_4$ 7 H_2O, 40 $C_{10}H_{12}O_8N_2NaFe$, 88 $CaCl_2$, 0.832 H_3BO_3, 0.946 $CuSO_4$ 5 H_2O, 3.294 $MnCl_2$ 4 H_2O, 0.172 $(NH_4)_6Mo_7O_{24}$ 4 H_2O, 2.678 $ZnSO_4$ 7 H_2O, 0.616 $CoSO_4$ 7 H_2O, and 0.0014 $(NH_4)VO_3$. The pH value was adjusted to 6.5–7.0 using 1 mol/L KOH before inoculation from an agar plate (Bránykiková et al., 2011).

1.2. Cell harvesting and COM extraction

Cells of *C. vulgaris* were harvested at the late stationary growth phase (20th day of cultivation) in order to acquire COM, the composition of which is similar to that of decline phase, which is most problematic from the perspective of coagulation performance. Moreover, carbohydrate production is favored at the stationary phase, while protein production prevails at the exponential phase (Lv et al., 2010). The cells were separated from the culture media by centrifugation (4000 r/min, 20 min) and then re-suspended in ultra-pure

water. Dissolved COM was extracted using ultrasonication in an ice bath using an ultrasonic homogenizer (UP400S, Hielscher Ultrasonics, Germany) at 60% amplitude of ultrasonication (240 W) in pulse mode for 5 min, followed by filtration through a 0.45 μm membrane filter. Filtrates were stored at −60 °C. The acquired COM sample was considered a fraction comprising intracellular (IOM), surface-retained organic matter (SOM), and possibly also organics loosely bound to the cell surface, i.e. EOM.

1.3. Isolation of non-proteinaceous COM

In our previous studies (Pivokonsky et al., 2012, 2015), which investigated the coagulation of proteinaceous COM, we used a salting out method adapted from Dawson et al. (1986) to separate proteinaceous matter (PM) from non-proteinaceous matter (NM). This method is, however, not suitable for acquiring NM for coagulation tests as NM is burdened with very high concentrations of $(NH_4)_2SO_4$. Approximately 17 g of $(NH_4)_2SO_4$ per 1 g of dissolved organic carbon (DOC) were present in the residual non-proteinaceous fraction after the protein precipitation. We found that, for the amounts of organic matter needed for coagulation tests, $(NH_4)_2SO_4$ is difficult to remove without a concurrent loss of NM (e.g., due to the sorption of organic compounds on dialysis membranes utilized for desalting). Therefore, PM was separated from NM by the thermal precipitation of proteins. This procedure assumes that most proteins denature predominantly at 40–80 °C and that denaturation is usually accompanied by aggregation and/or gelation (Bischof and He, 2005), while saccharide-like substances are generally stable at higher temperatures (Bothara and Singh, 2012). COM samples were, therefore, heated in a water bath (80 °C) for 30 min, and the precipitated proteins were then removed by filtration through a 0.45 μm membrane filter. PM and NM portions were expressed as DOC. NM was stored at −60 °C. The yields of PM and NM by thermal precipitation and salting out were compared. The protein content in NM after thermal precipitation was also controlled by additional salting out, which yielded no proteins, and by HPSEC (1260 Infinity, Agilent Technologies, USA) using the Agilent Bio SEC-5100 Å and 300 Å columns connected in series and coupled with a diode array detector (DAD) operating at 280 nm (Pivokonsky et al., 2015), which is used for peptide/protein detection.

1.4. Characterization of non-proteinaceous COM

NM obtained after thermal precipitation of proteins from the COM of *Chlorella vulgaris* was characterized in terms of N/C (nitrogen/carbon) ratio, charge, molecular weight distribution, total carbohydrates, proteins and lipids (as fatty acids). To describe the composition of NM utilized in this study and link it to the composition of the original algal material, the total carbohydrate, protein and fatty acid content was also determined in the total COM biomass (disrupted cells of *C. vulgaris*) and dissolved COM biomass (extracted from cells as described in Section 1.2.). DOC and total nitrogen (TN) concentrations were determined by a TOC/TN analyzer (Torch TN, TELEDYNE TEKMAR, USA). Determination of the amount of ionisable functional groups in whole NM and in its fractions with MW < 50 kDa and >50 kDa was undertaken by potentiometric titrations performed under the nitrogen atmosphere using an Orion 960 Autotitrator (Thermo Scientific, USA). Before the experiments, the system was standardized with dilute NaOH solutions to pH 10.5. The ionic strength (I = 0.05 mol/L) was controlled with NaCl. The aliquots (500 mL) of non-proteinaceous COM containing 250 mg DOC/L were titrated to pH 2.5 using 0.05 mol/L HCl at a constant temperature of 25.0 ± 0.2 °C. A blank titration was performed under the same conditions. The resultant titration curve (transformed for 1 g DOC/L) was determined as the difference between titration of non-proteinaceous COM and the blank titration (Newcombe 1994). Dissociation constants and equivalence points were determined as described by Safarikova et al. (2013). Molecular weight (MW) fractionation was performed using the Amicon Ultra-15 centrifugal filters of nominal MW cut-offs of 100, 50, 30, 10, and 3 kDa (Millipore, USA) as described by Pivokonsky et al. (2014). The MW distribution was expressed as a proportional part of DOC. To determine the total carbohydrates, the MBTH (3-methyl-2-benzothiazolinone hydrazone) method was employed. In brief, 25 mg of freeze-dried algal biomass was subjected to a two-step sulfuric acid hydrolysis to convert the polymeric forms of carbohydrates into monomeric subunits. The saccharide content was then determined spectrophotometrically at 620 nm after reaction with MBTH that yields a blue-green colored solution due to complexing with the aldehyde group of carbohydrates. Glucose was used as a calibration standard, while the calibration range was 0.01–0.05 mg/mL (Wychen and Laurens, 2015). To determine protein content, sequential extraction in trichloroacetic acid and NaOH from freeze-dried samples followed by a modified Lowry method was employed (Slocombe et al., 2013). The determination of total fatty acids from the samples was performed according to the methodology previously described by Řezanka et al. (2013). Briefly, samples were extracted using a mixture of chloroform, methanol and phosphate buffer (1:2:0.8; V/V/V). Fatty acid methyl esters (FAMEs) were prepared after saponification and further esterification using BF_3/MeOH. The products were dissolved in hexane and analyzed by gas chromatography–mass spectrometry (GC–MS; 450-GC, 240-MS ion trap detector, Varian, Walnut Creek, CA) according to Šnajdr et al. (2008). The individual fatty acids were identified and quantified using the respective chemical standards obtained from Sigma-Aldrich (Czech Republic) and Matreya, LLC (PA, USA). All the analyses were performed in triplicates.

1.5. Coagulation tests

Traditional jar tests were applied to study the coagulation of the non-proteinaceous COM of *C. vulgaris*. Model water was ultra-pure water with alkalinity adjusted to 1 mmol/L (utilizing 0.1 mol/L $NaHCO_3$), pH 8.0 and initial DOC concentration of 5 mg/L. Two coagulants were compared: aluminum sulphate ($Al_2(SO_4)_3{\cdot}18H_2O$; Sigma Aldrich, USA), the most common conventional coagulant, and polymeric coagulant polyaluminium chloride (PACl; Kemwater ProChemie, Czech Republic; basicity 43% ± 5%, Al content 9.0% ± 0.3%), which is utilized for its high efficiency in terms of charge neutralization and a wide range of coagulation pH values owing to the

high stability of Al_{13} polymers (Wu et al., 2007). Stock solutions of 1% coagulants were utilized in the tests. The doses of coagulants and pH values were optimized by testing with coagulant doses ranging from 1 to 15 mg/L Al (0.037–0.556 mmol/L Al; 0.2–3.0 mg Al/mg DOC) in the pH range 3.0–10.5. The target pH values were reached by adding predetermined amounts of 0.1 mol/L $NaHCO_3$, 0.1 mol/L NaOH or 0.1 mol/L HCl before supplementation with the coagulant. The experiments were performed using a variable speed eight position paddle stirrer (LMK 8–03, IH CAS, Czech Republic) and 2 L jars. The experimental procedure included 1 min of rapid mixing (shear rate of 200 sec^{-1}) after coagulant dosing, followed by 30 min of slow mixing (shear rate of 50 sec^{-1}) and 60 min of settling. The supernatants were analyzed for pH value, alkalinity, DOC, referring to the concentration of residual NM, and residual Al by ICP-OES (5110 Series, Agilent Technologies, USA). Each sample was analyzed in triplicate. MW fractionation and the determination of total carbohydrates in residual organics were also performed in triplicates in the samples treated under optimal coagulation conditions. Before these analyses, the samples were concentrated in a rotary evaporator (Laborota 4000 HB/G1, Germany).

2. Results and discussion

2.1. Character of non-proteinaceous COM

Non-proteinaceousCOM was isolated in two steps from the cells of *Chlorella vulgaris*, i.e., isolation of water-soluble COM from the cells and isolation of the non-proteinaceous fraction from water-soluble COM. To provide insight into the composition of original and isolated fractions, the carbohydrate, protein and lipid content in the total COM (cells including both water-soluble and insoluble components), water-soluble COM (extracted from cells) and NM (extracted from water-soluble COM) was quantified as detailed in Table 1. It can be seen that the portion of proteins and especially lipids differed in the total and dissolved COM biomass of *C. vulgaris*. This is given by the fact that some proteins and most lipids are insoluble in water. According to the literature, protein content in *C. vulgaris* dry biomass varies with growth conditions 4%–40% (Becker, 1994; Laurens et al., 2014; Safi et al., 2014; Yeh and Chang 2012). Some of the protein is bound to cell walls (about 20%) and the membranes of organelles, and some is soluble in cytoplasm (Becker, 1994; Safi et al., 2014). Herein, the portion of proteins in water-soluble COM of *C. vulgaris* determined by the modified Lowry method was about 10% of dry weight (DW), which conforms with the yield of the thermal precipitation method separating about 9% of DOC. The same amount of proteinaceous DOC (9%) was acquired with the salting out method. HPSEC-DAD at 280 nm analyses showed that some organics of apparent MW 800–6000 Da remained in the COM after thermal precipitation (data not shown), indicating the presence of low-MW peptides. The presence of nitrogenous compounds, which may contain amino acids, peptides, nucleotides and nucleic acids, was confirmed also by measuring TN. The N/C ratio was about 0.1.

Table 1 – Carbohydrate, protein and lipid content in total cellular organic matter (COM), water-soluble COM and non-proteinaceous COM of *Chlorella vulgaris* expressed as dry weight portions.

Fraction	Total COM	Water-soluble COM	Non-proteinaceous COM
Carbohydrate	21%	18%	20%
Protein	23%	10%	0%
Lipid	26%	0.04%	0.05%

In general, *C. vulgaris* can reach 5%–50% lipids per biomass DW depending on cultivation conditions (Becker, 1994; Yeh and Chang, 2012). During the separation of water-soluble COM, lipids apparently stayed in the solid parts of cells and were removed by filtration, as they are relatively insoluble in water. The analyses of fatty acids showed that they formed about 26% of the total COM biomass, while both water-soluble and non-proteinaceous COM contained negligible concentrations of lipids and fatty acids, composed mainly of palmitic and stearic acid. Similarly, Yeh and Chang (2012) identified palmitic (C16:0), stearic (C18:0) and oleic (C18:1) acids as major components of lipids produced by the *C. vulgaris* ESP-31 strain.

Carbohydrates formed 21%, 18% and 20% of the total COM, water-soluble COM and non-proteinaceous COM DW, respectively. In the literature, the carbohydrate content again varies with growth conditions and methods used and ranges 12%–60% of biomass DW (Laurens et al., 2014; Templeton et al., 2012; Yeh and Chang, 2012). Sui et al. (2012) extracted water-soluble polysaccharides of *C. vulgaris* forming about 13%–19% of biomass DW.

It should be noted that besides proteins, lipids and carbohydrates, algal biomass includes other substances, which forms majority in the case of water-soluble COM and NM. These substances are of low MW as indicated by MW fractionation (see Fig. 1) and comprise aldehydes,

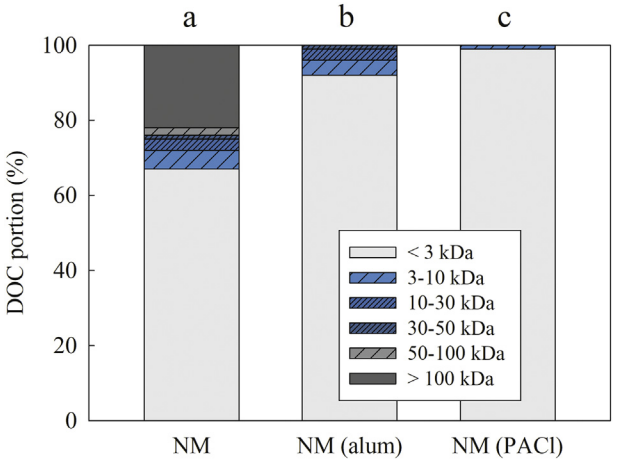

Fig. 1 – Molecular weight fractionation of non-proteinaceous COM (NM) of *Chlorella vulgaris* before coagulation (a) and after coagulation by aluminum sulphate–(alum) (Al dose 10 mg/L; pH 7.3) (b) and polyaluminium chloride (PACl) (Al dose 10 mg/L; pH 7.7) (c) expressed as DOC portions.

Table 2 – Comparison of molecular weight (MW) fractions of non-proteinaceous and proteinaceous COM of different algal species.

	Chlorella vulgaris	*Chlamydomonas geitleri*	*Fragilaria crotonensis*	*Merismopedia tenuissima*	*Microcystis aeruginosa*
Non-proteinaceous					
MW < 3 kDa	67%	66%[a]	63%[a]	41%[b]	48%[a]
MW > 100 kDa	22%	22%[a]	22%[a]	10%[b]	35%[a]
Proteinaceous					
MW < 3 kDa	NA	0%[a]	2%[a]	5%[b]	6%[a]
MW > 100 kDa	NA	3%[a]	6%[a]	86%[b]	22%[a]

NA – not analyzed.
[a] Pivokonsky et at. (2014).
[b] Baresova et at. (2017).

hydrocarbons, amines, glycolic acids, nucleotides and nucleic acids, amino acids, peptides and aminosugars (Pivokonsky et al., 2016).

MW fractionation through Amicon Ultra-15 centrifugal filters (Fig. 1a) showed that the NM of *C. vulgaris* contained a high portion (67%) of low-MW compounds (<3 kDa) and the second biggest fraction was >100 kDa (22%). Compared with other algal species (Baresova et al., 2017; Pivokonsky et al., 2014), MW distribution of the NM of *C. vulgaris* followed the same pattern as the NM of green alga *Chlamydomonas geitleri* and diatom *Fragilaria crotonensis*, while the NM of cyanobacteria *Microcystis aeruginosa* and *Merismopedia tenuissima* differed, but still contained large portions of low-MW substances (Table 2). The same MW fractions for PM are shown in Table 2 for comparison. In the case of PM, the portions of fractions under 3 kDa were small. The COM of both cyanobacteria species contained a substantial portion of high-MW proteins. In both studies indicated in Table 2 (Baresova et al., 2017; Pivokonsky et at., 2014), COM was acquired in the same way as in this study, and proteins were isolated from NM with the salting out method. Changes in MW fractions after coagulation by alum and PACl (Fig. 1b, c) are discussed in Section 2.2.

Since charge and the content of functional groups are important from the perspective of coagulation, potentiometric titration of NM was performed. The titration curve (Fig. 2) shows the number of protons which the NM is able to accept under the given pH value and which is equal to the amount of dissociated functional groups (in millimoles of H^+ ions per 1 g of DOC). The curve provides three buffer regions with equivalence points and dissociation constants, which may be attributed to various functional groups. The dissociation constant $pK_1 = 3.5$ may be attributed to carboxyl (–COOH) functional groups. For example, saccharide alginic acid is composed of poly-D-mannuronic and L-guluronic acid with –COOH of $pK_a = 3.38$ and 3.65,

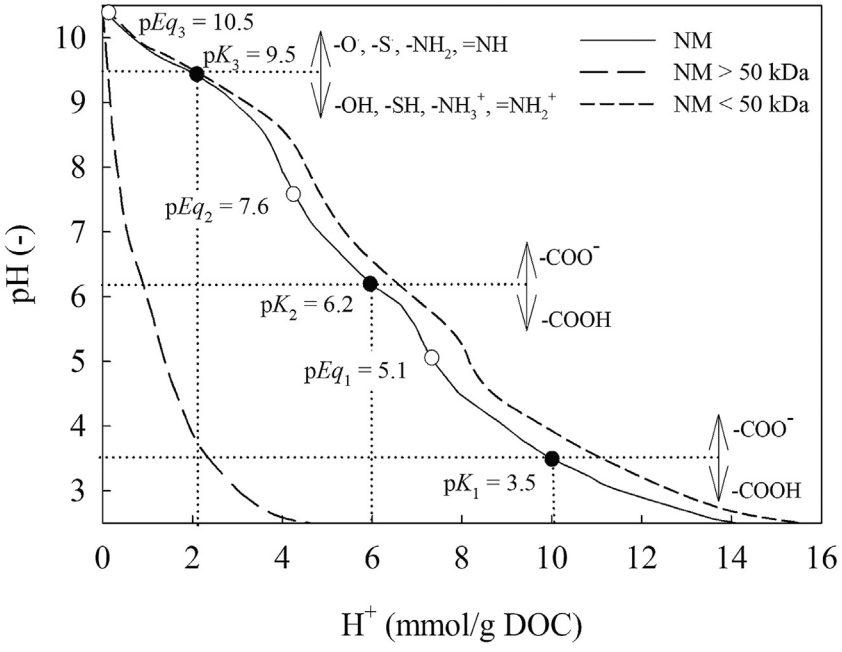

Fig. 2 – Titration curves of non-proteinaceous COM of *Chlorella vulgaris* (NM), and its fractions with molecular weight > 50 kDa (NM > 50 kDa) and < 50 kDa (NM < 50 kDa). Equivalence points (pEq_1-pEq_3) and dissociation constants (pK_1-pK_3) assigned to different functional groups are depicted for NM.

respectively. The constant $pK_2 = 6.2$ may be assigned to the second –COOH group of dicarboxylic acids. The constant $pK_3 = 9.5$ may be attributed to the collective effect of functional groups dissociating at alkaline pH values, such as –OH, –SH, $–NH_3^+$, and $= NH_2^+$ (Chang, 2005). It should be taken into consideration that NM is a mixture of compounds containing various functional groups whose dissociation constants depend not only on the type of group, but also on the overall net charge of the molecule. The number of titratable groups in whole NM is very similar to figures from our previous studies obtained for humic substances (Pivokonsky et al., 2015) or the COM of *Merismopedia tenuissima* (Baresova et al., 2017). The titration curves for NM fractions with MW > 50 kDa and < 50 kDa will be discussed in Section 2.2.

2.2. Coagulation of non-proteinaceous COM

Dose optimizations were performed for Al concentrations of 1–15 mg/L in a pH range of 3.0–10.5 with initial DOC concentration of 5 mg/L for both coagulants. The results are detailed in Figs. 3 and 4. In these figures, pH ranges 4.0–9.0 and 5.5–10.5 are indicated for alum and PACl, respectively, because no DOC and Al removal was observed outside these pH ranges. When alum was applied, coagulation started with a dose of 3 mg/L Al, and the highest DOC removal efficiencies (up to 25%) were achieved at doses of 8, 10 and 12 mg/L Al (1.6, 2 and 2.4 mg Al/mg DOC) at pH 6.6–8.0 (Fig. 3a). Residual aluminum dropped to the lowest level of 0.3 mg/L in the pH range 7.1–7.5 (Fig. 4a). In the case of PACl, coagulation started with a dose of 3 mg/L Al, and the highest DOC removal efficiencies (up to 25%) were achieved at doses of 8, 10, 12 and 15 mg/L Al (1.6, 2, 2.4 and 3 mg Al/ mg DOC; Fig. 3b). DOC removal efficiencies of 19%–25% were obtained at pH range 7.5–9.0, while residual aluminum reached the lowest level of 0.5 mg/L in a very narrow pH range of 7.6–7.8 (Fig. 4b). This narrow pH range can be better observed in Fig. 5, which details the coagulation curves for the optimal doses of PACl and alum (10 mg/L Al, i.e., 2 mg Al/mg DOC).

The coagulation of non-proteinaceousCOM has been poorly investigated up to now. Pivokonsky et al. (2009) coagulated COM of *M. aeruginosa* with ferric sulphate and aluminum sulphate and analyzed the PM and NM content before and after coagulation. They found that under optimal conditions ferric sulphate removed about 74% of PM and 12% of NM, while aluminum sulphate removed about 50% of PM and 22% of NM. Cui et al. (2016), who investigated the coagulation of effluent organic matter from wastewater by $AlCl_3$ and PACl, also demonstrated a higher removal of protein (75% and 69%, respectively; determined by the modified Lowry method) than saccharides (30% and 40%, respectively; determined by the colorimetric method) at Al dose of 3.2 mg Al/mg DOC.

Studies focusing on the coagulation of algal PM confirm higher DOC removal at lower coagulant doses (Pivokonsky et al., 2012, 2015) than those needed for NM removal. PM was also removed at lower pH values, at which metal coagulants hydrolyse to form positively charged hydroxopolymers (Stumm and Morgan, 1996), and was therefore prone to a charge neutralization mechanism. Specifically, Pivokonsky et al. (2012) found that peptides/proteins of *M. aeruginosa* in DOC concentrations of 1–8 mg/L were removed in the pH range 4–6 by ferric sulphate (at a dose of 7 mg/L Fe, i.e., 0.88–7 mg Fe/mg DOC) with a removal of 60%–85% depending on the initial DOC concentration. In the study by Pivokonsky et al. (2015), the same peptides/proteins of *M. aeruginosa* (DOC = 5 mg/L) were coagulated by alum (at a dose of 2 mg/L Al, i.e., 0.4 mg Al/mg DOC) in the pH range 5.2–6.7 with a removal efficiency of 75%.

DOC mean removal efficiencies (%) - aluminium sulphate

a

Al dose (mg/L) \ pH (-)	4.0-4.5	4.6-5.0	5.1-5.5	5.6-6.0	6.1-6.5	6.6-7.0	7.1-7.5	7.6-8.0	8.1-8.5	8.6-9.0
1	0	0	0	0	0	0	0	0	0	0
2	0	0	0	0	0	0	0	0	0	0
3	0	0	0	0	0	11	9	4	0	0
4	0	0	0	5	4	12	9	5	0	0
6	0	0	0	2	10	12	13	12	10	5
8	0	0	0	7	15	21	22	18	14	5
10	0	0	4	8	14	20	25	20	14	5
12	0	0	8	9	12	20	24	20	13	6
15	0	0	10	10	10	14	15	15	13	9
%	100	90	80	70	60	50	40	30	20	10	0

DOC mean removal efficiencies (%) - polyaluminium chloride

b

Al dose (mg/L) \ pH (-)	5.5-6.0	6.1-6.5	6.6-7.0	7.1-7.5	7.6-8.0	8.1-8.5	8.6-9.0	9.1-9.5	9.6-10.0	10.1-10.5
1	0	0	0	0	0	0	0	0	0	0
2	0	0	0	0	0	0	0	0	0	0
3	0	0	0	8	6	5	0	0	0	0
4	0	0	0	11	13	10	9	0	0	0
6	0	0	0	11	15	12	11	3	0	0
8	0	0	0	13	24	22	19	6	2	0
10	0	0	0	14	25	23	20	13	9	2
12	0	0	0	14	25	22	19	12	12	4
15	0	0	0	10	20	21	19	15	14	8
%	100	90	80	70	60	50	40	30	20	10	0

Fig. 3 – Optimization of coagulant dose and pH value – DOC removal efficiencies for aluminum sulphate (a) and polyaluminium chloride (b). At least three samples were analyzed in each pH interval for each coagulant dose. Initial DOC = 5 mg/L.

Mean residual Al concentrations (mg/L) - aluminium sulphate

a

Al dose (mg/L) \ pH (-)	4.0-4.5	4.6-5.0	5.1-5.5	5.6-6.0	6.1-6.5	6.6-7.0	7.1-7.5	7.6-8.0	8.1-8.5	8.6-9.0
1	1.0	1.0	1.0	1.0	1.0	1.0	0.7	0.8	1.0	1.0
2	2.0	2.0	2.0	1.9	1.8	1.4	0.9	1.1	1.5	1.8
3	3.0	3.0	2.9	2.8	2.5	1.8	1.5	1.2	2.2	2.7
4	4.0	4.0	3.8	3.7	3.5	1.8	1.4	1.0	2.9	3.8
6	6.0	5.8	5.6	5.5	2.5	1.1	0.5	0.8	2.1	4.3
8	8.0	7.5	7.1	5.5	1.6	0.8	0.3	0.8	2.0	5.5
10	10.0	9.2	7.4	5.5	1.4	0.7	0.3	0.8	2.3	7.5
12	12.0	11.2	8.5	4.7	1.2	0.7	0.3	0.9	2.1	7.0
15	15.0	14.4	9.4	4.0	1.0	0.7	0.3	1.0	1.2	3.2
Al	0	0.3	0.5	1	2	4	6	8	10	12	15

Mean residual Al concentrations (mg/L) - polyaluminium chloride

b

Al dose (mg/L) \ pH (-)	5.5-6.0	6.1-6.5	6.6-7.0	7.1-7.5	7.6-8.0	8.1-8.5	8.6-9.0	9.1-9.5	9.6-10.0	10.1-10.5
1	1.0	1.0	1.0	1.0	1.0	1.0	1.0	1.0	1.0	1.0
2	2.0	2.0	2.0	1.2	1.2	1.6	1.6	1.8	2.0	2.0
3	3.0	3.0	3.0	2.2	1.4	2.1	2.3	2.7	3.0	3.0
4	3.8	3.7	3.7	1.9	1.6	1.8	2.3	3.2	3.8	4.0
6	5.8	5.8	5.5	2.5	1.0	2.6	3.5	4.0	5.2	6.0
8	7.8	7.6	7.4	4.0	0.6	2.1	3.6	4.5	6.1	7.9
10	9.8	8.5	7.5	4.5	0.5	2.0	3.7	4.5	7.2	9.4
12	12.0	11.9	10.4	7.0	0.5	2.2	4.5	6.5	9.5	11.7
15	15.0	14.8	13.9	8.3	0.6	2.2	5.0	7.3	11.6	13.2
Al	0	0.3	0.5	1	2	4	6	8	10	12	15

Fig. 4 – Optimization of coagulant dose and pH value – Al residual concentrations for aluminum sulphate (a) and polyaluminium chloride (b). At least three samples were analyzed in each pH interval for each coagulant dose. Initial DOC = 5 mg/L.

Therefore, NM required four to five times more alum than PM. In both studies mentioned, Fe/Al residuals dropped below 0.1 mg/L.

Herein, relatively high residual aluminum concentrations, i.e., about 0.3 and 0.5 mg/L for alum and PACl, respectively, were achieved after coagulation under optimal conditions and 60 min of sedimentation (Fig. 4). These Al concentrations do not comply with the regulated limit of 0.2 mg/L of the EC drinking water directive (Directive 98/83/EC). High Al residuals stem from the high coagulant doses utilized to coagulate NM compared to the coagulation of COM peptides/proteins mentioned previously or the coagulation of AOM (Baresova et al., 2017; Henderson et al., 2010). For instance, Baresova et al. (2017) found that the ferric sulphate dose required to remove the COM of cyanobacterium *Merismopedia tenuissima* (removal rate of 43%–53%) was 1 mg Fe/mg DOC. Furthermore, Henderson et al. (2010) achieved the highest removals (71, 55 and 46%, respectively) of AOM produced by *Chlorella vulgaris*, *Microcystis aeruginosa* and diatom *Asterionella formosa* at alum doses of 0.8, 1.2 and 1.5 mg Al/mg DOC, respectively. The high Al residuals achieved in this study are further discussed in Section 2.3.

MW fractionation of residual organic matter after coagulation provides insights into the coagulation pathways. In the

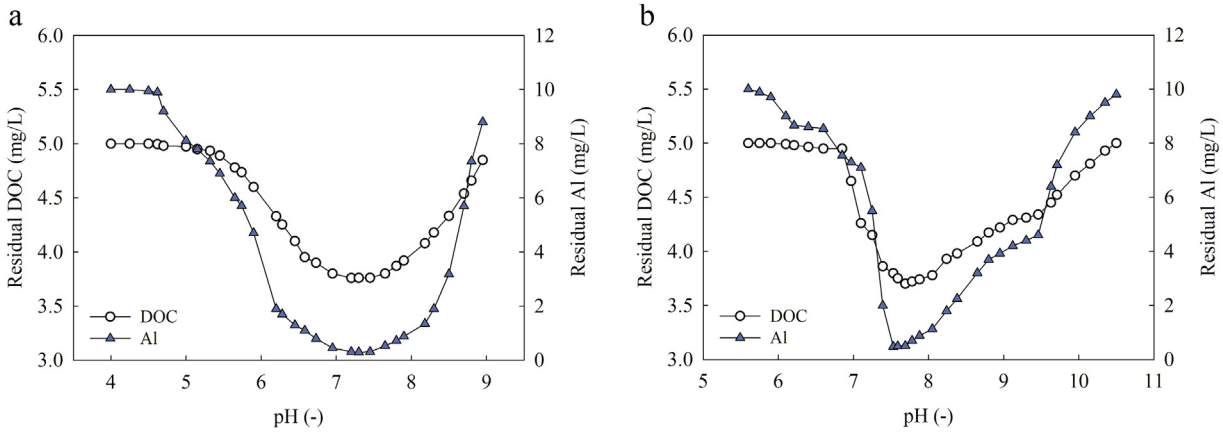

Fig. 5 – Residual DOC and aluminum concentrations as a function of pH value for the optimized doses (10 mg/L Al) of aluminum sulphate (a) and polyaluminium chloride (b). Initial DOC = 5 mg/L.

case of alum, fractions with MW > 50 kDa were fully removed by coagulation, whereas fractions with MW 3–50 kDa were removed partly and substances with MW < 3 kDa remained in the treated water (Fig. 1b). In the case of PACl, compounds larger than 10 kDa were fully removed by coagulation, while fraction with MW 3–10 kDa was removed partly and fraction under 3 kDa remained in the treated water (Fig. 1c). A number of previous studies ascertained that low-MW organics are reluctant to coagulate (Gregor et al., 1996; Liu et al., 2018; Pivokonsky et al., 2012, 2015). In the study by Liu et al. (2018), compounds of MW > 100 kDa isolated from the COM of *M. aeruginosa* were coagulated with a removal of 70% by $AlCl_3$ and 80% by PACl, while the fractions with MWs 30–100 kDa, 5–30 kDa and < 5 kDa exhibited a removal of 20%–40%. PACl showed higher DOC removal for the >100 kDa and < 5 kDa fractions than $AlCl_3$. This agrees with our results, where PACl was more efficient in removing 3–10, 10–30 and 30–50 kDa fractions than alum (Fig. 1b, c). For algal COM peptides/proteins, Pivokonsky et al. (2012, 2015) found that peptides of MW < 10 kDa were coagulated by neither ferric nor aluminum sulphate. Herein, NM contained a large portion of low-MW compounds <3 kDa (about 67%), which is most likely the reason for its low removal. Based on the data shown in Table 2, it can be assumed that the NM of the mentioned algal species will be also coagulated with low efficiencies due to the high content of low-MW compounds. The low-MW fraction includes intermediate products of algal metabolism, such as aldehydes, hydrocarbons, amines, glycolic acids, nucleotides and nucleic acids, amino acids, peptides, aminosugars and mono- and oligosaccharides (Pivokonsky et al., 2016). The portion of carbohydrates after coagulation substantially decreased from 20% of DW before coagulation to 0.5%–2% of DW after coagulation by both coagulants, indicating that carbohydrates (saccharides) were prone to coagulation. The N/C ratio after coagulation was very similar to before coagulation (0.11), suggesting that a part of nitrogen-containing compounds, e.g. high-MW aminosugars, were removed by coagulation.

As the fraction with MW > 50 kDa was fully removed by both coagulants utilized in this study, charge characterization by potentiometric titration was performed for fractions with MW > 50 kDa and MW < 50 kDa to determine whether these fractions differ in terms of charge. The results (Fig. 2) showed that fraction above 50 kDa carried substantially less ionisable groups than fraction under 50 kDa, the titration curve of which is comparable to the titration curve of whole NM. The results of titration curves and determination of saccharide content imply that the high-MW fraction of NM, which undergoes coagulation, consists of neutral or slightly acidic polysaccharides.

2.3. Comparison between alum and PACl

Table 3 summarizes and compares the performance of alum and PACl in the coagulation of NM. While the same maximum DOC removal under similar coagulant doses was achieved, the two coagulants differed in pH values effective for coagulation, the lowest Al residual concentrations reached and removal efficiencies for different MW fractions. As shown by many studies (Van Benschoten and Edzwald, 1990; Wang et al., 2004; Yan et al., 2007), hydrolysis products of Al may be divided into three groups: (1) Al_a – reactive monomeric species and small polymers; (2) Al_b – medium polymer species, correlated well to tridecamer $AlO_4Al_{12}(OH)_{24}(H_2O)_{12}^{7+}$, often denoted as Al_{13}; and (3) Al_c – colloidal or solid species of $Al(OH)_3$ precipitates. Regarding the mechanisms of coagulation, Al_b species are mainly involved in charge neutralization at slightly acidic pH values, while Al_c species are responsible for removals through adsorption and electrostatic patch effect (Yan et al., 2007). At pH values of the highest coagulation efficiency in the current study (6.6–8.0 for alum and 7.5–9.0 for PACl), the portion of Al_c is maximal for both alum and PACl, while the portion of Al_b decreases (Wang et al., 2004). These observations indicate that amorphous precipitates (Al_c) are playing a major role in interactions between coagulants and NM and adsorption via both electrostatic and non-electrostatic forces, such as hydrogen bonding and van der Waals forces, are more important than electrostatic neutralization by Al hydroxopolymers for the coagulation of NM. This is supported by the fact that high-MW fraction, which was amenable to coagulation, bears very low amount of ionisable functional groups (Fig. 2). Al_{13} species of PACl are stable across a wide pH range and up to higher pH values than in the case of alum (Van Benschoten and Edzwald, 1990; Wang et al., 2014; Wu et al., 2007). This is probably the reason why the coagulation of NM by PACl took place at higher pH values than by alum. At pH above 7.5, the hydrolysis of PACl was favored (Wang et al., 2014) and the formation of amorphous hydroxide precipitates (Al_c) from Al_{13} species enabled coagulation.

Difference in the lowest Al residual concentrations achieved for alum and PACl (see Table 3) also stem from different Al species distribution for alum and PACl. According to Wang et al. (2014) and Van Benschoten and Edzwald (1990), at pH values of the lowest Al residuals in this study, 5%-10% of dosed Al may be present in the form of Al_a. High residual Al concentrations may thus be expected, and the portion of Al_a for PACl is higher than for alum. This is in accordance with our results and explains higher residual Al concentrations for PACl than for alum achieved in our experiments. Moreover, different Al species distribution for alum and PACl is probably the reason for different efficiencies in removing various MW fractions by alum and PACl, as shown in Section 2.2 (Fig. 1b, c). Highly stable Al_b (mostly Al_{13}) species of PACl are able to interact with lower-MW

Table 3 – Comparison of aluminum sulphate and polyaluminium chloride.

	Aluminum sulphate	Polyaluminium chloride
Al doses investigated (mg Al/mg DOC)	0.2–3	0.2–3
Coagulation starts at Al dose (mg Al/mg DOC)	0.6	0.6
Optimal Al doses (mg Al/mg DOC)	1.6; 2; 2.4	1.6; 2; 2.4; 3
Maximum DOC removal (%)	25	25
pH of DOC removal	6.6–8.0	7.5–9.0
Lowest Al residuals (mg/L)	0.3	0.5
pH of lowest Al residuals	7.1–7.5	7.6–7.8

fractions through charge neutralization (Yan et al., 2007). Therefore, PACl was more efficient in removing 3–10, 10–30 and 30–50 kDa fractions than alum.

The different coagulation behaviors of PACl and traditional coagulant $AlCl_3$ was also observed by Liu et al. (2018) in the coagulation of the COM of *M. aeruginosa* together with kaolin. They ascertained that PACl removed 68% of COM at pH 7.8, while $AlCl_3$ removed 61% of COM at pH 6.9. PACl also demonstrated a slight advantage in removing fractions with MWs > 100 kDa and < 5 kDa and the hydrophilic fractions. $AlCl_3$ was slightly more effective in removing pigment-like organics, organics absorbing at 254 nm and transphilic fractions. Nevertheless, it is notable that neither the influence of kaolin particles nor the pH value was evaluated. The resultant pH value was based only on dose optimization experiments.

It can be concluded that the coagulation mechanisms for NM differ from those for whole AOM as well as proteinaceous AOM fractions and also for natural organic matter (NOM), which is usually represented by humic matter. Whole AOM and proteinaceous AOM were removed at acidic pH values through charge neutralization (Pivokonsky et al., 2015; Baresova et al., 2017). Similarly, as far as NOM is concerned, the aluminum-based coagulants, such as alum or aluminum chloride, are more efficient when positively-charged Al hydropolymers are generated under slightly acidic pH values, because NOM is mainly composed of organic compounds with negatively-charged functional groups (Sillanpää et al., 2018; Yan et al., 2008). Pre-hydrolysed metal-ion coagulants, such as PACl, also perform well at slightly acidic pH values (from pH 5) for NOM removal but may also be efficient in an alkaline pH up to 8.5–9.0 (Gao et al., 2006; Yan et al., 2008) owing to the stability of Al_{13} species in a wide pH range.

3. Conclusions

The study investigated coagulation of non-proteinaceous AOM to which only limited attention has been paid so far, compared to algal cells and proteinaceous AOM. The following conclusions have been drawn from this research: (1) Non-proteinaceous AOM of *Chlorella vulgaris* was removed by aluminum-based coagulants (alum, PACl) only by 25% under optimal conditions. (2) High-MW saccharide-like organics bearing low surface charge were removed, while low-MW ones (<3 kDa) with higher surface charge formed most of residual organics after coagulation. (3) The low removal of non-proteinaceous AOM was given by the high content of low-MW compounds and may also be expected for the non-proteinaceous AOM of other algal species. (4) The prevailing coagulation mechanism of high-MW saccharide-like AOM was adsorption onto aluminum hydroxide precipitates (Al_c species) at around neutral pH values in the case of alum (pH 6.6–7.5) and alkaline pH values in the case of PACl (pH 7.5–9.0). The lowest Al residuals were achieved at narrower pH ranges close to the minimum solubility of aluminum hydroxide. (5) Compared with previous studies dealing with the coagulation of proteinaceous AOM, NM requires higher coagulant doses and exhibits lower removal efficiencies than proteinaceous matter (25% vs. 60%–85%). Additionally, proteinaceous and non-proteinaceous matter is coagulated under different pH values (acidic vs. neutral/alkaline) due to the employment of different coagulation mechanisms.

Even though PACl is widely accepted to exhibit a better coagulation efficiency in a wider pH range than traditional hydrolysing coagulants ($AlCl_3$ or alum), alum appears to be more suitable for non-proteinaceous AOM removal because it exhibits lower Al residuals at a wider pH range at the same DOC removal compared to PACl. The results also indicate that the various AOM components are removed by different coagulation pathways and that their removal strategy should be carefully evaluated. Based on these observations, AOM coagulation might be approached as a two-stage process: coagulation at acidic pH values for removing charged proteinaceous AOM fraction through charge neutralization and coagulation at neutral/alkaline pH values for removing neutral non-proteinaceous AOM through adsorption. This two-stage process requires further investigation as well as evaluation of the benefit of the expected increased AOM removal compared to the expense of implementing two-stage coagulation. It is significant that low-MW AOM compounds of both proteinaceous and non-proteinaceous character remaining in water after coagulation require other removal processes, such as membrane filtration, adsorption onto activated carbon or oxidative degradation. Further work is needed to determine suitable conditions for these subsequent treatments and to evaluate their impact on water quality.

Acknowledgments

This work was supported by the Czech Science Foundation (No. GA18-14445S) and by the institutional support of the Czech Academy of Sciences (RVO: 67985874).

REFERENCES

Baresova, M., Pivokonsky, M., Novotna, K., Naceradska, J., Branyik, T., 2017. An application of cellular organic matter to coagulation of cyanobacterial cells (*Merismopedia tenuissima*). Water Res. 122, 70–77.

Becker, E.W., 1994. Microalgae: Biotechnology and microbiology. Cambridge University Press, Cambridge, New York.

Bischof, J.C., He, X., 2005. Thermal stability of protein. Ann. N. Y. Acad. Sci. 1066, 12–33.

Bothara, S.B., Singh, S., 2012. Thermal studies on natural polysaccharide. Asian Pac. J. Trop. Biomed. S1031–S1035.

Brányiková, I., Maršálková, B., Doucha, J., Brányik, T., Bišová, K., Zachleder, V., et al., 2011. Microalgae-novel highly efficient starch producers. Biotechnol. Bioeng. 108, 766–776.

Chang, R., 2005. Physical Chemistry for the Biosciences. second ed. University Science Books, USA.

Cui, X., Zhou, D., Fan, W., Huo, M., Crittenden, J.C., Yu, Z., et al., 2016. The effectiveness of coagulation for water reclamation from a wastewater treatment plant that has a long hydraulic and sludge retention times: A case study. Chemosphere 157, 224–231.

Dawson, R.M.C., Elliott, D.C., Elliott, W.H., Jones, K.M., 1986. Data for Biochemical Research. third ed. Oxford University Press, New York.

Gao, B.Y., Abbt-Braun, G., Frimmel, F.H., 2006. Preparation and evaluation of polyaluminum chloride sulfate (PACS) as a coagulant to remove natural organic matter from water. Acta Hydrochim. Hydrobiol. 34, 491–497.

Goslan, E.H., Seigle, C., Purcell, D., Henderson, R.K., Parsons, S.A., Jefferson, B., et al., 2017. Carbonaceous and nitrogenous disinfection by-product formation from algal organic matter. Chemosphere 170 (1–9).

Gregor, J.E., Fenton, E., Brokenshire, G., Van Den Brink, P., O'Sullivan, B., 1996. Interactions of calcium and aluminium ions with alginate. Water Res. 30 (6), 1319–1324.

Henderson, R.K., Baker, A., Parsons, S.A., Jefferson, B., 2008. Characterisation of algogenic organic matter extracted from cyanobacteria, green algae and diatoms. Water Res. 42, 3435–3445.

Henderson, R.K., Parsons, S.A., Jefferson, B., 2010. The impact of differing cell and algogenic organic matter (AOM) characteristics on the coagulation and flotation of algae. Water Res. 44 (12), 3617–3624.

Laurens, L.M.L., Wychen, S.V., McAllister, J.P., Arrowsmith, S., Dempster, T.A., McGowen, J., et al., 2014. Strain, biochemistry, and cultivation-dependent measurement variability of algal biomass composition. Anal. Biochem. 452, 86–95.

Liu, R., Guo, T., Ma, M., Yan, M., Qi, J., Hu, C., et al., van der Meer, W., 2018. Preferential binding between intracellular organic matters and Al13 polymer to enhance coagulation performance. J. Environ. Sci. https://doi.org/10.1016/j.jes.2018.05.011.

Lv, J.-M., Cheng, L.-H., Xu, X.-H., Zhang, L., Chen, H.-L., 2010. Enhanced lipid production of *Chlorella vulgaris* by adjustment of cultivation conditions. Bioresour. Technol. 101, 6797–6804.

Newcombe, G., 1994. Activated carbon and soluble humic substances: adsorption, desorption, and surface charge effects. J. Colloid Interface Sci. 164, 452–462.

Pivokonský, M., Pivokonská, L., Baumeltová, J., Bubáková, P., 2009. The effect of cellular organic matter produced by cyanobacteria *Microcystis aeruginosa* on water purification. J. Hydrol. Hydromech. 57 (2), 121–129.

Pivokonsky, M., Safarikova, J., Bubakova, P., Pivokonska, L., 2012. Coagulation of peptides and proteins produced by *Microcystis aeruginosa*: interaction mechanisms and the effect of Fe-peptide/protein complexes formation. Water Res. 46 (17), 5583–5590.

Pivokonsky, M., Safarikova, J., Baresova, M., Pivokonska, L., Kopecka, I., 2014. A comparison of the character of algal extracellular versus cellular organic matter produced by cyanobacterium, diatom and green alga. Water Res. 51, 37–46.

Pivokonsky, M., Naceradska, J., Brabenec, T., Novotna, K., Baresova, M., Janda, V., 2015. The impact of interactions between algal organic matter and humic substances on coagulation. Water Res. 84, 278–285.

Pivokonsky, M., Naceradska, J., Kopecka, I., Baresova, M., Jefferson, B., Li, X., et al., 2016. The impact of algogenic organic matter on water treatment plant operation and water quality: A review. Crit. Rev. Environ. Sci. Technol. 46 (4), 291–335.

Řezanka, T., Kolouchová, I., Čejková, A., Cajthaml, T., Sigler, K., 2013. Identification of regioisomers and enantiomers of triacylglycerols in different yeasts using reversed- and chiral-phase LC-MS. J. Sep. Sci. 36 (20), 3310–3320.

Safarikova, J., Baresova, M., Pivokonsky, M., Kopecka, I., 2013. Influence of peptides and proteins produced by cyanobacterium *Microcystis aeruginosa* on the coagulation of turbid waters. Sep. Purif. Technol. 118, 49–57.

Safi, C., Zebib, B., Merah, O., Pontalier, P.-Y., Vaca-Garcia, C., 2014. Morphology, composition, production, processing and applications of *Chlorella vulgaris*: A review. Renew. Sust. Energ. Rev. 35, 265–278.

Sillanpää, M., Ncibi, M.C., Matilainen, A., Vepsäläinen, M., 2018. Removal of natural organic matter in drinking water treatment by coagulation: A comprehensive review. Chemosphere 190, 54–71.

Slocombe, S.P., Ross, M., Thomas, N., McNeill, S., Stanley, M.S., 2013. A rapid and general method for measurement of protein in micro-algal biomass. Bioresour. Technol. 129, 51–57.

Šnajdr, J., Valášková, V., Merhautová, V., Herinková, J., Cajthaml, T., Baldrian, P., 2008. Spatial variability of enzyme activities and microbial biomass in the upper layers of *Quercus petraea* forest soil. Soil Biol. Biochem. 40, 2068–2075.

Stumm, W., Morgan, J.J., 1996. Aquatic Chemistry. third ed. John Wiley Sons, New York.

Sui, Z., Gizaw, Y., Bemiller, J.N., 2012. Extraction of polysaccharides from a species of *Chlorella*. Carbohyd. Polym. 90, 1–7.

Templeton, D.W., Quinn, M., Wychen, S.V., Hyman, D., Laurens, L. M.L., 2012. Separation and quantification of microalgal carbohydrates. J. Chromatogr. A 1270, 225–234.

Van Benschoten, J., Edzwald, J.K., 1990. Chemical aspects of coagulation using aluminum salts – I. Hydrolytic reactions of alum and polyaluminium chloride. Water Res. 24 (12), 1519–1526.

Villacorte, L.O., Ekowati, Y., Neu, T.R., Kleijn, J.M., Winters, H., Amy, G., et al., 2015. Characterisation of algal organic matter produced by bloom-forming marine and freshwater algae. Water Res. 73, 216–230.

Wang, D., Sun, W., Xu, Y., Tang, H., Gregory, J., 2004. Speciation stability of inorganic polymer flocculant–PACl. Colloids Surfaces A: Physicochem. Eng. Aspects 243, 1–10.

Wu, X., Ge, X., Wang, D., Tang, H., 2007. Distinct coagulation mechanism and model between alum and high Al13-PaCl. Colloids Surfaces A: Physicochem. Eng. Aspects 305, 89–96.

Wychen, S.V., Laurens, L.M.L., 2015. Determination of total carbohydrates in algal biomass, NREL/TP- 5100-60957. National Renewable Energy Laboratory, Golden, CO.

Yan, M., Wang, D., Qu, J., He, W., Chow, C.W.K., 2007. Relative importance of hydrolysed Al(III) species (Al_a, Al_b, Al_c) during coagulation with polyaluminum chloride. A case study with the typical micro-polluted source waters. J. Colloid. Interf. Sci. 316, 482–489.

Yan, M., Wang, D., Ni, J., Qu, J., Chow, C.W.K., Liu, H., 2008. Mechanism of natural organic matter removal by polyaluminum chloride: Effect of coagulant particle size and hydrolysis kinetics. Water Res. 42 (13), 3361–3370.

Yeh, K.-L., Chang, J.-S., 2012. Effects of cultivation conditions and media composition on cell growth and lipid productivity of indigenous microalga *Chlorella vulgaris* ESP-31. Bioresour. Technol. 105, 120–127.

PUBLIKACE 2

The impact of preozonation on coagulation of cellular organic matter produced by *Microcystis aeruginosa* and its toxin degradation

Magdalena Barešová, Jana Načeradská, Kateřina Novotná, **Lenka Čermáková** a Martin Pivokonský

Journal of Environmental Sciences 98 (2020) 124-133
DOI 10.1016/j.jes.2020.05.031

Journal of Environmental Sciences 98 (2020) 124–133

Contents lists available at ScienceDirect

Journal of Environmental Sciences

journal homepage: www.elsevier.com/locate/jes

The impact of preozonation on the coagulation of cellular organic matter produced by *Microcystis aeruginosa* and its toxin degradation

Magdalena Barešová, Jana Načeradská, Kateřina Novotná, Lenka Čermáková, Martin Pivokonský*

Institute of Hydrodynamics of the Czech Academy of Sciences, Pod Patankou 5, 166 12 Prague 6, Czech Republic

ARTICLE INFO

Article history:
Received 3 April 2020
Revised 18 May 2020
Accepted 30 May 2020

Keywords:
Algal organic matter
Coagulation
Microcystins
Microcystis aeruginosa
Ozonation

ABSTRACT

Ozonation pretreatment is typically implemented to improve algal cell coagulation. However, knowledge on the effect of ozonation on the characteristics and coagulation of associated algal organic matter, particularly cellular organic matter (COM), which is extensively released during algal bloom decay, is limited. Hence, this study aimed to elucidate the impact of ozonation applied before the coagulation of dissolved COM from the cyanobacteria *Microcystis aeruginosa*. Additionally, the degradation of microcystins (MCs) naturally present in the COM matrix was investigated. A range of ozone doses (0.1–1.0 mg O_3/mg of dissolved organic carbon – DOC) and ozonation pH values (pH 5, 7 and 9) were tested, while aluminium and ferric sulphate coagulants were used for subsequent coagulation. Despite negligible COM removal, ozonation itself eliminated MCs, and a lower ozone dose was required when performing ozonation at acidic or neutral pH (0.4 mg O_3/mg DOC at pH 5 and 7 compared to 0.8 mg O_3/mg DOC at pH 9). Enhanced MC degradation and a similar pattern of pH dependence were observed after preozonation-coagulation, whereas coagulation alone did not sufficiently remove MCs. In contrast to the benefits of MC depletion, preozonation using $\geq$ 0.4 mg O_3/mg DOC decreased the coagulation efficiency (from 42%/48% to 28%–38%/41%–44% using Al/Fe-based coagulants), which was more severe with increasing ozone dosage. Coagulation was also influenced by the preozonation pH, where pH 9 caused the lowest reduction in COM removal. The results indicate that ozonation efficiently removes MCs, but its employment before COM coagulation is disputable due to the deterioration of coagulation.

Introduction

Due to the anthropogenically intensified eutrophication of water sources, many drinking water treatment utilities worldwide currently face the development of seasonal algal blooms. While high removal efficiencies (> 90%) of algal and cyanobacterial cells can be achieved through conventional treatment processes based on coagulation, the removal of associated dissolved algal organic matter (AOM) is more challenging (Baresova et al., 2017; Henderson et al., 2010; Pivokonsky et al., 2016; Zhang et al., 2012). In addition to the extracellular organic matter (EOM) produced during the algal proliferation period and affecting cell separation itself (Henderson et al., 2010; Paralkar and Edzwald, 1996; Pranowo et al., 2013), considerable amounts of cellular organic matter (COM) are released and significantly affect water quality in the entire water column when algal bloom decay occurs accompanied by a breakdown of cells (Pivokonsky et al., 2016). The overall removal of dissolved AOM (either EOM or COM) by optimized coagulation ranges up to only 50% (Baresova et al., 2017; Henderson et al., 2010; Pivokonsky et al., 2009; Widrig et al., 1996). Coagulation is generally considered to have limited effectiveness, particularly for the removal of low-molecular-weight (MW) compounds, including harmful cyanobacterial toxins (Al Momani et al., 2008; Himberg et al., 1989; Onstad et al., 2007; Shang et al., 2018; Sharma et al., 2012; Westrick et al., 2010); hence, the application of additional treatment processes is often required. Chemical oxidation has previously been reported to be a promising treatment for cyanotoxin elimination (Sharma et al., 2012; Westrick et al., 2010), and among the commonly used oxidants, ozone was found to be most effective (Newcombe and Nicholson, 2004; Rodríguez et al., 2007; Sharma et al., 2012).

* Corresponding author.
E-mail address: pivo@ih.cas.cz (M. Pivokonský).

https://doi.org/10.1016/j.jes.2020.05.031
1001-0742/

Ozonation has also been proposed to enhance the coagulation of algae-laden waters. Most studies have focused on the impact of ozonation on the removal of algal and cyanobacterial cells, changes in cell integrity, the release of intracellular matter including cyanotoxins and their possible degradation (Coral et al., 2013; Miao and Tao, 2009; Plummer and Edzwald, 2002; Pranowo et al., 2013; von Gunten, 2003; Wen et al., 2017). The improvements in cell coagulation resulting from preozonation were usually ascribed to cell inactivation and destabilization, changes in external cell architecture and the release of high-MW AOM that contributes to cell coagulation (Plummer and Edzwald, 2002; Pranowo et al., 2013; von Gunten, 2003). On the other hand, excessive preozonation may alter cell permeability and induce toxin and internal cellular content release preceding actual cell lysis (Coral et al., 2013; Miao and Tao, 2009; Plummer and Edzwald, 2002; Xie et al., 2013). For instance, Coral et al. (2013) and Xie et al. (2013) observed an immediate loss of cell integrity of *M. aeruginosa* and *Anabaena flos-aquae* after exposure to an ozone dose as low as 0.4–0.5 mg/L. In contrast, studies on the ozonation of dissolved AOM in the absence of algal cells are very scarce and have mostly dealt with the ozonation of EOM released during the growth of algae (Paralkar and Edzwald, 1996; Wei et al., 2016; Widrig et al., 1996). Previous results showed that ozone induces the degradation of high-MW compounds to medium- and low-MW components (Paralkar and Edzwald, 1996; Wei et al., 2016), which is likely to be detrimental to subsequent coagulation (Pivokonsky et al., 2016). On the other hand, Widrig et al. (1996) observed a slight increase in the coagulation efficiency of EOM, up to 5%–15%, depending on the phytoplankton species and reaction conditions. This effect was ascribed to the chemical transformation of EOM components. However, the study reported only limited optimization of reaction conditions: the application of very high coagulant doses (up to 0.5 mmol Al/Fe per mg DOC) was considered, and only one ozone dose (0.8 mg O_3/mg DOC) and only two ozonation and coagulation pH values (both pH 5 and 8) were tested.

As already mentioned, ozonation is capable of efficiently destroying dissolved cyanotoxins (Al Momani et al., 2008; Rodríguez et al., 2007; Rositano et al., 1998). However, some investigations revealed an inhibition of toxin degradation in the presence of other organic compounds (Miao and Tao, 2009; Rodríguez et al., 2007; Rositano et al., 1998, 2001). For example, at a fixed initial concentration of microcystins (MCs), specifically MC-RR congener, the residual MC-RR increased from 10% to nearly 30% with increasing DOC of humic acids from 1 to 4 mg/L (Miao and Tao, 2009). In the same study, a decrease in MC-RR decomposition was also observed in samples containing algal supernatant (20% residual MC-RR, in contrast to complete toxin degradation in the absence of algal material). Rositano et al. (1998) reported similar findings in the effective ozonation of MC-LR and also indicated the role of competing ozone reactions between toxins and organic matter, in this case, an extract of *M. aeruginosa*. However, toxin degradation in the presence of a natural AOM matrix, as well as AOM/COM ozonation itself, has not been systematically evaluated.

The current study thus aimed to provide insights into the effects of ozone oxidation on dissolved COM derived from cyanobacteria *M. aeruginosa*, its subsequent coagulation, and the degradation of toxins naturally contained in the COM. To achieve this, a detailed optimization of reaction conditions was undertaken by testing various ozone and coagulant doses and ozonation and coagulation pH values. The specific objectives were (1) to evaluate changes in the COM concentration and MW distribution after ozonation, (2) to assess the influence of preozonation on the coagulation of COM by Al- and Fe-based hydrolysing coagulants, and (3) to evaluate the microcystin content after ozonation, coagulation, and preozonation-coagulation processes. The findings improve our understanding of ozonation mechanisms and the impact of preozonation on the characteristics and coagulation of COM, which has implications for algae-laden water treatment.

1. Material and methods

1.1. Cultivation of Microcystis aeruginosa and COM preparation

M. aeruginosa (strain Zap. 2006/2), a toxin-producing cyanobacterium that commonly occupies water reservoirs worldwide (Pivokonsky et al., 2016), was obtained from the Department of Culture Collection of the Algal Laboratory, Institute of Botany CAS (Czech Republic). *M. aeruginosa* was cultivated as described previously (Pivokonsky et al., 2009) and harvested at the late stationary growth phase (20th day of cultivation) when cell counts reached 10^7 cells/mL. Cells were separated from the culture media by centrifugation (4,000 r/min, 20 min) and re-suspended in ultra-pure water. To extract COM, the cells were disrupted using an ultrasonic homogenizer (UP400S, Hielscher Ultrasonics, Germany), and residual solids were removed by 0.22 μm membrane filtration. The COM sample was homogenized and stored in a freezer at -50°C prior to further use. The acquired COM matrix was considered to consist of intracellular (IOM) and surface-retained organic matter (SOM), as well as possibly some tightly bound EOM (Naceradska et al., 2019). The COM sample was analysed for the concentration of dissolved organic carbon (DOC), apparent MW distribution and microcystin content (methods described in Section 1.5).

1.2. Ozonation experiments

Samples for ozonation were prepared by diluting COM with ultra-pure water to an initial concentration of 10 mg/L DOC and adjusting the alkalinity to 1 mmol/L using 0.1 mol/L $NaHCO_3$. The target initial pH values (pH 5, 7 and 9) were reached by the addition of predetermined amounts of 0.1 mol/L HCl or NaOH.

Ozone was produced by a laboratory ozone generator (Ozontech, Czech Republic). Aliquots of freshly prepared ozone stock solution (20–30 mg/L O_3 in ultra-pure water) were promptly added to the samples (final sample volume 1 L) to reach the target ozone concentrations (1, 2, 4, 8 and 10 mg/L O_3 ~ 0.1, 0.2, 0.4, 0.8 and 1.0 mg O_3 per mg DOC). The ozonation experiments were performed at room temperature (20°C) in continuously stirred 1 L glass flasks equipped with lids to prevent ozone degassing. The concentrations of the ozone stock solution and ozone residuals in the treated samples were determined according to the standard colorimetric method 4500-O3 (Baird et al., 2017) using indigo trisulphonate and analysis at 600 nm with a UV–VIS 8453A spectrophotometer (Agilent Technologies, USA) and a 1 cm quartz cell. Ozonated samples were quenched after 30 min with sodium bisulphite (2.2 mg $NaHSO_3$/mg O_3) to stop the ozone reaction and analysed for DOC content, apparent MW distribution and microcystin concentration (see Section 1.5). Ozonation experiments and all analyses were performed in triplicate using the same COM material, and the results are expressed as the mean with one standard deviation.

1.3. Coagulation tests

For jar tests without ozone pretreatment, COM samples were prepared in the same way as for ozonation alone (initial COM DOC of 10 mg/L, alkalinity of 1 mmol/L, see Section 1.2).

First, the coagulant dose and coagulation pH were optimized. Aluminium or ferric sulphate (1% stock solutions of $Al_2(SO_4)_3 \cdot 18H_2O$ or $Fe_2(SO_4)_3 \cdot 9H_2O$; Sigma Aldrich, USA) were used as coagulants. Based on previous experiments (Pivokonsky et al., 2009), the tested doses ranged from 0.1 to 0.5 mmol/L Al or Fe (2.7–13.5 mg/L Al ~ 0.27–1.35 mg Al/mg DOC;

5.6–28.0 mg/L Fe ~ 0.56–2.80 mg Fe/mg DOC) in the coagulation pH range 4–9. The target pH values were reached prior to coagulant dosing by the addition of predetermined amounts of 0.1 mol/L HCl or NaOH. The coagulation tests were performed using a variable speed eight-position paddle stirrer (LMK 8–03, IH CAS, Czech Republic) and 2 L jars at a laboratory temperature of 20°C. The experimental procedure involved 1 min of rapid mixing (shear rate of 200 sec^{-1}), followed by slow mixing (50 sec^{-1}, 30 min) and 60 min of settling. The supernatants were analysed for pH, alkalinity, DOC, and residual Al/Fe. Additionally, the apparent MW distribution and microcystin content (see Section 1.5) of residual COM were measured in samples treated under optimal coagulation conditions. Jar tests were carried out in triplicate with the same COM material. Triplicate assays were conducted, and the results are expressed as the mean with one standard deviation.

1.4. Coagulation with ozone pretreatment

To evaluate the effect of ozone pretreatment under various reaction conditions, the above-mentioned ozone doses (0.1–1.0 mg O_3/mg DOC) were applied at three different ozonation pH values (pH 5, 7 and 9) prior to optimized coagulation of model water prepared as previously described (COM of 10 mg/L DOC, alkalinity of 1 mmol/L, see Section 1.2). The preozonation duration was also set to 30 min, similar to that for ozonation alone. After preozonation, the treated samples were poured into coagulation jars, and the pH of the samples was adjusted to reach the optimum coagulation pH. Thereafter, the optimized coagulant dose was added, and jar tests were performed following the same procedure as that described above for sole coagulation (see Section 1.3). Preozonation-coagulation tests were performed in triplicate, and the results from triplicate analyses are expressed as the mean with one standard deviation.

1.5. Analytical methods

DOC was analysed using a TOC-VCPH analyser (Shimadzu, Japan) after filtering samples through a 0.22 μm membrane filter (Millipore, USA). Al and Fe concentrations were measured by an inductively coupled plasma optical emission spectrophotometer (ICP-OES, 5110 Series, Agilent Technologies, USA).

MW fractionation was performed using Amicon Ultra-15 centrifugal filters with nominal MW cut-offs of 100, 50, 30, 10 and 3 kDa (Millipore, USA) as described by Naceradska et al. (2019). The MW distribution is expressed as the proportional part of DOC assigned to a distinct MW fraction. Furthermore, the apparent MWs were determined by high-performance size exclusion chromatography (HPSEC) coupled with a diode array detector (DAD) (Agilent 1260 Infinity, Agilent Technologies, USA) operated at 280 nm—a wavelength used for the detection of protein-like substances (Pivokonsky et al., 2009) —using Agilent Bio SEC-5 100 Å and 300 Å columns connected in series. The system was calibrated with an SEC protein standard mix (BEH450, Waters Corporation, USA) with an MW range of 244 Da to 1400 kDa. Apparent MWs were also determined by HPSEC coupled with a refractive index detector (RID) (Agilent 1260 Infinity, Agilent Technologies, USA) using three Agilent PL aquagel-OH MIXED-H columns connected in series. Polyethylene glycol/oxide standards (EasiVial PEG/PEO, Agilent, USA) with MWs ranging from 106 Da to 1258 kDa were used for calibration. Prior to the HPSEC analyses, the samples were concentrated with a rotary evaporator (23°C, 1.9 kPa) (Laborota 4002 control HB/G1, Heidolph Instruments, Germany) to reach a consistent DOC of 100 mg/L convenient for HPSEC performance. It should be noted that the response of low-MWs was higher after the treatment than in the raw COM sample. This result could be explained by the fact that the respective processes changed the content and ratio of COM components with different MWs in the treated samples.

Cyanobacterial toxin concentrations were determined by liquid chromatography with tandem mass spectrometry (LC-MS/MS) using a Nextera HPLC system (Shimadzu, Japan) coupled with a Qtrap 4500 mass spectrometer (Sciex, USA). LC separation of cyanotoxins was achieved using a Luna Omega 3 μm Polar C18 (150×2.1 mm) column with a mobile phase composed of water containing 0.1% (*V/V*) formic acid (A) and acetonitrile containing 0.1% (*V/V*) formic acid (B). The gradient elution was (time/%B): 0/15; 6/100; 7/100; 8/15. The mass spectrometer was equipped with an electrospray ionization (ESI) source operated in positive mode. Using multiple-reaction monitoring (MRM) mode, two transitions for each analyte were detected and used for consequent quantification and confirmation. Analyst software (version 1.6.3) was used for data processing. Prior to the analysis, samples were pre-concentrated to reach consistent DOC concentrations of 100 mg/L as described above, dried using a SpeedVac Concentrator Plus (Eppendorf, Germany) and reconstituted in water containing 0.1% (*V/V*) formic acid. The COM samples were tested for the concentrations of the following microcystins: MC-RR, MC-YR, MC-LR, MC-LY, MC-LW, and MC-LF. All of the microcystin congeners were detected in the raw COM matrix and thus monitored in subsequent experiments. The corresponding limits of detection (LODs) and limits of quantification (LOQs) were as follows (in μg/L): 0.5 and 2.0 for MC-RR, 1.0 and 2.0 for MC-YR, 1.0 and 1.5 for MC-LR, 0.8 and 1.0 for MC-LY, 2.0 and 4.0 for MC-LW, and 1.0 and 3.0 for MC-LF, respectively. Since the samples were pre-concentrated for LC-MS/MS analysis, the presented data represent adequately back-calculated arithmetic means corresponding to the actual DOC concentrations of the samples with standard deviations of individual analyses carried out in triplicate.

2. Results and discussion

2.1. Ozonation of M. aeruginosa COM

COM rapidly consumed significant amounts of ozone and accelerated ozone decomposition, especially under alkaline pH conditions, as derived from the ozone decay curves in the presence and absence of COM (Appendix A Section S1, **Fig. S1**). However, only a slight decrease (up to 7%) in COM from the initial DOC concentration of 10 mg/L was observed for applied ozone doses (0.1–1.0 mg O_3/mg DOC). As shown in **Fig. 1**, the DOC reduction was more significant at higher ozone doses and higher pH values. This result is consistent with the theory that at lower pH values, molecular ozone (O_3) is the primary oxidant, while at alkaline pH values, hydroxide ions (OH^-) initiate the ozone decomposition chain reaction, and molecular ozone rapidly breaks down into a series of free radicals, including •OH radicals, which are non-selective and more powerful oxidants than O_3 (von Gunten, 2003). Negligible DOC changes induced by ozonation were also observed by Paralkar and Edzwald (1996) for EOM of *Chlorella vulgaris*, *Scenedesmus quadricauda* and *Cyclotella* sp. (DOC 2.5–5.5 mg/L, no indication of pH value) under ozone doses of 1 and 3 mg/L. Similarly, low DOC reductions (0–3%) after ozonation were reported by Widrig et al. (1996), who applied an ozone dose of 0.8 mg O_3/mg DOC at pH values of 5 and 8 to EOM produced by *Dictyosphaerium pulchellum*, *S. quadricauda*, and *M. aeruginosa*.

Furthermore, MW fractionation of *M. aeruginosa* COM samples with and without ozonation showed that the proportions of high-MW fractions decreased and the proportions of lower-MW fractions increased with increasing ozone dosage, as depicted in **Fig. 1**. This trend was most noticeable at an ozonation pH of 5 (**Fig. 1a**). Under an acidic ozonation pH, COM decomposition was outweighed by the degradation of higher-MW fractions into low-MW (< 3 kDa) organics. At an ozonation pH of 7 (**Fig. 1b**) and

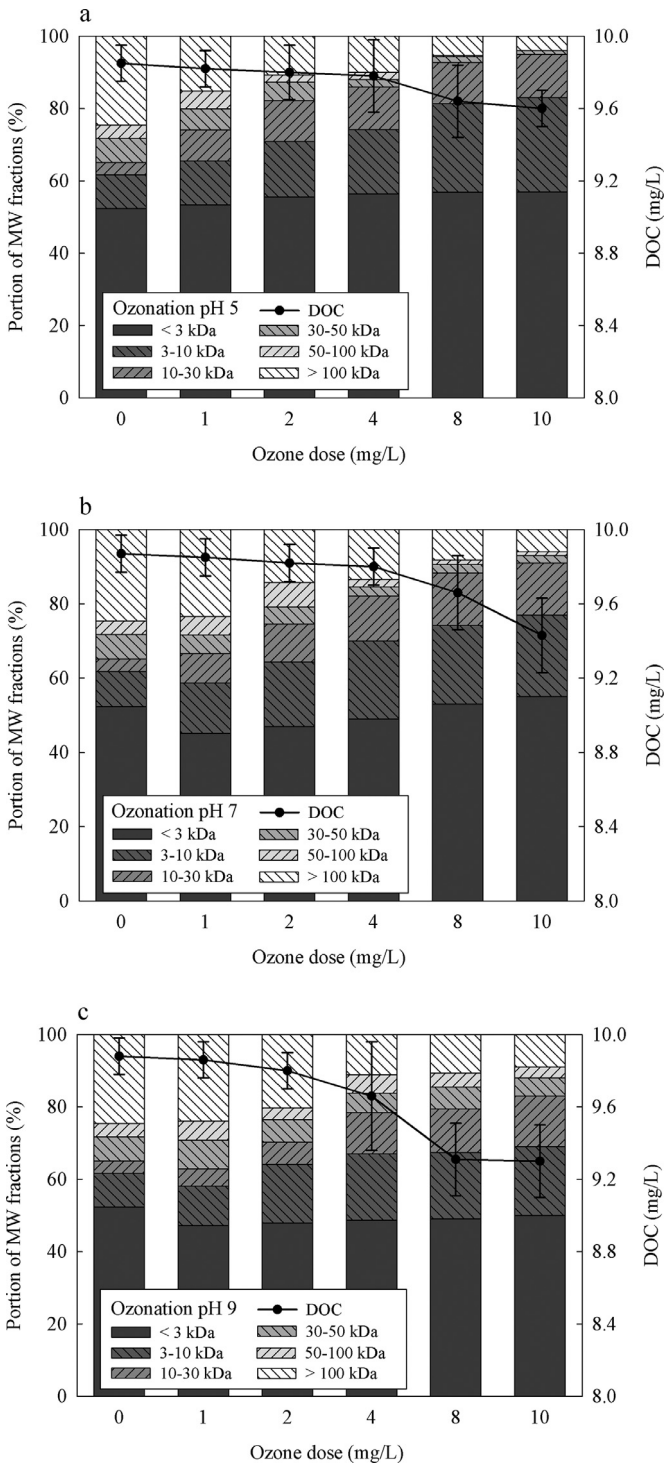

Fig. 1. – Effects of ozonation by 0–10 mg/L O_3 at different pH values—pH 5 (a), 7 (b) and 9 (c) —on the dissolved organic carbon (DOC) concentration and molecular weight (MW) distribution of *Microcystis aeruginosa* cellular organic matter (COM). Initial DOC = 10 mg/L, ozonation time 30 min. Errors represent the standard deviation from triplicate measurements.

9 (**Fig. 1c**), this process was accompanied by the partial mineralization of low-MW COM, as indicated by the DOC reduction and proportional decrease in the < 3 kDa fraction.

Similarly, HPSEC-RID analysis of raw COM (**Fig. 2a**) and COM samples after ozonation at 8 mg/L (0.8 mg O_3/mg DOC, **Fig. 2c**) performed under various pH values also revealed a decrease in apparent high-MW fractions and a corresponding increase in low-MW organics as a consequence of ozonation, and the effect was most pronounced at an ozonation pH of 5. The HPSEC-DAD results (**Fig. 2b, d**) illustrated significant reductions in high-MW compounds after ozonation as well. However, this reduction is probably also because ozone reacts quickly with double bonds in organic molecules and activated aromatic compounds (von Gunten, 2003), which provide the response at the operating wavelength of 280 nm. Interestingly, in contrast to the HPSEC-RID results, the HPSEC-DAD response increased with increasing pH (**Fig. 2d**), indicating enhanced ozone reactions with these structures in the acidic pH range. Decreased responses for UV-absorbing and fluorescent organics contained in *M. aeruginosa* EOM and IOM were also observed by Wei et al. (2016) after ozonation. Similarly, Widrig et al. (1996) observed the conversion of aromatic nitrogen to aliphatic nitrogen in proteinaceous EOM. A similar trend of a decreasing proportion of high-MW fractions and increasing proportions of medium- and low-MW fractions with increasing ozone dose was also observed by Paralkar and Edzwald (1996) for EOM of different species, by Wei et al. (2016) for EOM of *M. aeruginosa*, by Zhou et al. (2015) for EOM and IOM of *M. aeruginosa* and by (Xie et al., 2013) for organics released from *M. aeruginosa* cell surfaces during ozonation. For instance, Wei et al. (2016) found that in ozone-treated samples of *M. aeruginosa* EOM (DOC = 10.5 ± 0.5 mg/L), the amount of biopolymers (> 20 kDa) was reduced by 4%, 8%, 58% and 71% at ozone doses of 2, 5, 10 and 15 mg/L, respectively. The contents of building blocks (350–500 Da) and low-MW acids (< 350 Da) were also reduced after ozonation. In contrast, substances of 1–10 kDa MW increased due to the breakdown of biopolymers. These findings are also well supported by the results of studies on the ozonation of natural organic matter (Cheng et al., 2016; Huang et al., 2019) or model compounds such as humic acid, sodium alginate or bovine serum albumin (Bu et al., 2019; Cheng et al., 2016).

2.2. *Coagulation of* M. aeruginosa *COM*

Jar tests with coagulant doses ranging from 2.7 to 13.5 mg/L Al and 5.6 to 28.0 mg/L Fe revealed that the most suitable doses were 6.5 mg/L Al (0.024 mmol/mg DOC) and 13.0 mg/L Fe (0.023 mmol/mg DOC) for an initial COM concentration of 10 mg/L DOC. Increasing the coagulant dose (to 13.5 mg/L Al and 28.0 mg/L Fe) did not improve the coagulation efficiency and in turn increased undesired coagulant residuals (Appendix A **Fig. S2**).

Under the optimized coagulant doses, the highest DOC removals of 41–43% and 45–50% were attained within the pH range 6.0–7.0 and 5.8–6.8 for Al and Fe sulphate, respectively, while the coagulant residuals were sufficiently low, meeting the safe drinking water limit of 0.2 mg/L (Council Directive 98/83/EC) (Appendix A **Fig. S2**). Previously, *M. aeruginosa* COM was coagulated with similar maximum removal rates, i.e., 40% (pH 6.5–7.0) and 50% (pH 6.0–6.5), respectively, using approximately 0.021 mmol Al/mg DOC and 0.036 mmol Fe/mg DOC (Pivokonsky et al., 2009). Comparable removal efficiencies for different species were reported by some studies that investigated the coagulation of AOM in the absence of algal cells (Baresova et al., 2017; Henderson et al., 2010; Widrig et al., 1996). The current study confirmed that the optimum pH for COM coagulation lies in the acidic range where charge interactions between negatively charged COM and positively charged Al- or Fe-hydroxopolymers represent the underlying coagulation mechanism (Baresova et al., 2017; Pivokonsky et al., 2016). To illustrate, Baresova et al. (2017) achieved coagulation efficiencies ranging from 43% to 53% for COM of the cyanobacterium *Merismopedia tenuissima* within the pH range of 5.1–6.4 using 0.018 mmol Fe/mg DOC. Henderson et al. (2010) then observed removal efficiencies of 55%, 71% and 46% for EOM of *M. aeruginosa*, *C. vulgaris* and *Asterionella formosa* at pH 7 and doses of 0.044, 0.030 and 0.056 mmol

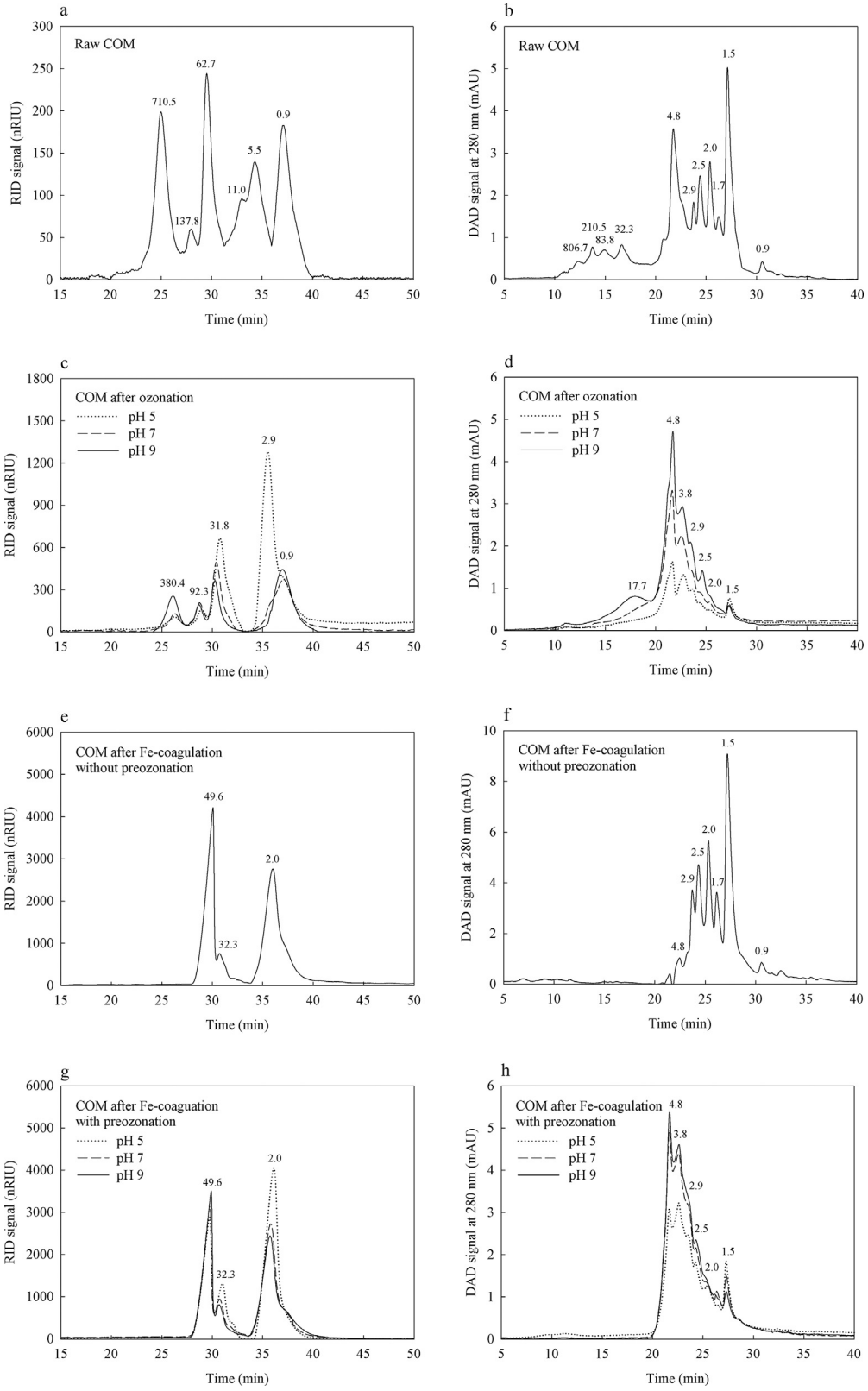

Fig. 2. – Apparent MW distribution of raw *M. aeruginosa* COM (a, b), COM after ozonation (c, d), and COM after optimized Fe coagulation without (e, f) and with preozonation by 0.8 mg O_3/mg DOC at pH 5, 7 and 9 (g, h), oxidation time 30 min. The results of high-performance size exclusion chromatography with refractive index (HPSEC-RID) and diode array detection (HPSEC-DAD) are depicted in (a, c, e, g) and (b, d, f, h), respectively. Numbers above peaks refer to the apparent MW in kDa.

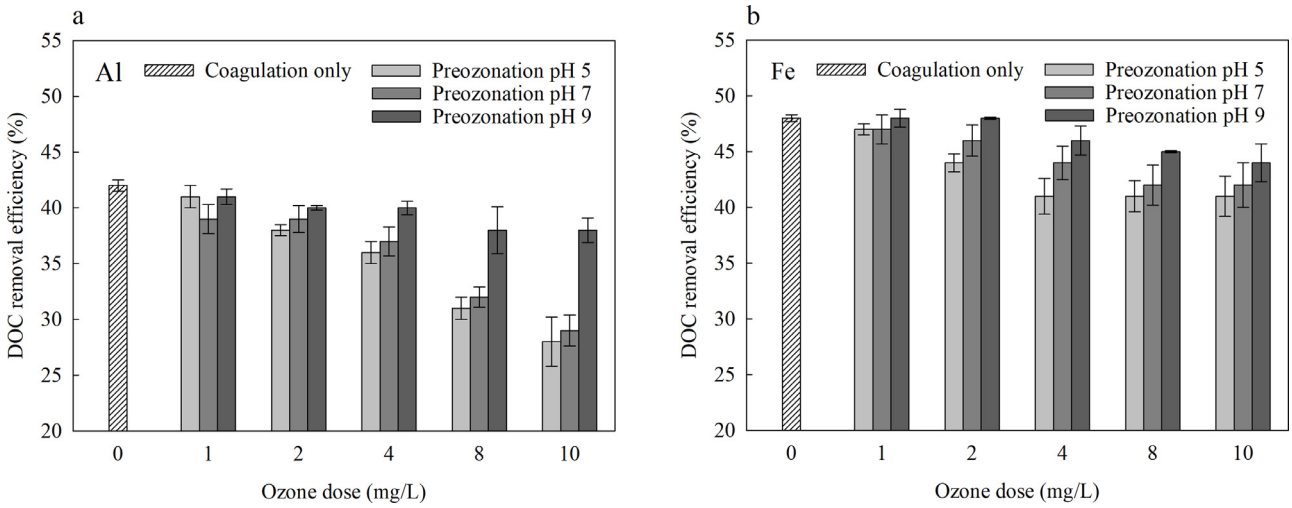

Fig. 3. – DOC removal efficiencies of *M. aeruginosa* COM after optimized coagulation by aluminium (a) or ferric sulphate (b) without and with preozonation by 1–10 mg/L O_3 at different preozonation pH values (5, 7 and 9). Initial DOC = 10 mg/L, preozonation time 30 min. Errors represent the standard deviation from triplicate measurements.

Al/mg DOC, respectively. Widrig et al. (1996), who examined the removal of EOM derived from *S. quadricauda*, *D. pulchellum* and *M. aeruginosa* by alum and ferric chloride (0.5 mmol Al/Fe per mg DOC), attained removals of approximately 25%, 50% and 20%, respectively, at pH 5, while the removals at pH 8 ranged from 5% to 10%. Ferric chloride performed better (5%) than alum at pH 5, which is consistent with the results of the current study.

Furthermore, HPSEC analyses of the apparent MW distribution illustrate that high-MW COM was removed by either Fe- or Al-based coagulation, while lower-MWs remained uncoagulated (**Fig. 2e, f** and Appendix A **Fig. S3a, S3b**, respectively). Specifically, protein-like compounds with an apparent MW under approximately 5 kDa were detected by DAD in COM samples after coagulation, while substances with an apparent MW < 50 kDa were detected by RID. The reluctance of low-MW components to coagulate was previously reported for COM of *M. tenuissima* (Baresova et al., 2017), COM peptides/proteins derived from *M. aeruginosa* (Naceradska et al., 2017; Pivokonsky et al., 2009), non-proteinaceous COM from the green alga *C. vulgaris* (Naceradska et al., 2019), and other organic compounds, such as humic substances (Matilainen et al., 2010).

2.3. *Coagulation of* M. aeruginosa *COM with ozone pretreatment*

Preozonation was employed before coagulation conducted under the optimized conditions (i.e., coagulant doses corresponding to 6.5 mg/L Al or 13.0 mg/L Fe and coagulation pH of 6.5 ± 0.2, see Section 2.2 and Appendix A **Fig. S2**). COM samples with an initial 10 mg/L DOC underwent ozone pretreatment with 1, 2, 4, 8 and 10 mg/L O_3 at pH values of 5, 7 and 9. The results show that preozonation led to decreased coagulation efficiency with increasing ozone dosage, and the effect was more pronounced at ozonation pH 5 and 7 than at pH 9, especially in the case of Al-based coagulation (**Fig. 3**). In the case of Al coagulation, preozonation with 10 mg/L O_3 decreased the average DOC removal efficiency from 42% to 28%, 29% and 38% at preozonation pH values of 5, 7 and 9, respectively (**Fig. 3a**). When the Fe coagulant was utilized, the average DOC removal decreased to a lesser extent, from 48% to 41%, 42% and 44% with preozonation by 10 mg/L O_3 at pH 5, 7 and 9, respectively (**Fig. 3b**). Both the residual Al and Fe concentrations were always below the safe drinking water limit of 0.2 mg/L (Council Directive 98/83/EC) without any observable pattern depending on ozonation conditions. The overall greater efficiency of Fe than Al coagulation can be ascribed to the higher effectiveness of Fe in the removal of medium- and low-MW organic matter fractions (Matilainen et al., 2010), the proportion of which increases after preozonation of the COM matrix, as illustrated by the changes in MW distribution.

The decreasing coagulation efficiencies with increasing ozone dose and decreasing ozonation pH value are mainly attributed to the degradation of high-MW COM to low-MW organics, which was consistently more pronounced at higher ozone doses and acidic ozonation pH values (see Section 2.1, **Fig. 1**). This result is in accordance with the HPSEC-RID results after ozonation alone (**Fig. 2c**) and after preozonation-coagulation (**Fig. 2g** for Fe and Appendix A **Fig. S3c** for Al), where more low-MW compounds in COM residuals were detected under preozonation at pH 5. Moreover, ozonation performed at pH 9 led to greater mineralization of DOC than that at pH 5 and 7 (**Fig. 1**). This mineralization also contributed to higher DOC removal after coagulation with ozone pretreatment at pH 9 than at pH 5 and 7. Alterations in coagulation may also stem from chemical changes in COM structure. Ozonation has been shown to increase ionisable functional groups in both EOM (Paralkar and Edzwald, 1996) and natural organic matter (Bose and Reckhow, 2007; von Gunten, 2003) and thus alter their negative charge. For instance, Paralkar and Edzwald (1996) observed an increase in carboxylic and phenolic charges with ozonation (ozone doses of 1 and 3 mg/L per 2.5–5.5 mg/L DOC) by hundreds of % in EOM and tens of % in alginic acid. They attributed the increase in charge mainly to the breakage of polysaccharides to monosaccharides followed by the oxidation of the alcoholic functions of monosaccharides, leading to the formation of aliphatic acids and aldehydes. In our study, the higher content of ionisable functional groups after ozonation might be expected to enhance coagulation performance, as the interaction of deprotonated carboxylic groups with positively charged Al/Fe coagulant species is usually recognized as an essential mechanism in the coagulation of COM (Baresova et al., 2017; Pivokonsky et al., 2016). However, as the increase in anionic charge is accompanied by the degradation of polymeric species to low-MW compounds, coagulation is hindered, and the residual DOC concentration increases. Furthermore, changes in the hydrophobic/hydrophilic character of compounds caused by ozonation may also affect coagulation performance since hydrophilic compounds are generally less amenable than hydrophobic compounds to coagulation (Baresova et al., 2017; Bu et al., 2019; Chiang et al., 2009; Pivokonsky et al., 2016). The conversion of hydrophobic to hydrophilic compounds after ozonation has been previously reported for natural organic mat-

ter (Cheng et al., 2016; Huang et al., 2019) and model compounds (Bu et al., 2019; Cheng et al., 2016). Widrig et al. (1996) observed the conversion of aromatic nitrogen to aliphatic nitrogen in EOM after ozonation. This conversion is consistent with our study, where the HPSEC-DAD results after preozonation-coagulation provided lower responses corresponding to protein-like substances due to the anticipated ozone reaction with double bonds and aromatic moieties in COM (**Fig. 2h** for Fe and Appendix A **Fig. S3d** for Al). Saturated compounds are typically formed as oxidation products, and their reactivity with ozone is very low (von Gunten, 2003), indicating that they remain in the water for further treatment.

Comparable studies on the ozonation and subsequent coagulation of AOM are very scarce. Widrig et al. (1996) investigated the preozonation-coagulation of EOM produced by *M. aeruginosa*, *D. pulchellum*, and *S. quadricauda*. In contrast to our findings, they reported that under certain conditions (ozone dose of 0.8 mg O_3/mg DOC applied at pH 8), preozonation increased the coagulation efficiency by 5%–15%, depending on the species. However, increased efficiency was achieved only under the highest examined dose of ferric chloride (27.5 mg Fe/mg DOC, i.e., 0.5 mmol Fe/mg DOC for an initial DOC of 6 mg/L), with no indication of residual Fe. At the median tested coagulant dose (2.8 mg Fe/mg DOC, i.e., 0.05 mmol Fe/mg DOC), the improvements in DOC removal resulting from preozonation were negligible (1%–2%). Moreover, they did not perform a consistent optimization of coagulation pH and thus possibly did not find optimal coagulation conditions. Nevertheless, as in the current study, Widrig et al. (1996) always attained better DOC removal when preozonation was conducted at higher pH (in their case at pH 8 rather than pH 5). Several authors investigated the effects of preozonation on DOC removal by coagulation in natural water samples. For example, Bose and Reckhow (2007) described a decrease in DOC coagulation efficiency for pond water (DOC 3.45 mg/L, 44% humic fraction, 22% hydrophilic neutral compounds) after preozonation conducted at pH 7. The deterioration was more significant with increasing ozone dose (from 0.3 to 1 mg O_3/mg DOC), which is consistent with our study. Chiang et al. (2009) coagulated lake water (DOC 7.8 mg/L, specific UV absorbance (SUVA) at 254 nm = 1.84 L/(mg m), 181 colour units (CU)) and reported that preozonation with 0.15, 0.45 and 0.85 mg O_3 per mg DOC at pH 5, 7 and 9 decreased DOC removal, and the effect was more pronounced at higher ozone doses and pH 5. This observation is also in agreement with the trends observed in our study.

The results clearly show that preozonation of COM deteriorates the coagulation efficiency at all tested ozonation pH values due to the degradation of COM to lower-MW compounds.

2.4. Degradation of microcystins in M. aeruginosa COM

M. aeruginosa produces a family of structurally similar microcystins (MCs), cyclic heptapeptide cyanotoxins with hepatotoxic effects (Bouhaddada et al., 2016; Díez-Quijada et al., 2019). We identified six different MC congeners as a natural part of *M. aeruginosa* COM, i.e., MC-RR, MC-YR, MC-LR, MC-LY, MC-LW, and MC-LF. The sum of these MCs accounted for approximately 24.15 µg/L in the raw COM sample with 10 mg/L DOC. MC-RR and MC-LR comprised the majority, followed by MC-YR, MC-LF, MC-LW and MC-LY in descending order (**Table 1**). Currently, MC-LR is the only cyanotoxin for which the World Health Organization has established a drinking water guideline value (WHO, 2011), and it has also been the most widely studied, as reviewed previously (Díez-Quijada et al., 2019). However, our results show that other MC congeners also deserve particular attention. For example, the MC-RR content (9.98 ± 0.36 µg/L) slightly exceeded that of MC-LR (8.66 ± 0.38 µg/L), and the MC-YR concentration was quite high (4.30 ± 0.35 µg/L). The significant content of congeners other than MC-LR was also reported for natural waters affected by cyanobacterial blooms (Bouhaddada et al., 2016; Díez-Quijada et al., 2019); thus, the COM sample used in the current study is representative in this regard.

2.4.1. Ozonation

COM samples comprising the natural mixture of MCs were subjected to ozonation under different conditions (i.e., ozone doses of 0.1–1.0 mg O_3/mg DOC and ozonation pH values of 5, 7 and 9). The degradation of all MC congeners by ozonation was both ozone dose- and pH-dependent (**Table 1**). In general, increasing ozone doses resulted in more efficient MC degradation. Interestingly, when using lower ozone doses, i.e., 0.1–0.4 mg O_3/mg DOC, the degradation rate of all MCs significantly decreased with increasing ozonation pH from 5 to 9. For example, at a fixed ozone dose of 0.1 mg O_3/mg DOC, the content of prevailing MCs (MC-RR, MC-LR, and MC-YR) after ozonation at pH 5 was approximately 5–10 times lower than those in the samples subjected to ozonation at pH 9. This pattern was even more pronounced at a dose of 0.2 mg O_3/mg DOC (7–18 times the difference). When using 0.4 mg O_3/mg DOC, MCs were not detected or were below the LOQ in the case of ozonation at pH 5 and 7, but at pH 9, the residual sum of MCs was still quite high (11.4 µg/L). The substantial effect of ozonation pH is attributable to the different actions of O_3 and ·OH, as well as the promotion of O_3 decomposition accompanied by ·OH formation at higher pH values (von Gunten, 2003). As shown in Appendix A **Fig. S1d**, in the presence of COM, O_3 decay after the reaction had started was much faster at pH 7 than at pH 5, and O_3 was hardly detectable after 3 min at pH 9. A deterioration in MC degradation due to an increase in ozonation pH has been reported previously (Al Momani et al., 2008; Rositano et al., 1998). For example, Rositano et al. (1998) oxidized MC-LR (250 µg/L) in *M. aeruginosa* COM (DOC 8.5 mg/L) with an ozone dose of 1 mg/L at pH values of 2.5–9.0. While no residual toxins were detected at pH 2.5–7.5, MC-LR residuals appeared when ozonation was performed at pH > 7.5.

MCs are highly amenable to react with O_3 owing to the presence of double bonds and amino groups in MC molecules, i.e., structures that are easily attacked by this oxidizing agent (Onstad et al., 2007; von Gunten, 2003). However, the capability of ·OH to degrade MCs must not be neglected. The second-order rate constant of ·OH with MC-LR was calculated to be 5 orders of magnitude higher than that of O_3 (Onstad et al., 2007). Moreover, the main reaction chains involved in MC degradation (Adda and Mdha degradation pathways) can result from both O_3 and ·OH oxidation (Chang et al., 2015). The decrease in MC degradation at higher pH values is thus associated with the different interactions of O_3 and ·OH with the COM matrix. While O_3 reacts selectively, ·OH is a powerful non-selective oxidant (von Gunten, 2003; Widrig et al., 1996) and is rapidly consumed by COM (Chang et al., 2015; Onstad et al., 2007). Onstad et al. (2007) showed that the contribution of ·OH to MC-LR degradation (at pH 8 and initial MC-LR concentration 0.15 µmol/L) decreases with increasing NOM concentration in natural lake water samples. In lake water with a DOC of 1.6 mg/L, sole O_3 (·OH was scavenged by added *tert*-butanol) eliminated MC-LR at an ozone dose of 2 mg/L, while an ozone dose as low as 0.2 mg/L was sufficient when MC-LR was oxidized by O_3 + ·OH (no scavenging applied). In contrast, in lake water with 13 mg/L DOC, 2 mg/L ozone was needed to oxidize MC-LR in both cases (sole O_3 and O_3 + ·OH) because ·OH radicals were almost completely consumed by NOM. Furthermore, decreased degradation rates of MCs and other cyanotoxins were recorded when they were spiked into either natural water samples (Rodríguez et al., 2007; Rositano et al., 2001) or algal supernatants (Miao and Tao, 2009; Rositano et al., 1998) compared to

Table 1. – Microcystin concentrations (μg/L) in *Microcystis aeruginosa* COM samples before and after ozonation by 0–10 mg/L O_3 at different pH values, after Al- and Fe-based coagulation and after preozonation-coagulation. Initial DOC = 10 mg/L, oxidation time 30 min.

Ozone dose (mg O_3/mg DOC)	Ozonation pH	MC-RR	MC-YR	MC-LR	MC-LY	MC-LW	MC-LF
Ozonation alone							
0	**–**	9.98 ± 0.36	4.30 ± 0.35	8.66 ± 0.38	0.30 ± 0.05	0.45 ± 0.02	0.46 ± 0.02
0.1	**5**	1.12 ± 0.01	0.69 ± 0.02	0.76 ± 0.01	< LOQ	< LOQ	< LOQ
	7	6.09 ± 0.19	3.09 ± 0.15	6.69 ± 0.28	0.20 ± 0.02	< LOQ	0.44 ± 0.04
	9	8.45 ± 0.43	3.52 ± 0.21	7.96 ± 0.49	0.28 ± 0.03	0.41 ± 0.02	0.46 ± 0.05
0.2	**5**	0.69 ± 0.04	0.37 ± 0.08	0.23 ± 0.07	< LOQ	n.d.	< LOQ
	7	1.83 ± 0.16	0.97 ± 0.04	1.41 ± 0.18	< LOQ	< LOQ	0.39 ± 0.01
	9	6.51 ± 0.27	2.59 ± 0.13	6.54 ± 0.58	0.24 ± 0.05	< LOQ	0.42 ± 0.03
0.4	**5**	< LOQ	n.d.	n.d.	n.d.	n.d.	n.d.
	7	< LOQ	n.d.	n.d.	n.d.	n.d.	n.d.
	9	4.27 ± 0.21	1.69 ± 0.17	4.79 ± 0.12	0.24 ± 0.03	< LOQ	0.41 ± 0.07
0.8	**5**	n.d.	n.d.	n.d.	n.d.	n.d.	n.d.
	7	n.d.	n.d.	n.d.	n.d.	n.d.	n.d.
	9	n.d.	n.d.	n.d.	n.d.	n.d.	n.d.
1.0	**5**	n.d.	n.d.	n.d.	n.d.	n.d.	n.d.
	7	n.d.	n.d.	n.d.	n.d.	n.d.	n.d.
	9	n.d.	n.d.	n.d.	n.d.	n.d.	n.d.
Prezonation + Al coagulation							
0	**–**	8.02 ± 0.22	3.67 ± 0.36	8.01 ± 0.59	0.30 ± 0.02	0.43 ± 0.06	< LOQ
0.1	**5**	0.68 ± 0.01	0.28 ± 0.04	0.41 ± 0.04	< LOQ	n.d.	< LOQ
	7	6.83 ± 0.47	3.25 ± 0.23	6.54 ± 0.44	0.21 ± 0.01	< LOQ	< LOQ
	9	6.46 ± 0.35	3.26 ± 0.38	5.59 ± 0.57	0.22 ± 0.01	< LOQ	< LOQ
0.2	**5**	< LOQ	n.d.	n.d.	n.d.	n.d.	n.d.
	7	1.36 ± 0.06	0.62 ± 0.03	1.06 ± 0.05	< LOQ	< LOQ	< LOQ
	9	5.67 ± 0.43	2.57 ± 0.36	6.03 ± 0.55	0.24 ± 0.02	< LOQ	< LOQ
0.4	**5**	n.d.	n.d.	n.d.	n.d.	n.d.	n.d.
	7	n.d.	n.d.	n.d.	n.d.	n.d.	n.d.
	9	< LOQ	< LOQ	< LOQ	n.d.	n.d.	< LOQ
0.8	**5**	n.d.	n.d.	n.d.	n.d.	n.d.	n.d.
	7	n.d.	n.d.	n.d.	n.d.	n.d.	n.d.
	9	n.d.	n.d.	n.d.	n.d.	n.d.	n.d.
1.0	**5**	n.d.	n.d.	n.d.	n.d.	n.d.	n.d.
	7	n.d.	n.d.	n.d.	n.d.	n.d.	n.d.
	9	n.d.	n.d.	n.d.	n.d.	n.d.	n.d.
Prezonation + Fe coagulation							
0	**–**	7.34 ± 0.34	3.55 ± 0.26	8.19 ± 0.59	0.29 ± 0.05	0.45 ± 0.16	0.32 ± 0.04
0.1	**5**	0.94 ± 0.03	0.41 ± 0.06	0.58 ± 0.05	< LOQ	n.d.	< LOQ
	7	4.55 ± 0.45	1.39 ± 0.23	2.87 ± 0.38	< LOQ	< LOQ	< LOQ
	9	6.83 ± 0.32	2.33 ± 0.36	5.96 ± 0.55	0.17 ± 0.01	< LOQ	< LOQ
0.2	**5**	< LOQ	n.d.	n.d.	n.d.	n.d.	n.d.
	7	1.61 ± 0.06	0.51 ± 0.04	1.30 ± 0.07	< LOQ	< LOQ	< LOQ
	9	7.26 ± 0.39	2.62 ± 0.32	6.78 ± 0.58	0.18 ± 0.02	< LOQ	< LOQ
0.4	**5**	n.d.	n.d.	n.d.	n.d.	n.d.	n.d.
	7	n.d.	n.d.	n.d.	n.d.	n.d.	n.d.
	9	1.19 ± 0.01	0.37 ± 0.03	0.75 ± 0.01	< LOQ	< LOQ	0.20 ± 0.01
0.8	**5**	< LOQ	n.d.	n.d.	n.d.	n.d.	n.d.
	7	n.d.	n.d.	n.d.	n.d.	n.d.	n.d.
	9	n.d.	n.d.	n.d.	n.d.	n.d.	n.d.
1.0	**5**	n.d.	n.d.	n.d.	n.d.	n.d.	n.d.
	7	n.d.	n.d.	n.d.	n.d.	n.d.	n.d.
	9	n.d.	n.d.	n.d.	n.d.	n.d.	n.d.

DOC: dissolved organic carbon; COM: cellular organic matter; MC-RR, MC-YR, MC-LR, MC-LY, MC-LW, and MC-LF: microcystin congeners; n.d.: not detectable; LOQ: limit of quantification.

Limits of detection (LODs) and LOQs were as follows (in μg/L): 0.5 and 2.0 for MC-RR, 1.0 and 2.0 for MC-YR, 1.0 and 1.5 for MC-LR, 0.8 and 1.0 for MC-LY, 2.0 and 4.0 for MC-LW, and 1.0 and 3.0 for MC-LF, respectively.

COM samples were pre-concentrated before MC analyses. The presented data support adequately back-calculated MC concentrations (μg/L); errors represent the standard deviation from triplicate measurements.

the degradation rates in samples without NOM content. As an example, in a study by Miao and Tao (2009), pure MC-LR and MC-RR (15 μg/L) were almost entirely removed by 3 mg/L ozone in 10 min, while in the presence of *M. aeruginosa* EOM (DOC 2.35 mg/L), approximately 20% of MC-LR and 10% of MC-RR were not oxidized. Moreover, in a study by Rositano et al. (1998), a sample containing 166 μg/L pure MC-LR was oxidized to below the detection limit by less than 0.2 mg/L ozone in 4 min. When 220 μg/L MC-LR was oxidized by ozone in *M. aeruginosa* COM (DOC 8.5 mg/L, pH 6.8), an increased ozone dose of 1.0 mg/L was required to eliminate MC-LR in 5 min.

When using the highest ozone doses in our study, i.e., $\geq$ 0.8 mg O_3/mg DOC, no MCs were detected at any ozonation pH. This result is also well illustrated by the vanishing of a 0.9 kDa peak attributable to MCs (Naceradska et al., 2017) from the HPSEC-DAD chromatograms after ozonation (**Fig. 2d**). In general, the results imply that when using a sufficient ozone dose, MCs can be efficiently degraded in a natural COM matrix, while lower ozone doses are required at acidic or neutral pH than under alkaline pH conditions.

2.4.2. Coagulation

MCs were also measured after sole coagulation of COM (initial DOC 10 mg/L) by both Al and Fe coagulants under the optimized conditions that resulted in the highest DOC removal (see Section 2.3, Appendix A **Fig. S2**). Although the concentrations of MCs slightly decreased after the treatment, coagulation alone was not sufficient for MC removal, as shown in **Table 1**. Samples after Al- and Fe-based coagulation still contained 8.01 $\pm$ 0.59 and 8.19 $\pm$ 0.59 μg/L MC-LR, respectively, thus exceeding by more than eight times the guideline value for the MC-LR content in drinking water of 1 μg/L (WHO, 2011). Moreover, similarly high concentrations of MC-RR were detected, and the sum of MCs after Al and Fe coagulation was 20.43 and 20.14 μg/L, respectively. The overall removal of MCs by coagulation was approximately 17%, although the DOC removal was 41–50%. This result is not surprising since conventional treatment processes have been shown to be ineffective in removing extracellular MCs (Himberg et al., 1989; Shang et al., 2018). Low MC removal is attributable to the fact that toxins are low-MW compounds, and the reluctance of the low-MW fraction to coagulate was previously documented for different kinds of AOM and NOM (e.g., Baresova et al., 2017; Henderson et al., 2010; Matilainen et al., 2010; Naceradska et al., 2019). Significant concentrations of MCs (1.4–11.2 μg/L as the sum of MC-LR, MC-RR and MC-YR for an initial 1–8 mg/L DOC) after coagulation without any additional treatment were also reported by Naceradska et al. (2017), who coagulated the peptide/protein COM fraction of *M. aeruginosa*, obtaining DOC removals of 55–82%.

2.4.3. Preozonation-coagulation

Microcystin concentrations determined after preozonation-coagulation (**Table 1**) showed similar patterns as the concentrations obtained after ozonation alone. The removal of MCs increased with rising ozone dose, and at $\leq$ 0.4 mg O_3/mg DOC, the influence of preozonation pH was noticeable. Again, the degradation rate of MCs decreased with increasing pH from 5 to 9. However, the overall removal of MCs by preozonation-coagulation was slightly higher than that by ozonation only conducted under the same conditions (ozone dose and ozonation pH), owing to partial toxin removal by coagulation itself.

The results show that ozone treatment efficiently degrades MCs contained in the natural COM matrix. However, complete MC elimination is achieved at the cost of a decreased coagulation efficiency of COM. These findings indicate that the pros and cons of including an ozonation step should be carefully considered when treating COM-containing waters and that attention must be paid to optimizing the ozonation conditions.

3. Conclusion

Investigating the effects of ozonation on dissolved COM from *M. aeruginosa* and its coagulation has shown the following: (1) A slight DOC decrease was observed after COM ozonation; however, ozonation led to the decomposition of high-MW to low-MW fractions, and the effect was most pronounced at higher ozone doses and acidic pH. (2) Preozonation decreased the coagulation efficiency, and the effect was more noticeable with increasing ozone dosage and decreasing ozonation pH; Fe-based coagulation was less affected than Al-based coagulation. (3) Ozonation completely eliminated microcystins (MC-LR, MC-RR, MC-YR, MC-LW, MC-LF and MC-LY); the ozonation pH governed microcystin degradation at lower ozone doses; and preozonation-coagulation followed a similar pattern.

These results indicate that ozonation is not unequivocally a suitable step before the coagulation of *M. aeruginosa* COM. Ozone has proven to be very effective in removing microcystins contained in a natural COM matrix, but it brings about an undesirable reduction in coagulation effectiveness. When preozonation is applied prior to coagulation, attention must be paid to optimizing the ozonation conditions to minimize the deterioration of coagulation. A question then arises whether ozonation would be a more convenient treatment for residual COM when employed after coagulation rather than before coagulation, i.e., whether it would destroy microcystins with the same or increased efficiency and reduce the concentration of total residual organics. Further research is therefore required in this regard.

Acknowledgments

This work was supported by the Czech Science Foundation (No. GA18-14445S) and by the institutional support of the Czech Academy of Sciences (RVO: 67985874).

Appendix A Supplementary data

Supplementary material associated with this article can be found, in the online version, at doi:10.1016/j.jes.2020.05.031.

References

Al Momani, F., Smith, D.W., Gamal El-Din, M., 2008. Degradation of cyanobacteria toxin by advanced oxidation processes. J. Hazard. Mater. 150 (2), 238–249.
Baird, R.B., Eaton, A.D., Rice, E.W., 2017. Standard Methods for the Examination of Water and Wastewater, 23rd edn. American Public Health Association (APHA), American Water Works Association (AWWA) and Water Environment Federation (WEF), Washington, DC, USA.
Baresova, M., Pivokonsky, M., Novotna, K., Naceradska, J., Branyik, T., 2017. An application of cellular organic matter to coagulation of cyanobacterial cells (*Merismopedia tenuissima*). Water Res. 122, 70–77.
Bose, P., Reckhow, D.A., 2007. The effect of ozonation on natural organic matter removal by alum coagulation. Water Res. 41, 1516–1524.
Bouhaddada, R., Nélieu, S., Nasri, H., Delarue, G., Bouaïcha, N., 2016. High diversity of microcystins in a *Microcystis* bloom from an Algerian lake. Environ. Pollut. 216, 836–844.
Bu, F., Gao, B., Shen, X., Wang, W., Yue, Q., 2019. The combination of coagulation and ozonation as a pre-treatment of ultrafiltration in water treatment. Chemosphere 231, 349–356.
Chang, J., Chen, Z.-L., Wang, Z., Kang, J., Chen, Q., Yuan, L., et al., 2015. Oxidation of microcystin-LR in water by ozone combined with UV radiation: The removal and degradation pathway. Chem. Eng. J. 276, 97–105.
Cheng, X., Liang, H., Ding, A., Qu, F., Shao, S., Liu, B., et al., 2016. Effects of pre-ozonation on the ultrafiltration of different natural organic matter (NOM) fractions: Membrane fouling mitigation, prediction and mechanism. J. Membr. Sci. 505, 15–25.
Chiang, P.-C., Chang, E.-E., Chang, P.-C., Huang, C.-P., 2009. Effects of pre-ozonation on the removal of THM precursors by coagulation. Sci. Total Environ. 407, 5735–5742.
Coral, L.A., Zamyadi, A., Barbeau, B., Bassetti, F.J., Lapolli, F.R., Prévost, J., 2013. Oxidation of *Microcystis aeruginosa* and *Anabaena flos-aquae* by ozone: Impacts on cell integrity and chlorination by-product formation. Water Res. 47 (9), 2983–2994.

Council Directive 98/83/EC of 3 November 1998 on the quality of water intended for human consumption, Official Journal of the European Communities, L 330/32-54, 5.12.1998.
Díez-Quijada, L., Prieto, A.I., Guzmán-Guillén, R., Jos, A., Cameán, A.M., 2019. Occurrence and toxicity of microcystin congeners other than MC-LR and MC-RR: A review. Food Chem. Toxicol. 125, 106–132.
Henderson, R.K., Parsons, S.A., Jefferson, B., 2010. The impact of differing cell and algogenic organic matter (AOM) characteristics on the coagulation and flotation of algae. Water Res. 44 (12), 3617–3624.
Himberg, K., Keijola, A.-M., Hiisvirta, L., Pyysalo, H., Sivonen, K., 1989. The effect of water treatment processes on the removal of hepatotoxins from *Microcystis* and *Oscillatoria* cyanobacteria: A laboratory study. Water Res. 23 (8), 979–984.
Huang, W., Lv, W., Zhou, W., Hu, M., Dong, B., 2019. Investigation of the fouling behaviors correlating to water characteristics during the ultrafiltration with ozone treatment. Sci. Total Environ. 676, 53–61.
Matilainen, A., Vepsäläinen, M., Sillanpää, M., 2010. Natural organic matter removal by coagulation during drinking water treatment: A review. Adv. Colloid Interface Sci. 159 (2), 189–197.
Miao, H., Tao, W., 2009. The mechanisms of ozonation on cyanobacteria and its toxins removal. Sep. Purif. Technol. 66, 187–193.
Naceradska, J., Novotna, K., Cermakova, L., Cajthaml, T., Pivokonsky, M., 2019. Investigating the coagulation of non-proteinaceous algal organic matter: Optimization of coagulation performance and identification of removal mechanisms. J. Environ. Sci. 79, 25–34.
Naceradska, J., Pivokonsky, M., Pivokonska, L., Baresova, M., Henderson, R.K., Zamyadi, A., et al., 2017. The impact of pre-oxidation with potassium permanganate on cyanobacterial organic matter removal by coagulation. Water Res. 114, 42–49.
Newcombe, G., Nicholson, B., 2004. Water treatment options for dissolved cyanotoxins. J. Water Supply Res. Technol. – AQUA 53 (4), 227–239.
Onstad, G.D., Strauch, S., Meriluoto, J., Codd, G.A., von Gunten, U., 2007. Selective oxidation of key functional groups in cyanotoxins during drinking water ozonation. Environ. Sci. Technol. 41, 4397–4404.
Paralkar, A., Edzwald, J.K., 1996. Effect of ozone on EOM and coagulation. J. Am. Water Works Assoc. 88 (4), 143–154.
Pivokonsky, M., Naceradska, J., Kopecka, I., Baresova, M., Jefferson, B., Li, X., et al., 2016. The impact of algogenic organic matter on water treatment plant operation and water quality: A review. Crit. Rev. Environ. Sci. Tech. 46 (4), 291–335.
Pivokonsky, M., Pivokonska, L., Baumeltova, J., Bubakova, P., 2009. The effect of cellular organic matter produced by cyanobacteria *Microcystis aeruginosa* on water purification. J. Hydrol. Hydromech. 57 (2), 121–129.
Plummer, J.D., Edzwald, J.K., 2002. Effects of chlorine and ozone on algal cell properties and removal of algae by coagulation. J. Water Supply Res. Technol. – AQUA 51, 307–318.
Pranowo, R., Lee, D.J., Liu, J.C., Chang, J.S., 2013. Effect of O_3 and O_3/H_2O_2 on algae harvesting using chitosan. Water Sci. Technol. 67 (6), 1294–1301.
Rodríguez, E., Onstad, G.D., Kull, T.P.J., Metcalf, J.S., Acero, J.L., von Gunten, U., 2007. Oxidative elimination of cyanotoxins: Comparison of ozone, chlorine, chlorine dioxide and permanganate. Water Res. 41 (15), 3381–3393.
Rositano, J., Newcombe, G., Nicholson, B., Sztajnbok, P., 2001. Ozonation of NOM and algal toxins in four treated waters. Water Res. 35, 23–32.
Rositano, J., Nicholson, B.C., Pieronne, P., 1998. Destruction of cyanobacterial toxins by ozone. Ozone Sci. Eng. 20, 223–238.
Shang, L., Feng, M., Xu, X., Liu, F., Ke, F., Li, W., 2018. Co-occurrence of microcystins and taste-and-odor compounds in drinking water source and their removal in a full-scale drinking water treatment plant. Toxins (Basel) 10 (1), 26–43.
Sharma, V.K., Triantis, T.M., Antoniou, M.G., He, X., Pelaez, M., Han, C., et al., 2012. Destruction of microcystins by conventional and advanced oxidation processes: A review. Sep. Purif. Technol. 91, 3–17.
von Gunten, U., 2003. Ozonation of drinking water: Part I. Oxidation kinetics and product formation. Water Res. 37, 1443–1467.
Wei, D., Tao, Y., Zhang, Z., Zhang, X., 2016. Effect of pre-ozonation on mitigation of ceramic UF membrane fouling caused by algal extracellular organic matters. Chem. Eng. J. 294, 157–166.
Wen, G., Zhu, H., Wei, Y., Huang, T., Ma, J., 2017. Formation of assimilable organic carbon during the oxidation of water containing *Microcystis aeruginosa* by ozone and an advanced oxidation process using ozone/hydrogen peroxide. Chem. Eng. J. 307, 364–371.
Westrick, J.A., Szlag, D.C., Southwell, B.J., Sinclair, J., 2010. A review of cyanobacteria and cyanotoxins removal/inactivation in drinking water treatment. Anal. Bioanal. Chem. 397 (5), 1705–1714.
Widrig, D.L., Gray, K.A., McAuliffe, K.S., 1996. Removal of algal-derived organic material by preozonation and coagulation: Monitoring changes in organic quality by pyrolysis-GC–MS. Water Res. 30 (11), 2621–2632.
WHO (World Health Organization), 2011. Guidelines for Drinking-Water Quality, 4th edn. World Health Organization, Geneva, Switzerland Available: http://www.who.int/water_sanitation_health/publications/dwq-guidelines-4/en/ .
Xie, P., Ma, J., Fang, J., Guan, Y., Yue, S., Li, X., et al., 2013. Comparison of permanganate preoxidation and preozonation on algae containing water: Cell integrity, characteristics, and chlorinated disinfection byproduct formation. Environ. Sci. Technol. 47, 14051–14061.
Zhang, X., Amendola, P., Hewson, J.C., Sommerfeld, M., Hu, Q., 2012. Influence of growth phase on harvesting of *Chlorella zofingiensis* by dissolved air flotation. Bioresour. Technol 116, 477–484.
Zhou, S., Zhu, S., Shao, Y., Gao, N., 2015. Characteristics of C-, N-DBPs formation from algal organic matter: Role of molecular weight fractions and impacts of pre-ozonation. Water Res. 72, 381–390.

Appendix A. Supplementary data

The impact of preozonation on the coagulation of cellular organic matter produced by *Microcystis aeruginosa* and its toxin degradation

Magdalena Barešová[1], Jana Načeradská[1], Kateřina Novotná[1], Lenka Čermáková[1], Martin Pivokonský[1,*]

1. Institute of Hydrodynamics of the Czech Academy of Sciences, Pod Patankou 5, 166 12 Prague 6, Czech Republic

---

* Corresponding author. E-mail: pivo@ih.cas.cz (M. Pivokonský)

This supplementary data contains the following section and figures:

S1 Ozone decay

Fig. S1 Ozone decay curves for ozone doses of 2 (a), 4 (b) and 8 mg/L (c) at pH 5, 7 and 9 in the absence of cellular organic matter (COM) and for ozone doses of 2, 4 and 8 mg/L at pH 5 and dose of 8 mg/L at pH 7 in the presence of COM (d). Initial dissolved organic carbon (DOC) concentration = 10 mg/L.

Fig. S2 Residual DOC and Al/Fe concentrations after coagulation of *Microcystis aeruginosa* COM as a function of pH value for the optimized doses of aluminium – 6.5 mg/L Al (a, c) and ferric sulphate – 13 mg/L Fe (b, d), depicting also selected low and high coagulant doses from the tested Al/Fe concentration range. Jar tests carried out in triplicate with the same COM matrix of an initial DOC of 10 mg/L exhibited very similar courses. Hence, for conciseness, we only report the results from one representative experiment.

Fig. S3 Apparent molecular weight (MW) distribution of *M. aeruginosa* COM after optimized Al coagulation without (a, b) and with preozonation by 0.8 mg O_3/mg DOC at pH 5, 7 and 9 (c, d), preozonation time 30 min. The results of high-performance size exclusion chromatography with refractive index (HPSEC-RID) and diode array detection (HPSEC-RID) are depicted in (a, c) and (b, d), respectively. Numbers above peaks refer to the apparent MW in kDa.

S1 Ozone decay

Ozone decay was monitored under various ozone doses (1, 2, 4 and 8 mg/L ~ 0.1, 0.2, 0.4 and 0.8 mg O_3 per mg DOC) and a range of ozonation pH values (pH 5, 7 and 9). Parallel experiments were performed in the absence and presence of COM at an initial DOC concentration of 10 mg/L. Ozone residuals were measured after 3, 5, 7, and 10 min and then in 10-min intervals until ozone was detected in the samples.

The ozone decay curves in the absence of COM are depicted in **Fig. S1a-c**, and those in the presence of COM are summarized in **Fig. S1d**. In the case of the lowest ozone dose (1 mg/L), no ozone (concentration < 0.01 mg/L O_3) was detectable after 3 min; therefore, curves for this dosage were not constructed. In agreement with the generally accepted theory (von Gunten, 2003), ozone decomposition was greatly accelerated under alkaline pH conditions, as evidenced by the significant differences between the decay curves for pH 5 and 7 and that of pH 9. As shown in **Fig. S1d**, COM obviously consumed significant amounts of ozone, and no ozone was detected after relatively short contact times. In the presence of COM, ozone decay curves could be constructed only for ozone doses of 2, 4 and 8 mg/L at pH 5 and for ozone dose of 8 mg/L at pH 7. For the other investigated conditions, no ozone (concentration < 0.01 mg/L O_3) was detectable after 3 min; thus, corresponding decay curves were not constructed. Similarly, in studies investigating the ozonation of algal suspensions, increased ozone decay was also observed with an increasing number of algal cells (Coral et al., 2013; Wen et al., 2017), indicating that organics bound to algal cells consumed ozone and accelerated ozone decay.

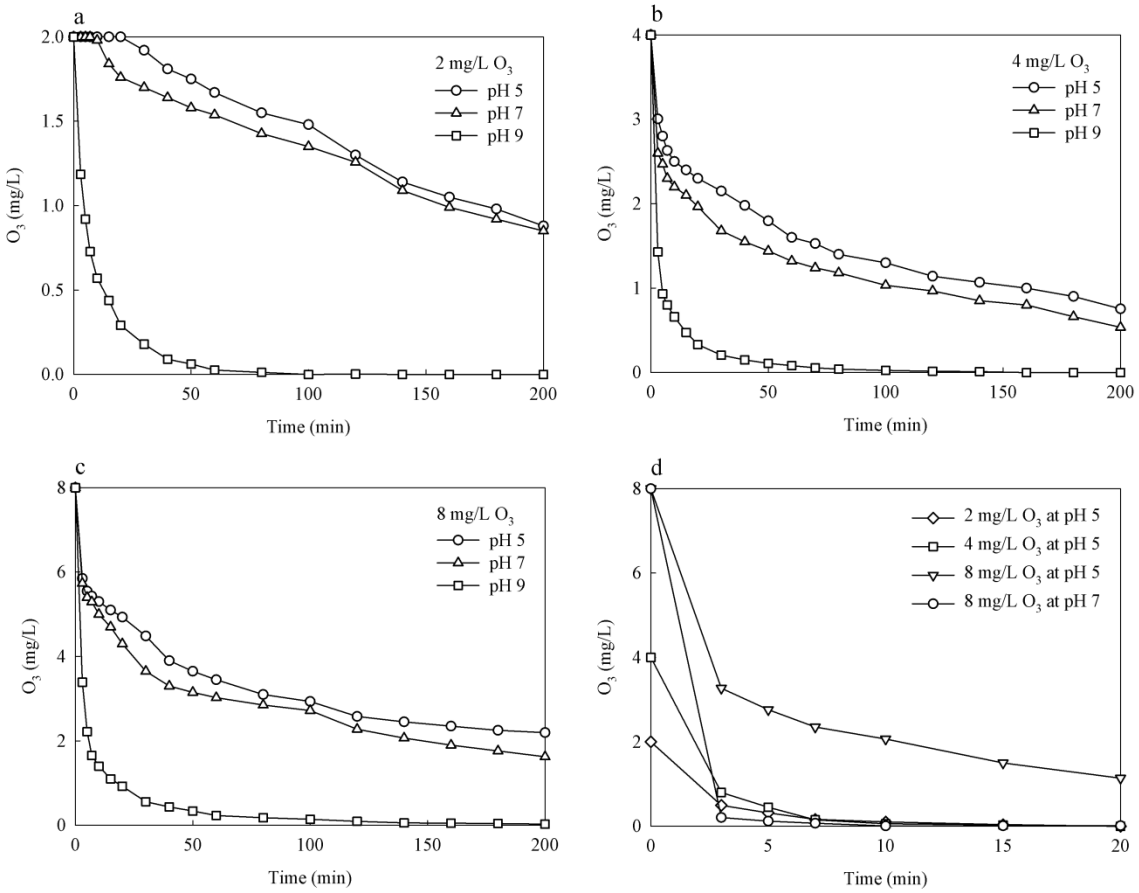

Fig. S1 Ozone decay curves for ozone doses of 2 (a), 4 (b) and 8 mg/L (c) at pH 5, 7 and 9 in the absence of cellular organic matter (COM) and for ozone doses of 2, 4 and 8 mg/L at pH 5 and dose of 8 mg/L at pH 7 in the presence of COM (d). Initial dissolved organic carbon (DOC) concentration = 10 mg/L.

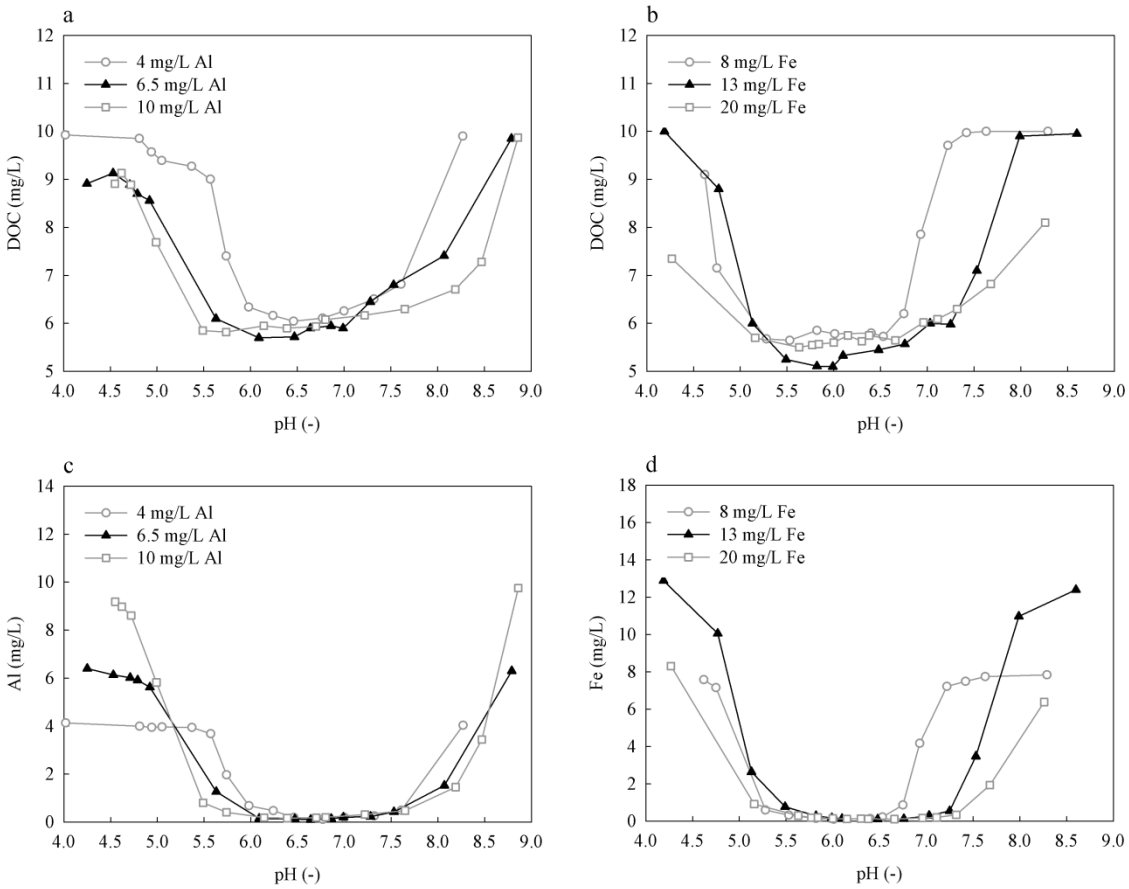

Fig. S2 Residual DOC and Al/Fe concentrations after coagulation of *Microcystis aeruginosa* COM as a function of pH value for the optimized doses of aluminium – 6.5 mg/L Al (a, c) and ferric sulphate – 13 mg/L Fe (b, d), depicting also selected low and high coagulant doses from the tested Al/Fe concentration range. Jar tests carried out in triplicate with the same COM matrix of an initial DOC of 10 mg/L exhibited very similar courses. Hence, for conciseness, we only report the results from one representative experiment.

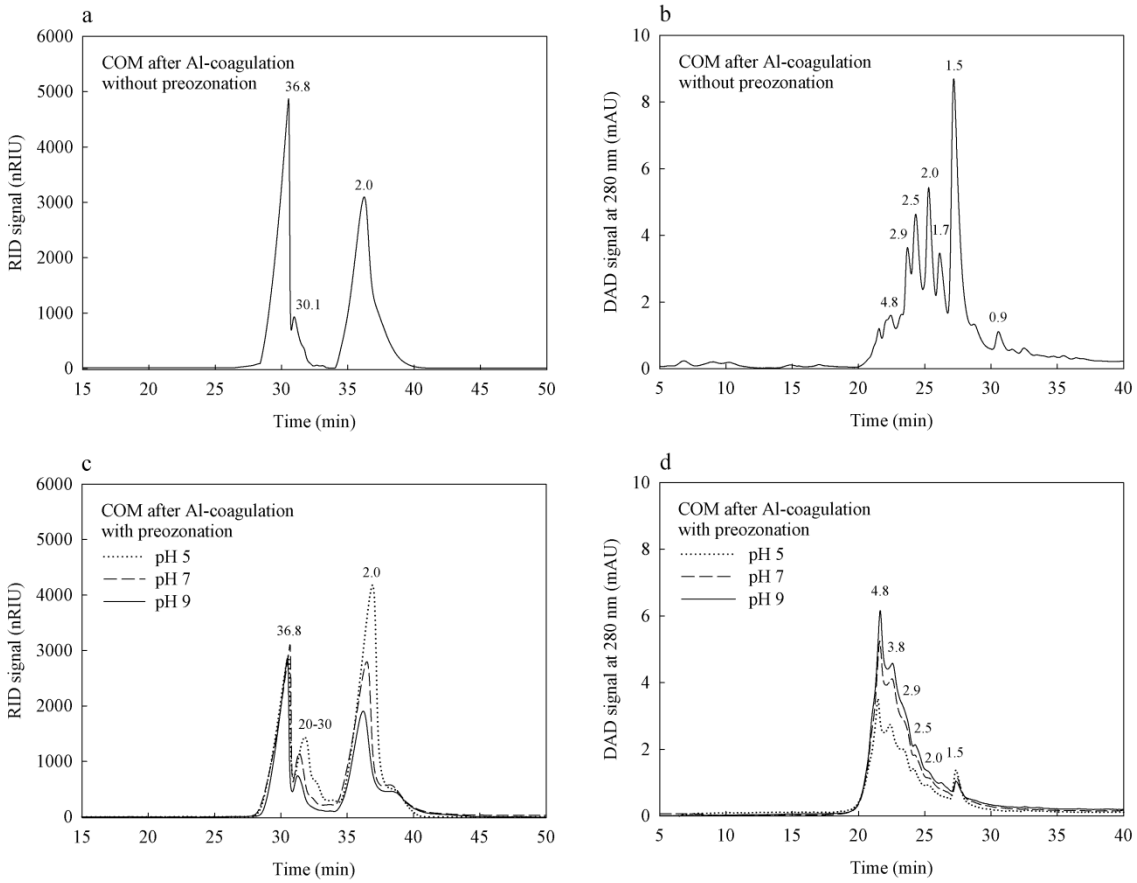

Fig. S3 Apparent molecular weight (MW) distribution of *M. aeruginosa* COM after optimized Al coagulation without (a, b) and with preozonation by 0.8 mg O_3/mg DOC at pH 5, 7 and 9 (c, d), preozonation time 30 min. The results of high-performance size exclusion chromatography with refractive index (HPSEC-RID) and diode array detection (HPSEC-RID) are depicted in (a, c) and (b, d), respectively. Numbers above peaks refer to the apparent MW in kDa.

References

Coral, L.A., Zamyadi, A., Barbeau, B., Bassetti, F.J., Lapolli, F.R., Prévost, J., 2013. Oxidation of *Microcystis aeruginosa* and *Anabaena flos-aquae* by ozone: Impacts on cell integrity and chlorination by-product formation. Water Res. 47(9), 2983–2994. https://doi.org/10.1016/j.watres.2013.03.012

von Gunten, U., 2003. Ozonation of drinking water: Part I. Oxidation kinetics and product formation. Water Res. 37, 1443–1467. https://doi.org/10.1016/S0043-1354(02)00457-8

Wen, G., Zhu, H., Wei, Y., Huang, T., Ma, J., 2017. Formation of assimilable organic carbon during the oxidation of water containing *Microcystis aeruginosa* by ozone and an advanced oxidation process using ozone/hydrogen peroxide. Chem. Eng. J. 307, 364–371. https://doi.org/10.1016/j.cej.2016.08.073

PUBLIKACE 3

Influence of COM-peptides/proteins on the properties of flocs formed at different shear rates

Monika Filipenská, Petra Vašatová, Lenka Pivokonská, Jana Načeradská,
Lenka Čermáková, Andrea Gonzalez-Torres, Rita K. Henderson
a Martin Pivokonský

Journal of Environmental Sciences 80 (2019) 116-127
DOI 10.1016/j.jes.2018.11.025

JOURNAL OF ENVIRONMENTAL SCIENCES 80 (2019) 116–127

Available online at www.sciencedirect.com

ScienceDirect

www.elsevier.com/locate/jes

JES JOURNAL OF ENVIRONMENTAL SCIENCES

www.jesc.ac.cn

Influence of COM-peptides/proteins on the properties of flocs formed at different shear rates

Monika Filipenska[1,2], *Petra Vasatova*[1], *Lenka Pivokonska*[1], *Lenka Cermakova*[1,2], *Andrea Gonzalez-Torres*[3], *Rita K. Henderson*[3], *Jana Naceradska*[1,2], *Martin Pivokonsky*[1,*]

1. *Institute of Hydrodynamics of the Czech Academy of Sciences, Pod Patankou 5, 166 12 Prague 6, Czech Republic*
2. *Institute for Environmental Studies, Faculty of Science, Charles University, Benatska 2, 128 01 Prague 2, Czech Republic*
3. *The bioMASS Lab, School of Chemical Engineering, The University of New South Wales, Sydney, NSW, Australia*

ARTICLE INFO

Article history:
Received 20 September 2018
Revised 21 November 2018
Accepted 22 November 2018
Available online 13 December 2018

Keywords:
Algal organic matter
Floc size
Coagulation
Image analysis
Water treatment

ABSTRACT

Coagulation followed by floc separation is a key process for the removal of algal organic matter (AOM) in water treatment. Besides optimizing coagulation parameters, knowledge of the properties of AOM-flocs is essential to maximizing AOM removal. However, the impact of AOM on the floc properties remains unclear. This study investigated how peptides/proteins derived from the cellular organic matter (COM) of the cyanobacterium *Microcystis aeruginosa* influenced the size, structure, and shape of flocs formed at different shear rates (G). Flocs formed by kaolinite, COM-peptides/proteins and a mixture of the same were studied, and the effect of intermolecular interactions between floc components on floc properties was assessed. The coagulation experiments were performed in a Taylor–Couette reactor, with aluminum (Al) or ferric sulphate (Fe) utilized as coagulants. Image analysis was performed to gauge floc size and obtain data on fractal dimension. It was found that floc properties were affected by the presence of the COM-peptides/proteins and the coagulant used. COM-peptides/proteins increased floc size and porosity and widened floc size distributions. The Fe coagulant produced larger and less compact flocs than Al coagulant. Moreover, the decrease in floc size that occurred in parallel with increase in shear rate was not smooth in progress. A rapid change for the kaolinite-coagulant suspension and two rapid changes for the suspensions containing COM were observed. These were attributed to various intermolecular interactions between floc components participating in coagulation at different G. Based on the results obtained, shear rates suitable for efficient separation of flocs containing COM were suggested.

Introduction

The presence of algae and cyanobacteria in drinking water has become a challenge for the water industry. During the increased growth and subsequent decay of algae and cyanobacteria, the concentration of algal/cyanobacterial cells and algal organic matter (AOM) increases in the source water. AOM comprises extracellular organic matter (EOM), stemming from algal metabolic activity and cellular organic matter (COM), sometimes also termed intracellular organic matter (IOM), released into the water during cell decay. AOM affects water quality and, since it is difficult to remove, it poses

* *Corresponding author. E-mail:* pivo@ih.cas.cz. (Martin Pivokonsky).

https://doi.org/10.1016/j.jes.2018.11.025
1001-0742 © 2018 The Research Center for Eco-Environmental Sciences, Chinese Academy of Sciences. Published by Elsevier B.V.

problems for water treatment plants (Zhang et al., 2010). Several studies have shown that AOM may exert a negative impact on the coagulation of algal/cyanobacterial cells (Henderson et al., 2010) and inorganic impurities, such as clay particles (Takaara et al., 2007). However, COM-peptides/proteins have been reported to improve the coagulation of clay particles and humic substances due to mutual interactions (Pivokonsky et al., 2015; Safarikova et al., 2013). Removal of AOM and its influence on the coagulation of other particles depends on the properties of AOM, e.g. protein/non-protein ratio, molecular weight, charge density and hydrophobicity, since it is these that determine the mechanism of interaction with the coagulant and other substances (Henderson et al., 2010; Pivokonsky et al., 2012).

In addition to efficient coagulation, an important role is played by floc properties (e.g. size, shape, porosity or density) in the efficiency of the downstream separation processes (i.e. filtration, sedimentation and flotation) (Bache and Gregory, 2010; Bubakova and Pivokonsky, 2012). Floc size and diameter is usually derived by the equation below (Bouyer et al., 2004; Jarvis et al., 2005a; Parker et al., 1972):

$$d_{\mathrm{av/\ max}} = CG^{-2\gamma} \quad (1)$$

where $d_{\mathrm{av/max}}$ is the average or maximal diameter of flocs in the system, G is the average/mean shear rate (velocity gradient) and C and γ are constants describing the strength of flocs and their tendency to break up, respectively (Jarvis et al., 2005a).

These constants, and thus also the floc size, are influenced by the composition and concentration of contaminants, type and dose of coagulant, reaction pH and the form of flow or energy dissipation, i.e. the effect of hydrodynamics. The balance that exists between forces of attraction and hydrodynamics then determines whether the flocs grow, break up or restructure (Bouyer et al., 2001; Selomulya et al., 2001; Spicer et al., 1998; Vlieghe et al., 2017). The shape and structure (represented by porosity and density) of flocs is often expressed using fractal dimension, since flocs are considered to be fractal objects which possess certain self-similarity in flocs, i.e. a repeated pattern of interconnected particles. In the equation below fractal dimension, D, describes the relationship between mass, M, and length, L:

$$M = L^{D} \quad (2)$$

An important feature of self-similar fractals is that their mass and density decrease as they grow larger (Meakin, 1990).

A number of studies have investigated the effect of hydrodynamics on floc properties, many of them employing artificial model particles, such as silica, kaolinite, latex and polystyrene (Jarvis et al., 2005b; Oles, 1992; Selomulya et al., 2001; Soos et al., 2007; Spicer et al., 1998). However, the effect of hydrodynamics on floc properties in natural water has largely been overlooked (Bubakova et al., 2013; Bubakova and Pivokonsky, 2012). Moreover, floc properties that arise through the presence of AOM or algal/cyanobacterial cells have received precious little attention (Gonzalez-Torres et al., 2017; Gonzalez-Torres et al., 2014; Henderson et al., 2006; Pivokonsky et al., 2009). In this context, it has been observed that flocs formed by algal cells and/or AOM were larger and more fragile than flocs stemming from inorganic particles or NOM (Gonzalez-Torres et al., 2014; Henderson et al., 2006). Furthermore, floc size was found to be more dependent on the initial concentration of AOM than the concentrations of coagulants (Pivokonsky et al., 2009).

However, information is very limited on floc properties arising through AOM, and thorough evaluation has yet to take place on differences between such flocs and those formed by other impurities. Furthermore, studies describing mutual interactions between AOM and other impurities during coagulation (Pivokonsky et al., 2016; Safarikova et al., 2013) indicate that said interactions may also alter the properties of flocs, and thus their separation.

Therefore, the aim of this study was to examine the properties of flocs instigated by AOM, namely COM-peptides/proteins derived from cyanobacterium *Microcystis aeruginosa*, at different shear rates. Specific objectives were to compare the properties of COM–flocs with floc properties initiated by inorganic particles (kaolinite) and those stemming from a mixture of COM and kaolinite. Moreover, the influence of COM–kaolinite interactions on floc properties was assessed. Finally, two types of coagulant – ferric sulphate and aluminum sulphate – were utilized in this study, and their impact on floc properties was evaluated. The significance of the presented research lies in the comparison of the influence of various floc components and their intermolecular interactions on the floc properties.

1. Materials and methods

1.1. Materials

1.1.1. Kaolinite

Kaolinite particles (Sedlecky kaolin a. s., Czech Republic) of size <4 μm were dispersed in ultrapure water. The point of zero charge (pzc) of kaolinite was determined to be at pH 2.9 by potentiometric titration, as described by Safarikova et al. (2013). Thus, at pH > 2.9, the negative charge prevailed in the kaolinite particles.

1.1.2. COM-peptides/proteins

Peptides/proteins were acquired from the COM of cyanobacterium *Microcystis aeruginosa* (strain Zap. 2006/2, CCALA, Institute of Botany, CAS, Czech Rep.) cultivated at the Institute of Hydrodynamics, CAS. The culture was harvested on the 16th day of cultivation, during the stationary growth phase, and separated from the culture media via a 0.45 μm membrane filter (Millipore, USA). COM was extracted by ultrasonication in an ice bath on an ultrasonic homogenizer (UP400S, Hielscher Ultrasonics, Germany), followed by filtration through a 0.45 μm membrane filter. The peptide/protein fraction was isolated from the COM by a two-step precipitation procedure utilizing ammonium sulphate, $(NH_4)_2SO_4$, at 0°C. The detailed methodology for cultivation, COM extraction and peptide/protein isolation is described by Safarikova et al. (2013). The COM-peptides/proteins were further characterized in terms of molecular weight (MW) distribution by high performance size exclusion chromatography (HPSEC) using

Agilent Bio SEC-5 columns connected in series. The HPLC system (Agilent Technologies, USA) was coupled with a diode array detector (DAD) operated at 280 nm. The methodology of HPSEC is described in detail elsewhere (Pivokonsky et al., 2012). Peptides/proteins of apparent MWs of approximately 1, 2.8, 4, 4.5, 5, 5.7, 6, 6.8, 8, 8.5, 12, 30, 40, 52, 106, 266, 470, and 1077 kDa were detected as components of *M. aeruginosa* COM. For the sake of simplification, the COM-peptides/proteins are referred to as "COM" hereinafter. Their concentrations in the experiments were expressed as dissolved organic carbon (DOC).

1.2. Methods

1.2.1. Coagulation tests

The coagulation of COM, kaolinite and a mixture of both by either aluminum sulphate ($Al_2(SO_4)_3 \cdot 18H_2O$; Sigma–Aldrich, USA) or ferric sulphate ($Fe_2(SO_4)_3 \cdot 9H_2O$; Sigma–Aldrich, USA) was performed in a Taylor–Couette reactor. The following suspensions were utilized in the coagulation experiments: (1) kaolinite (10 mg/L, 35 NTU), (2) COM (5 mg/L DOC), (3) a mixture of kaolinite and COM (10 mg/L kaolinite and 5 mg/L DOC). The mentioned concentrations were chosen with respect to concentrations usually present in raw water sources. Kaolinite and COM were dosed into the ultrapure water with alkalinity adjusted to 1.5 mmol/L (75 mg/L $CaCO_3$) using $NaHCO_3$. The target pH values were reached by adding predetermined amounts of 0.1 mol/L NaOH or 0.1 mol/L HCl prior to supplementation with the coagulant. The doses of coagulants and pH values were optimized by coagulation tests according to Pivokonsky et al. (2012) and Safarikova et al. (2013). Table 1 summarizes the optimized coagulant doses, optimized pH values, residual coagulants, and residual impurities (residual kaolinite is expressed as turbidity and residual COM is expressed as DOC) arrived at after the coagulation tests had been conducted. With respect to low coagulant doses, sweep flocculation (also called enmeshment) is not considered a coagulation mechanism (Gregory and Duan, 2001). The global shear rates applied during the coagulation experiments comprised G = 20, 30, 40, 50, 60, 70, 80, 90, 100, 110, 120, 140, 150, 160, and 180 sec^{-1}. The retention period of the suspension in the Taylor–Couette reactor was 60 min., which corresponded to its subsequent steady state. All tests were repeated five times. Image analysis was performed after each coagulation test.

1.2.2. Taylor–Couette mixing device

The Taylor–Couette reactor (TC) (IH CAS, Czech Rep.) was selected as the mixing device for the coagulation experiments due to its well-defined velocity field and the possibility for non-invasive observation of the resultant flocs. The TC comprises two concentric cylinders made from Plexiglas (Umaplex, Perspex), with an inner rotating cylinder. White and black inner cylinders were employed to give a contrasting background for the ferric and aluminum flocs, respectively. The outer cylinder was transparent and permitted photographic imaging of the aggregation process. The inner cylinder had a radius (R_1) of 73.5 mm while the outer one (R_2) was of radius 85.5 mm, which resulted in a gap of $d = R_2 - R_1$ = 12 mm in width and radius ratio of $\eta = R_1/R_2$ = 73/85.5 = 0.8596. The height of the cylinders was H = 385 mm, giving the aspect ratio of $\Gamma = H/d$ = 385/12 = 32.08. The inner cylinder was driven by a variable speed drive with a torquemeter. The hydrodynamic conditions in the TC were characterized by global shear rate, G, calculated according to the following equation:

$$G = \sqrt{\frac{P_i}{V\mu}} = \sqrt{\frac{\omega M}{V\mu}} = \sqrt{\frac{2\pi f M}{V\mu}} \quad (3)$$

where P_i represents the power dissipated in the aggregation space, V is the volume of the aggregation space, μ is the dynamic viscosity of the fluid, ω is the angular velocity of inner cylinder rotation, M is the torque and f is the rotation frequency.

1.2.3. Analyses of floc properties

The size, number, and size distribution of the flocs formed during coagulation in the TC reactor was determined by image analysis, which involved the following three steps: (1) illuminating flocs in the TC reactor with a laser light sheet (width = 1.2 ± 0.1 mm) generated by a laser diode (λ = 675 nm, power capacity 20 mW); (2) recording images of flocs on a Pentax K-3II digital camera (Asahi Co., Japan) with an smc PENTAX D FA Macro 50 mm *f*/2.8 lens (Asahi Co., Japan); (3) processing the images with image analysis software (Sigma Scan 5.0).

Table 1 – Coagulation conditions (optimal coagulant doses, optimal pH and temperature) and residual water parameters after coagulation (turbidity, DOC, Fe/Al).

	Al ($Al_2(SO_4)_3.18H_2O$)			Fe ($Fe_2(SO_4)_3.9H_2O$)		
	Kaolinite	COM	Kaolinite+COM	Kaolinite	COM	Kaolinite+COM
Optimal coagulant dose* (mmol/L Al/Fe)	0.037	0.149	0.149	0.054	0.126	0.126
Coagulation pH*	7.5	6.8	6	7.2	5.8	4.8
Temperature (°C)	25	25	25	25	25	25
Turbidity (NTU)	3	–	4	4	–	5
DOC (mg/L)	–	1.5	1.1	–	1.5	1.1
Fe (mg/L)	–	–	–	0.02	0.2	0.2
Al (mg/L)	0.01	0.01	0.01	–	–	–

* The optimal coagulant doses and optimal pH were determined on the basis of the highest removal efficiencies of all floc components (kaolinite as turbidity, COM as DOC and Al/Fe).

The digital images (23.5 × 15.6 mm) were taken in RAW format (6016 × 4000 pixels), which gave the pixel size of approximately 3.9 × 3.9 μm. Only flocs larger than 4 pixels (7.8 × 7.8 μm) were retained in the image analysis process to eliminate digital background noise. The images were then converted from RAW into BMP gray-scale format, after which thresholding was applied (Appendix A Fig. S1). Finally, Sigma Scan 5.0 software was employed to calculate the following: the projected area, A; the perimeter, P; the minimal and maximal dimension, l_{min} and l_{max}, respectively, of all the imaged flocs; and the total number of flocs. The equivalent floc diameter, d, of each floc was calculated from the projected area, as follows:

$$d = \sqrt{4A/\pi} \tag{4}$$

Furthermore, the average floc diameter, d_{avr}, (referred to as "floc size" hereinafter) was calculated from the d values for all the flocs present in one image (Bouyer et al., 2004; Bubakova and Pivokonsky, 2012). The structural characteristics of the flocs were derived from the two-dimensional fractal dimension, D_2, determined from the image analysis data. Said fractal dimension, D_2, represents the compactness or density of the flocs and is given by the following formula (Bubakova et al., 2013; Chakraborti et al., 2007):

$$A \propto d_{eq}^{D_2} \tag{5}$$

where A is the projected area, d_{eq} is the equivalent floc diameter calculated from the measured values for minimal and maximal dimensions l_{min} and l_{max}, respectively, according to the following equation:

$$d_{eq} = \sqrt{l_{min}.l_{max}} \tag{6}$$

This calculation of d_{eq} guarantees its independence of A (Bagheri et al., 2015). D_2 lies in the interval (1, 2). Dense flocs possess a higher value for D_2 than porous and lacunar flocs. Surface properties are calculated from the perimeter, P, and the projected area, A, as the perimeter-based fractal dimension, D_{pf}, see below (Bubakova et al., 2013; Chakraborti et al., 2007; Li et al., 2006):

$$A \propto P^{2/D_{pf}} \tag{7}$$

where D_{pf} lies in the interval (1, 2). Fractal objects increase their perimeter more rapidly than their size (projected area). Hence, if D_{pf} tends towards 2, the flocs are irregular and branched, whereas they are somewhat spherical in shape if D_{pf} tends towards 1.

1.2.4. Statistical processing and reproducibility of results

Statistical analysis was performed in Statistica 7.1 software (TIBCO Software, Inc.). Testing normality for the equivalent diameter, d, involved conducting a one-sample Kolmogorov–Smirnov test with a significance level of 0.95 ($\alpha = 0.05$). The null hypothesis, i.e. the size distribution of the flocs possesses normal distribution, was not rejected (Appendix A Table S1), thus the arithmetic mean was chosen to characterize the dataset.

Reproducibility of results was verified for all suspension variants at the G values of 40 and 160 sec^{-1}. The dataset of d and the number of flocs were tested by analysis of variance (ANOVA). The one-way ANOVA was used to test the null hypothesis that the means of parameters d and number (relevant floc components) were equal for individual measurements at both of the tested shear rates. At the significance level of 0.95 ($\alpha = 0.05$), the null hypothesis was not rejected for all suspensions. There was no statistically significant difference between the five experiments of each experimental variant (p-value > α-level and $F_{krit} > F$-value) (Appendix A Table S2).

2. Results and discussion

2.1. Number of flocs, size, and size distribution

The dependence of floc size on shear rate, G, is illustrated in Fig. 1a. In agreement with previous research, it was confirmed that the size of the flocs decreased concurrently with increase in shear rate (Bubakova et al., 2013; Bubakova and Pivokonsky, 2012; Dyer and Manning, 1999; Tambo and Hozumi, 1979). The extent of such decrease was greatly dependent on the substances participating in the coagulation, i.e. the primary components of the flocs, such as kaolinite, COM and the coagulant. The floc size increased in the following order: kaolinite+Al < kaolinite+Fe < COM+Al < kaolinite+COM+Al < COM+Fe < kaolinite+COM+Fe. Studies by Gonzalez-Torres et al. (2017, 2014), who coagulated cells of *M. aeruginosa* and *Chlorella vulgaris* together with the associated AOM released into cultivation media, also found that floc size diminished alongside a rise in G (evaluated in the range 9.4–167 sec^{-1}). Moreover, they showed that floc size was dependent on the composition of the AOM, specifically on the distribution of protein and carbohydrate throughout the flocs.

Two distinct trends are apparent in Fig. 1a. Firstly, the presence of COM in the flocs led to a substantial rise in floc size. It is not surprising that the peptide/protein fraction of COM, comprising large biopolymers with molecular weights of up to 1077 kDa (as determined by Safarikova et al. (2013)), created larger flocs than kaolinite particles. Similar observations were made by Henderson et al. (2006), who ascertained that cells + AOM produced substantially larger flocs than those formed either by natural organic matter (NOM, i.e. organic matter primarily humic in character) or kaolin. Likewise, Vandamme et al. (2014) who coagulated *Chlorella vulgaris* cells with and without AOM, reported that AOM caused a rise in floc size when alum and chitosan were applied as coagulants. These findings indicate that AOM polymers behave similarly to synthetic polymeric flocculants that increase floc size (Fabrizi et al., 2010).

Secondly, the results in Fig. 1a show that ferric sulphate (Fe) produced flocs almost twice as large as those created by aluminum sulphate (Al), regardless of the type of impurity. Similar results were achieved by Gonzalez-Torres et al. (2014) who investigated flocs formed by cells+AOM of *M. aeruginosa* and ferric chloride or aluminum sulphate. Furthermore, approximately twice the proportion of large flocs called macroaggregates (i.e. flocs larger than 1000 μm) was observed for the Fe coagulant than the Al coagulant by Pivokonsky et al. (2009) for coagulation of COM of *M. aeruginosa* at G = 70 sec^{-1}

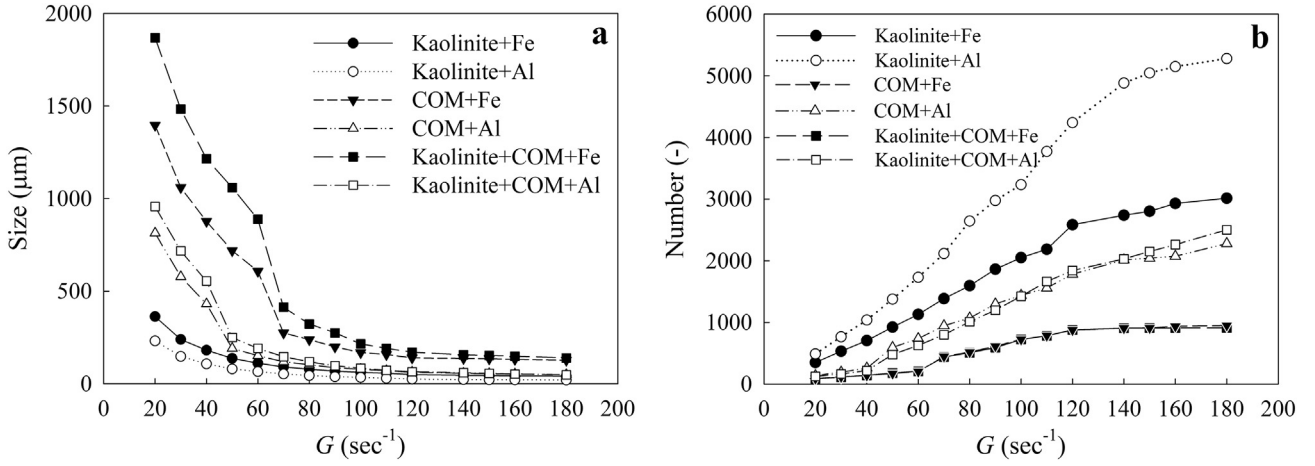

Fig. 1 – Dependence of size of flocs (a), and number of flocs (b), on the shear rate (G) applied for floc formation.

for 15 min. Additionally, Jarvis et al. (2012, 2005b) reported that their Fe-coagulant produced significantly larger NOM-flocs than Al.

Several explanations exist for such difference in floc size for ferric and aluminum coagulants. Fe tends to produce larger hydrolysis products than Al, as the Fe-O distance in Fe hydrolysis products is longer (2.00 Å) than the Al-O distance in Al hydrolysis products (1.89 Å) (Persson, 2010). In addition, higher coagulant doses of Fe than Al were applied to coagulate kaolinite particles, as shown in Table 1, thus producing a larger amount of Fe precipitates than Al. However, Fe doses were lower than those for Al for coagulation of COM and kaolinite + COM. Nevertheless, in the presence of COM, the size of proteins, which is known to differ with a change in pH value due to protein folding and unfolding, plays a crucial role in the resultant size of flocs. Many proteins unfold at pH values of less than 6 or greater than 9 (Creighton, 1993), which is accompanied by increase in their size. This may be the reason why flocs formed at pH values for coagulation by Fe are larger than flocs formed at pH values for coagulation by Al (see Table 1).

The most substantial differences in floc size were observed at the lowest shear rates (up to $G = 50\ sec^{-1}$ for Al-flocs and up to $G = 70\ sec^{-1}$ for Fe-flocs), potentially related to forces of attraction, i.e. interactions acting between primary components (further discussed in Section 2.3.), prevailing over hydrodynamic ones at the mentioned shear rates. As the shear rate increased, the forces (attraction vs. hydrodynamic) gradually attained balance. Finally, though, the effect of hydrodynamics prevailed over the forces of attraction (Coufort et al., 2005); therefore, the variances in floc size between the individual floc types became less pronounced at the highest shear rates.

Fig. 1b shows that the dependence of the number of flocs on G is inversely proportional to floc size. The flocs decreased in number in the following order: kaolinite+Al > kaolinite+Fe > COM+Al > kaolinite+COM+Al > COM+Fe > kaolinite+COM+Fe. However, the curves for rise in the number of flocs were relatively smooth compared to the behaviour of the equivalent ones for size (Fig. 1a).

Fig. 2 shows data on size distribution for three selected shear rates: 40, 80, and 140 sec^{-1}. With increase in the value G, size distributions became narrower, indicating that the floc suspensions were more homogeneous through increase in collision frequency (Bouyer et al., 2004; Bubakova et al., 2013), and the fact that hydrodynamic forces did not allow the flocs to grow any larger. The size distributions of COM+Al and kaolinite+COM+Al and of COM+Fe and kaolinite+COM+Fe were more similar to each other than the size distributions of COM+Al and COM+Fe and of kaolinite+COM+Al and kaolinite+COM+Fe; this suggested that the type of coagulant utilized had a greater impact on the size distribution of flocs formed by COM than the presence of kaolinite in the suspensions. The effects of coagulant type on floc size are discussed above.

2.2. Fractal dimension of flocs

The dependence of fractal dimensions, D_2 and D_{pf}, used to describe floc structure and shape, on shear rates is shown in Fig. 3. As expected, D_2 rose and D_{pf} dropped concurrently with rise in G. This indicated that the flocs became more compact, i.e. their density increased while porosity decreased (Fig. 3a), as well as more regular in shape, i.e. closer to a sphere/ellipsoid (Fig. 3b), with increase in G. Bubakova and Pivokonsky (2012) and Bubakova et al. (2013) reported similar results for natural water (turbidity 2.9 NTU for both and DOC 4.5 and 3.8 mg/L, respectively) coagulated by ferric sulphate at $G = 28–307$ and 21.2–347.9 sec^{-1}, respectively. Li et al. (2006) who coagulated kaolin by aluminum sulphate or cationic polyacrylamide at $G = 11.3–342\ sec^{-1}$, observed an analogous trend. They utilized a three-dimensional fractal dimension, D_F, (possessing values between 1 and 3) to describe the floc structure. Therein, D_F increased in parallel with rise in G, meaning that the floc structure was more compact. Furthermore, Wang et al. (2017) concluded that flocs became less porous and more compact with increase in G, when they coagulated wastewater using composited polyferric chloride–polydimethyldiallylammonium chloride (PFC-PDM) and non-composited polyferric chloride (PFC) under various coagulation mechanisms at $G = 24.8–547.9\ sec^{-1}$.

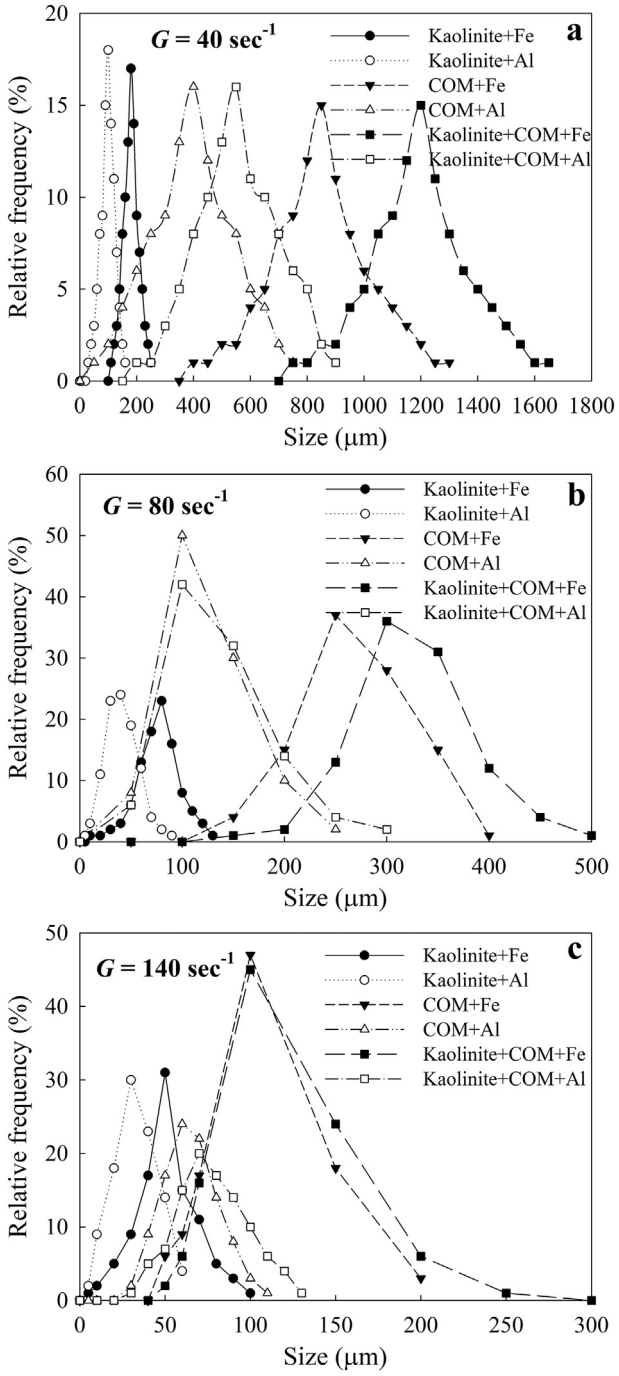

Fig. 2 – Size distributions of different types of flocs formed at (a) $G = 40\ sec^{-1}$ (size range 0–1600 μm in size), (b) $G = 80\ sec^{-1}$ (size range 0–500 μm in size) and (c) $G = 140\ sec^{-1}$ (size range 0–300 μm in size).

Herein, the compactness of flocs (Fig. 3a) decreased in the following order: kaolinite+Al > COM+Al > kaolinite +Fe > COM+Fe > kaolinite+COM+Fe > kaolinite+COM+Al. The higher value for D_2 for kaolinite+Al and COM+Al than the kaolinite+Fe and COM+Fe flocs probably stemmed from the shorter Al-O distance (1.89 Å) than Fe-O distance (2.00 Å) (Fabrizi et al., 2010). The most porous flocs were those formed by all three primary components – kaolinite, COM, and the coagulant. The variations in structure (compactness) between individual floc types could also be attributed to the distinct levels of pH at which coagulation took place (Table 1), this determining the formation of different Al/Fe hydrolysis products (Duan and Gregory, 2003). Moreover, in the case of the COM-flocs, the given pH value influenced protein folding (and thus floc structure), as mentioned in Section 2.1. This would also explain the inconsistency in the order of floc types according to their increase in D_2 and decrease in size. While the structure is influenced by the form of the primary component, which is pH-dependent (Gregory, 1998), size is determined additionally by the concentration of said component (or volume of mass) (Pivokonsky et al., 2009). Thus, the largest flocs are not necessarily the most porous.

The situation became more complicated for D_{pf} (Fig. 3b). At $G = 70–120\ sec^{-1}$, the order of D_{pf} for the various floc types was inversely proportional to D_2, meaning that the more compact the flocs, the more regular their shape. At $G < 70\ sec^{-1}$, the curves for D_{pf} crossed over each other. The shape of the flocs containing COM was obviously more affected by G than the kaolinite–flocs. This phenomenon is discussed in the following Section 2.3. At $G > 120\ sec^{-1}$, the differences between the fractal dimensions of flocs formed by different substances diminished, and the curves for kaolinite+Fe, COM+Fe, kaolinite+COM+Fe and kaolinite+COM +Al resembled each other. This was probably due to corrosion of the floc surfaces at high G, resulting in all of them obtaining a similar shape.

Although fractal dimensions have been used to describe floc structure in many studies (Bubakova et al., 2013; Chakraborti et al., 2007; Vlieghe et al., 2017; Wang et al., 2017, 2009), they varied in experimental conditions, i.e. type and concentration of coagulant and impurity, G value, method for gauging fractal dimension, and so on. Therefore, it is not possible to compare the absolute values derived for fractal dimension, either with each other or with the results given herein.

2.3. Floc components and their interaction mechanisms

Papers in the literature on the coagulation of kaolinite particles or/and AOM show that the interaction mechanisms between impurities and coagulants are primarily governed by their predominant net charge and/or the presence and amount of charged functional groups (Henderson et al., 2010; Pivokonsky et al., 2012; Safarikova et al., 2013). It should be noted that the charge of kaolinite, AOM, and Al/Fe coagulants is highly dependent on pH value, and that consistent pH optimization is a prerequisite for efficient floc formation and separation. The predominant net charges of the primary components coagulated in this study are detailed in Table 2, as derived from the titration curves of the individual primary components (Appendix A Fig. S2).

Kaolinite was effectively removed by the Fe and Al coagulants in the pH range 6.4–8.0 and 7.0–8.5, respectively, owing to the adsorption of positively charged Fe/Al hydroxide precipitates on the negatively charged surfaces of kaolin particles, thereby gradually neutralizing the charge of the kaolinite and leading to efficient coagulation (Safarikova et al.,

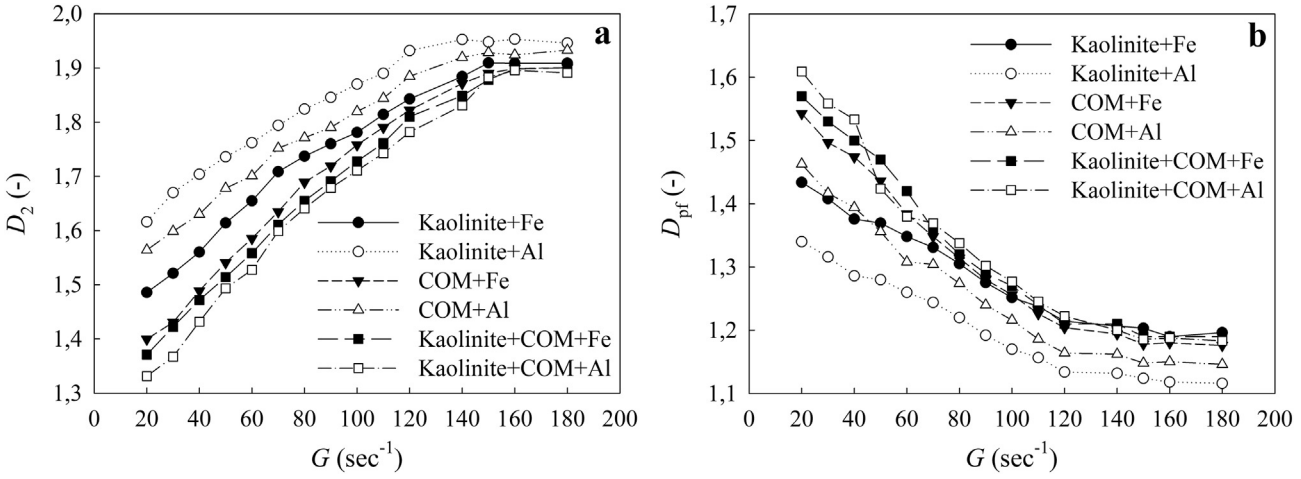

Fig. 3 – Dependence of fractal dimension on the shear rate used for floc formation: (a) D_2 – expressing the compactness (density) of flocs, and (b) D_{pf} – expressing the irregularity of flocs.

2013). In contrast, the COM-peptides/proteins of *M. aeruginosa* were coagulated by the Fe and Al coagulants in the pH ranges 4.0–6.0 and 5.0–6.5, respectively; this indicated that electrostatic interactions between the negatively charged acidic functional groups (–COO^-) of COM and positively charged Fe or Al hydroxopolymers were important to their coagulation (Pivokonsky et al., 2012, 2015). When kaolinite and COM were removed together by the Fe or Al coagulant, the process was also influenced by electrostatic interactions of attraction between the negatively charged kaolinite surface and peptide/protein –NH_3^+ groups. The kaolinite–COM clusters were then linked by positively charged Fe or Al hydroxopolymers at the same pH values (4.0–6.0 and 5.0–6.5, respectively) as when kaolinite was absent (Safarikova et al., 2013). It is of note that Van der Waals forces, hydrogen bonding and hydrophobic interactions also participated in the given coagulation processes (Shin et al., 2008). Polar functional groups, involved in hydrogen bonding, are contained within COM and kaolinite as well as Fe/Al hydrolysis products. Additionally, the nonpolar side chains of COM and hydrophobic silica surface planes of kaolinite may take part in hydrophobic interactions. The binding energies of the aforementioned interactions decrease in the following order: electrostatic interactions (binding energy ~20–30 kJ/mol) > hydrogen bonding (~15–17 kJ/mol) > hydrophobic interactions (~1.2–6 kJ/mol) (Israelachvili, 2011). Fig. 4 details the activity of these interactions, illustrating the dependence of floc size on the shear rate in log–log plots (in accordance with Eq. (1)). It can be inferred that the measured data did not follow a single dependence with a single γ constant. This phenomenon is also reported in data from the literature (Bouyer et al., 2004; Bubakova et al., 2013; Li et al., 2006; Wang et al., 2017; Wang et al., 2009) on floc properties. However, none of the referenced studies, except that by Bubakova et al. (2013), even observed, pursued or commented on this aspect. The results of all said authors, after applying Eq. (1), are depicted in Fig. 5. In the present study, one change in the γ constant, at approximately G ~120 sec^{-1}, was noted for all the types of floc (Fig. 4). This region can also be seen in works by others, as depicted in Fig. 5a–f. Furthermore, the flocs containing COM showed an additional change in γ, between values for G of 40–50 and 60–70 sec^{-1}, with reference to Al and Fe, respectively (Fig. 4c–f).

The changes in floc size can be explained by the activity of intermolecular interactions. As stated previously, electrostatic interactions, which are the strongest and most dominant ones in coagulation, are supported by other interactions with lower binding energies, such as Van der Waals forces, hydrogen bonds, and hydrophobic interactions. As the shear

Table 2 – Net charges of primary components prevailing at the pH value used for coagulation.

Coagulated primary components		Kaolinite+COM + Fe	COM + Fe	Kaolinite+COM + Al	COM + Al	Kaolinite+Fe	Kaolinite+Al
Coagulation pH		4.8	5.8	6	6.8	7.2	7.5
Kaolinite		⊖	N/A	⊖	N/A	⊖	⊖
COM	–COOH	⊖	⊖	⊖	⊖	N/A	N/A
	–NH_2	⊕	⊕	⊕	⊕	N/A	N/A
Al		N/A	N/A	⊕	⊕	N/A	⊕
Fe		⊕	⊕	N/A	N/A	⊕~ ⊖	N/A

N/A = Not Available.
The contents of Table 2 were derived from the titration curves of the individual primary components (see Appendix A Fig. S2).

rate increases, any weaker interactions are not strong enough to participate in floc formation, and floc size immediately drops away. The changes in floc size (also in D_{pf} value, as mentioned in the previous section) observed for the COM-flocs (at G ~ 40–50 and 60–70 sec^{-1} for Al and Fe, respectively) suggest that the presence of COM in the flocs leads to extra interactions, causing the formation of larger, irregularly shaped flocs at lower shear rates. Similar trends were reported by Li et al. (2006) and Williams et al. (1992) (Fig. 5g, h), who coagulated inorganic particles with polyacrylamide, which resemble peptides/proteins in certain properties (a ionic polymer with a nonpolar chain and $–NH_3^+$ and $–COO^-$ functional groups). Herein, the difference between G ranges for the change in floc size for the Al and Fe coagulants may stem from the various pH values applied for coagulation by Al and Fe. As stated in Section 2.1, proteins

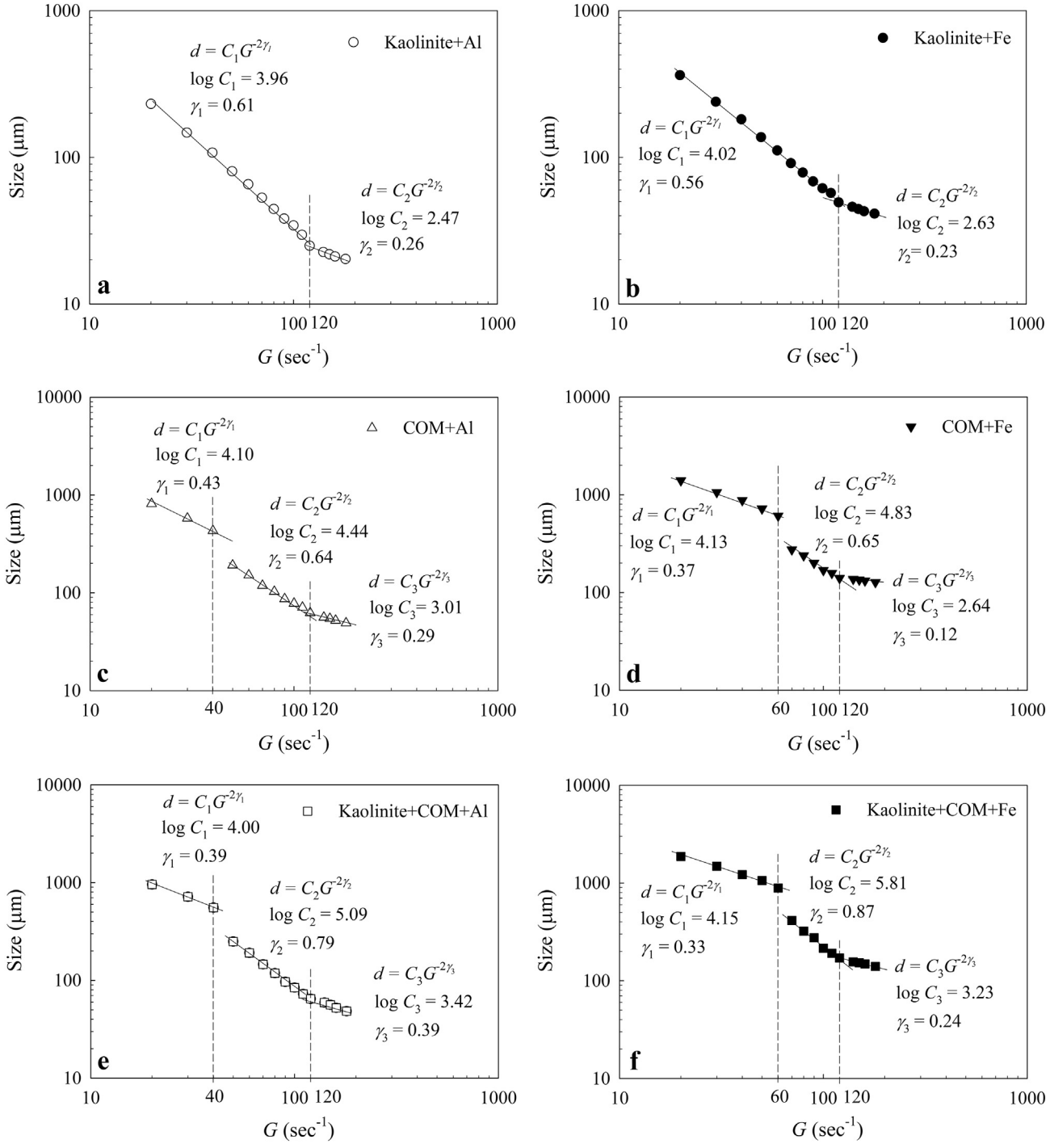

Fig. 4 – Dependence of floc size on the shear rate, G, in log–log plots: (a) kaolinite+Al-flocs, (b) kaolinite+Fe-flocs, (c) COM+Al-flocs, (d) COM+Fe-flocs, (e) kaolinite+COM+Al-flocs and (f) kaolinite+COM+Fe-flocs.

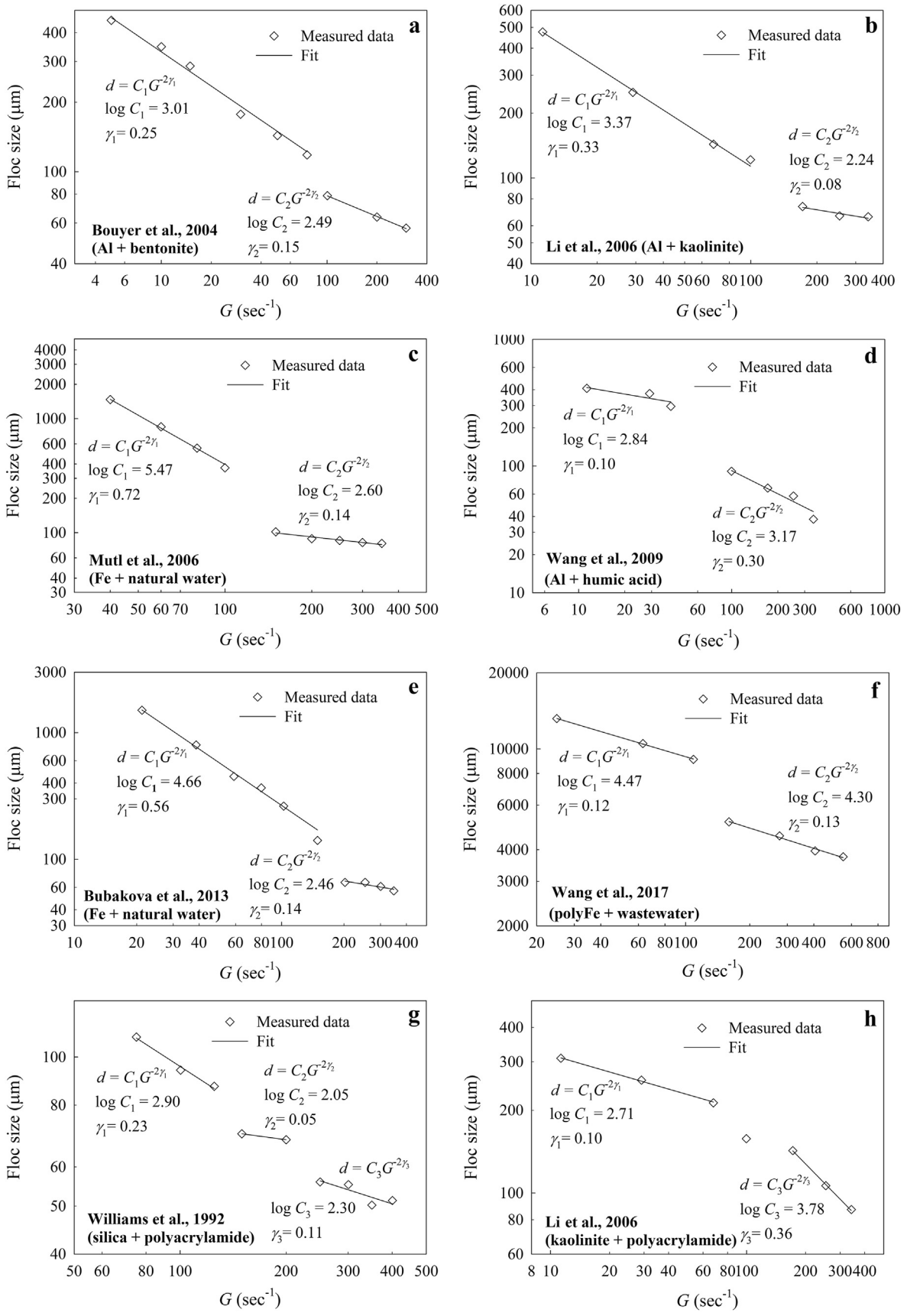

Fig. 5 – Log–log *d*-*G* plots of (a) Bouyer et al. (2004), (b) Li et al. (2006), (c) Mutl et al. (2006), (d) Wang et al. (2009), (e) Bubakova et al. (2013), (f) Wang et al. (2017), (g) Williams et al. (1992) and (h) Li et al. (2006). When a metal salt (Al/Fe) was used as a coagulant, only a single change in γ was seen (a–f). When polyacrylamide (PAM) was applied, two alterations in γ value occurred (g). The same trend was observed for COM-peptides/proteins, which have a similar structure to PAM (nonpolar parts and $-COO^-$, $-NH_3^+$ functional groups).

Table 3 – Separation processes suitable for the treatment of different types of floc; evaluation was made on the basis of the floc size attained by applying different levels of G, according to Edzwald (2010), and Bubakova and Pivokonsky (2012).

	Filtration [a]	Sedimentation-filtration [b]	Flotation-filtration [b]
Kaolinite + Al	$G > 40\ sec^{-1}$	$G \leq 40\ sec^{-1}$	$G = 70–120\ sec^{-1}$
Kaolinite + Fe	$G > 60\ sec^{-1}$	$G \leq 60\ sec^{-1}$	$G > 110\ sec^{-1}$
COM + Al	$G > 80\ sec^{-1}$	$G \leq 80\ sec^{-1}$	$G > 160\ sec^{-1}$
COM + Fe	–	$G = 20–180\ sec^{-1}$	–
Kaolinite+COM + Al	$G > 80\ sec^{-1}$	$G \leq 80\ sec^{-1}$	$G > 160\ sec^{-1}$
Kaolinite+COM + Fe	–	$G = 20–180\ sec^{-1}$	–

[a] Bubakova and Pivokonsky (2012).
[b] Edzwald (2010).

tend to unfold at the pH set for coagulation by Fe (Table 1). During the process of protein unfolding, the functional groups that are buried in non-ionized forms inside the folded proteins are able to ionize (Creighton, 1993), thus enabling more electrostatic interactions to participate in floc formation. These additional electrostatic interactions could result in the greater resistance of Fe-flocs to hydrodynamics (higher G values), compared to Al-flocs.

2.4. Implications of floc properties for separation

For efficient coagulation, it is necessary to consider conducting a thorough analysis of source water composition and selecting a suitable coagulant with the appropriate coagulation conditions, such as pH, shear rate and mixing time. Consistent optimization of these parameters will lead to flocs being produced with properties suitable for later separation processes, with respect to maximum efficiency and low energy costs. Table 3 summarizes the recommended separation methods for the flocs formed in this study, in accordance with Edzwald (2010) and Bubakova and Pivokonsky (2012).

Bubakova and Pivokonsky (2012) reported that flocs below 100 μm in size (optimally around 60 μm) are suitable for single-stage separation by direct filtration. Larger flocs do not penetrate deeply into the filter bed and shorten filtration runs, thus sedimentation has to be applied as the first stage of separation, followed by filtration. Edzwald (2010) recommended sedimentation for flocs at the size of hundreds of μm. Moreover, the same author (Edzwald, 2010) reported that flotation was suitable for separating out flocs at sizes between 25 and 50 μm. However, this range in size pertains to turbidity-based flocs produced through coagulation by metal salts. Algal and AOM-flocs were reported to float well, and removal efficiencies of algae/AOM via flotation were higher than or comparable to sedimentation (Henderson et al., 2010). Nevertheless, Henderson et al. (2010) did not report on the sizes of algal/AOM-flocs suitable for flotation, thus the recommendation given for flocs containing COM is based solely on Edzwald (2010).

In summary, COM+Fe- and kaolinite+COM+Fe-flocs do not comply with the size suitable for direct filtration or flotation-filtration (Fig. 1a) but can be removed by sedimentation-filtration. The other types of flocs in this study (kaolinite+Fe-flocs and Al-flocs) can be separated in dependence on their size by all the separation processes listed, as given by the respective shear rate (Table 3). It should be noted that floc size is influenced by AOM composition (Gonzalez-Torres et al., 2017; Gonzalez-Torres et al., 2014), suggesting that AOM produced by various species requires different shear rates to reach a definite floc size.

3. Conclusions

The following conclusions can be drawn from this research. Increase in shear rate results in a decrease in floc size depending on the substances forming the flocs. Growth in floc size (alongside a drop in the number of flocs) happens in the following order: kaolinite+Al < kaolinite+Fe < COM+Al < kaolinite+COM+Al < COM+Fe < kaolinite+COM+Fe; this indicates that COM boosts floc size, and the ferric coagulant produces larger flocs than the aluminum equivalent. However, floc size changes in dependence on shear rate are not smooth in progress. Observation was of a rapid change for the kaolinite-coagulant suspension and two rapid changes for the COM-coagulant and kaolinite–COM-coagulant suspensions. These can be attributed to the engagement of different interactions between COM, kaolinite, and the coagulants at various shear rates. Further, it was found that floc suspensions are more homogeneous, and variances between the sizes of the flocs formed by different substances lessen in line with increase in shear rate. In the case of the COM-flocs, the given type of coagulant exerts more of an impact on their size distribution than the presence of the kaolinite within them. Moreover, flocs become more compact and regular in shape, and the differences in these properties of flocs formed by different substances diminish alongside rise in shear rate. Floc structure also depends on the pH that determines the form of the primary components. Since floc properties determine the suitability of flocs for subsequent separation, based on the applied shear rate and floc components, separation processes for efficient flocs removal were suggested. Direct filtration is convenient for all types of flocs (except those containing COM and Fe) produced at higher shear rates. For COM+Fe- and kaolinite+COM+Fe-flocs, and other flocs produced at low shear rates, sedimentation is required.

Acknowledgements

The research project was funded by the Czech Science Foundation, under Project No. 1805007S, with institutional support RVO: 67985874, and by the Center for Geosphere

Dynamics (UNCE/SCI/006). The authors acknowledge this financial assistance with the project.

Appendix A. Supplementary data

Supplementary data to this article can be found online at https://doi.org/10.1016/j.jes.2018.11.025.

REFERENCES

Bache, D.H., Gregory, R., 2010. Flocs and separation processes in drinking water treatment: a review. J. Water Supply Res. Technol. 59, 16–30.

Bagheri, G.H., Bonadonna, C., Manzella, I., Vonlanthen, P., 2015. On the characterization of size and shape of irregular particles. Powder Technol. 270, 141–153.

Bouyer, D., Line, A., Cockx, A., Do-Quang, Z., 2001. Experimental analysis of floc size distribution and hydrodynamics in a jar-test. Chem. Eng. Res. Des. 79, 1017–1024.

Bouyer, D., Liné, A., Do-Quang, Z., 2004. Experimental analysis of floc size distribution under different hydrodynamics in a mixing tank. AICHE J. 50, 2064–2081.

Bubakova, P., Pivokonsky, M., 2012. The influence of velocity gradient on properties and filterability of suspension formed during water treatment. Sep. Purif. Technol. 92, 161–167.

Bubakova, P., Pivokonsky, M., Filip, P., 2013. Effect of shear rate on aggregate size and structure in the process of aggregation and at steady state. Powder Technol. 235, 540–549.

Chakraborti, R.K., Gardner, K.H., Kaur, J., Atkinson, J.F., 2007. In situ analysis of flocs. J. Water Supply Res Technol. 56, 1–11.

Coufort, C., Bouyer, D., Liné, A., 2005. Flocculation related to local hydrodynamics in a Taylor–Couette reactor and in a jar. Chem. Eng. Sci. 60, 2179–2192.

Creighton, T.E., 1993. Proteins: Structures and Molecular Properties. 2nd edition. Freeman, W. H, New York.

Duan, J., Gregory, J., 2003. Coagulation by hydrolysing metal salts. Adv. Colloid Interf. Sci. 100–102, 475–502.

Dyer, K.R., Manning, A.J., 1999. Observation of the size, settling velocity and effective density of flocs, and their fractal dimensions. J. Sea Res. 41, 87–95.

Edzwald, J.K., 2010. Dissolved air flotation and me. Water Res. 44, 2077–2106.

Fabrizi, L., Jefferson, B., Parsons, S.A., Wetherill, A., Jarvis, P., 2010. The role of polymer in improving floc strength for filtration. Environ. Sci. Technol. 44, 6443–6449.

Gonzalez-Torres, A., Putnam, J., Jefferson, B., Stuetz, R.M., Henderson, R.K., 2014. Examination of the physical properties of Microcystis aeruginosa flocs produced on coagulation with metal salts. Water Res. 60, 197–209.

Gonzalez-Torres, A., Rich, A.M., Marjo, C.E., Henderson, R.K., 2017. Evaluation of biochemical algal floc properties using Reflectance Fourier-Transform infrared Imaging. Algal Res. 27, 345–355.

Gregory, J., 1998. The role of floc density in solid-liquid separation. Filtr. Sep. 35, 367–376.

Gregory, J., Duan, J., 2001. Hydrolyzing metal salts as coagulants. Pure Appl. Chem. 73, 2017–2026.

Henderson, R.K., Sharp, E., Jarvis, P., Parsons, S., Jefferson, B., 2006. Identifying the linkage between particle characteristics and understanding coagulation performance. Water Sci. Technol.: Water Suppl. 6, 31–38.

Henderson, R.K., Parsons, S.A., Jefferson, B., 2010. The impact of differing cell and algogenic organic matter (AOM) characteristics on the coagulation and flotation of algae. Water Res. 44, 3617–3624.

Israelachvili, J.N., 2011. Intermolecular and Surface Forces. 3rd edition. Academic Press.

Jarvis, P., Jefferson, B., Gregory, J., Parsons, S.A., 2005a. A review of floc strength and breakage. Water Res. 39, 3121–3137.

Jarvis, P., Jefferson, B., Parsons, S.A., 2005b. Breakage, regrowth, and fractal nature of natural organic matter flocs. Environ. Sci. Technol. 39, 2307–2314.

Jarvis, P., Sharp, E., Pidou, M., Molinder, R., Parsons, S.A., Jefferson, B., 2012. Comparison of coagulation performance and floc properties using a novel zirconium coagulant against traditional ferric and alum coagulants. Water Res. 46, 4179–4187.

Li, T., Zhu, Z., Wang, D., Yao, C., Tang, H., 2006. Characterization of floc size, strength and structure under various coagulation mechanisms. Powder Technol. 168, 104–110.

Meakin, P., 1990. Fractal structures. Prog. Solid State Chem. 20, 135–233.

Mutl, S., Polasek, P., Pivokonsky, M., Kloucek, O., 2006. The influence of G and T on the course of aggregation in treatment of medium polluted surface water. Water Sci. Technol.: Water Suppl. 6, 39–48.

Oles, V., 1992. Shear-induced aggregation and breakup of polystyrene latex particles. J. Colloid Interface Sci. 154, 351–358.

Parker, D.S., Kaufman, W.J., David, J., 1972. Floc breakup in turbulent flocculation processes. J. Sanit. Eng. Div. 98, 79–99.

Persson, I., 2010. Hydrated metal ions in aqueous solution: how regular are their structures? Pure Appl. Chem. 82, 1901–1917.

Pivokonsky, M., Pivokonska, L., Bäumeltova, J., Bubakova, P., 2009. The effect of cellular organic matter produced by cyanobacteria micrcystis aeruginosa on water purification. J. Hydrol. Hydromech. 57, 121–129.

Pivokonsky, M., Safarikova, J., Bubakova, P., Pivokonska, L., 2012. Coagulation of peptides and proteins produced by *Microcystis aeruginosa*: interaction mechanisms and the effect of Fe-peptide/protein complexes formation. Water Res. 46, 5583–5590.

Pivokonsky, M., Naceradska, J., Brabenec, T., Novotna, K., Baresova, M., Janda, V., 2015. The impact of interactions between algal organic matter and humic substances on coagulation. Water Res. 84, 278–285.

Pivokonsky, M., Naceradska, J., Kopecka, I., Baresova, M., Jefferson, B., Li, X., et al., 2016. The impact of algogenic organic matter on water treatment plant operation and water quality: a review. Crit. Rev. Environ. Sci. Technol. 46, 291–335.

Safarikova, J., Baresova, M., Pivokonsky, M., Kopecka, I., 2013. Influence of peptides and proteins produced by cyanobacterium *Microcystis aeruginosa* on the coagulation of turbid waters. Sep. Purif. Technol. 118, 49–57.

Selomulya, C., Amal, R., Bushell, G., Waite, T.D., 2001. Evidence of shear rate dependence on restructuring and breakup of latex aggregates. J. Colloid Interface Sci. 236, 67–77.

Shin, J.Y., Spinette, R.F., O'Melia, C.R., 2008. Stoichiometry of coagulation revisited. Environ. Sci. Technol. 42, 2582–2589.

Soos, M., Wang, L., Fox, R.O., Sefcik, J., Morbidelli, M., 2007. Population balance modeling of aggregation and breakage in turbulent Taylor–Couette flow. J. Colloid Interface Sci. 307, 433–446.

Spicer, P.T., Pratsinis, S.E., Raper, J., Amal, R., Bushell, G., Meesters, G., 1998. Effect of shear schedule on particle size, density, and structure during flocculation in stirred tanks. Powder Technol. 97, 26–34.

Takaara, T., Sano, D., Konno, H., Omura, T., 2007. Cellular proteins of *Microcystis aeruginosa* inhibiting coagulation with polyaluminum chloride. Water Res. 41, 1653–1658.

Tambo, N., Hozumi, H., 1979. Physical characteristics of flocs-II. Strength of floc. Water Res. 13, 421–427.

Vandamme, D., Muylaert, K., Fraeye, I., Foubert, I., 2014. Floc characteristics of *Chlorella vulgaris*: influence of flocculation mode and presence of organic matter. Bioresour. Technol. 151, 383–387.

Vlieghe, M., Frances, C., Coufort-Saudejaud, C., Liné, A., 2017. Morphological properties of flocs under turbulent break-up and restructuring processes. AICHE J. 63, 3706–3716.

Wang, Y., Gao, B.Y., Xu, X.M., Xu, W.Y., Xu, G.Y., 2009. Characterization of floc size, strength and structure in various aluminum coagulants treatment. J. Colloid Interface Sci. 332, 354–359.

Wang, B., Shui, Y., He, M., Liu, P., 2017. Comparison of flocs characteristics using before and after composite coagulants under different coagulation mechanisms. Biochem. Eng. J. 121, 107–117.

Williams, R.A.A., Peng, S.J.J., Naylor, A., 1992. In situ measurement of particle aggregation and breakage kinetics in a concentrated suspension. Powder Technol. 73, 75–83.

Zhang, X.J., Chen, C., Ding, J.Q., Hou, A., Li, Y., Niu, Z.B., et al., 2010. The 2007 water crisis in Wuxi, China: analysis of the origin. J. Hazard. Mater. 182, 130–135.

Appendix A. Supplementary data

Influence of COM-peptides/proteins on the properties of flocs formed at different shear rates

Monika Filipenska[1,2], Petra Vasatova[1], Lenka Pivokonska[1], Lenka Cermakova[1,2], Andrea Gonzalez-Torres[3], Rita K. Henderson[3], Jana Naceradska[1,2], Martin Pivokonsky[1,*]

1. Institute of Hydrodynamics of the Czech Academy of Sciences, Pod Patankou 5, 166 12 Prague 6, Czech Republic
2. Institute for Environmental Studies, Faculty of Science, Charles University, Benatska 2, 128 01 Prague 2, Czech Republic
3. The bioMASS Lab, School of Chemical Engineering, The University of New South Wales, Sydney, NSW, Australia

*Corresponding author: Martin Pivokonsky, E-mail: pivo@ih.cas.cz

These supplementary data contain the following tables and figures:

Table S1 Evaluation of data normality.

Table S2 One-way ANOVA used for testing the data reproducibility.

Fig. S1 Images of COM-flocs.

Fig. S2 Titration curves of COM-peptides/proteins and kaolinite.

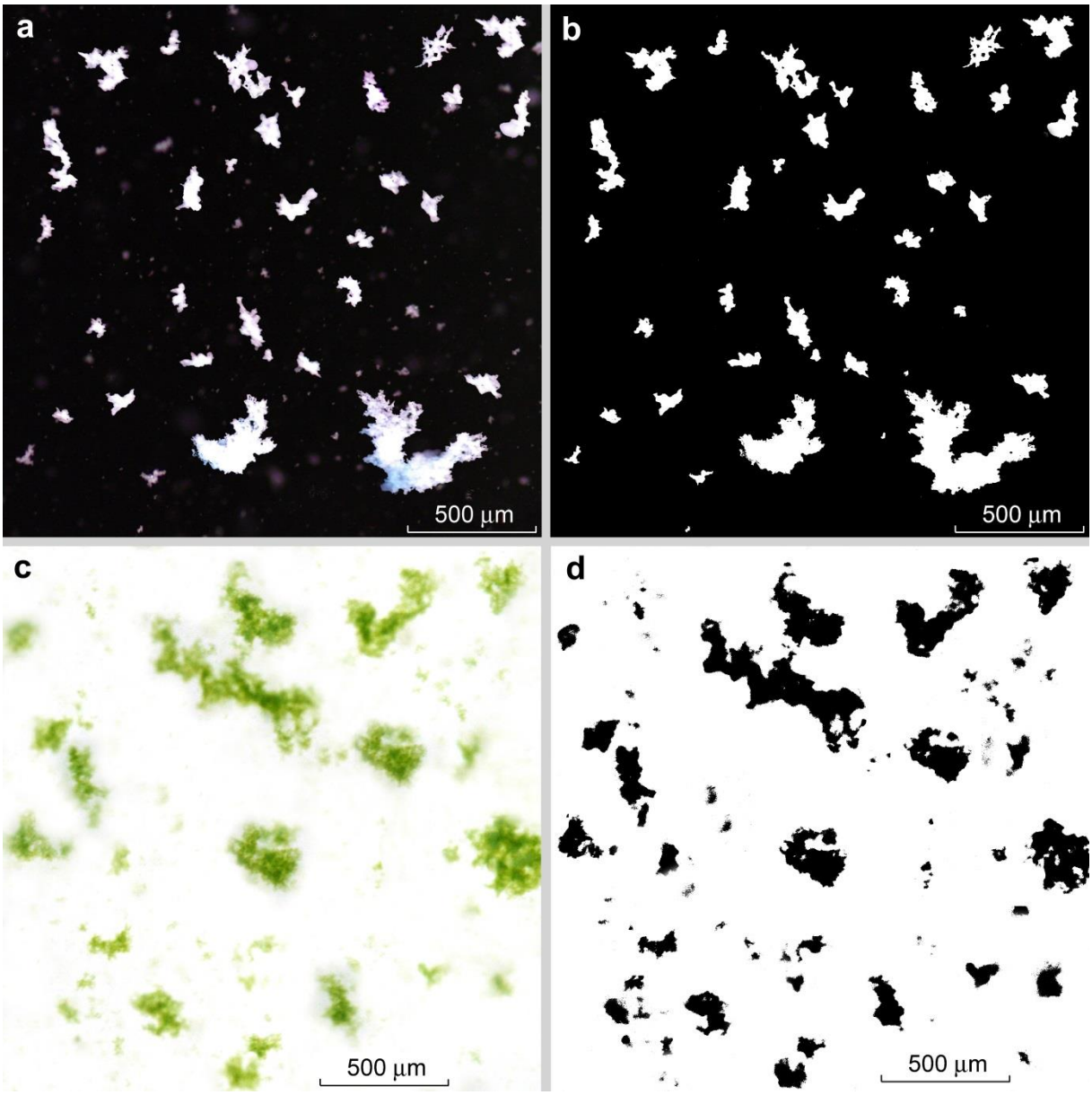

Fig. S1 Images of flocs at G = 40 sec^{-1}: (a) COM+Al - colour, (b) COM+Al - after thresholding, (c) COM+Fe - colour, and (d) COM+Fe - after thresholding.

Table S1 Evaluation of data normality. Testing normality for the equivalent diameter, *d*, involved conducting a one-sample Kolmogorov-Smirnov test with a significance level of 0.95 ($\alpha = 0.05$). The null hypothesis, i.e. the size distribution of the flocs possesses normal distribution, was not rejected.

	Kaolinite+Al		**COM+Al**		**Kaolinite+COM+Al**	
G (sec^{-1})	D_1	D_{1max}	D_1	D_{1max}	D_1	D_{1max}
20	0.0259	0.0616	0.0558	0.1162	0.0584	0.1216
30	0.0206	0.0491	0.047	0.0979	0.0511	0.1065
40	0.0177	0.0422	0.0406	0.0847	0.0443	0.0923
50	0.0154	0.0366	0.0268	0.0558	0.0299	0.0622
60	0.0137	0.0327	0.024	0.0501	0.0261	0.0543
70	0.0124	0.0296	0.0212	0.0442	0.0231	0.0481
80	0.0111	0.0265	0.0199	0.0416	0.0205	0.0428
90	0.0105	0.0249	0.0181	0.0377	0.0189	0.0393
100	0.01	0.0239	0.0172	0.0359	0.0173	0.036
110	0.0101	0.0221	0.0165	0.0344	0.016	0.0333
120	0.0101	0.0209	0.0155	0.0322	0.0152	0.0317
140	0.0082	0.0195	0.0145	0.0303	0.0145	0.0302
150	0.008	0.0191	0.0144	0.0301	0.0141	0.0293
160	0.008	0.019	0.0143	0.0299	0.0134	0.0286
180	0.0079	0.0187	0.0137	0.0285	0.0128	0.0272
	Kaolinite+Fe		**COM+Fe**		**Kaolinite+COM+Fe**	
G (sec^{-1})	D_1	D_{1max}	D_1	D_{1max}	D_1	D_{1max}
20	0.0035	0.0728	0.0669	0.1458	0.0778	0.1508
30	0.0028	0.059	0.058	0.1263	0.0608	0.13
40	0.0025	0.0512	0.0528	0.1149	0.0611	0.1221
50	0.0021	0.0448	0.0477	0.104	0.0544	0.1116
60	0.0019	0.0404	0.0439	0.0957	0.0512	0.109
70	0.0018	0.0365	0.0296	0.0644	0.0462	0.0925
80	0.0016	0.034	0.0274	0.0598	0.0393	0.0811
90	0.0015	0.0315	0.0252	0.0549	0.0333	0.0709
100	0.0014	0.03	0.0232	0.0505	0.0314	0.068
110	0.0015	0.0318	0.0223	0.0485	0.0273	0.0535
120	0.0014	0.0292	0.0211	0.046	0.0255	0.0491
140	0.0012	0.026	0.0207	0.0452	0.0233	0.0433
150	0.0012	0.0257	0.0207	0.0451	0.0219	0.0455
160	0.0012	0.0251	0.0204	0.0445	0.0211	0.0451
180	0.0012	0.0248	0.0202	0.0441	0.0209	0.0448

Table S2 The one-way ANOVA was used to test the null hypothesis that the means of parameters *d* and number (relevant floc components) were equal for individual measurements at both of the tested shear rates.

	$G = 40\ sec^{-1}$				$G = 160\ sec^{-1}$			
	α-level	***p-value***	***F-value***	F_{crit}	***α-level***	***p-value***	***F-value***	F_{crit}
Kaolinite+Al	0.05	0.009	0.142	2.62	0.05	0.162	0.163	3.40
Kaolinite+Fe	0.05	0.014	0.149	2.62	0.05	0.139	0.158	3.40
COM+Al	0.05	0.011	0.138	2.62	0.05	0.158	0.174	3.40
COM+Fe	0.05	0.052	1.142	2.62	0.05	0.125	0.146	3.40
Kaolinite+COM+Al	0.05	0.028	0.151	2.62	0.05	0.121	0.168	3.40
Kaolinite+COM+Fe	0.05	0.011	0.116	2.62	0.05	0.122	0.150	3.40

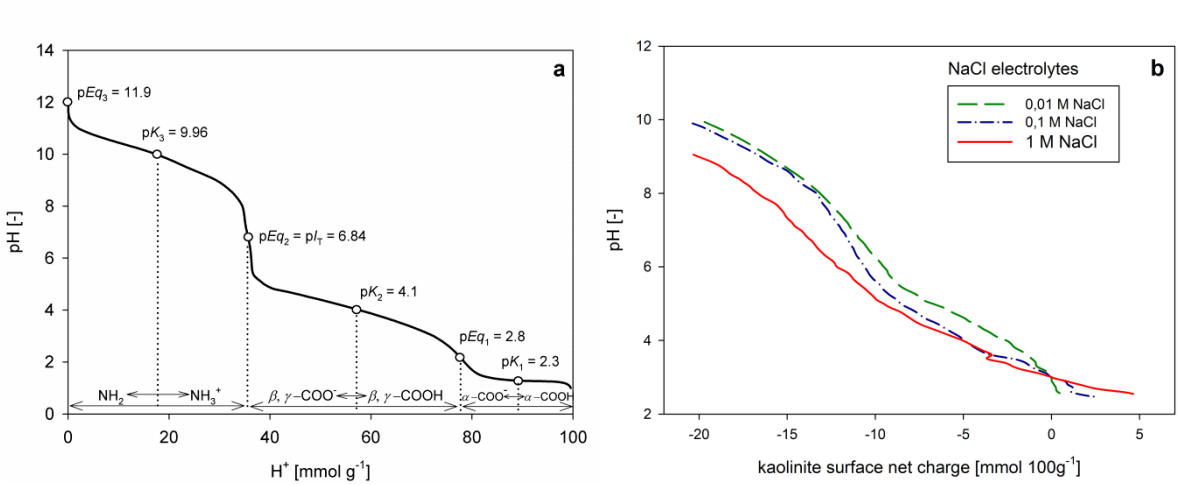

Fig. S2 Titration curves of (a) COM-peptides/proteins, and (b) kaolinite, as measured by Safarikova et al. (2013). These data were used for the determination of the net charge of individual floc components used in Table 2.

References:

Safarikova, J., Baresova, M., Pivokonsky, M., Kopecka, I., 2013. Influence of peptides and proteins produced by cyanobacterium *Microcystis aeruginosa* on the coagulation of turbid waters. Sep. Purif. Technol. 118, 49–57.

PUBLIKACE 4

Removal of cyanobacterial amino acids in water treatment by activated carbon adsorption

Lenka Čermáková, Ivana Kopecká, Martin Pivokonský, Lenka Pivokonská a Václav Janda

Separation and Purification Technology 173 (2017) 330-338
DOI 10.1016/j.seppur.2016.09.043

Separation and Purification Technology 173 (2017) 330–338

Contents lists available at ScienceDirect

Separation and Purification Technology

journal homepage: www.elsevier.com/locate/seppur

Removal of cyanobacterial amino acids in water treatment by activated carbon adsorption

Lenka Cermakova [a,b], Ivana Kopecka [a], Martin Pivokonsky [a,b,*], Lenka Pivokonska [a], Vaclav Janda [c]

[a] Institute of Hydrodynamics, Academy of Sciences of the Czech Republic, Pod Patankou 30/5, 16612 Prague 6, Czech Republic
[b] Institute for Environmental Studies, Faculty of Science, Charles University, Benatska 2, 12801 Prague 2, Czech Republic
[c] Department of Water Technology and Environmental Engineering, University of Chemistry and Technology, Prague, Technicka 5, 16628 Prague 6, Czech Republic

ARTICLE INFO

Article history:
Received 23 June 2016
Received in revised form 21 September 2016
Accepted 25 September 2016
Available online 28 September 2016

Keywords:
Amino acids
Activated carbon
Adsorption
Algal organic matter
Water treatment

ABSTRACT

The applicability of activated carbon for the adsorption of *phenylalanine*, *arginine* and *aspartic acid* from aqueous solution was evaluated in this study. These amino acids are plentiful in low-molecular weight algal organic matter produced by cyanobacteria, which is not satisfactorily removed by chemical coagulation. Because of this they may gravely disturb the water treatment process. Equilibrium adsorption of amino acids was studied on well-characterized activated carbons, Picabiol (PIC) and Filtrasorb (FTL), possessing different chemical and charge properties evaluated by Boehm titration. Adsorption experiments were conducted at various adsorbate initial concentrations, pH values and ionic strengths to elucidate the effect of solution properties on the amino acid removal. Distinct adsorption mechanisms were observed for individual amino acids depending on the pH and the type of carbon applied. Electrostatic interactions between functional groups of the adsorbents and *arginine* were deemed the predominant adsorption mechanism. The maximum *arginine* uptake was achieved through electrostatic attraction at pH 9 on PIC, which bears a higher number of acidic functionalities. Hydrogen bonds between protonated functionalities of adsorption participants were suggested as a possible explanation for the observed *arginine* adsorption on FTL in unfavourable conditions at pH 5 and 7, when electrostatic repulsion prevailed. *Phenylalanine* adsorption was dominated by hydrophobic interactions under all experimental conditions. Electrostatic interactions then caused the final differences in *phenylalanine* uptakes at particular pH values. Besides the direct hydrophobic interactions, *phenylalanine* removal was enhanced by intermolecular hydrophobic interactions leading to the formation of associates consisting of several *phenylalanine* molecules, which were then adsorbed as a unit. Insignificant adsorption of *aspartic acid* was observed on both carbons owing to its strong hydrophilicity. Generally, adsorption of amino acids decreased as the ionic strength of the solution increased. The added salt screened attractive electrostatic interactions, altered surface charge of the adsorbents or changed adsorbate solubility.

1. Introduction

Free and combined amino acids (AAs) can be found in all types of natural waters including water sources used for drinking water production. AAs form together with peptides and proteins a dominant fraction of nitrogenous compounds of algal organic matter (AOM) [1]. Many deleterious effects on water treatment are related to AOM presence in raw water, e.g. coagulation failures accompanied by increased consumption of chemical reagents [2,3], membrane fouling [4,5] or production of harmful cyanobacterial toxins [6]. Metabolic activity of cyanobacteria and green algae is the primary source of AOM nitrogenous compounds [1,7–9]. Cyanobacteria produce high amounts of polypeptides composed of *glycine* units, *aspartic* and *glutamic acid*, *alanine* and *serine* [10]. High concentrations of AAs have been detected during a period of rapid algal decomposition and subsequent degradation of their cells [11]. Concentrations of dissolved peptides/proteins and free AAs in raw water depend on biological activity of the microorganisms and increase with the age of the culture [1,9]. They can reach high mg L^{-1} concentrations during the period of algal blooms [1]. Concentration of free AAs usually ranges between 20 and 1000 μg L^{-1} [7,11] and it may account for 2–13% of the total dissolved organic carbon (DOC) in natural waters [7,8]. The incidence of peptides/proteins is up to 5 times higher than for free AAs in

* Corresponding author at: Institute of Hydrodynamics, Academy of Sciences of the Czech Republic, Pod Patankou 30/5, 16612 Prague 6, Czech Republic.
E-mail address: pivo@ih.cas.cz (M. Pivokonsky).

http://dx.doi.org/10.1016/j.seppur.2016.09.043
1383-5866/

natural waters [11]. The amount of AAs is stable throughout the water column, but decreases with water depth in the case of peptides/proteins [7,8].

Glycine, *glutamic acid*, *alanine*, *aspartic acid*, *leucine* and *serine* belong to the most frequent AAs in natural waters [7,8], and *arginine*, *lysine* and *glycine* dominate the cellular organic matter (COM) [9].

Amino acids are non-toxic compounds acting mainly as the building blocks of microorganisms' DNA, RNA, proteins, etc. [12] but their occurrence in the treated water is undesirable [8,11,13–15]. This brings about numerous problems across water treatment process. AAs may increase Cl_2 consumption during chlorination of water [11]. Under this treatment process, their presence also leads to the production of aldehydes, nitriles and other compounds negatively affecting the organoleptic properties of water, especially its taste and odour [12,13,15]. They also present a potential source of biodegradable organic carbon serving as a nutritive substrate for the growth of detrimental microorganisms in the water distribution network [8,14]. Finally, AAs belong to identified precursors of disinfection by-products (DBPs) and contribute to the formation of trihalomethanes (THMs) and haloacetic acids (HAAs) [10]. Hong et al. [8] discovered that especially aromatic AAs and two AAs with aliphatic side chain, *aspartic* and *glutamic acid*, are problematic in this context.

A coagulation-based treatment is often ineffective in removing organic compounds of high polarity and low molecular weight (MW) such as AAs [3]. Various concentrations of AAs are measured in all stages of the water treatment process [8,11,12], and increasing concentrations have been detected in some cases [11].

For the reasons mentioned above, it is necessary to pay attention to the removal of AAs from raw water sources and to search for effective ways how to do it. Adsorption onto activated carbon (AC) seems to be an appropriate method since it is effectively applied in drinking water production for the uptake of other organic nitrogenous compounds with a very low MW, e.g. cyanobacterial toxins [6] or AOM peptides [16]. Studies focusing exclusively on the adsorption of AAs onto AC in the water treatment process are rare, although numerous researches have been made to investigate the adsorption of AAs for applications in medicine, biochemistry, geochemistry and the food industry [17]. Various adsorbents have been assessed in these studies including zeolites [18], kaolinite [19], polymeric adsorbent [20], mesoporous silica [21,22] or activated carbon, which demonstrated adsorption capacity comparable to mesoporous carbon, a sorption material with well ordered pore system [23]. Carbon nanotubes have also been found to be promising adsorbent for AAs with sorption capacities much higher than those of many other macroporous and mesoporous sorption materials [24].

Recent adsorption studies have brought several conclusions. Adsorption efficiency for AAs is affected by their MW, size or geometry of molecules. Solubility, polarity and content of functional groups (e.g. —COOH, —NH_2, —OH, —S—) are also responsible for adsorption ability of AAs [22,25]. Besides the adsorbate properties, the adsorption is governed by the adsorbent nature (e.g. surface charge, pore structure, functional groups on the adsorbent surface) and solution properties (e.g. pH, ionic strength (IS), initial adsorbate concentration, temperature) [12,18–21,23–27]. Finally, a combination of these factors determines both the adsorption character and the mechanisms [18,22]. Hydrophobic interactions [23,27], electrostatic interactions [21] and hydrogen bonds [19] have been identified as the most common mechanisms in amino acid adsorption, unfortunately often on adsorbents other than activated carbon.

The aim of this study was to investigate the effect of several adsorption factors (adsorbate initial concentration, pH and IS) on the adsorption of three amino acids belonging to the major AAs commonly identified in natural waters containing AOM and also in treated water after coagulation/flocculation – aromatic *phenylalanine* (*Phe*), basic *arginine* (*Arg*) and acidic *aspartic acid* (*Asp*). The AAs were adsorbed in laboratory scale operation on two types of commercially applied granular activated carbon (GAC) with different textural and charge properties to clarify which mechanisms govern their adsorption.

2. Materials and methods

2.1. Characterization of adsorbents

GAC Picabiol 12 × 40 (PIC) and Filtrasorb TL 830 (FTL) were used for the adsorption of AOM amino acids based on the results of our previous adsorption study with AOM peptides [15]. Both GACs are microporous and designed for drinking water treatment including adsorption of natural organic matter, taste and odour compounds, cyanobacterial toxins and other organic matter with a low molecular weight. Textural and charge properties of the GACs are summarized in Table S1 (see Supplementary material). Details of the performed characterization methods can be found in our previous study [16].

The characterization of surface functional groups was made by Boehm titration [28]. Carbon suspensions were prepared with 1 g of GAC and 50 mL of 0.05 M NaOH and HCl solutions, equilibrated for 48 h at room temperature (22 ± 0.5 °C). Twenty mLs of these solutions were filtered through a 0.22 μm membrane filter (Millipore, USA) and then titrated either with 0.05 M HCl or 0.05 M NaOH. The amount of acidic and basic functional groups was calculated from the uptake of titration agent according to the methodology in literature [29].

2.2. Adsorbates

Three amino acids with different molecular structure and chemical properties were selected as the adsorbates in this study: L-*aspartic acid*, L-*arginine* and L-*phenylalanine* (Sigma-Aldrich, USA). They represent the dominant amino acids identified in natural waters [9]. The characteristics of selected AAs are shown in Table S2 (see Supplementary material).

2.2.1. DOC analysis

Concentrations of AAs in the samples were quantified before and after the adsorption as the concentration of DOC (Dissolved Organic Carbon) measured by a total organic carbon analyser TOC-V_{CPH} (Shimadzu Corporation, Japan) according to the methodology described in our previous studies [1,3]. Each sample was performed in triplicate with the relative error <3%. The dependence of the DOC content on the concentration of AAs in mg L^{-1} is depicted in Fig. S1 (see Supplementary material).

2.2.2. Quantitative analysis of natural amino acids in cellular organic matter

The quantitative analysis of free AAs was performed to verify the proportional representation of the studied AAs in cyanobacterial cellular organic matter (COM). COM produced by cyanobacterium *Microcystis aeruginosa* of MW <500 Da was used for this analysis. The cultivation of the cyanobacterium and the preparation of COM samples were done according to the methodology described in our previous studies [1,3]. Free amino acids included in COM were determined after derivatization by fluorenylmethyl chloroformate (FMOC) by the HPLC system [9] (see Section S1 in Supplementary material).

2.3. Adsorption experiments and isotherm models

The equilibrium batch experiments were performed to determine the impact of solution pH value and IS on the adsorption of selected AAs onto GACs. AA stock solutions (500 mg L^{-1} DOC) were diluted in ultra-pure water (alkalinity of 1.5 mmol L^{-1} adjusted by 0.125 M $NaHCO_3$) to prepare samples of AAs (250 mL) with the final concentration of 1–200 mg L^{-1} DOC. Then, the samples were adjusted by 0.1 M or 2 M HCl and by 0.1 M or 2 M NaOH to reach different pH values of 5, 7 and 9. Sodium azide (50 mg L^{-1}) was added to all samples to eliminate the biological activity. Further, a series of samples in 0.01 M (low ionic strength) and 0.3 M (high ionic strength) NaCl background electrolyte were prepared to determine the effect of solution IS on the adsorption process.

Doses of 400 mg L^{-1} of GAC PIC or FTL were added to each solution and agitated on a magnetic stirrer (100 rpm) at room temperature (22 ± 0.5 °C) for 48 h, a time interval pre-determined to be sufficient to reach adsorption equilibrium. Subsequently, the solutions were filtered through a membrane filter 0.22 μm (Millipore, USA) to remove GAC particles, and residual concentrations of AAs after the adsorption were measured as DOC. For each concentration of AAs, a blank sample without adsorbent was prepared and served as a control of the adsorbate loss during the experiments.

The amount of AAs adsorbed onto GAC was calculated according to the following Eq. (1):

$$q_e = (C_0 - C_e)\frac{V}{m} \quad (1)$$

where q_e is the amount of AAs adsorbed per mass unit of GAC at equilibrium (mg g^{-1}), C_0 and C_e are the initial and equilibrium concentrations of AAs in the solution (mg L^{-1}), respectively, V is the volume of the solution (L) and m is the mass of the adsorbent (g).

The data obtained from the adsorption isotherm experiments were fitted to the Langmuir (2) and Freundlich (3) models, respectively

$$q_e = \frac{a_m b C_e}{1 + bC_e} \quad (2)$$

and

$$q_e = K_f C_e^{1/n} \quad (3)$$

where q_e (mg g^{-1}) and C_e (mg L^{-1}) represent adsorbate uptake and solution concentration at equilibrium, respectively. Parameters a_m (mg g^{-1}) and K_f [(mg g^{-1}) (L $mg^{-1})^{1/n}$] are reflective to adsorption capacity; constants b (L mg^{-1}) and $1/n$ represent the surface affinity and the heterogeneity of surface site energy distribution, respectively.

3. Results and discussion

3.1. Amino acids in cellular organic matter

Arg, *Asp* and *Phe* were chosen to represent adsorbates in this study as they have earlier been referred to count among the major AAs naturally occurring in cyanobacterial COM, particularly in that produced by *Microcystis aeruginosa* [9]. They are resistant to coagulation and may form a potential source of DBPs during water treatment [11]. As shown by analyses of free AAs included in COM produced by *M. aeruginosa* (Fig. S2 in Supplementary material), the studied AAs comprised together 53.1% of all free AAs in the sample (*Phe* 22.7%, *Asp* 17.6%, *Arg* 12.8%). The analysis confirmed that *Phe*, *Asp* and *Arg* belong to the most abundant AAs of cyanobacterial COM.

3.2. Charge characteristics of adsorption system

AAs have several functional groups with different acidities, of which the amino and carboxylic groups are the most important ones. These groups can be in protonated or dissociated state according to the solution pH value so they produce charged AA molecules [18]. In the case of GAC, oxygen complexes of acidic (e.g. carboxyl, phenol, lactone) and basic character (e.g. pyrone, chromene, quinone) belong to the most important ionisable functional groups that affect GAC net surface charge as well as its adsorption ability [30]. Thanks to these active functional groups, AAs and GAC can exhibit complex adsorption behaviour via different types of interactions, as will be discussed in Section 3.3. Fig. 1 depicts specific charge conditions occurring during the adsorption of studied AAs on selected GACs.

3.3. Adsorption from aqueous solution

The dependence of PIC and FTL adsorption capacity on the initial concentration of AAs was evaluated through the single-component isotherms at pH 5, 7 and 9.

3.3.1. Aspartic acid

Insignificant *Asp* adsorption was observed at pH 5, 7 and 9 on PIC (Fig. 2a) thanks to *Asp* strong hydrophilicity, i.e. the propensity of its side chain to be in contact with water molecules through the hydrogen bonds, and electrostatic repulsion between its —COO^- groups and PIC negative charge (see Fig. 1). *Asp* was absorbed on FTL better than on PIC (Fig. 2b) but the adsorbed amounts (following the order of pH 9 > pH 7 > pH 5) were still lower than for *Phe* and *Arg*, again because of *Asp* hydrophilicity. Since FTL carried a lower acidity compared to PIC (see Table S1 in Supplementary material), *Asp* adsorption was not so limited by electrostatic repulsion.

3.3.2. Phenylalanine

The amount of *Phe* adsorbed on PIC decreased as follows: pH 5 > pH 7 > pH 9 (Fig. 3a). Hydrophobic interactions between hydrophobic parts of PIC surface and hydrophobic side chain of the *Phe* molecules enabled the adsorption under all experimental conditions [17,23], as well as π-π interactions acting between delocalized π-electrons of aromatic ring in *Phe* side chain and graphene rings of GAC [27,31]. The significant differences of *Phe* uptakes at individual pH values were then caused by electrostatic interactions. The highest uptake of 141.00 mg g^{-1} observed at pH 5 can be interpreted in various ways. Firstly, solution pH was lower than *Phe* p*I* = 5.48, thus the molecule had overall positive charge due to the protonated amino group. A negative charge dominated on PIC surface at pH > pH_{pzc} = 3.5 (Fig. 1). The opposite charges resulted in attractive electrostatic interactions enhancing the adsorption. Secondly, the maximum adsorption at pH 5 can be explained by the proximity of solution pH to the *Phe* p*I*. A solution at the p*I* has a large concentration of zwitterions (including both charged amino and carboxyl groups) that are considered to be net-neutral with respect to the charge. Therefore, the strength of coulomb repulsive interactions between *Phe* molecules at a pH close to the p*I* was minimal and allowed the PIC adsorption capacity to have the greatest value [22–24].

The negative charge increased at pH 7 on PIC and it developed also in *Phe* molecules owing to the dissociation of carboxylic group (Fig. 1). Besides the attractive electrostatic interactions, the repulsive ones have formed between *Phe* and PIC surface and the adsorption decreased from 141.00 mg g^{-1} to 106.50 mg g^{-1} compared to pH 5. This effect was even more evident at pH 9, because the negative charge of adsorption participants increased and

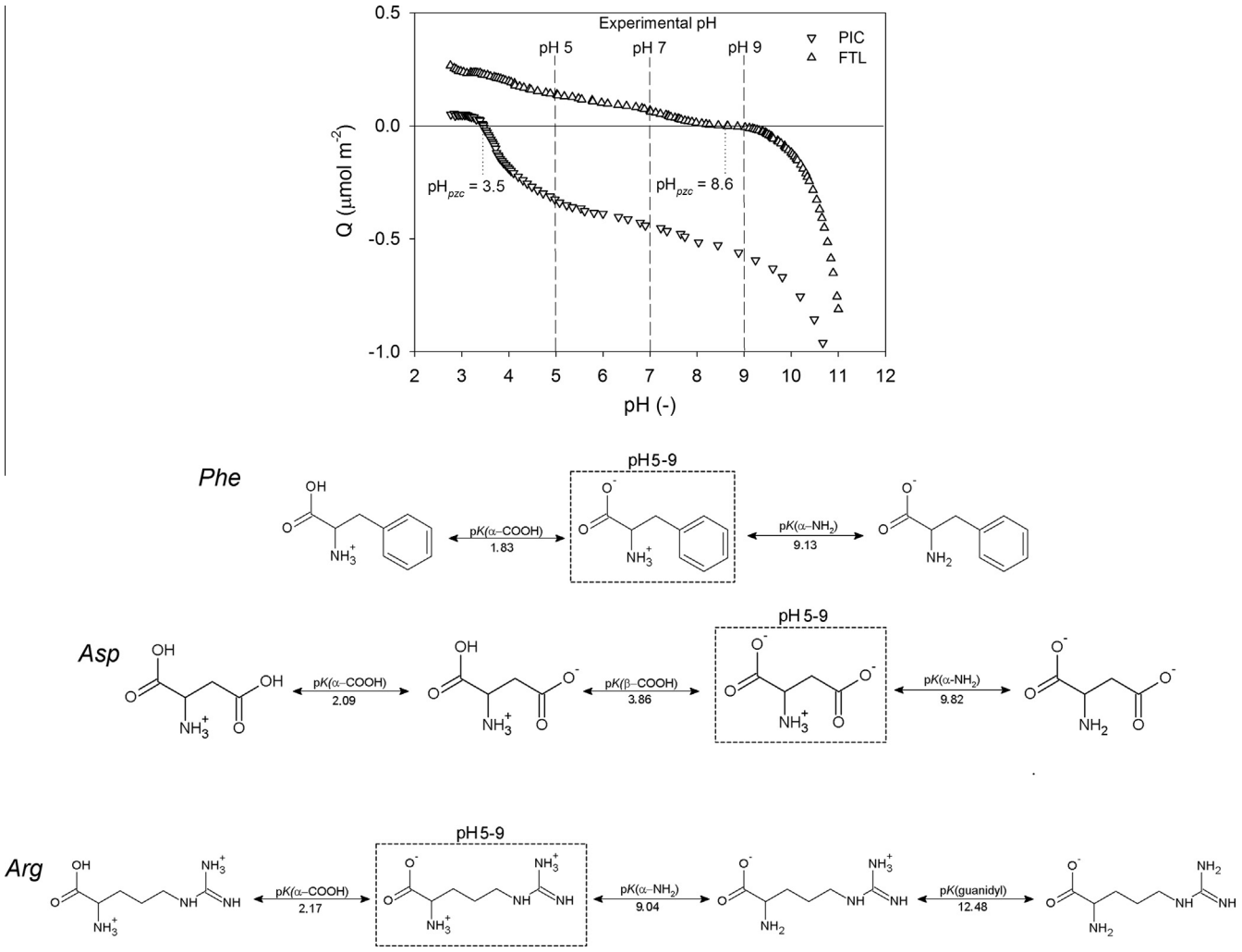

Fig. 1. Surface charge of GAC PIC and FTL and particular forms of *Phe*, *Arg* and *Asp* according to the solution pH.

strengthened the repulsion. The highest adsorbed amount of 71.75 mg g^{-1} at pH 9 was half of the amount at pH 5.

The amount of *Phe* adsorbed on FTL was higher and it decreased in an opposite order: pH 9 > pH 7 > pH 5 (Fig. 3a). Hydrophobic interactions and π-π interactions contributed to the adsorption on FTL as it was in the case of PIC. Acid-base characterization (Table S1 in Supplementary material) showed the FTL is generally less charged than PIC. Hydrophobic interactions, which are essential for *Phe* adsorption, thus could be more pronounced. This was most evident at pH 9 where they outweighed the anticipated electrostatic repulsion between dissociated carboxylic groups of *Phe* molecules and the negative charge prevailed slightly on the FTL surface, so the highest adsorption capacity of 188.75 mg g^{-1} was reached. On the other hand, an electrostatic attraction enhanced adsorption between oppositely charged functionalities of adsorption partners at pH 7. The lowest adsorption capacity of 127.80 mg g^{-1} was observed at pH 5, though *Phe* was closest to its p*I* and the same positive adsorption effect could be expected as on PIC. Both carbons have different chemical structures that influenced their surface charge as apparent from Fig. 1 and acid-base characterization based on Boehm titration (see Table S1 in Supplementary material). FTL had more than three times higher amount of basic surface groups producing the positive charge than PIC. The repulsive electrostatic interactions between FTL strong positive charge and protonated amino groups of *Phe* at pH 5 then reduced the adsorption. Similar results of *Phe* adsorption have been described on various adsorbents by Clark et al. [27].

3.3.3. Arginine

The amount of *Arg* adsorbed on PIC decreased as follows: pH 9 > pH 7 > pH 5 (Fig. 3b). All studied pH values were below the *Arg* p*I* = 10.76, thus its overall charge can be considered as positive. Charges of *Arg* and PIC were always opposite and allowed a formation of attractive electrostatic interactions. Differences in the amount of *Arg* adsorbed at pH 9 (103.25 mg g^{-1}), pH 7 (86.25 mg g^{-1}) and pH 5 (62.00 mg g^{-1}) were given by the growth of PIC negative charge. Similar results reflecting electrostatic interactions and a higher adsorption of basic AAs with increasing pH have been described in literature [17,21]. Vinu et al. [23] observed the highest adsorption of basic *histidine* at pH 7.5, which was close to its p*I* = 7.47. Repulsive electrostatic interactions between *histidine* and adsorbent surface were reduced under these conditions, while attractive intramolecular forces allowed a conformation of *histidine* more favourable for entering adsorbent internal structure. Since the *Arg* p*I* of 10.76 is high above the highest experimental pH, it was not possible to verify this phenomenon in this study.

Arg was adsorbed on FTL less than on PIC. The adsorbed amounts decreased in the order of pH 9 > pH 7 ⩾ pH 5 (Fig. 3b).

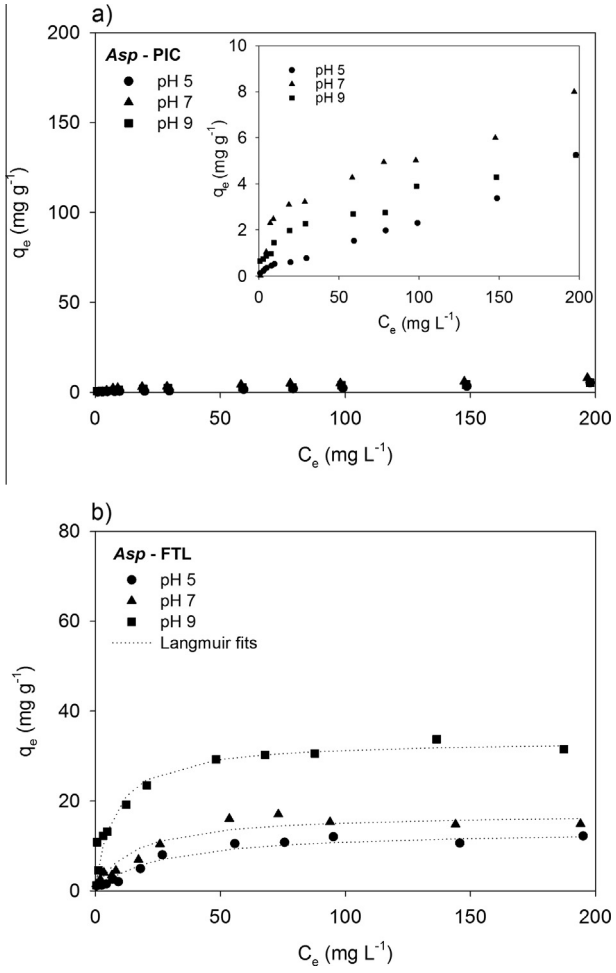

Fig. 2. Adsorption isotherms for *Asp* on GAC PIC (a) and FTL (b) at pH 5, 7 and 9.

Since the overall charge of FTL at pH 9 was minimal, the highest uptake of 56.77 mg g^{-1} achieved at this pH was caused primarily by hydrogen bonds formed between functional groups of adsorption partners (e.g. N heteroatoms of guanidyl group in *Arg* and FTL hydroxyl or carboxyl groups). The adsorption capacity markedly decreased at lower pH values owing to repulsive electrostatic interactions that have developed between the strong positive charges of *Arg* and FTL (see Fig. 1). The difference in maximal *Arg* uptakes at pH 7 (26.90 mg g^{-1}) and pH 5 (22.40 mg g^{-1}) was negligible. *Arg* adsorption occurred probably by hydrogen bonds under these unfavorable conditions [32].

If compared *Arg* and *Phe* isotherms on PIC at pH 5, pH 7 and pH 9, the described adsorption differences between these AAs are more evident. *Arg* was adsorbed in a greater extent compared to *Phe* at all experimental pH values at lower initial concentrations (C_0 < 30 mg L^{-1}) but *Phe* adsorption was more effective at pH 5 and pH 7 at higher initial concentrations (C_0 > 100 mg L^{-1}). This was well reflected also by the isotherm crossing that can be seen at pH 5 and pH 7. On the other hand, no isotherm crossing was observed at pH 9 because *Arg* adsorbed on PIC more than *Phe* at all C_0. This trend is apparent also from the values of Langmuir parameter *b* (Table 1 – *Section A*), which were on average 6 times higher for *Arg* than for *Phe*.

Phe was adsorbed on FTL more than *Arg* at all pH values independently on C_0 (compare Fig. 3a and b), thus no isotherm crossing was observed on FTL compared to PIC. This was caused probably by the charge differences between the GACs as apparent from Fig. 1 and acid-base characterization summarized in Table S1 in Supplementary material.

3.3.4. Adsorption isotherm models

Experimental adsorption data for PIC and FTL were evaluated using Langmuir and Freundlich isotherm models. Model parameters for *Phe* and *Arg* are summarized in Table 1 (*Section A*). As a negligible adsorption of *Asp* on PIC was observed in the study, data obtained for FTL were included in the Table 1 only.

The Langmuir model provided a better fit for experimental data (higher coefficients of determination R^2) compared to the Freundlich model and was therefore included in Figs. 2 and 3. Langmuir parameter a_m (representing a maximum adsorbate uptake at monolayer coverage) described *Arg* and *Phe* adsorption trends at various pH values more accurately than the Freundlich capacity parameter K_f. Parameters *b* and 1/*n* were markedly different for *Phe* and *Arg*, and indicated that adsorption of diverse nature occurred. Since this was obvious mainly for PIC, the discussion below is focused on parameters obtained for this carbon. Higher *b* values (representing the surface affinity and reflecting the rate of uptake change) for *Arg* correlated well with a higher initial steepness of its isotherms (see Fig. 3a and b). On the other hand, low *b* values for *Phe* indicated adsorption occurring in larger and

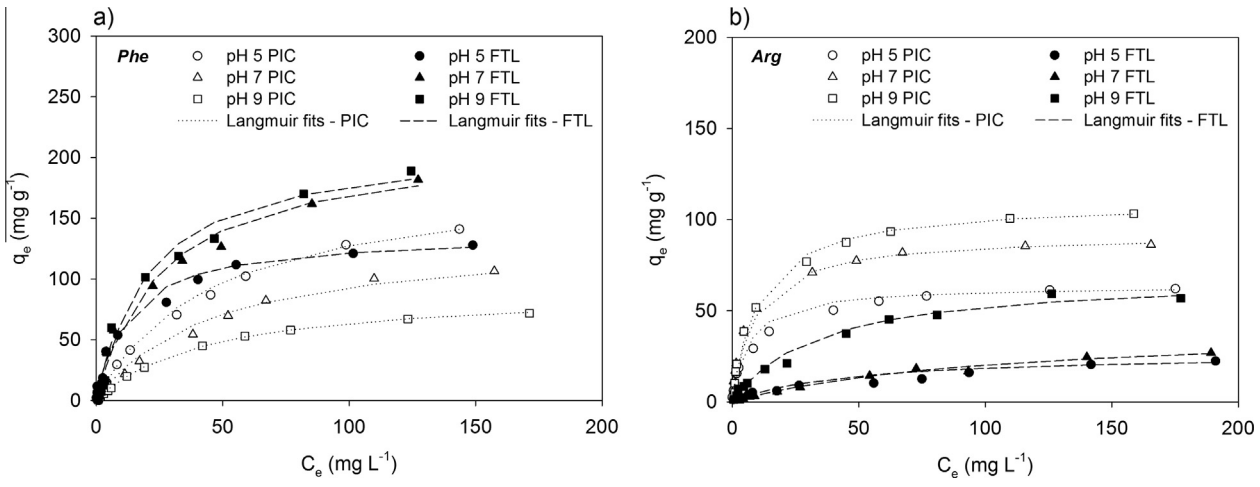

Fig. 3. Adsorption isotherms for *Phe* (a) and *Arg* (b) on GAC PIC and FTL at pH 5, 7 and 9.

Table 1
Freundlich and Langmuir model parameters for adsorption of amino acids (AA) on PIC and FTL from the solutions without (*Section A*) and with NaCl (*Section B*).

	AA	GAC	pH	Freundlich			Langmuir		
				K_f	$1/n$	R^2	a_m	b	R^2
Section A									
Ultra-pure water	*Arg*	PIC	5	14.57	0.390	0.971	63.69	0.153	0.998
			7	20.27	0.400	0.904	91.74	0.111	0.986
			9	18.42	0.490	0.885	109.90	0.095	0.997
		FTL	5	1.24	0.559	0.974	26.60	0.023	0.975
			7	0.73	0.703	0.931	41.15	0.010	0.962
			9	2.88	0.643	0.967	69.44	0.029	0.982
	Phe	PIC	5	5.43	0.707	0.988	185.19	0.022	0.990
			7	4.02	0.700	0.977	135.14	0.022	0.962
			9	2.59	0.700	0.978	90.91	0.023	0.994
		FTL	5	12.40	0.534	0.947	136.99	0.078	0.991
			7	12.28	0.700	0.919	202.77	0.038	0.975
			9	6.37	0.692	0.874	212.77	0.047	0.988
	Asp	PIC	5	–	–	–	–	–	–
			7	–	–	–	–	–	–
			9	–	–	–	–	–	–
		FTL	5	0.98	0.527	0.922	13.57	0.040	0.966
			7	2.14	0.416	0.916	17.30	0.068	0.963
			9	8.27	0.294	0.830	33.56	0.136	0.996
Section B									
0.01 M NaCl	*Arg*	PIC	5	9.16	0.374	0.954	54.64	0.103	0.999
			7	11.80	0.408	0.933	80.65	0.074	0.984
			9	14.83	0.864	0.864	100.00	0.070	0.997
		FTL	5	1.61	0.542	0.968	24.27	0.040	0.989
			7	1.70	0.570	0.987	30.58	0.033	0.988
			9	2.59	0.624	0.978	58.82	0.030	0.984
	Phe	PIC	5	4.82	0.719	0.984	178.57	0.020	0.991
			7	3.56	0.712	0.979	136.99	0.018	0.978
			9	2.77	0.692	0.970	90.09	0.023	0.995
		FTL	5	7.94	0.566	0.978	129.87	0.036	0.992
			7	7.55	0.693	0.927	196.08	0.032	0.966
			9	10.62	0.642	0.985	196.08	0.050	0.985
	Asp	PIC	5	–	–	–	–	–	–
			7	–	–	–	–	–	–
			9	–	–	–	–	–	–
		FTL	5	1.82	0.293	0.897	8.62	0.059	0.988
			7	1.92	0.462	0.869	17.76	0.061	0.983
			9	8.12	0.316	0.918	34.72	0.174	0.999
0.3 M NaCl	*Arg*	PIC	5	2.66	0.501	0.948	31.85	0.047	0.995
			7	2.49	0.543	0.925	45.05	0.044	0.989
			9	2.49	0.632	0.930	55.25	0.031	0.992
		FTL	5	2.00	0.551	0.978	26.74	0.040	0.979
			7	1.36	0.363	0.978	31.35	0.030	0.993
			9	2.08	0.609	0.927	41.67	0.034	0.985
	Phe	PIC	5	3.68	0.644	0.968	94.34	0.026	0.992
			7	4.34	0.529	0.984	65.79	0.030	0.996
			9	2.67	0.642	0.930	86.97	0.022	0.995
		FTL	5	5.81	0.604	0.979	111.11	0.035	0.993
			7	6.06	0.650	0.865	131.58	0.035	0.953
			9	7.33	0.656	0.940	133.33	0.053	0.996
	Asp	PIC	5	–	–	–	–	–	–
			7	–	–	–	–	–	–
			9	–	–	–	–	–	–
		FTL	5	0.75	0.434	0.843	6.43	0.052	0.983
			7	1.44	0.509	0.885	15.60	0.067	0.978
			9	9.37	0.320	0.900	40.82	0.173	0.999

Units: K_f [$(mg\ g^{-1})\ (L\ mg^{-1})^{1/n}$], n [–], R [–], a_m [$mg\ g^{-1}$], b [$L\ mg^{-1}$].

lower-energy pores compared to *Arg*. This is peculiar as both AAs are comparatively small (see Table S2 in Supplementary material) and *Phe* mean kinetic diameter of 0.58 nm [18] allows its package into supermicropores (diameter <0.80 nm). A possible explanation based on *Phe* hydrophobicity is proposed below. Parameter $1/n$ (symbolizing the heterogeneity of surface site energy distribution) for *Phe* was on average twice as for *Arg*, and confirmed that higher *Phe* adsorption at higher C_0 was not induced only by the direct interactions between adsorbent and adsorbate [6]. Higher $1/n$ values are the result of weaker adsorption bonds between the adsorbent and the adsorbate and suggest a cooperative adsorption between AA molecules [23].

Hydrophobic character of *Phe* molecules played a crucial role in the observed uptake differences between studied AAs. *Phe* molecules prefer to minimize a contact with water via hydrophobic interactions, and thus arranged together by hydrophobic parts. Displacing water molecules from the space between the hydrophobic parts of *Phe* molecules led to the formation of associates

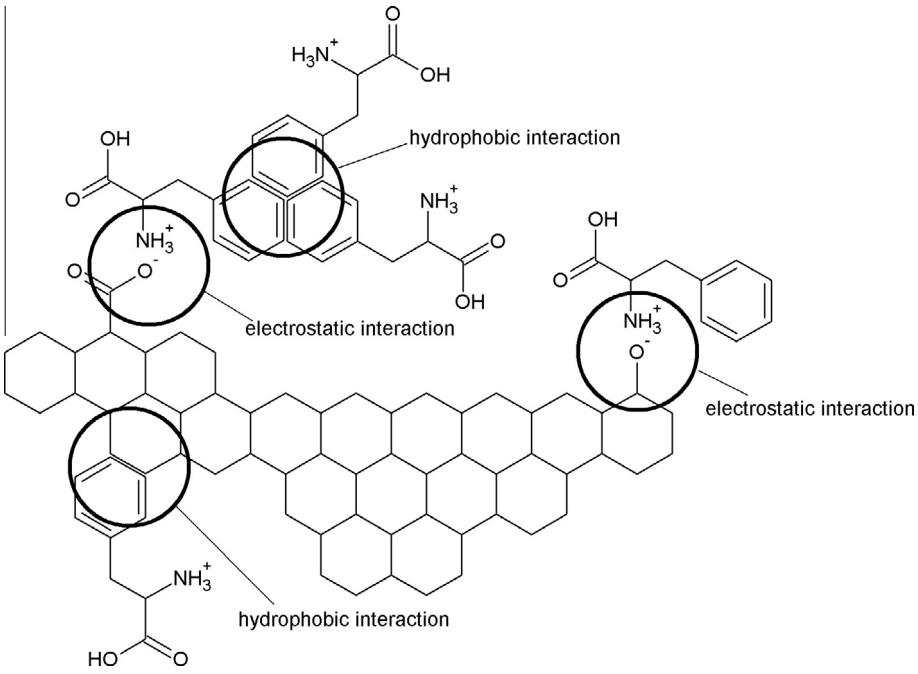

Fig. 4. Interaction forces involved in adsorption of *Phe* on activated carbon.

consisting of several *Phe* molecules. These associates were then adsorbed as a complex on GAC surface, e.g. by electrostatic interactions (Fig. 4). The effect of associate formation asserted oneself at higher initial concentrations ($C_0 > 30$ mg L^{-1}) and therefore may be the main reason of increased adsorption efficiency for *Phe* at higher C_0. Besides the intermolecular hydrophobic interactions, the direct ones with GAC surface affected *Phe* uptake [18,23,27] as is discussed in Section 3.3.2. *Arg* adsorption isotherms reached lower equilibrium adsorption capacities (q_e) but were significantly steeper compared with *Phe* isotherms. This suggests that electrostatic interactions governing *Arg* adsorption proved even at low C_0 [21].

3.4. Adsorption from sodium chloride solution

The presence of dissolved salts has been confirmed to affect the adsorption efficiency of AC in aqueous solutions [32]. Adsorption of *Phe*, *Arg* and *Asp* was studied in the presence of 0.01 M and 0.3 M NaCl background electrolyte to simulate the effect of dissolved salt and consequent change of IS on AA uptake. The impact of IS is further described in the cases of the most effective adsorption observed for individual AAs (i.e. for *Phe* on FTL, *Arg* on PIC and *Asp* on FTL). These results are illustrated in Fig. 5 and corresponding model parameters are summarized in Table 1 (*Section B*). See Supplementary material for additional results (Fig. S3).

Phe adsorption decreased at all pH values on FTL (Fig. 5a), if compared the experiments with and without NaCl. This was more apparent in 0.3 M NaCl solution, as the *Phe* uptake was reduced by 38.2% (pH 9, pH 7) and by 25.9% (pH 5) compared with NaCl free solution. This change was also reflected by the model parameters (Table 1 – *Section B*) – e.g. Langmuir parameter a_m decreased by 79.4 mg g^{-1} (pH 9), 81.2 mg g^{-1} (pH 7) and 25.9 mg g^{-1} (pH 5), respectively. *Phe* adsorption in the absence of NaCl was governed by hydrophobic interactions with the cardinal assistance of electrostatic interactions, which were responsible for the variations of *Phe* uptakes at single pH values (for details see Section 3.3.2 and Fig. 1). The influence of IS was manifested just through the electrostatic interactions. A large quantity of electrolyte ions screened attractive electrostatic interactions in the adsorption system [17,20,32] at pH 9 but strengthened the repulsive ones at pH 7 and 5 so the adsorption decreased in all cases. Both the solvated sodium and chloride ions have been shown to affect the acid-base nature of the adsorbents [32].

Arg uptake dropped by 55.6% (pH 9), by 55.0% (pH 7) and by 51.8% (pH 5), respectively, on PIC as NaCl concentration increased from 0 to 0.3 mol L^{-1} (Fig. 5b). Parameter a_m decreased correspondingly by 54.7 mg g^{-1} (pH 9), by 46.7 mg g^{-1} (pH 7) and by 31.8 mg g^{-1} (pH 5). Attractive electrostatic interactions governed *Arg* adsorption on PIC at all pH values (see Section 3.3.2 and Fig. 1). However, they were diminished by sodium ions forming a positively charged electric double layer around the negatively charged PIC, altering its apparent surface charge and leading finally to lower adsorption of positively charged *Arg* molecules in the presence of background electrolyte [17,32].

Asp behaved differently than the other two AAs in the presence of NaCl (Fig. 5c). Its uptake increased by 26.4% at pH 9 (corresponding increase of a_m by 7.26 mg g^{-1}) and decreased by 51.6% at pH 5 (corresponding decrease of a_m by 7.14 mg g^{-1}) on FTL as NaCl concentration changed from 0 to 0.3 mol L^{-1}. *Asp* uptake decreased very slightly at pH 7, if compared 0.01 M and 0.3 M NaCl solutions, and changed insignificantly compared with experiments without NaCl. A nonspecific adsorption trend under various salt concentrations can probably be related to the hydrophilic nature of *Asp*. NaCl could reduce the solubility of *Asp* [17] and to allow its higher uptake at pH 9. This assumption was not further verified since *Asp* was adsorbed on AC to a limited extent and the study was more focused on the remaining two AAs.

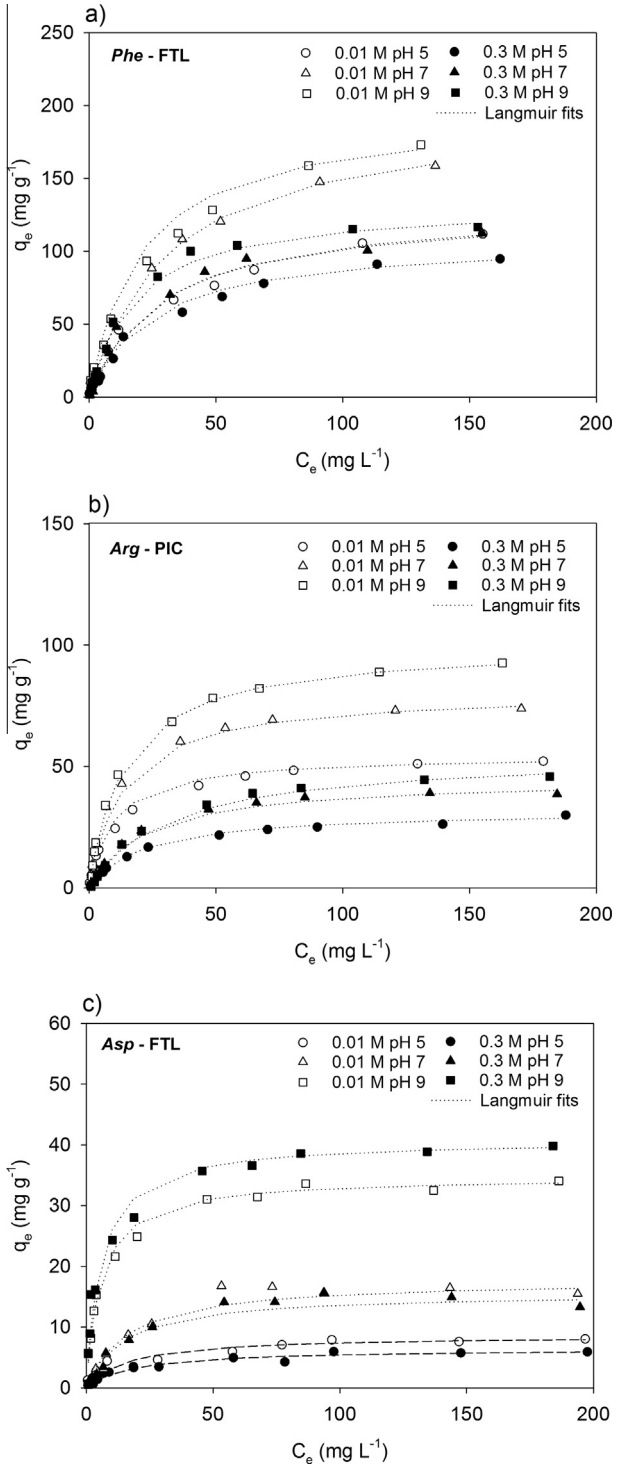

Fig. 5. Adsorption of amino acids from 0.01 M and 0.3 M NaCl solution at pH 5, 7 and 9: (a) adsorption isotherms for *Phe* on FTL, (b) adsorption isotherms for *Arg* on PIC and (c) adsorption isotherms for *Asp* on FTL.

4. Conclusions

Granular activated carbon is an effective adsorbent for amino acids included in algal organic matter, but the adsorption may be impaired by hydrophilicity (polarity/water solubility) of the adsorbate, as was evident during the experiments with *aspartic acid*.

Adsorption of *phenylalanine*, *arginine* and *aspartic acid* onto GAC occurred by electrostatic interactions, hydrophobic interactions and hydrogen bonding and/or by a combination of them. Adsorption efficiency for individual amino acids fundamentally depends on solution pH because it affects the adsorbate and the adsorbent charge and finally the dominating adsorption mechanism. Basic amino acid *arginine* was preferably adsorbed on negatively charged carbon PIC thanks to the attractive electrostatic interactions. The highest amount of *arginine* was removed at pH 9, when PIC carried the highest negative charge. *Phenylalanine* was more adsorbed on carbon FTL, which has different chemical properties than carbon PIC. FTL posed more balanced ration between the acidic and basic surface groups, and allowed therefore a formation of different types of interactions simultaneously. Hydrophobic interactions, which control adsorption independently on solution pH, were dominant in *phenylalanine* uptake on this carbon.

The removal of amino acids was reduced in the presence of NaCl background electrolyte. This was evident mainly in the cases where the adsorption occurred via attractive electrostatic interactions because the added salt screened them. Adsorbed amounts of amino acids also changed according to their initial solution concentration. At higher initial concentrations, adsorption was affected by the direct interactions between the carbon surface and the amino acids, as well as by the forces between the adsorbate molecules.

The results herein presented indicate that adsorption of amino acids onto activated carbon is a complex interplay of many factors that should be taken into account if the effective and optimized treatment is required. The study brings one of the first insights into the field of water treatment applying activated carbon for the removal of cyanobacterial amino acids. More detailed research will need to be undertaken in the future, but the conclusions from the study of *phenylalanine*, *arginine* and *aspartic acid* should be applicable for other amino acids with the similar chemical structure.

Acknowledgements

Financial support from RVO: 67985874 is greatly acknowledged.

Appendix A. Supplementary material

Supplementary data associated with this article can be found, in the online version, at http://dx.doi.org/10.1016/j.seppur.2016.09.043.

References

[1] M. Pivokonsky, J. Safarikova, M. Baresova, L. Pivokonska, I. Kopecka, A comparison of character of algal extracellular versus cellular organic matter produced by cyanobacterium, diatom and green algae, Water Res. 51 (15) (2014) 37–46.
[2] M. Ma, R. Liu, H. Liu, J. Qu, W. Jefferson, Effects and mechanisms of pre-chlorination on *Microcystis aeruginosa* removal by alum coagulation: significance of the released intracellular organic matter, Sep. Purif. Technol. 86 (2012) 19–25.
[3] M. Pivokonsky, J. Safarikova, P. Bubakova, L. Pivokonska, Coagulation of peptides and proteins produced by *Microcystis aeruginosa*: interaction mechanisms and the effect of Fe-peptide/protein complexes formation, Water Res. 46 (17) (2012) 5583–5590.
[4] N. Her, G. Amy, H.R. Park, M. Song, Characterizing algogenic organic matter (AOM) and evaluating associated NF membrane fouling, Water Res. 38 (6) (2004) 1427–1438.
[5] B.K. Pramanik, F.A. Roddick, L. Fan, Treatment of secondary effluent with biological activated carbon to reduce fouling of microfiltration membranes caused by algal organic matter from *Microcystis aeruginosa*, J. Membr. Sci. 496 (2015) 125–131.
[6] M. Campinas, M.A. Rosa, The ionic strength effect on microcystin and natural organic matter surrogate adsorption on PAC, Colloid Interface Sci. 299 (2) (2006) 520–529.
[7] E.M. Thurman, Organic Geochemistry of Natural Waters, Martinus Nijhoff/Dr. W. Junk, Dordrecht, 1985.
[8] H.C. Hong, M.H. Wong, Y. Liang, Amino acids as precursors of trihalomethane and haloacetic acid formation during chlorination, Arch. Environ. Contam. Toxicol. 56 (4) (2009) 638–645.

[9] J. Fang, X. Yang, J. Ma, C. Shang, Q. Zhao, Characterization of algal organic matter and formation of DBPs from chlor(am)ination, Water Res. 44 (20) (2010) 5897–5906.
[10] G.E. Fogg, Extracellular products of algae in freshwater, Archiv für Hydrobiologie – Beiheft Ergebnisse der Limnologie 5 (1971) 1–25.
[11] L. Hureiki, J.P. Croué, B. Legube, Chlorination studies of free and combined amino acids, Water Res. 28 (12) (1994) 2521–2531.
[12] L. Elsellami, F. Vocanson, F. Dappozze, E. Puzenat, O. Païsse, A. Houas, C. Guillard, Kinetic of adsorption and photocatalytic degradation of phenylalanine effect of pH and light intensity, Appl. Catal., A 380 (2010) 142–148.
[13] K.L. Froese, A. Wolanski, S.E. Hrudey, Factors governing odorous aldehyde formation as disinfection by-products in drinking water, Water Res. 33 (6) (1999) 1355–1364.
[14] G.A. Gagnon, R.M. Slawson, P.M. Huck, Effect of easily biodegradable organic compounds on bacterial growth in a bench-scale drinking water distribution system, Can. J. Civ. Eng. 27 (3) (2000) 412–420.
[15] I. Freuze, S. Brosillon, A. Laplanche, D. Tozza, J. Cavard, Effect of chlorination on the formation of odorous disinfection byproducts, Water Res. 39 (2005) 2636–2642.
[16] I. Kopecka, M. Pivokonsky, L. Pivokonska, P. Hnatukova, J. Safarikova, Adsorption of peptides produced by cyanobacterium *Microcystis aeruginosa* onto granular activated carbon, Carbon 69 (2014) 595–608.
[17] Q. Gao, W. Xu, Y. Xu, D. Wu, Y. Sun, F. Deng, W. Shen, Amino acid adsorption on mesoporous materials: influence of types of amino acids, modification of mesoporous materials, and solution conditions, Phys. Chem. B 112 (7) (2008) 2261–2267.
[18] E. Titus, A.K. Kalkar, V.G. Gaikar, Equilibrium studies of adsorption of amino acids on NaZSM-5 zeolite, Colloids Surf., A 223 (1–3) (2003) 55–61.
[19] J. Ikhsan, B.B. Johnson, J.D. Wells, M.J. Angove, Adsorption of aspartic acid onto kaolinite, Colloid Interface Sci. 273 (1) (2004) 1–5.
[20] M. Liu, J. Huang, Y. Deng, Adsorption behaviors of L-arginine from aqueous solutions on a spherical cellulose adsorbent containing the sulfonic group, Bioresour. Technol. 98 (2007) 1144–1148.
[21] A.J. O'Connor, A. Hokura, J.M. Kisler, S. Shimazu, G.W. Stevens, Y. Komatsu, Amino acids adsorption onto mesoporous silica molecular sieves, Sep. Purif. Technol. 48 (2) (2006) 197–201.
[22] J. Goscianska, A. Olejnik, R. Pietrzak, Adsorption of L-phenylalanine onto mesoporous silica, Mater. Chem. Phys. 142 (2013) 586–593.
[23] A. Vinu, K.Z. Hossain, G. Satish Kumar, K. Ariga, Adsorption of L-histidine over mesoporous carbon molecular sieves, Carbon 44 (3) (2006) 530–536.
[24] J. Goscianska, W. Nowicki, R. Pietryak, Physicochemical and sorption properties of multi-walled carbon nanotubes decorated with silver nanoparticles, Chem. Eng. J. 250 (2014) 295–302.
[25] E. Greiner, K. Kumar, M. Sumit, A. Giuffre, W. Zhao, J. Pedersen, N. Sahai, Adsorption of L-glutamic acid and L-aspartic acid to γ-Al_2O_3, Geochim. Cosmochim. Acta 133 (2014) 142–155.
[26] B. Schreiber, T. Brinkmann, V. Schamlz, E. Worch, Adsorption of dissolved organic matter onto activated carbon – the influence of temperature, absorption wavelength, and molecular size, Water Res. 39 (2005) 3449–3456.
[27] H.M. Clark, C.C.C. Alves, A.S. Franca, L.S. Oliveira, Evaluation of the performance of an agricultural residue-based activated carbon aiming the removal of phenylalanine from aqueous solutions, LWT-Food Sci. Technol. 49 (1) (2012) 155–161.
[28] H.P. Boehm, Chemical identification of surface groups, in: D.D. Eley, H. Pines, P.B. Weisz (Eds.), Advances in catalysis, vol. 16, Academic Press, London, 1966, pp. 179–274.
[29] S.L. Goertzen, K.D. Thériault, A.M. Oickle, A.C. Tarasuk, H.A. Andreas, Standardization of the Boehm titration. Part I. CO_2 expulsion and endpoint determination, Carbon 48 (2010) 1252–1261.
[30] C. Moreno-Castilla, Adsorption of organic molecules from aqueous solutions on carbon materials, Carbon 42 (1) (2004) 83–94.
[31] C. Rajesh, C. Majumder, H. Mizuseki, Y. Kawazoe, A theoretical study on the interaction of aromatic amino acids with graphene and single walled carbon nanotubes, J. Chem. Phys. 130 (12) (2009) 1–6.
[32] D. Sebben, P. Pendleton, Analysis of ionic strength effect on the adsorption of simple aminoacids, Colloid Interface Sci. 443 (2015) 153–161.

Supplementary Material for

Removal of cyanobacterial amino acids in water treatment by activated carbon adsorption

Lenka Cermakova[a,b], Ivana Kopecka[a], Martin Pivokonsky[a,b,*], Lenka Pivokonska[a], Vaclav Janda[c]

[a]*Institute of Hydrodynamics, Academy of Sciences of the Czech Republic, Pod Patankou 30/5, 16612 Prague 6, Czech Republic*

[b]*Institute for Environmental Studies, Faculty of Science, Charles University, Benatska 2, 12801 Prague 2, Czech Republic*

[c]*Department of Water Technology and Environmental Engineering, University of Chemistry and Technology, Prague, Technicka 5, 16628 Prague 6, Czech Republic*

*Corresponding author:

Martin Pivokonsky

Tel.: +420 233 109 068; fax +420 233 324 361

E-mail: pivo@ih.cas.cz

This supplementary material contains the following section, tables and figures:

S1. Analysis of COM amino acids

Free amino acids included in COM produced by cyanobacterium *Microcystis aeruginosa* were analysed after derivatization by fluorenylmethyl chloroformate [1] by the HPLC system (Agilent 1260 series, Agilent Technologies, USA) with Agilent Eclipse Plus C18 column (2.1 × 150 mm, 3.5 μm) and a diode array detector operated at 338 nm, then switched to 280 nm at 15 min of analysis. The HPLC mobile phases used for the AAs analysis were 10 mM Na_2HPO_4, 10 mM Na_2O_7 and 0.5 mM NaN_3 (pH 8.0) (A) and acetonitrile: methanol: water (45%: 45%: 10%) (B) mixed during gradual gradient elution from 100% A: 0% B at the start to 0% A: 100% B at the end of analysis (25 min). The flow rate was 1 mL min^{-1} at the temperature of 23 °C and the sample injection volume was 10 μL. The system was calibrated using Amino acids standard kit (Sigma Aldrich, USA) included aspartic acid (*Asp*), glutamic acid (*Glu*), asparagine (*Asn*), serine (*Ser*), glutamine (*Gln*), histidine (*His*), glycine (*Gly*), threonine (*Thr*), arginine (*Arg*), alanine (*Ala*), tyrosine (*Tyr*), cystine (*Cy2*), valine (*Val*), methyonine (*Met*), norvalin (*Nva*), tryptophan (*Trp*), phenylalanine (*Phe*), isoleucine (*Ile*), leucine (*Leu*), lysine (*Lys*), hydroxyproline (*Hyp*), sarcosine (*Sar*) and proline (*Pro*). Reproducibility of AAs analyse was very good with deviation of all AAs concentrations of less than 5% from repeated measurement.

Table S1. General characteristics of GAC PIC and FTL

	PIC	FTL	Ref.
General characteristics			
Precursor	Vegetal material	Bituminous coal	
Activation agent	Phosphoric acid	Water steam	
Form	Granular	Granular	
Textural properties			
S_{BET} (m^2 g^{-1})	1668	1039	[2]
S_{mezo} (m^2 g^{-1})	770	421	[2]
V_{total} (cm^3 g^{-1})	1.20	0.63	[2]
$V_{meso+macro}$ (cm^3 g^{-1})	0.75	0.33	[2]
V_{micro} (cm^3 g^{-1})	0.45	0.30	[2]
(V_{micro}/V_{total})·100 (%)	37	48	[2]
Surface charge			
pH_{pzc}	3.5	8.6	[2]
Acid-base characterization of surface			
Acidity (mmol g^{-1})	2.175	0.310	This study
Basicity (mmol g^{-1})	0.081	0.270	This study

Table S2. Characteristics of amino acids *Arg*, *Asp* and *Phe*

Adsorbate	Molecular formula	Structural formula	MW (Da)	p*I*	Functional groups
L-arginine (*Arg*)	$C_6H_{14}N_4O_2$	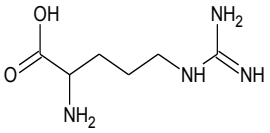	174.20	10.76	α-COOH (pK_a = 2.17) α-NH_2 (pK_a = 9.04) guanidyl group (pK_a = 12.48)
L-aspartic acid (*Asp*)	$C_4H_7NO_4$	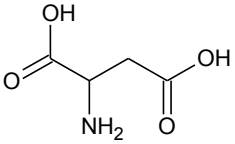	133.10	2.98	α-COOH (pK_a = 2.09) α-NH_2 (pK_a = 9.82) β-COOH (pK_a = 3.86)
L-phenylalanine (*Phe*)	$C_9H_{11}NO_2$	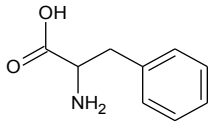	165.19	5.48	α-COOH (pK_a = 1.83) α-NH_2 (pK_a = 9.13)

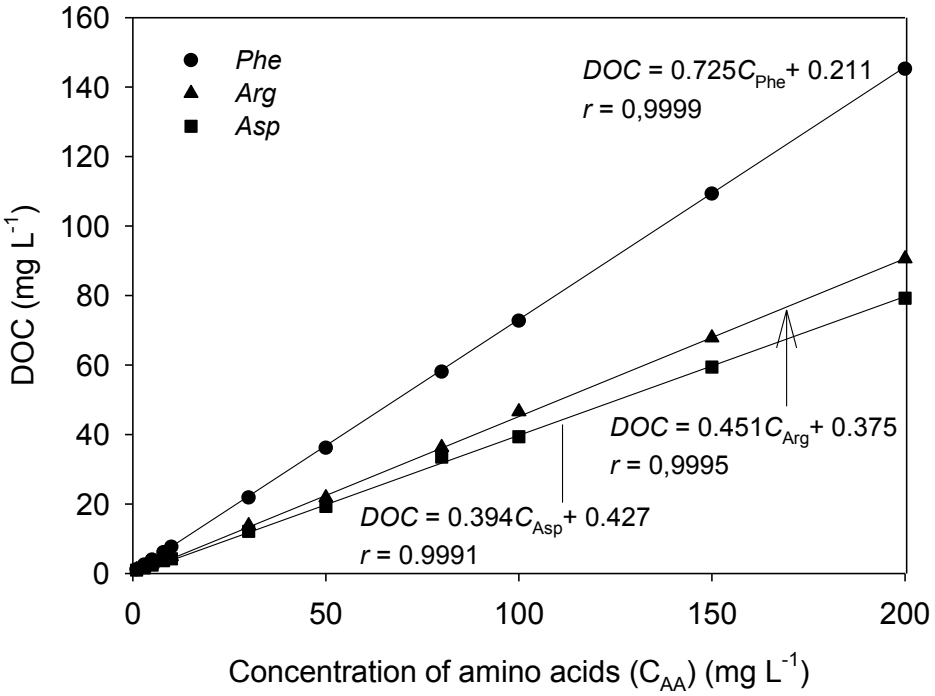

Fig. S1. Calibration curve for amino acid concentrations (C_{AA}) expressed as dissolved organic matter (DOC) in mg L^{-1}.

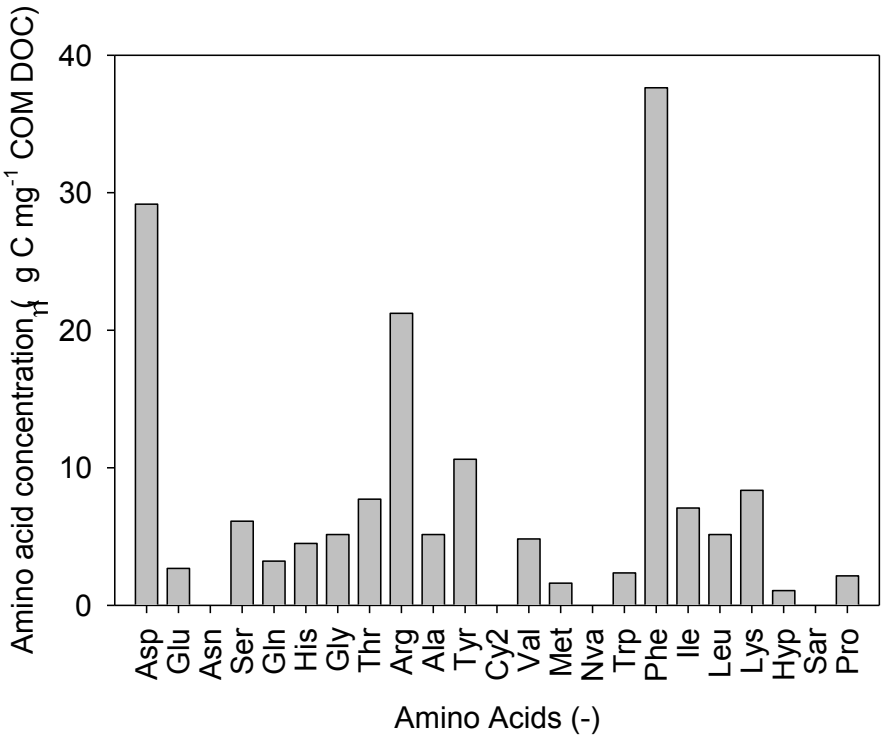

Fig. S2. Concentration of free amino acids (C_{AA}) identified in cellular organic matter (COM) produced by cyanobacterium *Microcystis aeruginosa* expressed as µg of carbon in mg dissolved organic matter (DOC) of cellular organic matter (COM).

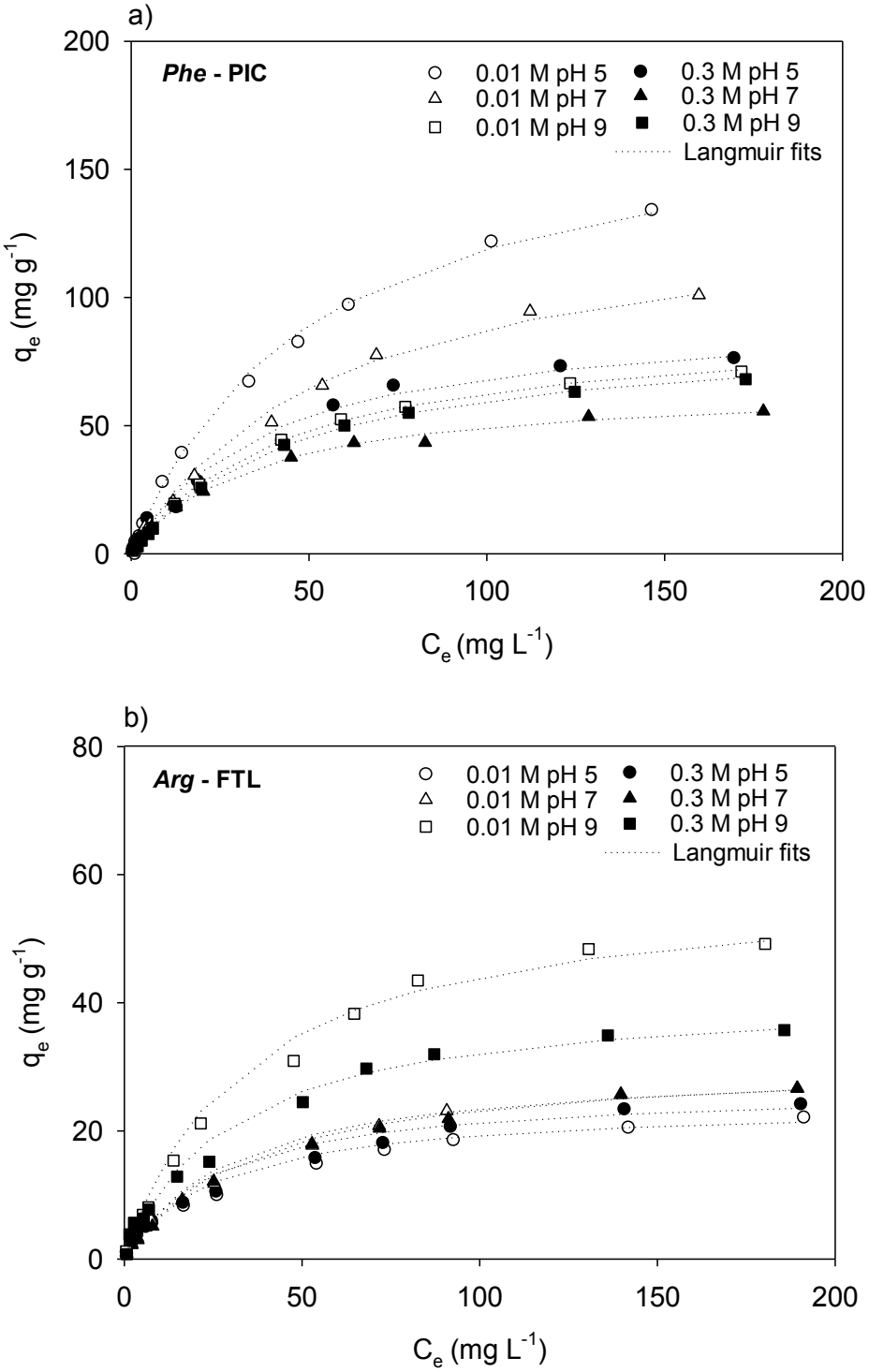

Fig. S3. Adsorption of amino acids in the presence of 0.01 M and 0.3 M NaCl solutions at pH 5, 7 and 9: (a) adsorption isotherms for *Phe* on PIC and (b) adsorption isotherms for *Arg* on FTL (q_e is the amount of amino acids adsorbed per mass unit of granular activated carbon at equilibrium (mg g^{-1}), C_0 and C_e are the initial and equilibrium concentrations of amino acids in the solution (mg L^{-1})).

Reference

[1] J. Fang, X. Yang, J. Ma, C. Shang, Q. Zhao, Characterization of algal organic matter and formation of DBPs from chlor(am)ination, Water Res. 44 (20) (2010) 5897-5906.

[2] I. Kopecka, M. Pivokonsky, L. Pivokonska, P. Hnatukova, J. Safarikova, Adsorption of peptides produced by cyanobacterium *Microcystis aeruginosa* onto granular activated carbon, Carbon 69 (2014) 595-608.

PUBLIKACE 5

Investigating adsorption of model low-MW AOM components onto different types of activated carbon – influence of temperature and pH value

Lenka Čermáková, Kateřina Fialová, Ivana Kopecká, Magdalena Barešová a Martin Pivokonský

Environmental Technology – v recenzním řízení

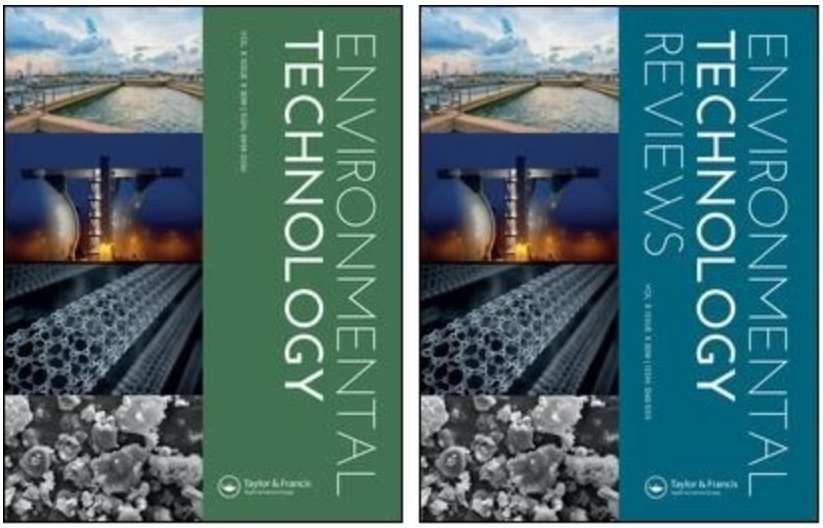

Investigating adsorption of model low-MW AOM components onto different types of activated carbon – influence of temperature and pH value

Journal:	*Environmental Technology*
Manuscript ID	TENT-TENT-2020-0724
Manuscript Type:	Original Article
Date Submitted by the Author:	02-Jun-2020
Complete List of Authors:	Cermakova, Lenka; Institute of Hydrodynamics Czech Academy of Sciences, Department of Water Resources; Charles University Faculty of Science, Institute for Environmental Studies Fialova, Katerina; Institute of Hydrodynamics Czech Academy of Sciences, Department of Water Resources Kopecka, Ivana; Institute of Hydrodynamics Czech Academy of Sciences, Department of Water Resources Baresova, Magdalena; Institute of Hydrodynamics Czech Academy of Sciences, Department of Water Resources Pivokonsky, Martin; Institute of Hydrodynamics Czech Academy of Sciences, Department of Water Resources
Keywords:	adsorption, algal organic matter, amino acid, temperature, water treatment

ABSTRACT

Low molecular weight algal organic matter (AOM), as a frequent water contaminant with poor coagulation efficiency, adversely affects the quality of produced water and serves as a source of potentially carcinogenic disinfection by-products. AOM removal from water is inevitable to eliminate the negative health and environmental impacts. This research evaluates the removal of arginine, phenylalanine and aspartic acid, which are amino acids abundant in AOM. Adsorption experiments were performed at 10, 18 and 25 °C and pH 5, 7 and 9 using two different activated carbons (FTL, PIC). Amino acids showed endothermic adsorption behaviour, with a higher removal at higher temperature. Higher temperature increased the diffusion of amino acid molecules, reduced the solution viscosity, or enhanced the hydrophobic interactions contributing to adsorption. The effect of temperature manifested differently during experiments depending on the chemical nature of the amino acids, the pH value and the surface properties of the carbon. Phenylalanine isotherms showed specific waves (Langmuir type 4). The pH value had a greater effect on arginine adsorption than temperature did. Aspartic acid isotherms exhibited a decrease in adsorption at higher pH values and higher temperatures. The principal mechanisms involved in amino acid adsorption were hydrophobic interactions, electrostatic interactions or hydrogen bonds.

Highlights

Amino acids were adsorbed on different carbons at temperatures of 10, 18 and 25 °C.

Amino acids adsorption was an endothermic process under the given conditions.

Temperature affects the adsorption of amino acids depending on their concentration.

The effect of temperature depends on the dominant mechanism involved in adsorption.

Phenylalanine may exhibit Langmuir type 4 adsorption isotherms.

Investigating adsorption of model low-MW AOM components onto different types of activated carbon – influence of temperature and pH value

Lenka Cermakova[a,b], Katerina Fialova[a], Ivana Kopecka[a], Magdalena Baresova[a], Martin Pivokonsky[a,*]

[a]*Institute of Hydrodynamics of the Czech Academy of Sciences, Pod Patankou 30/5, 166 12 Prague 6, Czech Republic*

[b]*Institute for Environmental Studies, Faculty of Science, Charles University, Benatska 2, 128 01 Prague 2, Czech Republic*

*Corresponding author:

Tel: +420 233 109 068, E-mail: pivo@ih.cas.cz (Martin Pivokonsky)

ABSTRACT

Low molecular weight algal organic matter (AOM), as a frequent water contaminant with poor coagulation efficiency, adversely affects the quality of produced water and serves as a source of potentially carcinogenic disinfection by-products. AOM removal from water is inevitable to eliminate the negative health and environmental impacts. This research evaluates the removal of arginine, phenylalanine and aspartic acid, which are amino acids abundant in AOM. Adsorption experiments were performed at 10, 18 and 25 °C and pH 5, 7 and 9 using two different activated carbons (FTL, PIC). Amino acids showed endothermic adsorption behaviour, with a higher removal at higher temperature. Higher temperature increased the diffusion of amino acid molecules, reduced the solution viscosity, or enhanced the hydrophobic interactions

contributing to adsorption. The effect of temperature manifested differently during experiments depending on the chemical nature of the amino acids, the pH value and the surface properties of the carbon. Phenylalanine isotherms showed specific waves (Langmuir type 4). pH had a greater effect on arginine adsorption than did temperature. Aspartic acid isotherms exhibited a decrease in adsorption at higher pH values and higher temperatures. The principal mechanisms involved in amino acid adsorption were hydrophobic interactions, electrostatic interaction or hydrogen bonds.

Keywords: adsorption; algal organic matter; amino acid; temperature; water treatment

1. Introduction

The problems associated with the presence of low-molecular-weight algal organic matter (AOM) in waters treated for drinking purposes have become increasingly important over the last few years. This organic material, produced by cyanobacteria and green algae as extracellular organic matter (EOM) or originating from the lysis of their cells as cellular organic matter (COM), has been reported to be more difficult to remove by coagulation processes than are algal products with high molecular weights (MW > 10 kDa) [1]. Both EOM and COM contain a variety of peptides and free and combined amino acids (AAs), which together represent the dominant part of the low-MW fraction (MW < 10 kDa) [2]. These compounds adversely affect the quality of produced water, the consumption of the coagulation agent or the disinfection efficiency [3,4]. Free AAs have been reported to be among the most reactive nitrogenous organic compounds; these compounds can interfere with aqueous chlorine and are associated with the formation of harmful disinfection by-products, such as trihalomethanes and haloacetic acids [5]. AAs cause taste and odour problems [6], and they may also serve

as a potential source of biodegradable organic carbon for microorganisms in the water distribution network [7,8].

Many studies have revealed the importance of algal removal in drinking water treatment plants [4,9,10]. However, as far as we know, there is only one study aimed at eliminating cyanobacterial AAs concerning potable water production [11]. Most studies have been performed in the fields of biochemistry, medicine, geochemistry or the food industry [12]. It is clear from the available research that the removal efficiency of conventional water treatment approaches based on destabilization and aggregation is negligible for low-MW compounds such as AAs [1] and other treatment methods should be used for their elimination. Adsorption onto activated carbon (AC) represents a possibility for addressing this challenge because AC adsorbents are commonly used by water utilities to control other natural or anthropogenic pollutants, such as humic substances, cyanotoxins and pesticides [10,13]. AC adsorbents are often part of a treatment line, and minimal additional costs are required. If the AC and specific treatment conditions are appropriately selected, low-MW organic substances of various origins and chemical properties (e.g., with different functional groups, such as -OH, -SH, -COOH, $=NH_2^+$, and $-NH_3^+$) will be effectively removed [14,15,16]. Our previous study revealed that the adsorption efficiency of cyanobacterial AAs fundamentally depends on the pH and ionic strength of the solution. Electrostatic interactions, hydrophobic interactions and/or hydrogen bonds were identified as the dominant mechanisms of *Arg*, *Asp* and *Phe* adsorption on AC [11]. However, there is little information in the literature concerning the influence of water temperature on the removal of AAs by AC, although temperature is one of the main factors influencing the adsorption process [17].

The temperature of raw water varies from 4 to 20 °C depending on the season, which affects the entire water treatment process, from coagulation through adsorption to disinfection [18]. Temperature affects not only the adsorption equilibrium but also the adsorption kinetics [19]. It has been proven that the solution viscosity, the solubility of organic compounds [20], the Brownian and diffusion motion of molecules [21], the kinetic energy of molecules [22] and adsorbent chemistry are temperature-dependent variables. A detailed analysis of adsorption thermodynamics can provide insight into intermolecular interactions between the adsorbate and adsorbent at the phase interface [23].

Adsorption is generally considered to be a spontaneous process with an exothermic nature, and an increased uptake of organic molecules is expected when the adsorption temperature decreases [17]. Sebben and Pendleton [23] observed an exothermic response for AAs adsorbed onto mineral silica with an oxide surface. Glycine and lysine experienced a greater negative effect with increased temperature than did glutamic acid. An increase in uptake with reduced temperature was also described by Titus et al. [24] for phenylalanine, alanine, tyrosine and tryptophan on highly hydrophobic NaZSM-5 zeolite. The isotherms were essentially independent of pH, but they varied significantly with temperature. The same adsorption pattern was confirmed by the study of Clark et al. [25]. The performance of an agricultural residue-based AC was evaluated with respect to the removal of phenylalanine from aqueous solutions, and the results showed that the higher the temperature was, the lower the adsorbed amount. However, some studies have reported that the amount of organic compounds adsorbed on AC increases with increasing temperature; hence, the process is endothermic [26,27]. Liu et al. [28] observed that the adsorption of arginine from diluted aqueous solution onto spherical cellulose is also an endothermic process. The

adsorbed amount of arginine increased with temperature from 20 to 50 °C. One possible explanation for the endothermic nature of the adsorption process is related to hydration. For a compound to adsorb to the adsorbent surface, it must first lose part of its hydration coating, which occurs at the same time as energy consumption [29]. The increase in adsorption efficiency due to higher temperature can also be explained by the fact that with increasing temperature, molecules interact more easily with each other. This behaviour results in the formation of larger associates that are able to bind to the active centres on the AC surface [26]. It is even possible that a change from monolayer adsorption to multilayer adsorption may occur at higher concentrations of a given substance due to higher temperature [30].

A number of studies have compared the effect of different temperatures on adsorption and then concluded whether the process is exothermic or endothermic. However, these studies often do not explain the possible reasons for the thermodynamic behaviour of the investigated substances. The results are sometimes inconsistent, and more detailed research on this issue is needed.

The purpose of this study was twofold. First, we investigated the effect of different solution temperatures (10, 18 and 25 °C) on the adsorption behaviour of arginine (*Arg*), phenylalanine (*Phe*) and aspartic acid (*Asp*) on AC. These amino acids are the major amino acids in AOM; they are commonly identified in natural waters and in treated water after coagulation/flocculation. Second, we focused on complementing the findings of AA adsorption from our previous study [11], which may help elucidate the removal of low-MW AOM in water treatment. Since the adsorption of AAs is highly pH dependent, thermodynamic experiments were performed at three different pH values of 5, 7 and 9. Two types of granular activated carbon (GAC) with different chemical

properties (Filtrasorb TL830 and Picabiol 12x40) were used. Both adsorbents are designed for water treatment technologies.

2. Materials and methods

All experimental solutions were prepared from analytical reagent-grade chemicals and demineralized water (GW 65, Goldman Water, CZ) with a total alkalinity of 1.5 mmol L^{-1} adjusted with 0.125 M $NaHCO_3$ to approximate the typical alkalinity of raw surface water.

2.1. Adsorbates and their analysis

Adsorption experiments were performed with three AAs with different chemical and structural properties (Table 1): *L*-arginine (*Arg*), *L*-phenylalanine (*Phe*) and *L*-aspartic acid (*Asp*) (Sigma-Aldrich, USA). The adsorbates were selected based on the results of our previous study, where we evaluated the concentrations of AAs in AOM and summarized the effects of solution pH and ionic strength on the removal of cyanobacterial AAs by GAC [11]. Significant concentrations of free AAs have been detected in AOM produced by *Microcystis aeruginosa*, a cyanobacterium responsible for serious problems in water reservoirs in many countries, including the Czech Republic [5]. *Arg, Phe* and *Asp* have been identified as the most abundant AAs in the cellular portion of AOM [11]. Cyanobacterial cells are generally rich in *Arg* and *Asp* because these AAs together form cyanophycin, a co-polymer that serves as a nitrogen reservoir [31].

The side chain of *Phe* is formed by an aromatic ring that gives the amino acid a non-polar character and allows it to participate in hydrophobic interactions. *Arg* is classified as a basic amino acid with amino and guanidyl groups in the side chain. It carries a

predominantly positive charge in the experimental pH range of 5 - 9 due to the protonation of amino groups. *Asp* is a hydrophilic amino acid with acidic character due to the presence of carboxylic groups. It is negatively charged in the experimental pH range of 5 - 9. The pH-dependent forms of all three AAs are shown in Fig. 1.

Amino acid quantification was accomplished based on dissolved organic carbon (DOC) analysis before and after the adsorption experiments. DOC was calculated as the difference between total carbon (TC) and inorganic carbon (IC). All samples were first filtered through a 0.22 µm membrane filter (Millipore, USA). A total organic carbon analyser (TOC-V_{CPH}) with an autosampler (ASI-V, Shimadzu Corporation, Japan) was used for the measurements. Calibration was performed using potassium hydrogen phthalate as a TC standard and sodium bicarbonate and sodium carbonate as IC standards. Each sample was analysed in triplicate, and the relative error was < 2%. The calibration curve for amino acid concentrations (C_{AA}), expressed as DOC in mg L^{-1}, is given in our previous study [11-Supplementary data].

2.2. Adsorbents and their characterization

The granular activated carbons Filtrasorb TL830 (FTL) (Chemviron Carbon, USA) and Picabiol 12x40 (PIC) (Jacobi Carbons, Japan), manufactured for the treatment of water samples containing AOM, taste and odour compounds, cyanobacterial toxins or AAs, were applied in adsorption experiments. The textural properties of the GACs were characterized in terms of the specific surface area (S_{BET}), total pore volume (V_{total}) or volume of micropores (V_{micro}). The point of zero charge (pH_{pzc}), indicating the surface charge of an adsorbent at different pH values, was also determined for both GACs according to the methodology of Álvarez-Merino et al. [32]. A negative charge predominates on the surface of the adsorbent at a pH lower than pH_{pzc}. If the

experimental pH is higher than pH_{pzc}, the total charge on the adsorbent surface is considered to be positive. The details of the performed characterization methods, as well as more reasons for choosing these types of adsorbents, are explained in our previous paper [16]. All other characteristics of the GACs including for example the amount of acidic and basic functional groups, are summarized in Table 1. Overview of the charge conditions in the adsorption system under the experimental pH values can be seen in Fig. 1. Based on the characteristics given in Table 1, it is evident that adsorption of target amino acids will occur in the micropore region due to their very low molecular weight. The representation of this pore category is significant in both GAC samples (about 40% and more). Moreover, based on the information provided by the manufacturers, both types of GAC are suitable for the adsorption of target pollutants even in the presence of high molecular weight organics. Competition for sites or pore blocking is not expected.

2.3. Adsorption experiments and data evaluation

Adsorption isotherms of *Arg*, *Phe* and *Asp* were obtained by batch experiments performed by shaking samples (250 mL) of each of the AAs (5 – 300 mg L^{-1} DOC) for 48 h with 400 mg L^{-1} of adsorbent (FTL or PIC) at pH 5, 7 and 9. Each experiment was performed in triplicate, and the data were reported as the average value ± standard deviation (SD). Standard deviations of equilibrium surface concentrations (q_e) are summarized in Table S1 in Supplementary Material. The time interval required to establish adsorption equilibrium was predetermined by kinetic tests. An example of this kinetic test is presented in Fig. S1 in Supplementary Material. The effect of solution temperature on the removal of AAs was simulated by performing the tests at different temperatures of 10, 18 and 25 °C. Full details of sample preparation and treatment

methods are given in our previous work [11]. The amount of AAs adsorbed per unit mass of adsorbent at equilibrium (q_e, mg g^{-1}) was calculated as follows:

$$q_e = (C_0 - C_e)\frac{V}{m} \quad (1)$$

where C_0 and C_e are the initial and equilibrium solution concentrations of AAs (mg L^{-1}), respectively, V is the solution volume (L), and m is the mass of the adsorbent (g).

The correlation of the experimental adsorption data with the Langmuir (2) and Freundlich (3) isotherm models was undertaken to gain an understanding of the adsorption behaviour. The isotherm models are given by the following equations:

$$q_e = \frac{a_m b C_e}{1 + bC_e} \quad (2)$$

and

$$q_e = K^f C_e^{\frac{1}{n}} \quad (3)$$

where q_e (mg g^{-1}) and C_e (mg L^{-1}) represent the adsorbate uptake and solution concentration at equilibrium, respectively. The parameters a_m (mg g^{-1}) and K_f [(mg g^{-1})(L $mg^{-1})^{1/n}$] reflect the adsorption capacity; the constants b and $1/n$ represent the surface affinity and the heterogeneity of surface site energy distribution, respectively.

3. Results and discussion

3.1. Adsorption of amino acids at different temperatures

The effect of solution temperature on *Arg, Phe* and *Asp* adsorption was investigated by a series of batch equilibrium tests at three different temperatures of 10, 18 and 25 °C and at pH 5, 7 and 9. The experimental data were fitted to the Freundlich and Langmuir adsorption isotherm models. The parameters of both models are summarized in Table S2 in the Supplementary Material. The Freundlich parameter K_f reflects the adsorption capacity, and the constant $1/n$ describes the heterogeneity of

the surface site energy distribution. The Langmuir parameter a_m represents the maximum adsorbate uptake at monolayer coverage, and the parameter *b* reflects the surface affinity and the rate of change in uptake. The values of the coefficients of determination (R^2) were higher for the Langmuir model, which more accurately represented the experimental data and was therefore included in the figures predicting amino acid adsorption.

3.2. Equilibrium adsorption of arginine

Fig. 2 shows the experimental and model data for the adsorption of *Arg* on the GACs (FTL and PIC). The equilibrium data are displayed as a function of solution temperature at individual pH values. The Langmuir isotherm model was used to predict adsorption data based on the higher R^2 values obtained using this model than the Freundlich model (Table S2). *Arg* was the only investigated AA that was more efficiently adsorbed on PIC than on FTL. The highest efficiency was achieved at pH 9 and at 25 °C (q_e = 76.8 ± 2.64 mg g^{-1}); on the other hand, the lowest efficiency was measured at pH 5 and 10 °C (q_e = 31.5 ± 2.71 mg g^{-1}). The functional groups on the PIC surface were negatively charged because the experimental pH values were higher than the PIC pH_{pzc} of 4.45 (see Table 1). The overall negative charge of the adsorbent continued to increase with increasing pH from 5 to 9 (Fig. 1). *Arg* had a predominantly positive charge under all experimental conditions, and thus, attractive electrostatic interactions between the PIC surface and *Arg* occurred. The manifestation of these interactions was also supported by the high amount of acidic functional groups on PIC (Table 1) [11]. As the pH of the solution decreased, the PIC negative charge also decreased, and the adsorption efficiency gradually declined. The effect of pH on *Arg* adsorption on PIC was much greater than the dependency on solution temperature [12]. The effect

of temperature was clearly observable only at pH 9, when the electrostatic interactions between PIC and *Arg* were the strongest. The difference in *Arg* uptake at 10 and 25 °C was ~ 20 mg g^{-1} at pH 9, while only half this difference was observed at pH 7. The temperature trend was inconsistent at pH 5 and pH 7. A higher adsorption efficiency was achieved at 18 °C than at 25 °C at lower concentrations of *Arg*; however, at higher concentrations (C_e ≥ 120 mg L^{-1}), the adsorption efficiency measured at 25 °C was greater, and the overall process showed signs of endothermic adsorption (i.e., q_e at 10 °C < q_e at 18 °C < q_e at 25 °C). The link between the effect of temperature and the concentration of adsorbate in the solution was also confirmed by the study of Liu et al. [28]. A detailed view of the isotherms measured at 25 °C showed that these isotherms were initially more linear at lower *Arg* concentrations than isotherms measured at 10 or 18 °C. The initial slope of an isotherm depends on the rate of change of site availability with an increasing amount of solute adsorbed. Linearity of an isotherm usually means that the availability of adsorption sites remains constant at certain concentrations. Similar isotherm characteristics have been observed for the adsorption of certain amino acids and peptides in water on silica. The mechanism under such conditions is rather obscure, and it probably involves a contribution from the hydrogen bonding of amino groups with silica [33].

Similar trends were obtained for *Arg* adsorption on FTL. The effect of pH on *Arg* adsorption on FTL was significant, and *Arg* removal decreased in the order of pH 9 > pH 7 > pH 5. This result corresponded well with the trends in data and parameters predicted by both isotherm models in Table S1. However, the adsorption efficiency on FTL was lower than that of PIC (pH 9 and 25 °C: q_e = 50.8 ± 2.55 mg g^{-1}; pH 5 and 10 °C: q_e = 7.8 ± 2.36 mg g^{-1}). The dominant adsorption mechanism on FTL was electrostatic interactions, as in the case of PIC. These interactions were weaker due

to the less negative charge of FTL caused by less amount of acidic functional groups, and thus, the overall adsorption efficiency was lower. Similar results and the dominant influence of electrostatic interactions were confirmed in a study by O' Connor et al. [34]. Hydrogen bonds formed between *Arg* and FTL functional groups probably also contributed to adsorption, especially at pH 5 and pH 7, at which values electrostatic interactions were less dominant [11].

The adsorption efficiency increased with an increase in temperature from 10 to 25 °C at all pH values, and the adsorption process could be considered endothermic. A hydrating coating can be formed around water-soluble substances to stabilize them. A higher temperature probably provides the energy needed to break the bonds with water and thereby allows the adsorption of *Arg* [29,35]. A higher solution temperature may also increase the diffusion rate of molecules, which can then more easily penetrate into the inner structure of the adsorbent and bind there [36]. However, the effect of temperature on *Arg* adsorption was generally less pronounced than the effect of pH. This effect can clearly be seen from the *Arg* isotherms measured at pH 7 (Fig. 2). A small effect of temperature was also described by Sebben and Pendleton [23] in the case of lysine adsorption.

3.3. Equilibrium adsorption of phenylalanine

Fig. 3 shows experimental and model data for the adsorption of *Phe* on FTL and PIC. The equilibrium data are displayed as a function of solution temperature at individual pH values. The results of equilibrium adsorption tests with *Phe* differ significantly from those with *Arg* (Fig. 2). *Phe* adsorbed on FTL better than on PIC and this can be related to the manifestation of hydrophobic interactions. According acid-base characterization of GACs based on Boehm titration (Table 1), FTL is generally

less charged than PIC, thus hydrophobic bonds could be more pronounced. The highest adsorption efficiency was achieved at 25 °C, with almost no difference between individual pH values (pH 5: q_e = 148.8 ± 3.20 mg g^{-1}, pH 7: q_e = 146.5 ± 3.10 mg g^{-1}, pH 9: q_e = 145.5 ± 3.15 mg g^{-1}). This behaviour was also reflected in the small differences between the a_m parameters of the Langmuir model (Table S2). Temperature had a greater effect on *Phe* adsorption than did pH. The equilibrium surface concentration of *Phe* increased with increasing temperature on both GACs in the order 10 °C < 18 °C < 25 °C, so the adsorption process can be characterized as endothermic under all experimental pH values (see Fig. 3). A higher temperature imparted more kinetic energy to the *Phe* molecules, which led to an increase in their diffusion [26], and the molecules could penetrate more rapidly into the internal porous structure of the GACs [37]. The properties of *Phe* are influenced by the aromatic nucleus in its side chain, which makes this amino acid strongly hydrophobic in nature. *Phe* prefers to minimize contact with water at all pH values by changing its conformation or by adsorption from solution [38]. *Phe* molecules can be oriented parallel to the adsorbent surface due to the aromatic nucleus. This position is more energy efficient than other positions [39,40]. Hydrophobic interactions between *Phe* molecules are enhanced at higher temperatures, and the molecules cluster into larger associates that can be adsorbed as a complex. Thus, more *Phe* molecules are adsorbed to GAC than expected due to the number of action centres [26]. *Phe* molecules need to interact through hydrophobic bonds, not only with themselves but also directly with the surface of GAC [11]. According to Alves et al. [40], adsorbed *Phe* molecules can further react with *Phe* molecules that are still dissolved in solution by means of hydrogen bonds, which contributes to a further increase in adsorption. These interactions are supported by higher temperatures.

The adsorption of AAs including *Phe* to a silicate adsorbent at 20 – 60 °C was studied by Basiuk et al. [41], and the results showed the exothermic nature of the adsorption of all investigated AAs. Silvério et al. [42] also evaluated *Phe* adsorption on layered hydroxides and found that the process was exothermic at experimental temperatures of 25 – 37 °C. The differences in the results of these individual studies are probably related to the different characteristics of the adsorbents and different experimental conditions applied.

The adsorption efficiency of *Phe* on PIC was lower than that on FTL due to the different surface charges of the two GACs (see Fig. 1). In addition to hydrophobic interactions, which are considered to be the dominant forces controlling the adsorption of *Phe* on GAC, electrostatic interactions are present in the case of PIC. Because of the high acidity of PIC, the repulsive interactions between the dissociated carboxyl group of *Phe* and the negatively charged PIC surface groups reduce adsorption [more details in 11].

A detailed examination of Fig. 3 reveals a wave in the *Phe* isotherms for both GACs. The wave occurs at all pH values and temperatures but is particularly evident at pH 5 and 25 °C (see Fig. S2 in the Supplementary Material). Moreover, the wave is probably influenced by the initial concentration of adsorbate, since it can always be observed at approximately C_e ~ 50 mg L^{-1}. According to Giles et al. [33], the isotherms were classified as sub-group 4 of the Langmuir type (L4). The isotherms were also included in the same classification group in the study by El Shafei et al. [38] examining the amino acid histidine, which is very similar to *Phe* in properties. The study of Scheufele et al. [30] explains this wave phenomenon by the change in adsorption mechanism from monolayer to multilayer at a higher initial adsorbate concentration (C_e > 100 mg

L^{-1}). Waves in adsorption isotherms can also be found in other studies [14,43], but these studies do not provide a further explanation.

3.4. Equilibrium adsorption of aspartic acid

Fig. 4 shows experimental and model data for the adsorption of *Asp* on FTL and PIC. The equilibrium data are displayed as a function of solution temperature at individual pH values. The Langmuir isotherm model was used to predict adsorption data based on the higher R^2 values obtained for this model than the Freundlich model (Table S2). *Asp,* a hydrophilic compound, differs significantly from the other examined AAs because it prefers interactions with water molecules over adsorption on GAC [11]. This behaviour was particularly evident during adsorption on PIC when the repulsive electrostatic interactions between the dissociated *Asp* carboxylic groups and negative PIC surface with a high amount of acidic functional groups (see Fig. 1 and Table 1) resulted in a reduction in adsorption at all experimental pH values [11]. The amount of *Asp* adsorbed onto PIC decreased as the pH increased in the order of pH 9 > pH 7 > pH 5. This trend was also confirmed by the study of Greiner et al. [44] on the adsorption of aspartic and glutamic acid on an Al_2O_3 mineral surface. *Asp* adsorption was endothermic in nature, and q_e decreased with decreasing temperature. Because of the negligible q_e values at pH 7 and pH 9, the effect of temperature was clearly noticeable only at pH 5. At this pH and at 25 °C, the overall highest adsorption efficiency of *Asp* on PIC was achieved (25 °C: q_e = 24.0 ± 3.90 mg g^{-1}; 18 °C: q_e = 16.0 ± 3.87 mg g^{-1}; 10 °C: q_e = 3.8 ± 2.53 mg g^{-1}). Due to the hydrophilicity of *Asp* and the predominant repulsive electrostatic forces, hydrogen bonds appeared to be the dominant adsorption mechanism [11]. The importance of this type of interaction in glutamic acid adsorption was also demonstrated by the study of Sebben and Pendleton [23] on nonporous silica.

However, *Asp* adsorption on PIC under other experimental conditions was negligible compared to that of the other examined AAs.

Asp adsorption on FTL was more efficient than adsorption on PIC. One possible explanation is the different acid-base character of FTL and PIC, when the less amount of negative charged acidic functional groups on FTL probably led to the decrease of repulsive electrostatics interactions. The higher adsorption efficiency for FTL was also reflected by the differences in adsorption model parameters (see Table S1). The solution temperature had a greater effect on *Asp* adsorption than did pH, as shown in Fig. 4. Adsorption increased with increasing temperature from 10 to 25 °C at all experimental pH values and was considered to be endothermic. The highest adsorption efficiency on FTL was achieved at pH 5, when the FTL net surface charge was positive, while the *Asp* charge was negative at all experimental pH values. Attractive electrostatic interactions between opposite charges in the adsorption system increased the adsorption efficiency under these experimental conditions [11]. The *Asp* isotherms had a shape corresponding to the L4 group in the classification system by Gilles et al. [33], as was observed in the case of *Phe*. The typical wave was evident mainly at pH 7 and pH 9, when the positive effect of attractive electrostatic interactions was weaker. The *Asp* isotherms also showed a decrease in the adsorbed amount at higher pH values and higher temperatures. This phenomenon appears to be related to the concentration of *Asp* in solution. At lower concentrations, *Asp* was adsorbed mainly due to hydrogen bonds, but at higher concentrations (C_e > 80 mg L^{-1}), *Asp* molecules strongly manifested their hydrophilic character and formed something like a hydration layer, which stabilized them in solution and prevented their adsorption. There could even be desorption. However, we are currently unable to confirm these assumptions, and further research is needed. Neither the Langmuir nor Freundlich model considers

the desorption of molecules in its assumptions, which was also evident from the low R^2 values in Table S1. In particular, the Freundlich model was not practically applicable to describe *Asp* adsorption on either adsorbent. A better correlation between the experimental and model data was achieved by the Langmuir adsorption model, as observed in the study of He et al. [43].

4. Conclusions

The study provided insight into the GAC adsorption of arginine (*Arg*), phenylalanine (*Phe*) and aspartic acid (*Asp*). The effect of temperature on the removal of these amino acids from water solution was investigated through laboratory equilibrium experiments at 10, 18 and 25 °C with the activated carbons FTL and PIC at pH 5, 7 and 9.

It was found that the solution temperature had an effect on the adsorption efficiency of *Arg*, *Phe* and *Asp* and that this effect was different depending mainly on the chemical nature of the amino acids, the pH value and the surface properties of the GAC. *Phe* and *Asp* were removed more efficiently on FTL, while *Arg* was adsorbed better on PIC. The overall greatest adsorption efficiency was achieved for *Phe*.

The adsorption efficiency increased with increasing temperature from 10 to 25 °C for all three investigated amino acids, and thus, the adsorption was considered to be endothermic. This nature applies to both GACs used. Higher temperature probably increased the diffusion of amino acid molecules, reduced the solution viscosity, and/or enhanced the hydrophobic interactions that contribute to adsorption.

If the dominant adsorption mechanism is based on interactions controlled by the solution pH, then the effect of solution temperature on adsorption will not be very apparent. This behaviour was confirmed in the case of *Arg*, which was adsorbed mainly due to electrostatic interactions that are strongly dependent on the solution pH. The

temperature had the least effect on the studied amino acids in this case. On the other hand, the effect of temperature was the most noticeable during the adsorption of *Phe*. The dominant mechanism in *Phe* adsorption was due to hydrophobic interactions, which are minimally affected by pH. The hydrophobic interactions between *Phe* molecules were enhanced at higher temperatures, and the molecules clustered into larger associates that could be adsorbed as a complex.

Asp adsorption was mainly influenced by the hydrophilic nature of this amino acid, which hinders adsorption. The adsorption isotherms even showed a decrease in the adsorbed amount at higher concentrations. The effect of temperature differed according to the applied GAC. In the case of adsorption on PIC, where strong repulsive electrostatic interactions were involved, temperature showed little effect. In the case of FTL, however, effects of both temperature and pH were observed, and the adsorption of *Asp* on this GAC was up to twice that of PIC.

5. Practical aspects

The results of the study indicate that the temperature of the solution (water) affects the adsorption efficiency, and this effect is more pronounced when hydrophobic interactions are the main adsorption mechanism. However, it is obvious that in real operation under applied conditions at the water treatment plant, solution temperature is not a decisive influencing adsorption factor. The pH value of the solution (water) is a more important parameter in relation to water treatment than the temperature. It is due to that pH value determines the protonation/deprotonation of the functional groups on the surface of the GACs and in the adsorbate structure, and thus controls the manifestation and extent of involved interactions and significantly affects the adsorption efficiency. Therefore, we should focus primarily on the pH value in

optimization of water treatment. An important finding is also that adsorption of low molecular weight AOM such as amino acids seems to be endothermic. This is advantageous due to the fact that the development of algal bloom is associated with the warm season of the year.

Acknowledgements

This work was supported by the institutional support of the Czech Academy of Sciences [RVO: 67985874].

References

[1] M. Pivokonsky, J. Safarikova, P. Bubakova, and L. Pivokonska, *Coagulation of peptides and proteins produced by Microcystis aeruginosa: Interaction mechanisms and the effect of Fe-peptide/protein complexes formation*, Water Res. 46 (2012), pp. 5583-5590.

[2] M. Pivokonsky, J. Safarikova, M. Baresova, L. Pivokonska, and I. Kopecka, *A comparison of the character of algal extracellular versus cellular organic matter produced by cyanobacterium, diatom and green alga*, Water Res. 51 (2014), pp. 37-46.

[3] L. Li, N. Gao, Y. Deng, J. Yao, and K. Zhang, *Characterization of intracellular & extracellular algae organic matters (AOM) of Microcystis aeruginosa and formation of AOM-associated disinfection byproducts and odor & taste compounds*, Water Res. 46 (2012), pp. 1233-1240.

[4] M. Ma, R. Liu, H. Liu, J. Qu, and W. Jefferson, *Effects and mechanisms of pre-chlorination on Microcystis aeruginosa removal by alum coagulation: significance of the released intracellular organic matter*, Sep. Purif. Technol. 86 (2012), pp. 19-25.

[5] J. Fang, X. Yang, J. Ma, C. Shang, and Q. Zhao, *Characterization of algal organic matter and formation of DBPs from chlor(am)ination*, Water Res. 44 (2010), pp. 5897-5906.

[6] I. Freuze, S. Brosillon, A. Laplanche, D. Tozza, and J. Cavard, *Effect of chlorination on the formation of odorous disinfection byproducts*, Water Res. 39 (2005), pp. 2636-2642.

[7] G.A. Gagnon, R.M. Slawson, and P.M. Huck, *Effect of easily biodegradable organic compounds on bacterial growth in a bench-scale drinking water distribution system*, Can. J. Civ. Eng. 27 (2000), pp. 412-420.

[8] H.C. Hong, M.H. Wong, and Y. Liang, *Amino acids as precursors of trihalomethane and haloacetic acid formation during chlorination*, Arch. Environ. Contam. Toxicol. 56 (2009), pp. 638-645.

[9] N. Her, G. Amy, H.-R. Park, and M. Song, *Characterizing algogenic organic matter (AOM) and evaluating associated NF membrane fouling*. Water Res. 38 (2004), pp. 1427-1438.

[10] M.B. Dixon, Y. Richard, L. Ho., C.W.K. Chow, B.K. O'Neill, and G. Newcombe, 2011. *A coagulation–powdered activated carbon–ultrafiltration – Multiple barrier approach for removing toxins from two Australian cyanobacterial blooms*, J. Hazard. Mater. 186 (2011), pp. 1553-1559.

[11] L. Cermakova, I. Kopecka, M., Pivokonsky, L. Pivokonska, and V. Janda, *Removal of cyanobacterial amino acids in water treatment by activated carbon adsorption*, Sep. Purif. Technol. 173 (2017), pp. 330-338.

[12] Q. Gao, W. Xu, Y. Xu, D. Wu, Y. Sun, F. Deng, and W. Shen, *Amino acid adsorption on mesoporous materials: Influence of types of aminoacids, modification of*

mesoporous materials, and solution conditions, J. Phys. Chem. B 112 (2008), pp. 2261-2267.

[13] H. Qiu, L. Lv, B.-C. Pan, Q.-J. Zhang, W.-M. Zhang, and Q.-X. Zhang, *Critical review in adsorption kinetic models*, J. Zhejiang Univ.-Sc. A 10 (2009), pp. 716-724.

[14] W.-J. Huang, B.-L. Cheng, and Y.-L. Cheng, *Adsorption of microcystin-LR by three types of activated carbon*, J. Hazard. Mater. 141 (2007), pp. 115-122.

[15] L. Ho, P. Lambling, H. Bustamante, P. Duker, and G. Newcombe, *Application of powdered activated carbon for the adsorption of cylindrospermopsin and microcystin toxins from drinking water supplies*. Water Res. 45 (2011), pp. 2954-2964.

[16] I. Kopecka, M. Pivokonsky, L. Pivokonska, P. Hnatukova, and J. Safarikova, *Adsorption of peptides produced by cyanobacterium Microcystis aeruginosa onto granular activated carbon*, Carbon 69 (2014), pp. 595-608.

[17] C. Moreno-Castilla, *Adsorption of organic molecules from aqueous solutions on carbon materials*, Carbon 42 (2004), pp. 83-94.

[18] J.T. Marois-Fiset, A. Carabin, A. Lavoie, and C.C. Dorea, *Effects of temperature and pH on reduction of bacteria in a point-of-use drinking water treatment product for emergency relief*, Appl. Environ. Microbiol. 79 (2013), pp. 2107-2109.

[19] M. Rabe, D. Verdes, and S. Seeger, *Understanding protein adsorption phenomena at solid surfaces*, Adv. Colloid Interface Sci. 162 (2011), pp. 87-106.

[20] J.P. Amend, and H.C. Helgeson, *Solubilities of the common L-α-amino acids as a function of temperature and solution pH*, Pure and Applied Chemistry, 69 (1997), pp. 935-942.

[21] F.F., Liu, J.L. Fan, S.G. Wang, and G.H. Ma, *Adsorption of natural organic matter analogues by multi-walled carbon nanotubes: Comparison with powdered activated carbon*, Chem. Eng. J. 219 (2013), pp. 450-458.

[22] A.P. Terzyk, G. Rychlicki, S. Biniak, S., and J.P. Łukaszewicz, *New correlations between the composition of the surface layer of carbon and its physicochemical properties exposed while paracetamol is adsorbed at different temperatures and pH*, J. Colloid Interface Sci. 257 (2003), pp. 13-30.

[23] D. Sebben, and P. Pendleton, *(Amino acid + silica) adsorption thermodynamics: Effects of temperature*. J. Chem. Thermodyn. 87 (2015), pp. 96-102.

[24] E. Titus, A.K. Kalkar, and V.G. Gaikar, *Equilibrium studies of adsorption of amino acids on NaZSM-5 zeolite*, Colloids Surf. A Physicochem. Eng. Asp. 223 (2003), pp. 55-61.

[25] H.M. Clark, C.C.C. Alves, A.S. Franca, and L.S. Oliviera, *Evaluation of the performance of an agricultural residue-based activated carbon aiming at removal of phenylalanine from aqueous solutions*, LWT-Food Sci. Technol. 49 (2012), pp. 155-161.

[26] B. Schreiber, T. Brinkmann, V. Schamlz, and E. Worch, *Adsorption of dissolved organic matter onto activated carbon – the influence of temperature, absorption wavelength, and molecular size*. Water Res. 39 (2005), pp. 3449-3456.

[27] I.A.W. Tan, A.L. Ahmad, and B.H. Hameed, *Adsorption isotherms, kinetics, thermodynamics and desorption studies of 2,4,6-trichlorophenol on oil palm empty fruit bunch-based activated carbon*, J. Hazard. Mater. 164 (2009), pp. 473–482.

[28] M. Liu, J. Huang, and Y. Deng, *Adsorption behaviors of L-arginine from aqueous solutions on a spherical cellulose adsorbent containing the sulfonic group*, Bioresour. Technol. 98 (2007), pp. 1144-1148.

[29] I. Anastopoulos, and G.Z. Kyzas, *Are the thermodynamic parameters correctly estimated in liquid-phase adsorption phenomena?*, J. Mol. Liq. 218 (2016), pp. 174-185.

[30] F.B. Scheufele, A.N. Módenes, C.E. Borba, C. Ribeiro, F.R. Espinoza-Quiñones, R. Bergamasco, and N.C. Pereira, *Monolayer - multilayer adsorption phenomenological model: Kinetics, equilibrium and thermodynamics*, Chem. Eng. J. 284 (2016), pp. 1328-1341.

[31] E. Flores, S. Arévalo, and M. Burnat, *Cyanophycin and arginine metabolism in cyanobacteria*, Algal Res. 42 (2019), pp. 1-10.

[32] M.A., Álvarez-Merino, M.A. Fontecha-Cámara, M.V. López-Ramón, and C. Moreno-Castilla, *Temperature dependence of the point of zero charge of oxidized and non-oxidized activated carbons*, Carbon 46 (2008), pp. 778-787.

[33] C.H. Giles, T.H. MacEwan, S.N. Nakhwa, and D. Smith, *Studies in adsorption. Part XI. A system of classification of solution adsorption isotherms, and its use in diagnosis of adsorption mechanisms and in measurement of specific surface areas of solids*, J. Soc. Dye. Colour. 786 (1960), pp. 3973-3993.

[34] A.J., O' Connor, A. Hokura, J.M. Kisler, S. Shimazu, G.W. Stevens, and Y. Komatsu, *Amino acid adsorption onto mesoporous silica molecular sieves*, Sep. Purif. Technol. 48 (2006), pp. 197-201.

[35] S. Yang, D. Zhao, H. Zhang, S. Lu, L. Chen, and X. Yu, *Impact of environmental conditions on the sorption behavior of Pb(II) in Na-bentonite suspensions*, J. Hazard. Mater. 183 (2010), pp. 632-640.

[36] Y.S. Al-Degs, M.I. El-Barghouthi, A.H. El-Sheikh, and M. Wakler, *Effect of solution pH, ionic strength, and temperature on adsorption behavior of reactive dyes on activated carbon*, Dyes Pigm. 77 (2008), pp. 16-23.

[37] F. Jiao, Z. Fu, L. Shuai, and X. Chen, X., *Removal of phenylalanine from water with calcined CuZnAl-CO_3 layered double hydroxides*, T. Nonferr. Metal. Soc. 22 (2012), pp. 476-482.

[38] G.M.S. El Shafei, and N.A. Moussa, *Adsorption of Some Essential Amino Acids on Hydroxyapatite*. J. Colloid. Interface Sci. 238 (2001), pp. 160–166.

[39] C. Rajesh, C. Majumder, H. Mizuseki, and Y. Kawazoe, *A theoretical study on the interaction of aromatic amino acids with graphene and single walled carbon nanotube*, J. Chem. Phys. 130 (2009), p. 124911.

[40] C.C.O Alves, A.S. Franca, and L.S. Oliveira, *Removal of phenylalanine from aqueous solutions with thermo-chemically modified corn cobs as adsorbents,* LWT-Food Sci. Technol. 51 (2013), pp. 1-8.

[41] V.A. Basiuk, and T.Y. Gromovoy, *Comparative study of amino acid adsorption on bare and octadecyl silica from water using high-performance liquid chromatography*, Colloids Surf. A Physicochem. Eng. Asp. 118 (1996), pp. 127-140.

[42] F. Silvério, M.J. dos Reis, J. Tronto, and J.B. Valim, *Adsorption of phenylalanine on layered double hydroxides: effect of temperature and ionic strength*, J. Mater. Sci. 43 (2007), pp. 434-439.

[43] J. He, R. Lin, H. Long, Y. Liang, and Y. Chen, Y., *Adsorption characteristics of amino acids on to calcium oxalate*, J. Colloid. Interface Sci. 454 (2015), pp. 144-151.

[44] E. Greiner, K. Kumar, M. Sumit, A. Giuffre, W. Zhao, J. Pedersen, and N. Sahai, *Adsorption of L-glutamic acid and L-aspartic acid to ∂-Al_2O_3*, Geochimica et Cosmochimica Acta 133 (2014), pp. 142-155.

Table 1. General characteristics of the amino acids and granular activated carbons.

Characteristics of adsorbate	*L*-arginine (*Arg*)	*L*-phenylalanine (*Phe*)	*L*-aspartic acid (*Asp*)
MW (Da)	174.20	165.19	133.10
p*I*	10.76	5.48	2.98
Solubility (mg 100 mL^{-1})	14.87	2.69	0.45
Functional groups	α-COOH (pK_a=2.17) α-NH_2 (pK_a=9.04) guanidyl group (pK_a=12.48)	α-COOH (pK_a=1.83) α-NH_2 (pK_a=9.13)	α-COOH (pK_a=2.09) α-NH_2 (pK_a=9.82) β-COOH (pK_a=3.86)
Characteristics of adsorbent	Filtrasorb TL830 (FTL)		Picabiol 12x40 (PIC)
Precursor	Bituminous coal		Vegetal material
Activation agent	Water steam		Phosphoric acid
S_{BET} (m^2 g^{-1})	1036		1692
S_{mezo} (m^2 g^{-1})	419		765
V_{total} (cm^3 g^{-1})	0.61		1.21
V_{micro} (cm^3 g^{-1})	0.29		0.47
(V_{micro}/V_{total})·100 (%)	47		39
pH_{pzc}	7.75		4.45
Acidity (mmol g^{-1})	0.295		2.045
Basicity (mmol g^{-1})	0.255		0.112

Note: Surface characteristics of FTL and PIC samples are slightly different in the present study and the former study of Cermakova et al. (2017) (mainly in pH_{pzc} values), even if the GACs was of the same type. This may be because the manufacturer provided for both studies identical types of GACs but different series of them. However, there was no change in the fact that the charge of PIC was negative throughout the whole experimental pH 5 – 9 and that it changed from positive to negative in the case of FTL when the experimental pH exceeded its pH_{pzc} in both studies.

Figure 1. Schematic representation of the charge conditions for the adsorption of the amino acids *Phe*, *Asp* and *Arg* from water solution on the granular activated carbons FTL and PIC (p*I* – isoelectric point of the amino acid, pH_{pzc} – point of zero charge of the activated carbon, Q – surface charge of the activated carbon in μmol m^{-2}).

Figure 2. Isotherms and fits to the Langmuir model for the adsorption of *Arg* on FTL and PIC at different temperatures (10, 18 and 25 °C) and at a) pH 5, b) pH 7 and c) pH 9.

Figure 3. Isotherms and fits to the Langmuir model for the adsorption of *Phe* on FTL and PIC at different temperatures (10, 18 and 25 °C) and at a) pH 5, b) pH 7 and c) pH 9.

Figure 4. Isotherms and fits to the Langmuir model for the adsorption of *Asp* on FTL and PIC at different temperatures (10, 18 and 25 °C) and at a) pH 5, b) pH 7 and c) pH 9.

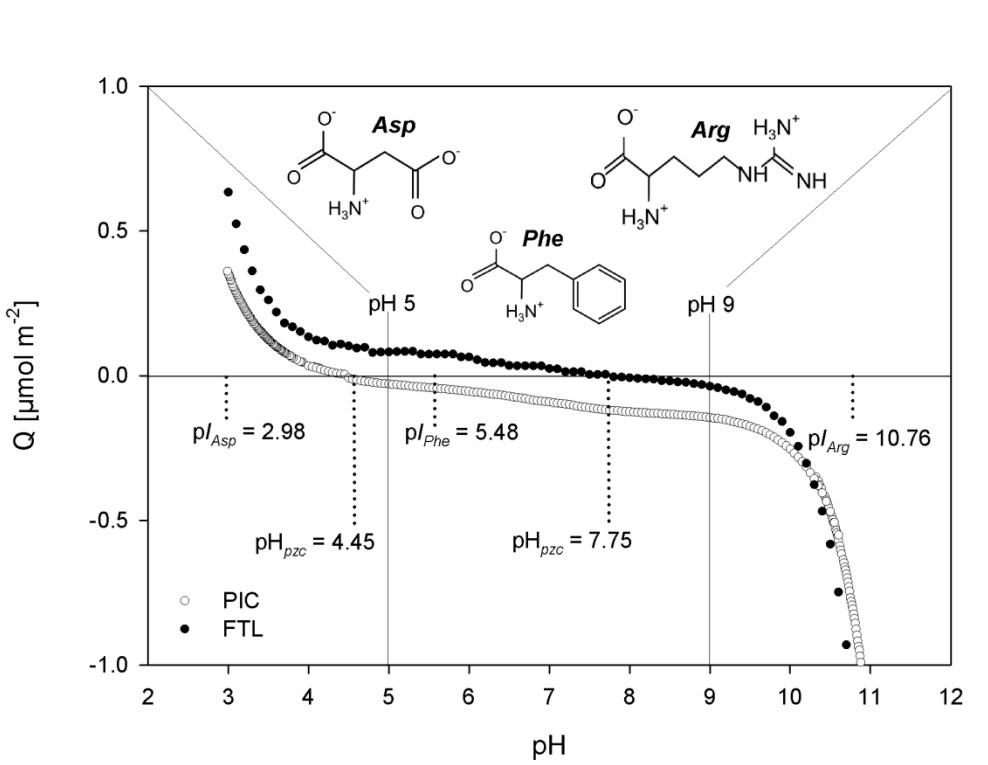

Figure 1. Schematic representation of the charge conditions for the adsorption of the amino acids *Phe*, *Asp* and *Arg* from water solution on the granular activated carbons FTL and PIC (p*I* – isoelectric point of the amino acid, pH_{pzc} – point of zero charge of the activated carbon, Q – surface charge of the activated carbon in µmol m^{-2}).

156x119mm (300 x 300 DPI)

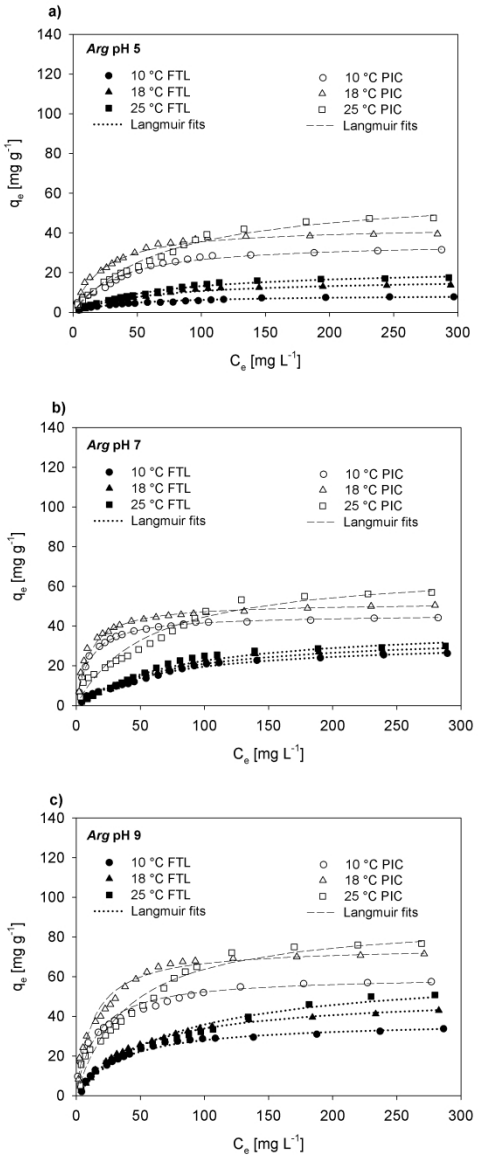

Figure 2. Isotherms and fits to the Langmuir model for the adsorption of *Arg* on FTL and PIC at different temperatures (10, 18 and 25 °C) and at a) pH 5, b) pH 7 and c) pH 9.

169x389mm (300 x 300 DPI)

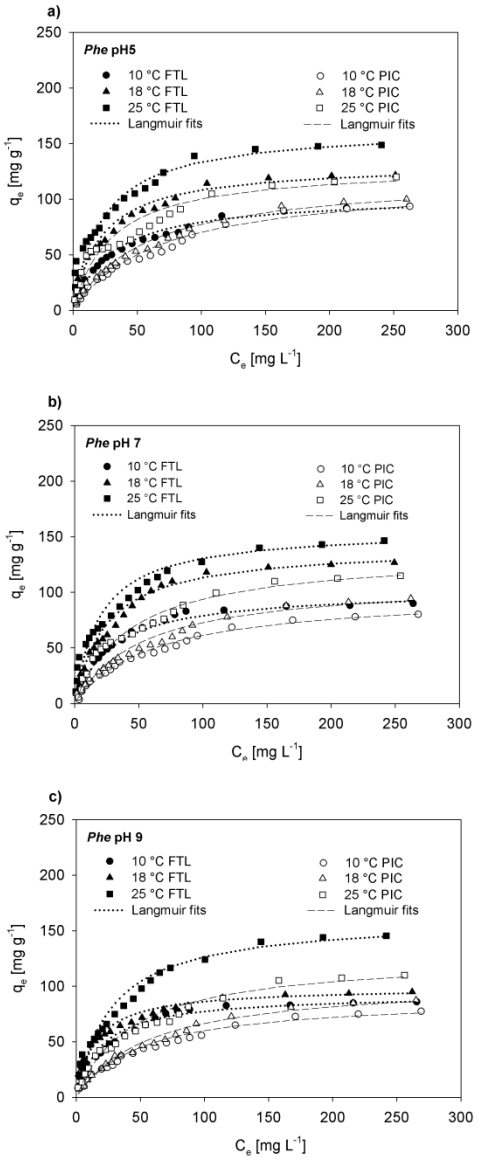

Figure 3. Isotherms and fits to the Langmuir model for the adsorption of *Phe* on FTL and PIC at different temperatures (10, 18 and 25 °C) and at a) pH 5, b) pH 7 and c) pH 9.

169x389mm (300 x 300 DPI)

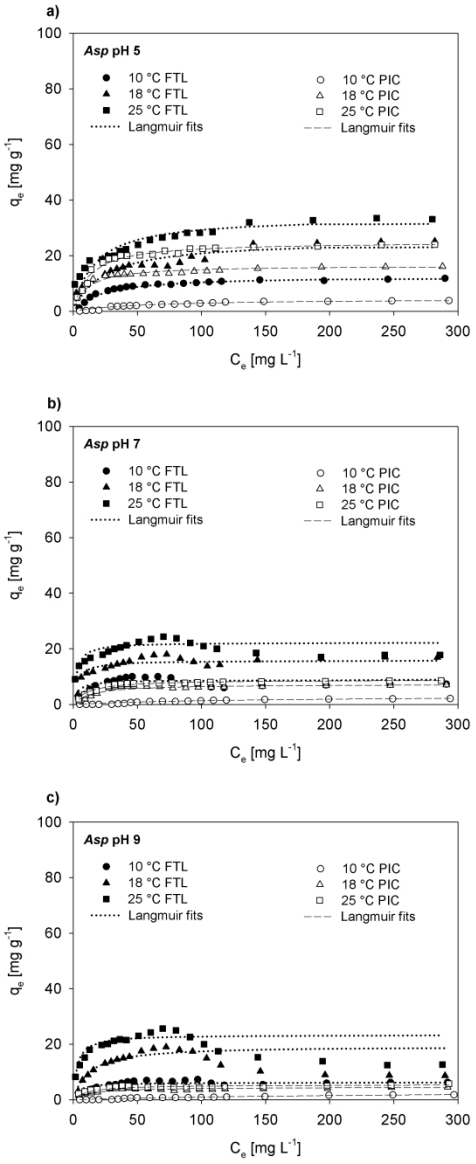

Figure 4. Isotherms and fits to the Langmuir model for the adsorption of *Asp* on FTL and PIC at different temperatures (10, 18 and 25 °C) and at a) pH 5, b) pH 7 and c) pH 9.

169x389mm (300 x 300 DPI)

Supplementary Material for

Investigating adsorption of model low-MW AOM components onto different types of activated carbon – influence of temperature and pH value

Lenka Cermakova[a,b], Katerina Fialova[a], Ivana Kopecka[a], Magdalena Baresova[a], Martin Pivokonsky[a,*]

[a]Institute of Hydrodynamics of the Czech Academy of Sciences, Pod Patankou 30/5, 166 12 Prague 6, Czech Republic
[b]Institute for Environmental Studies, Faculty of Science, Charles University, Benatska 2, 128 01 Prague 2, Czech Republic

[*]Corresponding author:
E-mail: pivo@ih.cas.cz (Martin Pivokonsky)
Tel: +420 233 109 068

This Supplementary Material contains the following tables and figures:

Table S1. Standard deviations (SD) of equilibrium surface concentrations (q_e) measured in adsorption of amino acids on FTL and PIC at different pH values and solution temperature.

Figure S1. An example of the kinetic test for *Phe* adsorption on GAC FTL and PIC at pH 7 and 10, 18 and 25 °C.

Table S2. Parameters of the Langmuir and Freundlich isotherm models for the adsorption of AAs on FTL and PIC at different solution pH values and temperatures.

Figure S2. Detailed view of the waves in *Phe* adsorption isotherms on a) FTL and b) PIC at pH 5 and 10, 18 and 25 °C.

Table S1. Standard deviations (SD) of equilibrium surface concentrations (q_e) measured in adsorption of amino acids on FTL and PIC at different pH values and solution temperature.

AA	Conditions		SD* GAC FTL [mg g^{-1}]	SD* GAC PIC [mg g^{-1}]
Arg	pH5	25 °C	0.19-3.20	0.22-3.14
		18 °C	0.20-3.09	0.24-3.29
		10 °C	0.23-3.15	0.21-3.21
	pH7	25 °C	0.18-3.21	0.19-3.23
		18 °C	0.21-3.14	0.22-3.18
		10 °C	0.22-3.23	0.21-3.22
	pH9	25 °C	0.22-3.15	0.22-3.24
		18 °C	0.21-2.98	0.22-3.19
		10 °C	0.18-3.11	0.24-3.20
Phe	pH5	25 °C	0.20-3.60	0.23-3.52
		18 °C	0.24-3.45	0.25-3.49
		10 °C	0.26-3.51	0.21-3.48
	pH7	25 °C	0.19-3.20	0.24-3.49
		18 °C	0.21-3.23	0.23-3.50
		10 °C	0.22-3.52	0.20-3.43
	pH9	25 °C	0.22-3.19	0.25-3.42
		18 °C	0.20-3.49	0.20-3.61
		10 °C	0.23-3.50	0.22-3.41
Asp	pH5	25 °C	0.26-4.11	0.30-4.30
		18 °C	0.24-3.92	0.29-4.13
		10 °C	0.28-3.90	0.31-3.89
	pH7	25 °C	0.24-3.85	0.32-3.62
		18 °C	0.21-4.24	0.29-3.83
		10 °C	0.30-3.72	0.28-3.78
	pH9	25 °C	0.29-3.93	0.33-3.99
		18 °C	0.31-3.89	0.32-4.03
		10 °C	0.32-4.01	0.33-3.65

*SD is given in the range of experimental concentrations 5 – 300 mg L^{-1} DOC

Table S2. Parameters of the Langmuir and Freundlich isotherm models for the adsorption of AAs on FTL and PIC at different solution pH values and temperatures.

AA	Conditions		FTL						PIC					
			Langmuir			Freundlich			Langmuir			Freundlich		
			a_m	b	R^2	K_f	$1/n$	R^2	a_m	b	R^2	K_f	$1/n$	R^2
Arg	pH5	25 °C	22.22	0.015	0.988	0.76	0.61	0.947	61.35	0.014	0.984	2.11	0.602	0.978
		18 °C	17.33	0.016	0.982	0.58	0.627	0.925	43.48	0.045	0.991	4.30	0.462	0.788
		10 °C	8.84	0.024	0.991	0.80	0.433	0.950	35.59	0.029	0.994	3.13	0.454	0.951
	pH7	25 °C	40.49	0.013	0.974	0.96	0.68	0.949	69.44	0.018	0.973	3.69	0.527	0.947
		18 °C	36.23	0.014	0.972	1.21	0.607	0.965	51.81	0.103	0.999	11.75	0.307	0.769
		10 °C	32.68	0.031	0.987	1.24	0.587	0.951	45.87	0.099	0.999	9.65	0.321	0.793
	pH9	25 °C	63.29	0.016	0.977	2.16	0.597	0.966	89.29	0.025	0.984	6.17	0.500	0.904
		18 °C	50.76	0.02	0.994	2.20	0.591	0.900	75.19	0.078	0.999	12.58	0.367	0.878
		10 °C	37.74	0.029	0.985	2.48	0.527	0.821	60.24	0.067	0.997	12.27	0.310	0.952
Phe	pH5	25 °C	163.93	0.044	0.963	18.61	0.431	0.727	129.87	0.034	0.979	12.51	0.445	0.938
		18 °C	131.58	0.046	0.995	14.55	0.437	0.955	120.48	0.018	0.984	5.48	0.565	0.972
		10 °C	103.09	0.034	0.995	8.89	0.472	0.948	117.65	0.015	0.981	4.07	0.610	0.970
	pH7	25 °C	156.25	0.051	0.991	19.46	0.413	0.938	135.14	0.023	0.985	6.61	0.579	0.894
		18 °C	140.85	0.041	0.994	13.05	0.471	0.958	111.11	0.019	0.970	6.84	0.496	0.990
		10 °C	102.04	0.034	0.967	7.17	0.533	0.788	99.01	0.016	0.978	3.63	0.609	0.915
	pH9	25 °C	161.29	0.036	0.989	14.23	0.474	0.923	126.58	0.023	0.979	8.19	0.505	0.977
		18 °C	99.01	0.068	0.997	16.48	0.362	0.912	105.26	0.017	0.979	5.12	0.543	0.978
		10 °C	92.59	0.051	0.996	11.69	0.411	0.923	90.09	0.02	0.977	5.90	0.487	0.974
Asp	pH5	25 °C	34.01	0.061	0.985	8.95	0.250	0.986	25.00	0.085	0.999	5.27	0.314	0.804
		18 °C	25.64	0.043	0.956	5.03	0.300	0.971	16.5	0.097	0.998	5.52	0.213	0.823
		10 °C	12.71	0.044	0.985	1.13	0.498	0.806	4.53	0.018	0.993	0.47	0.384	0.959
	pH7	25 °C	22.27	0.435	0.984	9.81	0.194	0.881	8.87	0.091	0.999	2.10	0.289	0.770
		18 °C	16.47	0.204	0.983	5.08	0.262	0.635	7.27	0.071	0.992	1.18	0.371	0.665
		10 °C	8.77	0.318	0.911	1.79	0.402	0.716	3.13	0.007	0.967	0.13	0.496	0.939
	pH9	25 °C	23.36	0.362	0.973	10.26	0.176	0.515	5.43	0.093	0.991	2.29	0.161	0.741
		18 °C	16.47	0.197	0.910	4.57	0.267	0.419	4.62	0.071	0.984	1.64	0.191	0.723
		10 °C	6.22	0.262	0.959	1.23	0.375	0.625	3.41	0.004	0.738	0.01	0.973	0.700

Units: K_f [(mg g^{-1}) (L mg^{-1})$^{1/n}$], n [–], R [–], a_m [mg g^{-1}], b [L mg^{-1}]

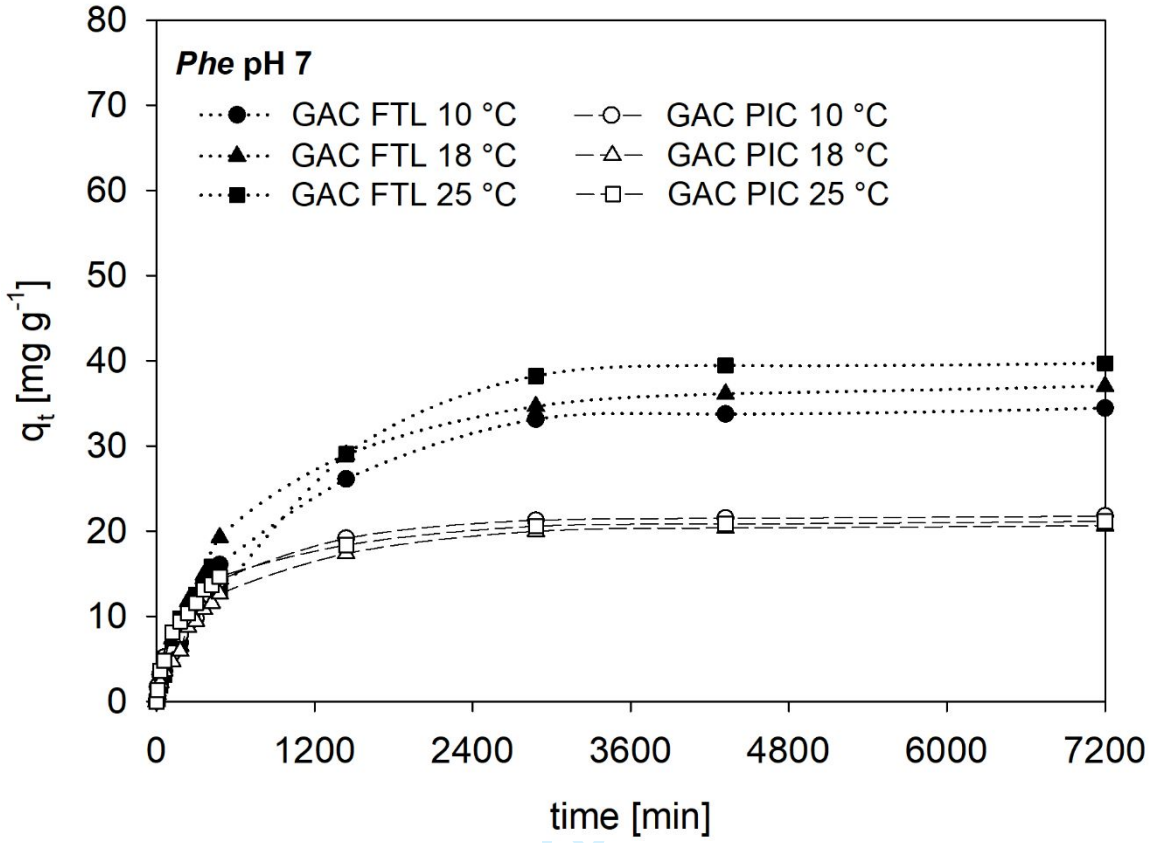

Figure S1. An example of the kinetic test for *Phe* adsorption on GAC FTL and PIC at pH 7 and 10, 18 and 25 °C.

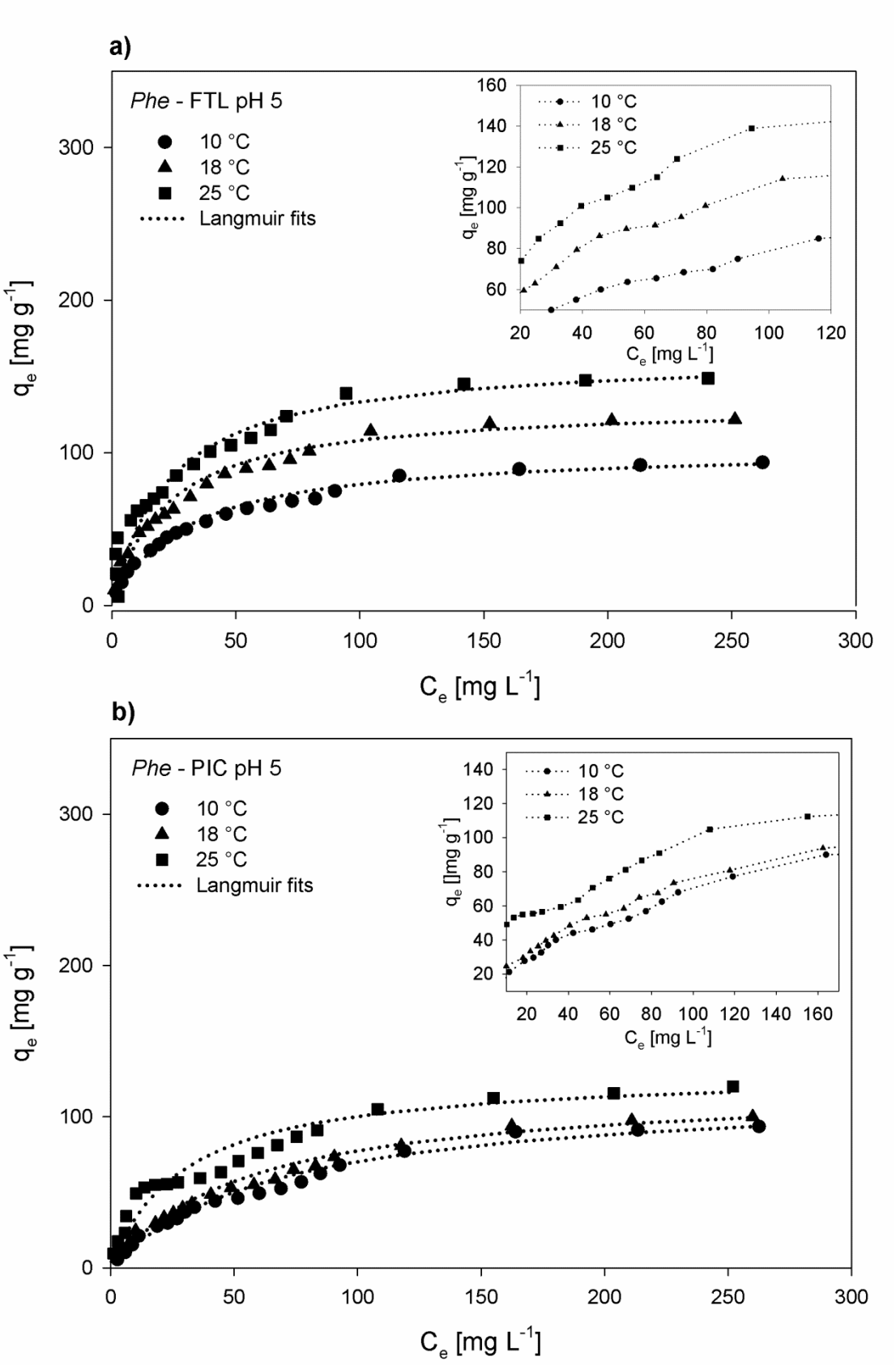

Figure S2. Detailed view of the waves in *Phe* adsorption isotherms on a) FTL and b) PIC at pH 5 and 10, 18 and 25 °C.

Declaration of interests

☒ The authors declare that they have no known competing financial interests or personal relationships that could have appeared to influence the work reported in this paper.

☐The authors declare the following financial interests/personal relationships which may be considered as potential competing interests:

PUBLIKACE 6

Adsorpce peptidů produkovaných fytoplanktonem na aktivním uhlí

Lenka Čermáková, Lenka Pivokonská, Ivana Kopecká, Martin Pivokonský a Václav Janda

Chemické listy 109 (2015) 176-179
ISSN 0009-2770
chemicke-listy.cz/ojs3/index.php/chemicke-listy/article/view/1303/1303

Chem. Listy *109*, 176–179 (2015) Referát

ADSORPCE PEPTIDŮ PRODUKOVANÝCH FYTOPLANKTONEM NA AKTIVNÍM UHLÍ

LENKA ČERMÁKOVÁ[a,b], LENKA PIVOKONSKÁ[a], IVANA KOPECKÁ[a] , MARTIN PIVOKONSKÝ[a,b] a VÁCLAV JANDA[c]

[a] *Ústav pro hydrodynamiku AV ČR, v. v. i., Pod Paťankou 5, 166 12 Praha 6,* [b] *Ústav pro životní prostředí, Přírodovědecká fakulta, Univerzita Karlova v Praze, Albertov 6, 128 43 Praha 2,* [c] *Ústav technologie vody a prostředí VŠCHT Praha, Technická 5, 166 28 Praha 6*
pivo@ih.cas.cz

Došlo 26.6.14, přijato 17.7.14.

Klíčová slova: aktivní uhlí, adsorpce, organické látky produkované fytoplanktonem, peptidy

Obsah

1. Úvod

Povrchové vody užívané pro úpravu na vodu pitnou obsahují celou řadu organických látek přírodního původu (NOM – natural organic matter). Kromě huminových látek (především huminové kyseliny a fulvokyseliny)[1] jsou významnou součástí NOM také organické látky produkované sinicemi a řasami (AOM – algal organic matter)[2]. AOM se do vody dostávají v důsledku metabolických pochodů mikroorganismů jako tzv. extracelulární organické látky (EOM), ale vznikají také autolýzou buněk v průběhu odumírání těchto mikroorganismů jako tzv. celulární organické látky (COM)[3]. Složení AOM se mění v závislosti na druhu organismu, jeho růstové fázi a abiotických faktorech (teplota, světelné podmínky, pH, množství a dostupnost živin). EOM zahrnují převážně polysacharidy, oligosacharidy, monosacharidy a částečně také proteiny a peptidy[2,3]. Hlavními složkami COM jsou naopak především proteiny, dále ale také i nabité a neutrální polysacharidy, nukleové kyseliny a lipidy[2,3].

Právě AOM způsobují při úpravě vody na vodu pitnou značné problémy. Zhoršují organoleptické vlastnosti vody[4], snižují účinnost koagulace[5–8], způsobují zanášení membránových filtrů[9,10] a jsou významnými prekurzory vedlejších produktů desinfekce vody (disinfection by-product DBPs), především trihalogenmethanů a halogenderivátů kyseliny octové[11,12]. Vedle těchto zjevných negativních účinků byl také prokázán významný inhibiční vliv nízkomolekulární složky AOM na adsorpci antropogenních mikropolutantů (pesticidů)[13]. Z hlediska úpravy vody se jako značně problematické ukazují především nízkomolekulární peptidy s molekulovou hmotností < 10 kDa, které jsou velmi obtížně koagulovatelné[6–8], a potenciálně se tak stávají zdrojem pro tvorbu vedlejších desinfekčních produktů při hygienickém zabezpečení vody[7]. Bylo rovněž prokázáno, že tato zbytková frakce AOM peptidů obsahuje vysoké koncentrace (až 1,2 μg mg^{-1} rozpuštěného organického uhlíku) cyanotoxinů na bázi cyklických NRP (neribozomálních peptidů)[14,15].

Z výše uvedených důvodů je zřejmé, že je třeba hledat další metody pro účinné odstranění AOM peptidů při úpravě vody. Jednou z takových potenciálně vhodných metod je adsorpce na granulovaném nebo práškovém aktivním uhlí (AU)[12,16].

2. Adsorpce AOM na aktivním uhlí

Při úpravě pitné vody je adsorpce na aktivním uhlí často využívána zejména pro odstraňování nežádoucích organických nečistot přírodního i antropogenního původu[17]. Převážná většina studií věnujících se odstraňování NOM adsorpcí na AU se zabývá vodami se zvýšeným obsahem huminových látek[18–21] nebo organické látky definuje sumárně jako rozpuštěné organické látky DOC (dissolved organic matter)[22,23]. Přestože zařazení sorpce na AU do procesu úpravy pitné vody může výrazně zvýšit účinnost odstraňování nežádoucích AOM, studie zabývající se výhradně adsorpcí produktů sinic a řas, vyjma cyanotoxinů, se doposud vyskytují sporadicky[13,15].

Při úpravě pitné vody se používá adsorpce na AU nejčastěji ve spojení s chemickou úpravu vody, tj. koagulací/flokulací a pískovou filtrací. Aktivní uhlí bývá aplikováno ve fázi koagulace jako práškové (PAU), častěji však v granulované formě (GAU) za pískovou filtrací. Práškové aktivní uhlí se obvykle dávkuje přímo do upravované vody (před nebo častěji současně s dávkováním koagulačního činidla) a obvykle se používá pouze krátkodobě při neočekávaném zhoršení kvality surové vody. Použité práškové aktivní uhlí se nerecykluje a po použití v úpravně vody se stává odpadem. Granulované aktivní uhlí tvoří náplň atmosférických či tlakových filtrů a představuje tak zpravidla předposlední technologický krok před desinfekcí vody.

Granulované aktivní uhlí lze regenerovat, např. teplotně, popř. s přídavkem vodní páry.

3. Faktory ovlivňující adsorpci AOM

Účinnost adsorpce organických látek je ovlivněna nejen vlastnostmi adsorbentu (tj. velikostní distribucí pórů, strukturou povrchu a jeho chemickým složením) a povahou adsorbátu (např. molekulovou hmotností, konformací molekul, typem a rozmístěním funkčních skupin, povrchovým nábojem, rozpustností atd.), ale také vlastnostmi roztoku, jako je hodnota pH, iontová síla (IS) a jeho chemické složení[16,24].

3.1. Velikostní distribuce pórů AU a velikost molekul AOM peptidů

Účinnost adsorpce většiny nízkomolekulárních organických sloučenin (mikropolutanty, fulvokyseliny) je dána hodnotou specifického povrchu adsorbentu. Čím je tato hodnota vyšší, tím je i vyšší sorpční kapacita adsorbentu[24]. V případě AOM peptidů má ale na jejich adsorpci podstatnější vliv velikostní distribuce pórů AU, resp. její poměr k molekulové hmotnosti adsorbátu. Adsorpční kapacita je v tomto případě ovlivněna tedy spíše velikostí molekul AOM a tím jejich prostupností do vnitřní struktury AU[15]. Přednostně jsou tak zaplňovány póry velikostně odpovídající velikosti AOM molekul, kdy se uplatňuje větší počet kontaktních bodů mezi molekulou peptidu a pórem AU[13,15]. Vzhledem k tomu, že molekulové hmotnosti AOM peptidů se pohybují v rozmezí od několika set Da po zhruba 10 kDa (cit.[2,7]), uplatňují se při adsorpci především mezopóry (d > 2 nm) a mikropóry (d = 0,8–2 nm)[25].

Bylo zjištěno, že v důsledku velikosti mezo a mikropóru AU je nejúčinnější adsorpce pro peptidy o molekulových hmotnostech < 2 kDa. Naopak koncentrace peptidů s molekulovými hmotnostmi > 2 kDa se i při použití vysokých dávek AU (100 mg l^{-1}) odstraňuje jen z části (< 30% účinnost)[13]. Naopak bylo prokázáno, že peptidy o MW > 2 kDa významně snižují účinnost adsorpce ucpáváním mikro a mezopórů GAU. Také další studie prokázala účinnější odstranění AOM peptidů s molekulovými hmotnostmi < 4 kDa v porovnání s AOM peptidy o molekulové hmotnosti 8,3 a 9,5 kDa (cit.[15]).

3.2. Vliv pH roztoku na adsorpci

Při procesu adsorpce AOM na AU hraje významnou roli i hodnota pH roztoku, která ovlivňuje jak disociaci funkčních skupin na povrchu AOM peptidů, tak i funkčních skupin na povrchu AU.

V závislosti na hodnotě pH převládají na povrchu AOM peptidů kladně (=NH_2^+, –NH_3^+), nebo záporně (–COO^-, –O^-) nabité funkční skupiny[8]. Tyto skupiny se pak během adsorpce účastní elektrostatických interakcí s nabitými skupinami na povrchu aktivního uhlí. Protonizované funkční skupiny na povrchu peptidů především –COOH, –OH a –SH skupiny) mohou také vytvářet vodíkové vazby s funkčními skupinami na povrchu AU (cit.[15]). S ohledem na zjištěné střední disociační konstanty karboxylových ($pK_{a\ \alpha\text{-COOH}}$ = 2,5; $pK_{a\ \beta,\gamma\text{-COOH}}$ = 4,2), hydroxylových ($pK_{a\ \text{-OH}}$ = 10,1) a sulfo ($pK_{a\ \text{-SH}}$ = 8,3) skupin AOM peptidů se při tvorbě vodíkových můstků uplatňují především –OH a –SH skupiny[8,15].

Obdobně jako v případě AOM peptidů ovlivňuje hodnota pH také charakter (protonizaci/deprotonizaci) funkčních skupin na povrchu AU. Platí, že v roztocích s pH nižším než pH_{pzc} (pH nulového bodu náboje) je povrchový náboj AU kladný, zatímco v roztocích s pH vyšším než pH_{pzc} nese AU záporný náboj[15]. Pokud je adsorbentem AU kyselého charakteru (na povrchu převládají kyselé funkční

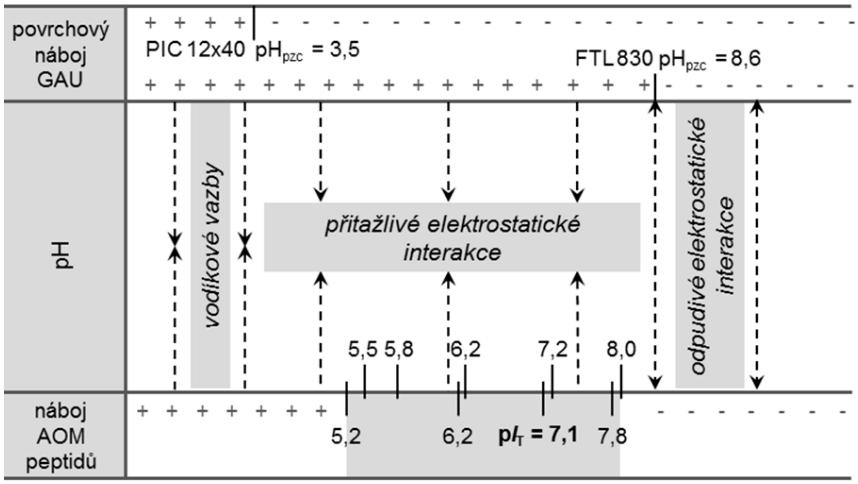

Obr. 1. **Základní mechanismy adsorpce organických látek produkovaných sinicemi a řasami (AOM) peptidů na granulované aktivní uhlí (GAU) kyselého (Picabiol 10x40) a zásaditého (Filtrasorb TL 830) charakteru v závislosti na hodnotě pH**

skupiny, především $–COO^–$) má povrch AU při pH nad pH_{pzc} převážně záporný náboj. Protonizace/deprotonizace funkčních skupin na povrchu AU a AOM peptidů a jejich vzájemná nábojová bilance pak rozhodují o převládajícím charakteru vzájemných elektrostatických interakcí, viz obr. 1. V případě uhlí kyselého charakteru se při nižších hodnotách pH (pH okolo 5) uplatňují silné přitažlivé elektrostatické interakce mezi deprotonizovanými záporně nabitými funkčními skupinami na jeho povrchu a kladně nabitými skupinami peptidů ($=NH_2^+$, α-NH_3^+, ε-NH_3^+), což vede k rychlé a účinné adsorpci[15]. Se zvyšující se hodnotou pH dochází z důvodu velkého množství disociovaných kyselých funkčních skupin k postupnému nárůstu koncentrace záporného náboje na povrchu AU a současně se také zvyšuje množství disociovaných karboxylových skupin na povrchu peptidů. V důsledku toho vznikají mezi záporně nabitým povrchem kyselého AU a disociovanými $–COO^–$ skupinami peptidů odpudivé elektrostatické interakce, a účinnost adsorpce tak s rostoucím pH klesá[13,15].

V případě AU zásaditého charakteru (nese na svém povrchu převážně zásadité funkční skupiny) bude situace trochu jiná (obr. 1). V oblasti nižších hodnot pH (v závislosti na funkčních skupinách na povrchu AU a peptidů) spolu budou interagovat protonované zásadité funkční skupiny AU a deprotonované $–COO^–$ skupiny peptidů. Postupný nárůst hodnoty pH povede k zmenšování kladného náboje na povrchu AU, a účinnost adsorpce tak bude postupně klesat v důsledku postupně klesajících přitažlivých elektrostatických interakcí. Postupně se naopak začnou výrazně uplatňovat odpudivé interakce způsobené postupnou deprotonizací funkčních skupin na povrchu AU (cit.[13,15]).

Obecně tedy můžeme konstatovat, že pro AOM peptidy klesá adsorpční kapacita na povrchu AU s rostoucí hodnotou pH. Zvýšená adsorpce peptidů při nižších hodnotách pH (okolo pH 5) může být také podpořena tvorbou vodíkových vazeb mezi protonovanými funkčními skupinami peptidů a protonovanými povrchovými funkčními skupinami aktivního uhlí i přes převládající kladný náboj obou účastníků adsorpce. Naopak při vysokých hodnotách pH jsou peptidy i aktivní uhlí nabity záporně, což způsobuje vznik odpudivých elektrostatických sil vedoucí ke snižování adsorpční účinnosti.

3.3. Vliv iontové síly na adsorpci

Kromě hodnoty pH je dalším důležitým faktorem ovlivňujícím adsorpci AOM peptidů na AU iontová síla (IS). Iontová síla má vliv především na elektrostatické interakce a mění se v závislosti na typu AU a pH roztoku.

V případě záporně nabitého povrchu AU, vede nárůst IS ke zvyšování účinnosti adsorpce AOM peptidů[15] v širokém rozsahu pH (pH 5–8). Toto zvýšení adsorpční účinnosti je pravděpodobně způsobeno stíněním záporného náboje AU kationty podílejícími se na hodnotě IS. Toto stínění tak brání elektrostatickým repulzím mezi povrchem AU a disociovanými funkčními skupinami peptidů (např. $–COO^–$). Pozitivní vliv tohoto efektu se projevuje především při vyšších hodnotách pH nad 7, kdy se odpudivé elektrostatické síly v roztoku projevují nejvýrazněji, a jsou tak účinně zastiňovány vlivem účinku kationtů přítomných v roztoku[15].

V případě AU s převažujícím kladným nábojem je situace odlišná. Celková míra adsorpce AOM peptidů se s nárůstem iontové síly sice zvyšuje, ale ne při všech hodnotách pH. Vliv iontové síly je tedy silně závislý na hodnotě pH. V kyselé a zásadité oblasti pH dochází s nárůstem IS ke zvýšení účinnosti adsorpce AOM peptidů. Při nízkých hodnotách pH (okolo pH 5), kdy jsou hlavními mechanismy adsorpce elektrostatické interakce, je však tento účinek nárůstu IS prakticky zanedbatelný. Účinek IS se však významně projevuje v oblasti zásaditých hodnot pH, zejména pak v blízkosti pH_{pzc}, kdy růst IS pravděpodobně přispívá k posílení přitažlivých elektrostatických interakcí mezi povrchem uhlíku a opačně nabitými funkčními skupinami peptidů (např. α-, β-, γ-$COO^–$). Zcela opačný je pak vliv IS u AU s převažujícím kladným nábojem v neutrální oblasti pH. Zvýšení iontové síly roztoku zde patrně vede k zastínění elektrostatických přitažlivých interakcí mezi povrchem AU a disociovanými funkčními skupinami peptidů[15]. Dalším možným důvodem, proč v neutrální oblasti pH vede zvýšení IS k poklesu míry adsorpce peptidů na AU zásaditého charakteru, je třeba hledat ve struktuře AOM peptidů. Protože AOM peptidy/proteiny mají celkový izoelektrický bod (pI_T) při pH 7,1 (cit.[8,15]), lze předpokládat, že jednotlivé AOM peptidy mají v blízkosti pI_T díky velmi silným intramolekulárním interakcím kompaktní složenou strukturu[26]. Nárůst IS může vést ke změně v poměru nábojů na povrchu peptidů a tím oslabit interakce uvnitř jejich molekul. To se projeví změnou konformace molekul peptidů, natažením jejich řetězců a následně pravděpodobně i jejich horší adsorbovatelností. Nicméně je třeba podotknout, že zvyšování IS může mít za určitých okolností i opačný efekt. Za předpokladu velmi vysokých koncentrací AOM peptidů, kdy jsou jejich molekuly v těsné blízkosti, mohou být totiž intra- a mezimolekulární elektrostatické repulze mezi funkčními skupinami na jejich skeletu potlačeny právě nárůstem koncentrací iontů opačného náboje, v důsledku čehož dojde k složení molekuly peptidů do struktur vyšších řádů[16,27]. Tato změna konformace vede ke zmenšení velikosti (průměru) molekuly peptidů a tím pravděpodobně také ke zvýšení účinnosti jejich adsorpce[15].

4. Závěr

Nízkomolekulární peptidová složka sinicových a řasových produktů, tzv. AOM, je při koagulaci odstraňována s velmi nízkou účinností, což způsobuje v procesu úpravy pitné vody celou řadu problémů. Pro její následné odstranění se jako velmi vhodná metoda ukazuje být adsorpce na aktivním uhlí. Účinnost adsorpce nízkomolekulárních AOM na AU je však ovlivněna celou řadou faktorů. Zcela zásadní je volba vhodného druhu AU s odpovídající velikostní distribucí pórů a charakterem povrchového náboje.

Dalšími významnými faktory jsou hodnota pH a iontová síla roztoku.

Nízkomolekulární složka COM je v závislosti na charakteru AU přednostně adsorbována při nižších hodnotách pH. Se zvyšujícím se pH adsorpční kapacita AU pro COM peptidy značně klesá. Pro účinnou adsorpci této složky je tedy vhodné odstraňovat jejich zbytkové koncentrace po koagulaci při slabě kyselých hodnotách pH (pH < 6). Vzhledem k tomu, že i samotná koagulace probíhá pro organické látky s největší účinností v rozmezí hodnot pH 4–6 (cit.[7]), nemuselo by zavedení adsorpce do procesu úpravy pitné vody způsobovat větší technologické problémy. Účinnost adsorpce může být podpořena i zvýšením iontové síly roztoku, avšak je nutné brát v úvahu charakter adsorbentu a hodnotu pH, při které je voda upravována.

V současné době se adsorpce na aktivním uhlí využívá převážně při úpravě problematických vod s obsahem antropogenních mikropolutantů nebo krátkodobě při náhlém zhoršení kvality surové vody. Avšak s ohledem na nárůst eutrofizace vod v posledních letech bude odstraňování AOM z vody jistě nabírat na významu a bude zapotřebí zlepšovat dosavadní technologii, například právě zavedením dalšího stupně úpravy – adsorpce na aktivním uhlí.

Práce je řešena v rámci grantového projektu GA ČR P105/11/0247 a projektu MSM 6046137308.

LITERATURA

1. Pivokonský M., Pivokonská L., Bubáková P., Janda V.: Chem. Listy *104*, 1015 (2010).
2. Pivokonský M., Šafaříková J., Barešová M., Pivokonská L., Kopecká I.: Water Res. *51*, 37 (2014).
3. Henderson R .K., Baker A., Parsons S. A., Jefferson B.: Water Res. *42*, 3435 (2008).
4. Zhang K., Gao N., Deng Y., Shui M., Tang Y.: Desalination *266*, 231 (2011).
5. Henderson R. K., Parsons S. A., Jefferson B.: Water Res. *44*, 3617 (2010).
6. Pivokonský M., Polášek, P., Pivokonská, L., Tomášková, H.: Water Environ. Res. *81*, 514 (2009).
7. Pivokonský M., Šafaříková J., Bubáková P., Pivokonská L.: Water Res. 46, 5583 (2012).
8. Šafaříková J., Barešová M., Pivokonský M., Kopecká I.: Sep. Purif. Technol. *118*, 49 (2013).
9. Her N., Amy G., Park H. R., Song M.: Water Res. *38*, 1427 (2004).
10. Teixeira M. R., Sousa V. S.: Desalination *315*, 149 (2013).
11. Fang J., Yang X., Ma J., Shang C., Zhao Q.: Water Res. *44*, 5897 (2010).
12. Bond T., Goslan E. H., Parsons S. A., Jefferson B.: Environ. Technol. *32*, 1 (2011).
13. Hnaťuková P., Kopecká I., Pivokonský M.: Water Res. *45*, 3359 (2011).
14. Li L., Gao N., Deng Y., Yao J., Zhang K.: Water Res. 46, 1233 (2012).
15. Kopecká I., Pivokonský M., Pivokonská L., Hnaťuková P., Šafaříková J.: Carbon *69*, 595 (2014).
16. Campinas M., Rosa M. J.: J. Colloid Interface Sci. *299*, 520 (2006).
17. Delgado L. F., Charles P., Glucina K., Morlay C.: Sci. Total Environ. *435*, 509 (2012).
18. Kristiana I., Joll C., Heitz A.: Chemosphere *83*, 66 (2011).
19. Velten S., Knappe D. R. U., Traber J., Kaiser H. P., von Guten U., Boller M., Meylan S.: Water Res. *45*, 3951 (2011).
20. Matsui Y., Yoshida T., Nakao, S., Knappe D. R. U., Matsushita T.: Water Res. 46, 4741 (2012).
21. Gibert O., Lefèvre B., Fernández M., Bernat X., Paraira M., Pons M.: Water Res. *47*, 2821 (2013).
22. Schreiber B., Brinkmann T., Schmalz V., Worch E.: Water Res. *39*, 3449 (2005).
23. Wei L., Zhao Q., Xue S., Jia T.: J. Zhejiang Univ., Sci., A *9*, 994 (2008).
24. Newcombe G., v knize: *Interface Science In Drinking Water Treatment* (Newcombe G., Dixon D., ed.), str. 133. Elsevier, Amsterdam 2006.
25. Dastgheib S. A., Karanfil T., Cheng W.: Carbon *42*, 547 (2004).
26. Gorham J. M., Wnuk J. D., Shin M., Fairbrother H.: Environ. Sci. Technol. *41*, 1238 (2007).
27. Newcombe G., Drikas M.: Carbon *35*, 1239 (1997).

L. Čermáková[a,b], L. Pivokonská[a], I. Kopecká[a], M. Pivokonský[a,b], and V. Janda[c] *([a] Institute of Hydrodynamics, Academy of Sciences of the Czech Republic, Prague, [b] Institute of Environment, Charles University, Prague, [c] Department of Water Technology and Environmental Engineering, University of Chemistry and Technology, Prague):* **Adsorption of Peptides Produced by Phytoplankton on Activated Carbon**

The paper deals with adsorption of AOM peptides during water treatment. The adsorption is affected by many circumstances. However, the principal factors are size distribution of the adsorbent pores, pH value of the solution and its ionic strength. For the adsorption of peptides having molecular weight lower than 4 kDa, the most important role play mesopores (d > 2 nm) and micropores (d = 0.8–2 nm). Charge characteristics of AOM functional groups and surface activated carbon functional groups are determined by pH value of the solution. These charge relationships affect prevailing mechanisms of interactions between peptides and the activated carbon surface. The biggest adsorption capacities are reached at weakly acidic region of pH due to an effect of attractive electrostatic forces between the activated carbon surface and AOM peptides. The next factor influencing the AOM adsorption is ionic strength of the solution. Its increasing value can have a positive effect on the adsorption efficiency, but the adsorbent character and pH value of the water to be treated, should be taken into account.

PUBLIKACE 7

Vliv aminokyselin produkovaných fytoplanktonem na úpravu vody a jejich adsorpce na aktivním uhlí

Lenka Čermáková, Lenka Pivokonská, Ivana Kopecká, Martin Pivokonský a Václav Janda

Chemické listy 110 (2016) 418-423
ISSN 0009-2770
chemicke-listy.cz/ojs3/index.php/chemicke-listy/article/view/190/190

Chem. Listy *110*, 418–423 (2016) Referát

VLIV AMINOKYSELIN PRODUKOVANÝCH FYTOPLANKTONEM NA ÚPRAVU VODY A JEJICH ADSORPCE NA AKTIVNÍM UHLÍ

LENKA ČERMÁKOVÁ[a,b], LENKA PIVOKONSKÁ[a], IVANA KOPECKÁ[a], MARTIN PIVOKONSKÝ[a,b] a VÁCLAV JANDA[c]

[a] Ústav pro hydrodynamiku AV ČR, v. v. i., Pod Paťankou 5, 166 12 Praha 6, [b] Ústav pro životní prostředí, Přírodovědecká fakulta, Univerzita Karlova v Praze, Albertov 6, 128 43 Praha 2, [c] Ústav technologie vody a prostředí VŠCHT Praha, Technická 5, 166 28 Praha 6
cermakova@ih.cas.cz; pivo@ih.cas.cz

Došlo 9.10.15, přijato 8.12.15.

Klíčová slova: aktivní uhlí, adsorpce, organické látky produkované fytoplanktonem, aminokyseliny

Obsah

1. Úvod

Ve všech povrchových vodách využívaných jako zdroje surové vody pro úpravu na vodu pitnou jsou v různé míře obsaženy organické látky přírodního původu (NOM – natural organic matter)[1,2]. Jedná se o složitou směs řady látek různého původu, charakteru, s odlišnou strukturou, velikostí a molekulovou hmotností[1,3–6]. Lze je rozdělit na dvě základní skupiny – na huminové látky (především huminové kyseliny a fulvokyseliny) a na látky produkované fytoplanktonem (AOM – algal organic matter)[7]. AOM se do vody uvolňují jako tzv. extracelulární organické látky (EOM – extracellular organic matter) v důsledku metabolických pochodů sinic a řas, nebo také jako celulární organické látky (COM – cellular organic matter) v průběhu odumírání těchto organismů[4,5,8–10]. Složení AOM je velmi proměnlivé a závisí na mnoha biotických (druh organismu, růstová fáze organismu) a abiotických (teplota, pH, světelné podmínky, dostupnost a množství živin) faktorech[4,8]. EOM mají charakter především poly-, oligo- a monosacharidů, v menší míře pak také peptidů a proteinů. Naopak hlavní složkou COM jsou peptidy, proteiny a aminokyseliny, dále pak obsahují také polysacharidy, nukleové kyseliny a lipidy[4,5,8,11].

Z hlediska úpravy pitné vody právě AOM způsobují značné problémy. Mají negativní vliv na organoleptické vlastnosti vody (především chuť a zápach)[10,12,13], zabraňují účinné koagulaci[6,14,15], způsobují zanášení membrán filtrů[11,16–18] a v neposlední řadě jsou významnými prekurzory vedlejších produktů vznikajících při hygienickém zabezpečení upravené vody[10,19,20]. Kromě zmíněného byl zejména u nízkomolekulární složky AOM prokázán inhibiční vliv na adsorpci mikropolutantů (např. pesticidů)[21]. Při samotném procesu úpravy vody se jako problematická jeví především nízkomolekulární frakce peptidů pod 10 kDa a značně menší aminokyseliny (AMK)[21,22]. Kompletní přehled vlivu AOM na jednotlivé procesy je podrobně popsán v review[23].

2. Výskyt aminokyselin produkovaných fytoplanktonem v povrchových vodách

Z přírodních nízkomolekulárních látek způsobujících při úpravě vody značné problémy se v zdrojích surové vody kromě fulvokyselin[1] a peptidů[8] vyskytují především volné a vázané aminokyseliny[24]. Jejich zdrojem je zejména metabolická činnost sinic a řas a degradace jejich buněk[8,20,25,26]. Koncentrace rozpuštěných peptidů/proteinů a volných AMK v přírodních vodách závisí na mikrobiologické aktivitě a v době rozvoje vodního květu může dosahovat až několika jednotek mg l^{-1} (cit.[23]). Koncentrace samotných AMK se pak obvykle pohybuje mezi 50 až 1000 μg l^{-1} (cit.[24–26]). Ačkoli množství peptidů/proteinů může až 5× převyšovat množství volných AMK[24], je koncentrace AMK na rozdíl od koncentrace peptidů/proteinů stabilní v celém vodním sloupci[25]. Nejčastěji se vyskytujícími AMK jsou glycin (Gly), kyselina glutamová (Glu), alanin (Ala), leucin (Leu) a serin (Ser)[25,26]. COM složka je pak velmi bohatá především na arginin (Arg), lysin (Lys) a Gly[20].

3. Vliv aminokyselin produkovaných fytoplanktonem na úpravu vody

Jak již bylo řečeno, účinnost konvenční úpravy, tedy koagulace/flokulace, je pro tyto látky téměř nulová[6,8,15]. Aminokyseliny se tak v různém množství vyskytují ve

všech stupních úpravy vody[24,26,27] a jejich koncentrace se může v některých stupních úpravy dokonce i zvyšovat[24]. Přítomnost AMK, které mohou být příčinou hned několika závažných problémů, je však v upravované vodě nežádoucí[12,13]. Aminokyseliny významně ovlivňují dávku desinfekčních činidel používaných při hygienickém zabezpečování upravené vody[24]. Například mohou velmi významně zvyšovat spotřebu chloru při efektivním zabezpečování upravené vody chlorací. Důležitou roli přitom hraje hlavně struktura molekuly aminokyseliny, především charakter jejího řetězce. Ten ovlivňuje míru reaktivity s chlorem, a tím i jeho spotřebované množství. Čím více elektrondonorových skupin (–OH, –S–, $–NH_2$) a dvojných vazeb molekula nese, tím větší množství chloru dokáže ve své struktuře navázat[26]. Nejmenší množství chloru (< 3 mol Cl_2/mol AMK) spotřebují pro svou velmi malou reaktivitu s tímto oxidačním činidlem neutrální aminokyseliny s alkyl-substituenty – alanin (Ala), valin (Val), leucin (Leu), izoleucin (Ile)[24]. O něco vyšší spotřebu chloru (5–6 mol Cl_2/mol AMK) vykazují AMK, jejichž řetězec nese hydroxylovou (serin, Ser; threonin, Thr) nebo sulfidickou (methionin, Met; cystein, Cys) skupinu[24,26]. U AMK se zásaditým charakterem řetězce velmi ovlivňuje spotřebu chloru počet aminoskupin a přítomnost např. dvojné vazby. Obecně se pohybuje nad 3 mol Cl_2/mol AMK, ale u argininu (Arg) a histidinu (His) může dosahovat vzhledem k jejich struktuře až 12 mol Cl_2/mol AMK[24,26]. Aminokyseliny asparagová (Asp) a glutamová (Glu), jejichž řetězec má charakter kyselý, se ze zatím nezjištěného důvodu ve spotřebě chloru velmi liší. Jeden mol molekul Asp dokáže pojmout až dvojnásobné množství chloru (5,5 mol Cl_2/mol AMK) oproti Glu[24]. Nejvíce pak dávku chloru zvyšují aromatické AMK tyrosin (Tyr) a tryptofan (Trp), kdy se spotřeba chloru pohybuje mezi 13–16 mol Cl_2/mol AMK[24,26].

Z AMK přítomných v upravené vodě často vznikají chlorací látky negativně ovlivňující její organoleptické vlastnosti, především chuť a zápach, a jsou to zejména aldehydy, nitrily a imidy[12,13,28]. Nejčastějšími produkty chlorace AMK jsou následující aldehydy: isobutylaldehyd vznikající z Val, isovaleraldehyd vznikající z Leu, 2-methylbutyraldehyd vznikající z Ile a fenylacetaldehyd vznikající chlorací fenylalaninu (Phe). Aldehydy byly přitom dlouhou dobu považovány za produkty vznikající pouze při ozonizaci vody, nikoli při chloraci vody obsahující volné AMK. Vznikající množství těchto látek závisí na řadě faktorů, především pak na hodnotě pH a teplotě upravované vody, na reakčním čase a na molárním poměru desinfekčního činidla a AMK. Bylo zjištěno, že nejvyšší množství pak vzniká při hodnotě pH 9, teplotě vody 20 °C, reakčním čase 2 h a molárním poměru volný chlor/AMK 1,5 (cit.[12]).

Aminokyseliny jsou také potenciálním zdrojem biodegradabilního uhlíku, který vytváří v distribuční síti živný substrát pro růst nežádoucích heterotrofních mikroorganismů[29].

Nejzávažnější problém v upravované vodě však představují AMK v podobě prekurzorů vzniku karcinogenních vedlejších produktů desinfekce vody (DBPs) – především trihalogenmethanů (THMs) a haloderivátů kyseliny octové (HAAs)[24,30]. Důležitou roli při vzniku těchto látek opět hraje struktura molekuly AMK, tedy počet a charakter funkčních skupin řetězce[20,24,26,31]. Bylo zjištěno, že za tvorbu THMs jsou zodpovědné především aromatické AMK a že jsou produkovány v menší míře než HAAs[24,26]. Aminokyseliny poskytující halogenderiváty kyseliny octové lze rozdělit na dvě skupiny podle lineární závislosti mezi spotřebou Cl_2 a potenciálem k tvorbě HAAs. Aminokyseliny s řetězovou strukturou vykazují pomalý nárůst tvorby HAAs se spotřebou Cl_2. Jejich elektrodonorové funkční skupiny ochotně reagují s Cl_2, čímž zvyšují jeho spotřebu, ale nejsou hlavními prekurzory vzniku HAAs. Těmi jsou hlavně aromatické AMK (aromatický kruh je důvodem vysoké reaktivity s Cl_2) a dvě aminokyseliny s řetězovou strukturou – kyselina asparagová a kyselina glutamová[26]. Schéma vzniku HAA chlorací kyseliny asparagové ukazuje obr. 1.

Z výše uvedených důvodů je nutné věnovat odstranění AMK z pitné vody při její úpravě zvýšenou pozornost. Jako potenciální způsob eliminace AMK v pitné vodě se nabízí adsorpce na aktivním uhlí (AU).

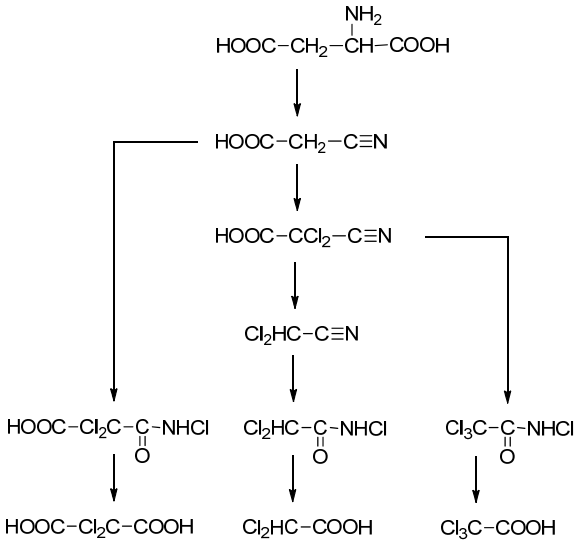

Obr. 1. **Schéma vzniku halogenderivátů kyseliny octové chlorací kyseliny asparagové[26]**

4. Adsorpce aminokyselin produkovaných fytoplanktonem na aktivním uhlí

Adsorpce je velice složitý proces, který je ovlivňován celou řadou faktorů určujících jeho charakter a řídící mechanismy. Adsorpční účinnost aminokyselin se odvíjí zejména od struktury molekuly, především molekulové hmotnosti, velikosti a geometrie molekuly. Dále závisí na rozpustnosti, polaritě a přítomnosti funkčních skupin – karboxylových skupin, aminoskupin a dalších funkčních

skupin (–OH, –S–) řetězce[32,33]. Na adsorpci mají kromě struktury a charakteru adsorbátu vliv také povaha adsorbentu a vlastnosti roztoku. Mezi nejvýznamnější charakteristiky roztoku, které ovlivňují proces a průběh adsorpce AMK, patří hodnota pH, iontová síla, teplota a počáteční koncentrace adsorbátu[33,34]. Kombinace těchto faktorů pak určuje charakter a mechanismy adsorpce[35,36]. Nejčastějšími mechanismy adsorpce AMK jsou elektrostatické interakce[37], hydrofobní interakce[34,38] a vodíkové vazby[39].

4.1. Vliv hodnoty pH

Hodnota pH má vliv na povrchový náboj AU a disociační schopnost funkčních skupin na povrchu AMK, čímž následně ovlivňuje adsorpční mechanismy[40–42]. Z tohoto důvodu hrají zcela zásadní roli při adsorpci struktura molekuly AMK a charakter povrchu AU[43]. V závislosti na pH roztoku se funkční skupiny AMK a AU nacházejí v protonované či deprotonované formě, čímž dochází k uplatňování různých interakcí, které následně určují charakter a míru adsorpce. Nejvýrazněji se uplatňujícím mechanismem adsorpce jsou elektrostatické interakce. Projevují se jako přitažlivé, nebo odpudivé, a to vzhledem k povaze náboje mezi účastníky adsorpce[42,44]. Každá aminokyselina nese ze své povahy vždy minimálně jednu karboxylovou skupinu a jednu aminoskupinu, které mají různé hodnoty disociačních konstant, a tím ovlivňují převažující náboj molekuly. S rostoucí hodnotou pH se mění forma molekul aminokyselin, resp. náboj, a to z kladného, přes převážně kladný, neutrální (forma amfiontu – při hodnotě pH odpovídajícímu izoelektrickému bodu dané AMK) a převážně záporný na záporný. Průběh adsorpce a její účinnost je tedy závislá na kombinaci převažujících nábojů (a také jejich velikosti) obou účastníků adsorpce, které závisí na charakteru funkčních skupin na povrchu AU a AMK[33,43,45]. Pokud adsorpce probíhá na AU s pH_{nbn} (pH nulového bodu náboje, hodnota pH, při které se mění převažující náboj AU z kladného na záporný) v kyselé oblasti, je adsorpční účinnost ovlivněna strukturou molekuly AMK, tedy charakterem funkčních skupin jejího řetězce. V případě aminokyseliny, v jejíž molekule převažují zásadité funkční skupiny (např. Arg), se účinnost adsorpce s rostoucí hodnotou pH zvyšuje. Na povrchu AU narůstá množství záporného náboje, zatímco AMK nese stále kladný náboj. Tím dochází k silnému elektrostatickému přitahování opačně nabitých funkčních skupin AU a AMK a míra adsorpce roste[37,43,45].

Pokud molekula AMK nese ve svém řetězci funkční skupiny kyselého charakteru, např. další karboxylovou skupinu (např. Asp), nemá pH (v případě AU s kyselým charakterem povrchu) na její adsorpci žádný vliv, resp. k adsorpci u takovéto AMK téměř nedochází[33,39,43,46]. Přítomnost další karboxylové skupiny v řetězci (kromě α-COOH) způsobuje, že již v poměrně nízkých hodnotách pH převažuje na molekule AMK záporný náboj. Zároveň dochází ke stejnému jevu i u AU (viz výše). Téměř nulová adsorpční účinnost AMK s kyselým charakterem řetězce je způsobena silnými odpudivými elektrostatickými interakcemi vlivem růstu záporného náboje AMK i AU se zvyšujícím se pH[33,43,45]. Důležitou roli přitom hraje i skutečnost, že AMK s kyselým charakterem řetězce jsou hydrofilní, a raději tak upřednostňují interakce s vodným roztokem (vodíkové můstky) než s povrchem AU[39,47].

Má-li řetězec AMK neutrální, navíc hydrofobní, charakter (např. Phe), kombinuje se při adsorpci vliv elektrostatických interakcí s hydrofobními. S ohledem na hodnotu pH určují míru adsorpce jednak elektrostatické interakce probíhající mezi protonovanými nebo deprotonovanými

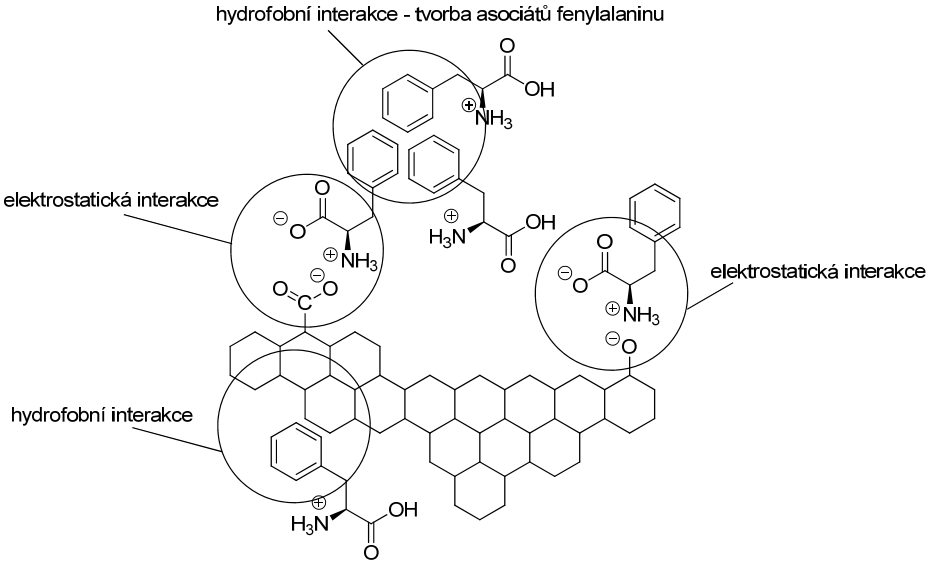

Obr. 2. **Mechanismy adsorpce fenylalaninu na aktivním uhlí[43]**

α-COOH a α-NH_2 skupinami, jednak hydrofobní interakce mezi povrchem AU a aromatickým kruhem v řetězci AMK[34,35,43,45]. Při nízkých hodnotách pH nesou molekuly AMK kladný náboj a AU náboj záporný (stále v případě AU s kyselým charakterem povrchu). Adsorpce probíhá vlivem působení přitažlivých elektrostatických sil mezi opačně nabitými funkčními skupinami AMK a AU. S rostoucím pH pak míra adsorpce klesá. Na molekulách AMK začne převažovat vlivem disociace α-COOH záporný náboj, který narůstá i na povrchu AU, a začnou se projevovat odpudivé elektrostatické interakce[43,45].

Vzhledem k tomu, že molekula AMK má ale hydrofobní řetězec, hrají při adsorpci důležitou roli také i hydrofobní interakce, kterými se molekuly AMK snaží minimalizovat svůj styk s molekulami vody[35,43,45]. Zejména dominují hydrofobní interakce při adsorpci při hodnotách pH, kdy nemůže vlivem opačně nabitých funkčních skupin AMK a AU docházet k přitažlivým elektrostatickým interakcím, a také při vyšších počátečních koncentracích AMK. S rostoucí počáteční koncentrací AMK roste v roztoku množství molekul, které se mohou této interakce účastnit, a také pravděpodobnost, že k takové interakci dojde[43]. Interakce uplatňující se při adsorpci AMK s neutrálním hydrofobním řetězcem jsou na příkladu fenylalaninu ukázány na obr. 2.

4.2. Vliv iontové síly

Kromě hodnoty pH dále významně ovlivňuje adsorpci AOM aminokyselin na AU iontová síla (IS)[37,38,43,45,48]. Iontová síla má vliv především na elektrostatické interakce a mění se v závislosti na typu AU a pH roztoku. Obecně dochází vlivem zvýšené IS v systému k potlačení odpudivých elektrostatických interakcí, a tím ke zvýšení účinnosti adsorpce[1,40,41,44]. Velice však záleží i na povrchové koncentraci adsorbátu. V případě, že je povrchová koncentrace nízká a mezi účastníky adsorpce převládají přitažlivé síly, vede zvýšení IS k poklesu účinnosti adsorpce[1,44]. Tento jev se významně uplatňuje i při adsorpci AMK[43]. V případě zvýšení IS roztoku, kde probíhá adsorpce opačně nabitých účastníků sorpce na základě přitažlivých elektrostatických interakcí, dojde vlivem přidaných iontů soli k oslabení těchto sil a míra adsorpce se sníží. Velmi výrazně je míra adsorpce snížena především při adsorpci AMK se zásaditým charakterem řetězce na AU s kyselým charakterem povrchu[38,45,48]. Tyto AMK jsou totiž spíše hydrofobní, upřednostňují reakci s AU než s molekulami vodného roztoku, čemuž je ionty přidané soli bráněno. Míra adsorpce pak může klesnout až o cca 90 % (cit.[37,45]). Možnými důvody jsou např. pokles rozpustnosti dané AMK s přidáním soli nebo také větší afinita iontů Na^+ k povrchu adsorbentu, což způsobuje omezení působení přitažlivých sil mezi adsorbentem a molekulami AMK. Tedy, při nízkých koncentracích adsorbátu na povrchu AC zvýšení IS ovlivňuje adsorpci opačně nabitých účastníků (převládají přitažlivé síly) negativně[45].

V případě adsorpce AMK s řetězcem kyselého charakteru je situace složitější. Ačkoli by zvýšením IS roztoku mohlo dojít k oslabení odpudivých elektrostatických sil, když u opačně nabitých účastníků adsorpce způsobí ionty přidané soli oslabení přitažlivých sil, při adsorpci AMK se tento jev neuplatňuje[39,43,47]. Aminokyseliny s kyselým řetězcem mají totiž hydrofilní povahu a upřednostňují reakce s molekulami vodného roztoku[39,47]. Navíc jsou molekuly AMK tak malé, že ani odstínění odpudivých sil mezi stejně nabitou částí molekuly a povrchem AU nestačí k projevu přitažlivých sil mezi povrchem AU a tou částí molekuly, která je vůči němu nabitá opačně[43].

Téměř žádný nebo velmi malý vliv má IS na adsorpci AMK, jejichž řetězec je neutrálního hydrofobního charakteru. Při adsorpci takovýchto AMK se totiž kromě elektrostatických sil uplatňují ještě síly hydrofobní (viz výše), na které nemá zvýšení IS žádný vliv[34,35,43].

5. Závěr

Aminokyseliny, které jsou součástí nízkomolekulární složky sinicových a řasových produktů, tzv. AOM, jsou při konvenční úpravě vody koagulací/flokulací odstraňovány s malou účinností. Zbytkové koncentrace AMK v upravené vodě následně způsobují celou řadu problémů, z nichž pravděpodobně nejvýznamnější je zvyšování spotřeby desinfekčních činidel a tvorba vedlejších produktů desinfekce, které se řadí mezi prokázané nebo potenciální karcinogeny. Z uvedených důvodů je zřejmé, že je třeba hledat další metody pro účinné odstranění nízkomolekulárních AOM při úpravě vody. Jednou z takových potenciálně vhodných metod je jejich adsorpce na aktivním uhlí.

Adsorpce aminokyselin je závislá především na jejich struktuře a povrchovém náboji, charakteru povrchu AU a vlastnostech roztoku. V případě AU je určující především chemismus povrchu – přítomnost funkčních skupin určující charakter povrchového náboje. Obdobně je tomu i u AMK, kde také zásadní roli hraje přítomnost a charakter funkčních skupin řetězce ovlivňující jejich náboj. Vliv uvedených charakteristik AU a AMK přitom úzce souvisí s chemismem roztoku, především s hodnotou pH, která ovlivňuje disociaci povrchových funkčních skupin u AU i AMK, a tím určuje i povahu mechanismů probíhajících při adsorpci.

Adsorpce AOM aminokyselin také vykazuje určitá specifika spojená především s velmi malou velikostí a homogenností jejich molekul. Zatímco např. COM peptidy (také nízkomolekulární složka AOM) se jako několikanásobně větší molekuly s různorodým charakterem funkčních skupin adsorbují snadněji a lze pro jejich odstraňování stanovit jisté optimum, v případě aminokyselin je situace složitější. Optimální podmínky sice lze vzhledem k charakteru molekuly nalézt i pro odstranění jednotlivých volných AMK, avšak vezmeme-li v úvahu, že ve vodě se vyskytují různé AMK s odlišnými strukturami, dojde při použití jednoho druhu AU k odstranění jen některých aminokyselin. Jistý podíl AMK tedy bude i po adsorpci na AU v upravené vodě zůstávat. Otázkou pak je, zda toto zbytkové množství představuje potenciální riziko pro tvorbu

DBPs. Protože však tvorba DBPs je značně specifická (některé látky se mohou prakticky kompletně transformovat na vedlejší produkty desinfekce, jiné naopak vůbec) a aminokyseliny jsou velmi účinnými prekurzory, představují jejich zbytkové aminokyseliny riziko i při relativně nízkých zbytkových koncentracích např. v řádech desítek $\mu g\ l^{-1}$. Pro odstranění specifických aminokyselin je nepochybně důležitá volba vhodného aktivního uhlí. Protože hlavním mechanismem adsorpce aminokyselin jsou elektrostatické interakce (v menší míře pak hydrofobní interakce), je třeba volit sorbent s dostatečným opačným nábojem než při daném pH mají sorbované aminokyseliny. Tato skutečnost vyžaduje detailní charakterizaci zvoleného AU (velikostní distribuci pórů, charakter povrchových funkčních skupin, závislost povrchového náboje na pH roztoku) i potenciálních adsorbovaných látek (struktura molekuly, molekulová hmotnost, závislost celkového náboje na pH roztoku).

Adsorpce na AU se v současné době využívá převážně při úpravě problematických vod s obsahem antropogenních mikropolutantů nebo krátkodobě při náhlém zhoršení kvality surové vody. S ohledem na nárůst eutrofizace vod v posledních letech se však bude problematika odstraňování AOM dostávat do popředí zájmu nejen vědeckého výzkumu, ale také provozovatelů úpraven vody.

LITERATURA

1. Newcombe G., Drikas M.: Carbon *35*, 1239 (1997).
2. Matilainen A, Gjessing E. T., Lahtinen T., Hed L., Bhatnagar A., Sillanpää M.: Chemosphere *83*, 1431 (2011).
3. Pelekani, C., Snoeyink, V. L.: Water Res. *33*, 1209 (1999).
4. Pivokonsky M., Kloucek O., Pivokonska L.: Water Res. *40*, 3045 (2006).
5. Henderson R. K., Baker A., Parsons S. A., Jefferson B.: Water Res. *42*, 3435 (2008).
6. Safarikova J., Baresova M., Pivokonsky M., Kopecka I.: Sep. Purif. Technol. *118*, 49 (2013).
7. Pivokonský M., Pivokonská L., Bubáková P., Janda V.: Chem. Listy *104*, 1015 (2010).
8. Pivokonsky M., Safarikova J., Baresova M., Pivokonska L., Kopecka I.: Water Res. *51*, 37 (2014).
9. Takaara T., Sano D., Konno H., Omura T.: Water Res. *41*, 1653 (2007).
10. Li L., Gao N., Deng Y., Yao J., Zhang K.: Water Res. *46*, 1233 (2012).
11. Qu F., Liang H., Wang Z., Wang H., Yu H., Li G.: Water Res. *46*, 1490 (2012).
12. Froese, K. L., Wolanski, A., Hrudey, S. E.: Water Res. *33*, 1355 (1999).
13. Freuze, I., Brosillon, S., Laplanche, A., Tozza, D., Cavard, J.: Water Res. *39*, 2636 (2005).
14. Pivokonsky M., Safarikova J., Bubakova P., Pivokonska L.: Water Res. 46, 5583 (2012).
15. Pivokonsky M., Polasek, P., Pivokonska, L., Tomaskova, H.: Water Environ. Res. *81*, 514 (2009).
16. Her N., Amy G., Park H. R., Song M.: Water Res. *38*, 1427 (2004).
17. Zhang X., Fan L., Roddick F. A.: J. Membr. Sci. *425*, 23 (2013).
18. Zhang X., Fan L., Roddick F. A.: J. Membr. Sci. *447*, 362 (2013).
19. Nguyen M. L., Westerhoff P., Baker L., Hu Q., Esparza-Soto M., Sommerfeld M.: J. Environ. Eng. *131*, 1574 (2005).
20. Fang J., Yang X., Ma J., Shang C., Zhao Q.: Water Res. *44*, 5897 (2010).
21. Hnatukova P., Kopecka I., Pivokonsky M.: Water Res. *45*, 3359 (2011).
22. Pivokonsky M., Naceradska J., Kopecka I., Baresova M., Jefferson B., Li X., Henderson R. K.: Crit. Rev. Env. Sci. Tec., DOI: 10.1080/10643389.2015.1087369.
23. Čermáková L., Pivokonská L., Kopecká I., Pivokonský M., Janda V.: Chem. Listy *109*, 176 (2015).
24. Thurman E. M.: *Organic Geochemistry of Natural Waters.* Nijhoff/Junk, Hague 1985.
25. Hong H. C., Wong M. H., Liang Y.: Arch. Environ. Contam. Toxicol. *56*, 638 (2009).
26. Hureiki L., Croue J. P., Legube B.: Water Res. *28*, 2521 (1994).
27. Elsellami L., Vocanson F., Dappozze F., Puzenat E., Païsse, O., Houas A., Guillard C.: Appl. Catal., A *380*, 142 (2010).
28. Manar K. F., Al-Sheikh A. M.: Water Res. *35*, 1304 (2001).
29. Gagnon G. A., Slawson R. M., Huck P. M.: Can. J. Civ. Eng. *27* (3), 412 (2000).
30. Trehy M. L., Yost R. A., Miles C. J.: Environ. Sci. Technol. *20*, 1117 (1986).
31. Hong H. C., Mazumder A., Wong M. H., Liang Y.: Water Res. *42*, 4941 (2008).
32. Pászti Z., Guczi L.: Vib. Spectrosc. *50*, 48 (2009).
33. Greiner E., Kumar K., Sumit M., Giuffre A., Zhao W., Pedersen J., Sahai N.: Geochim. Cosmochim. Acta *133*, 142 (2014).
34. Clark H. M., Alves C. C. C., Franca A. S., Oliveira L. S.: LWT – Food Sci. Technol. *49*, 155 (2012).
35. Titus E., Kalkar A. K., Gaikar V. G.: Colloids Surf., A *233*, 55 (2003).
36. Goscianska J., Olejnik A., Pietrzak R.: Mater. Chem. Phys. *142*, 586 (2013).
37. O´Connor A. J., Hokura A., Kisler J. M., Shimazu S., Stevens G. W., Komatsu Y.: Sep. Purif. Technol. *48*, 197 (2006).
38. Vinu A., Hossain K. Z., Kumar G. S., Ariga K.: Carbon *44*, 530 (2006).
39. Ikhsan J., Johnson B. B., Wells J. D., Angove M. J.: J. Colloid Interface Sci. *273*, 1 (2004).
40. Moreno-Castilla, C.: Carbon *42*, 83 (2004).
41. Campinas M., Rosa M. J.: J. Colloid Interface Sci. *299*, 520 (2006).
42. Kopecka I., Pivokonsky M., Pivokonska L., Hnatuko-

va P., Safarikova J.: Carbon *69*, 595 (2014).
43. Čermáková L.: *Diplomová práce*. Univerzita Karlova, Praha 2015.
44. Bjelopavlic M., Newcombe G., Hayes R.: J. Colloid Interface Sci. *210*, 271 (1999).
45. Gao Q., Xu W., Xu Y., Wu D., Sun Y., Deng F., Shen W.: J. Phys. Chem. B *112*, 2261 (2008).
46. Tentorio A., Canova L.: Colloids Surf. *39*, 311 (1989).
47. Sebben D., Pendleton P.: J. Colloid Interface Sci. *443*, 153 (2015).
48. Liu M., Huang J., Deng Y.: Bioresour. Technol. *98*, 1144 (2007).

L. Čermáková[a,b], L. Pivokonská[a], I. Kopecká[a], M. Pivokonský[a,b], and V. Janda[c] *([a]Institute of Hydrodynamics, Academy of Sciences of the Czech Republic; [b] Institute for Environmental Studies, Faculty of Science, Charles University in Prague; [c] Dept. of Water Technology and Environmental Engineering, University of Chemistry and Technology, Prague):* **Effect of Amino Acids Produced by Phytoplancton on Water Treatment and Their Adsorption onto Activated Carbon**

The paper deals with the influence of amino acids (AAs) from algal organic matter (AOM) on the water treatment process and with their adsorption onto activated carbon (AC). The structure of the molecule, especially the character of functional groups in the chain, plays the most important role in the adsorption of AOM AAs. In terms of the nature of the solution, adsorption is affected especially by pH and ionic strength (IS). The largest adsorption capacities for a particular AA are achieved under conditions, where the molecules of AAs carry a charge opposite to the AC surface and, therefore, attractive electrostatic forces between the AC and AOM AAs can manifest themselves. Furthermore, the hydrophobic interactions are applied in the adsorption of neutral AAs with hydrophobic chain. Depending on the conditions, an increase of IS can significantly reduce the adsorption efficiency or have no effect.

PUBLIKACE 8

Occurrence of microplastics in raw and treated drinking water

Martin Pivokonský, **Lenka Čermáková**, Kateřina Novotná, Petra Peer, Tomáš Cajthaml a Václav Janda

Science of the Total Environment 643 (2018) 1644-1651
DOI 10.1016/j.scitotenv.2018.08.102

Science of the Total Environment 643 (2018) 1644–1651

Contents lists available at ScienceDirect

Science of the Total Environment

journal homepage: www.elsevier.com/locate/scitotenv

Occurrence of microplastics in raw and treated drinking water

Martin Pivokonsky [a,*], Lenka Cermakova [a,b], Katerina Novotna [a,c], Petra Peer [a], Tomas Cajthaml [b], Vaclav Janda [c]

[a] Institute of Hydrodynamics of the Czech Academy of Sciences, Pod Patankou 30/5, 16612 Prague 6, Czech Republic
[b] Institute for Environmental Studies, Faculty of Science, Charles University, Benatska 2, 12801 Prague 2, Czech Republic
[c] Department of Water Technology and Environmental Engineering, Faculty of Environmental Technology, University of Chemistry and Technology, Prague, Technicka 5, 16628 Prague 6, Czech Republic

HIGHLIGHTS

- Microplastics were present in all water samples from different treatment plants.
- The concentration of microplastics was higher in raw water than in treated water.
- Particles of 1–10 μm were the most abundant, accounting for up to 95%.
- Polyethylene terephthalate, polypropylene and polyethylene microplastics prevailed.

GRAPHICAL ABSTRACT

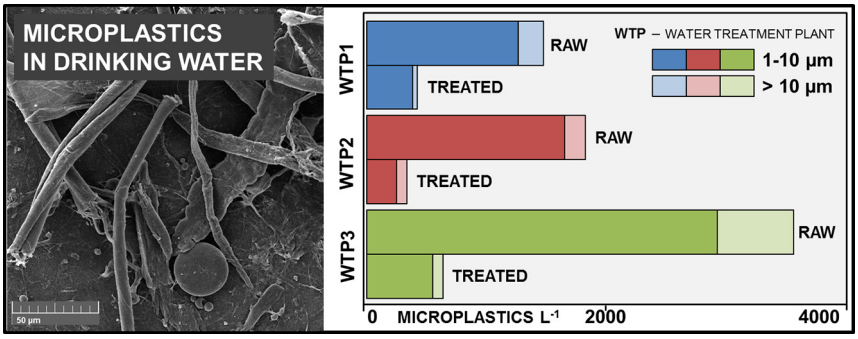

ARTICLE INFO

Article history:
Received 2 July 2018
Received in revised form 6 August 2018
Accepted 7 August 2018
Available online 8 August 2018

Editor: D. Barcelo

Keywords:
Drinking water sources
Microplastics
Nanoplastics
Plastic contamination
Water treatment

ABSTRACT

The study investigates the content of microplastic particles in freshwater and drinking water. Specifically, three water treatment plants (WTPs) supplied by different kinds of water bodies were selected and their raw and treated water was analysed for microplastics (MPs). Microplastics were found in all water samples and their average abundance ranged from 1473 ± 34 to 3605 ± 497 particles L^{-1} in raw water and from 338 ± 76 to 628 ± 28 particles L^{-1} in treated water, depending on the WTP. This study is one of very few that determine microplastics down to the size of 1 μm, while MPs smaller than 10 μm were the most plentiful in both raw and treated water samples, accounting for up to 95%. Further, MPs were divided into three categories according to their shape. Fragments clearly prevailed at two of the WTPs and fibres together with fragments predominated at one case. Despite 12 different materials forming the microplastics being identified, the majority of the MPs (>70%) comprised of PET (polyethylene terephthalate), PP (polypropylene) and PE (polyethylene). This study contributes to fill the knowledge gap in the field of emerging microplastic pollution of drinking water and water sources, which is of concern due to the potential exposure of microplastics to humans.

1. Introduction

Recently, residuals of plastic materials have been increasingly detected in aquatic environments, including oceans, seas and freshwater bodies. Not only plastic litter that is visible to the naked eye, but also smaller debris has gained attention. Microplastics (MPs) are usually defined as particles smaller than 5 mm (Andrary, 2011; Eerkes-Medrano et al., 2015; Koelmans et al., 2015), nevertheless, a lower limit is not clearly defined as various methods have been used for sampling of the particles among the studies (Eerkes-Medrano et al., 2015; Mason et al., 2016; Su et al., 2016; Di and Wang, 2018). For example, 333 μm

* Corresponding author.
E-mail address: pivo@ih.cas.cz (M. Pivokonsky).

https://doi.org/10.1016/j.scitotenv.2018.08.102
0048-9697/

mesh size nets are commonly employed (Andrary, 2011; Eerkes-Medrano et al., 2015; Anderson et al., 2017). However, smaller MPs (including particles <100 μm) have been found in bulk water samples (Su et al., 2016; Di and Wang, 2018). The smallest plastic particles are sometimes referred to as nanoplastics (NPs), while the definition varies in the literature, i.e. it stands for particles <100 nm in some studies (Koelmans et al., 2015; Hahladakis et al., 2018) and <1 μm in another (da Costa et al., 2016). To date, plastic particles within this size range have only rarely been subjected to investigation and have not been satisfactorily quantified in natural waters (da Costa et al., 2016). However, substantial amounts of small-sized MPs were detected in bottled waters, i.e. up to 118 ± 88 MPs L^{-1} > 5 μm (Schymanski et al., 2018) and up to 6292 ± 10,521 MPs L^{-1} > 1 μm (Oßmann et al., 2018). Microplastics were suspected to originate from the materials of which the bottles and the caps were made. Nevertheless, with regard to the composition of detected microplastics (including polymers such as polyethylene, polypropylene or styrene-butadien-copolymer), other sources of MPs besides the packaging materials were suggested by the authors (Oßmann et al., 2018).

In the aquatic environment, MPs of various compositions have been identified, including acrylic, polyamide, polyester, polyethylene, polypropylene and polystyrene (Eerkes-Medrano et al., 2015; Di and Wang, 2018). MPs also differ in their shape and morphotypes such as fibres, films, foams, foils, fragments, pellets and spheres are commonly distinguished (Mason et al., 2016; Su et al., 2016; Anderson et al., 2017; Leslie et al., 2017). Although plastics are recognized as light and buoyant materials and substantial amounts of MPs were quantified as floating debris when sampling from surface water layer, e.g. ranging from $1 \cdot 10^3$ to $68 \cdot 10^5$ particles per km^2 in various freshwater bodies (Free et al., 2014; Su et al., 2016; Anderson et al., 2017), denser plastics can easily submerge (Andrary, 2011) and they have been detected in sediments (Su et al., 2016; Leslie et al., 2017; Di and Wang, 2018). However, a significant portion of plastic particles tends to remain suspended in the water column (da Costa et al., 2016; Leslie et al., 2017). For example, concentrations ranging from 1.6 to 12.6 pieces (48 μm–5 mm) per litre were measured in the Three Gorges Reservoir, China, depending on the sampling location (Di and Wang, 2018). Particles smaller than 0.5 mm were always the most abundant (comprising 31.2–74.4% of the total number). Su et al. (2016) determined MPs (>5 μm) content in Taihu Lake, China, where the concentrations were 3.4–25.8 items per litre, again varying among the sampling points, while particles of sizes 100–1000 μm were prevalent. Concentrations of MPs (approx. 10 μm–5 mm) ranged from 48 to 187 particles per litre in Amsterdam canal water (Leslie et al., 2017).

The sources of plastics in aquatic environments include sewage discharge (Browne et al., 2011; Eerkes-Medrano et al., 2015; Mason et al., 2016; Mintenig et al., 2017), plastic manufacturing plants and other industrial activities, decomposition of plastic litter etc. (da Costa et al., 2016). Conventional waste water treatment plants (WWTPs) have shown an ability to remove a portion of the plastic MPs, however, large amounts still pass through the process, accounting for up to hundreds to thousands of particles per m^3 effluent (Mason et al., 2016; Leslie et al., 2017; Mintenig et al., 2017), while smaller particles are less likely to be retained by the treatment plants (da Costa et al., 2016; Mintenig et al., 2017; Talvitie et al., 2017). Interestingly, to the best of our knowledge, no studies have been conducted to examine the removability of plastic particles at drinking water treatment plants (WTPs) or their concentrations in treated water. Despite the ecological and toxicological impacts of MPs are still largely unknown, microplastics are considered to be an emerging contaminant, including concerns about possible influence on human health. Virgin microplastics have been already demonstrated to have adverse effect on various organisms (Chae and An, 2017; Lei et al., 2018a, b). Besides intrinsic impacts of MPs, they can also serve as a transfer medium for other harmful chemicals (Andrary, 2011; Eerkes-Medrano et al., 2015). Although a couple of studies on MPs presence in selected foodstuff and packaged beverages have been conducted (Liebezeit and Liebezeit, 2014; Van Cauwenberghe and Jenssen, 2014; Yang et al., 2015; Oßmann et al., 2018; Schymanski et al., 2018), the research on microplastics in potable water is lacking.

With respect to the research gaps regarding the content of microplastic particles in drinking water, we focused on the presence of MPs in freshwaters that directly enter WTPs and subsequently on microplastics determination in treated water. Different kinds of water bodies were selected – a large valley water reservoir, a small water reservoir and a river. Aims of our study were (i) to quantify MPs and compare their content in raw and treated water originating from diverse sources, (ii) to provide size classification of the particles and (iii) to identify prevailing morphotypes and material composition of the microplastics.

2. Materials and methods

2.1. Sampling sites

Samples of raw and treated water were obtained from three drinking water treatment plants. All are located in urban areas of the Czech Republic and provide water for a considerable number of inhabitants, but they are supplied by diverse kinds of water bodies and differ in the treatment technology. Our main reason for selecting the different water bodies and WTPs was to avoid random absence or presence of microplastics, potentially possible if we had analysed samples from only one location. For confidentiality reasons, the WTPs are not named and are referred as WTP1, WTP2 and WTP3. WTP1 (usual/maximum capacity: 3700/7000 L s^{-1}, supplies approx. 1.5 million inhabitants) takes water from a large valley water reservoir and the applied technology involves coagulation/flocculation and sand filtration. The water source for WTP2 (usual/max capacity: 100/200 L s^{-1}, supplies approx. 60 thousand inhabitants) is a smaller water reservoir and coagulation/flocculation, sedimentation, sand and granular activated carbon filtration are operated. WTP3 (usual/max capacity: 90/150 L s^{-1}, contributes to supply approx. 130 thousand inhabitants) uses water from a river and the treatment process includes coagulation-flocculation, flotation, sand filtration and granular activated carbon filtration. The quality of both raw and treated water samples is specified in Table S1 (Supplementary data).

2.2. Water samples collection

Samples were collected in the winter period (November 2017–January 2018). This timing was chosen because of a minimal occurrence of phytoplankton that might hinder the analysis. Raw water was sampled at the WTP inlet and treated water at the outflow to the treated water accumulation. One sample of raw water and one sample of treated water (volume of 1 L each) were taken into autoclavable borosilicate glass bottles (pre-cleaned as described in Section 2.6). Sampling was conducted three times (every 8 h) within a 24 hour period and such sampling event was repeated three times within the given period, while the selection of sampling days was random. These samples (54 L in total; i.e. 27 L of raw water and 27 L of treated water) were used to determine the number, size and morphology of contained particles by using SEM (scanning electron microscopy) analysis. Additionally, extra 1 L samples were taken for qualitative analysis (Fourier transform infrared spectroscopy – FTIR; Raman spectroscopy; elemental microanalysis) at the first sampling occasion every sampling day (18 L in total; i.e. 9 L of raw water and 9 L of treated water). The samples were stored at 4 °C prior to analysis, while particular attention was paid to avoid contamination of the samples (see Section 2.6 for details).

2.3. Sample preparation and filtration

At first, wet peroxide oxidation was conducted to remove organic material from the water samples, as described in Anderson et al. (2017). The pre-treated samples were passed through a series of polytetrafluoroethylene (PTFE) membrane filters (Merck Millipore, USA) of 5 μm and subsequently 0.2 μm pore sizes. These filters were used for SEM analysis of retained particles. This two-step filtration through descending mesh size was applied in order to pass the entire sample volume through the filter of diameter 25 mm without clogging. Previously, filters made of various materials were tested (including also aluminium oxide, glass-fibre or polycarbonate filters). PTFE was selected as these filters appeared not to pose any interference to the SEM analysis (Fig. S6, Supplementary data) or any sample contamination, compared to e.g. glass-fibre filters that might release the fibres and subsequently disturb the analysis. Al_2O_3 filters (Whatman, UK) were chosen for filtration of the samples for qualitative analysis to assure no matrix interference (Leslie et al., 2017; Mintenig et al., 2017). A glass vacuum filtration device (GV 025 series, Whatman, UK) connected to a vacuum pump (Laboport series, KNF Neuberger GmbH, Germany) were used for filtration. Thereafter, the filters were dried in an oven (30 °C, 30 min) and stored in capped glass petri dishes placed in a desiccator before being analysed.

2.4. Quantification of plastic particles and their size and shape determination

The obtained filters served for the analysis of the retained particles, using a Vega high resolution scanning electron microscope (Tescan, Czech Republic). Three cut-outs (3 mm × 8 mm) from each filter were prepared (one from the middle, one from the edge of a filter and one from in between). Prior to imaging, a conductive gold layer was sputtered onto the samples. The images were taken with an optimized acceleration voltage of 10 kV, detector working distance of approximately 9 mm.

Number, size and shape (morphology) of particles were determined for each individual filter cut-out by using SigmaScan 5 software (Systat Software, Inc., USA). Values obtained from the cut-outs of one filter were then used to calculate total numbers per filter (quantity of particles and their distribution in size and shape categories). Results derived for 5 μm and 0.2 μm filters were summarized to provide final information on all the detected particles in each individual 1 L sample. The homogeneity of results among the three filter cut-outs was evaluated and their similar profiles demonstrated that they satisfactorily represent the sample as a whole, see Section 2.7 Statistical analysis and Section S1, Figs. S1, S2 and Tables S2–S4, Supplementary data, for details. Further, average values (including standard deviations) per sampling day and whole period at each WTP were calculated, while the differences between the raw and treated water were emphasized.

The particles were divided into six size categories (0.2–1 μm; 1–5 μm; 5–10 μm; 10–50 μm; 50–100 μm; >100 μm) and three morphotypes (fibres, spherical and fragments). Fibres were defined as particles with a long and thin appearance (size measured as the fibre diameter), spherical particles as those of a clearly circular shape (size = diameter) and remaining particles are referred as fragments (size as a distance between two most remote points of a particle).

The qualitative analyses (see Section 2.5 for methods) revealed that 8–83% (depending on the sample) of the particles were not composed of plastic. Thus, particular percentage of particles was always subtracted from the results obtained from SEM analysis. A similar approach (recalculation of microplastic number according to qualitative analysis of selected particles) was applied also in other studies, e.g. Su et al. (2016) or Schymanski et al. (2018).

Additionally, particles smaller than 1 μm cannot be credibly analysed in terms of material composition. Therefore, these particles (size category 0.2–1 μm) were excluded from our results on microplastics. Unless otherwise stated, all data on particle abundance, size, shape and material composition presented hereafter in this study describes only plastic particles >1 μm. Such particles are referred to as "microplastics" as none of the particles exceeded the size of 5 mm that is most often presented as an upper boundary for MPs (Andrary, 2011; Eerkes-Medrano et al., 2015; Koelmans et al., 2015).

2.5. Qualitative analysis

Particles >10 μm were analysed by using FTIR spectrometer Nicolet 6700 (Thermo Fisher Scientific, USA) complemented by microscope Continuum (MCT detector, beam splitter KBr). The band from 4000 to 650 cm^{-1} was collected, resolution of 4 cm^{-1} was applied and each spectrum was an average of 128 scans. Collected data were processed by Omnic software (Thermo Fisher Scientific, USA) and the composition of particles was determined by comparing obtained spectra to a database (Restaurator library, UCT Prague, Czech Republic), while the match factor threshold was set to 0.80.

For the analysis of particles in the size range 1–10 μm, DXR2xi micro-Raman imaging microscope system (Thermo Fisher Scientific, USA) was employed (532 nm laser, laser spot size around 0.5 μm, Raman shift 50–3550 cm^{-1}, spectral resolution of 5 cm^{-1}). Collected spectra were processed by Omnic software and identified by comparing to a database (Thermo Fisher Scientific, USA). The match factor threshold always exceeded 0.80.

The qualitative analysis using FTIR and Raman spectroscopy was performed for a circular sector covering 25% of the Al_2O_3 filter, thus approximately one quarter of the particles was analysed per filter and the results were extrapolated to all the particles on the filter being examined. Analysing of a whole filter is not feasible due to the demanding and time-consuming methods applied. Thus, selecting a representative part of a filter for the analysis and subsequent extrapolation of results is a common approach (Oßmann et al., 2018; Schymanski et al., 2018). Additionally, elemental analysis of selected particles was performed by using SEM-EDX (energy dispersive X-ray spectroscopy) to provide more information on their composition. See Section S2 and Fig. S7, Supplementary data.

2.6. Avoiding contamination and blank sample analysis

Any direct contact of samples with plastic materials was avoided during the sampling, sample preparation and analysis. All utilized glassware were cleaned using sonication in HPLC-grade water (30 min) and repeatedly rinsed with HPLC-grade water prior to being used so as to prevent any contamination of the samples. In order to avoid airborne contamination, processing of the samples was performed in a laboratory with air filtration provided by HEPA air filters (KS BESTFIL, KS Klima-Service, Czech Republic). Only cotton clothing was worn during manipulation with the samples.

In order to assure if any additional plastic contamination happened during the sample preparation and filtration, blank filters using HPLC-grade water as a sample were prepared and analysed, applying the very same procedure as for real samples, including storing in the sampling bottle and the oxidation step. Three blanks were performed with each set of samples (set = samples from one sampling day).

2.7. Statistical analysis

The number and distribution of microplastics in each 1 L sample was calculated based on the individual cut-out results, while the homogeneity of such derived data was tested (exact data for one sampling day and each WTP are shown in Tables S2–S4, Supplementary data). Firstly, a profile of every cut-out was created, including the information on microplastic number in each shape category. It was shown that the profiles for one sample do not differ considerably (example is shown in Fig. S1a–c, Supplementary data). Subsequently, the cut-out profiles

from individual samples collected during one day were aggregated into a datasets representing each WTP (separate datasets for raw and treated water were created). These were used for profile analysis (Morrison, 1990) performed in programming language R, applying the profileR package. Two hypotheses (a hypothesis of parallel sample profiles and a hypothesis of the same level of sample profiles) were tested (see Section S1 and Fig. S2a, b, Supplementary data, for details). As these hypotheses were not rejected in any case ($p > 0.05$), it appears that the samples were satisfactorily representative.

3. Results and discussion

3.1. Microplastic abundance

All samples were shown to contain microplastics. Their number varied among the WTPs and also differed between the raw and treated water in every case (see Table 1 for details). The background contamination (determined by analysing blank filters, as described in Section 2.6) represented <5% of the abundance of microplastics detected in the samples and was considered negligible (see Supplementary data, Section S3, Table S5).

The content of MPs in raw water samples (average for the entire sampling period) was 1473 ± 34, 1812 ± 35 and 3605 ± 497 particles L^{-1} at WTP1, WTP2 and WTP3, respectively. The differences in MPs abundance in raw water are expected to be caused by various factors such as the kind of water body and especially its ambient environment, including human activities in its surroundings, current weather conditions etc. The quality of water samples that were used for the determination of microplastics is described in Table S1, Supplementary data. As WTP1 is supplied by water from a large reservoir with a possibility to adjust sampling profile according to the water quality, the uptake of undesirable particles (including microplastics) is likely to be avoided to some limited extent. WTP2 takes water from a reservoir which is much smaller and where the residence time of water is much shorter. Furthermore, there are more industrial activities nearby and the area is more populated compared to WTP1 source. WTP3 takes water directly from a river that flows through a rather industrial region. However, despite the fact that these factors are likely to have some impact on the MPs content in the surface waters, detailed research would be needed to monitor sources and the fate of microplastics in freshwater systems.

The amounts of MPs were generally much lower in treated water, accounting for 443 ± 10, 338 ± 76 and 628 ± 28 particles L^{-1} at WTP1, WTP2 and WTP3, respectively. These results demonstrate that a significant portion of the microplastics were removed by the treatment processes, i.e. 70% at WTP1, 81% at WTP2 and 82% at WTP3 on average. The difference between raw and treated water samples at each WTP and sampling day is expressed as "removal" in Table 1. The distinctions in the MP removal percentage between WTP1 versus WTP2 and WTP3 might be related to the applied treatment technologies. While WTP1 operates only conventional sand filtration, the latter two treatment plants run two-stage separation (sedimentation + sand filtration at WTP2, flotation + sand filtration at WTP3) with additional granular activated carbon filtration. Flotation especially seems to be suitable for the removal of MPs because many of the plastic materials are generally recognized as light and buoyant (da Costa et al., 2016; Di and Wang, 2018). However, further research would be necessary to prove any relation between the technological arrangement of a water treatment plant and plastic particles removal efficiency. The number of microplastics in treated water is also given by their occurrence in raw water. Thus, for example, despite the fact that the percentage of the MPs removed is lowest in the case of WTP1, their content in treated water is similar to WTP2 because of the initial water quality.

Table 1
Quantification of microplastics – daily, average and min and max numbers of microplastics in raw versus treated water at water treatment plants 1 (WTP1), 2 (WTP2) and 3 (WTP3).

	Microplastics L^{-1}		Removal (%)
	Raw water	Treated water	
WTP1			
Day 1	1436 ± 60	434 ± 56	70
Day 2	1478 ± 87	442 ± 57	70
Day 3	1504 ± 14	453 ± 43	70
Average	1473 ± 34	443 ± 10	70
Minimum	1383	369	66
Maximum	1575	485	74
WTP2			
Day 1	1830 ± 195	418 ± 44	77
Day 2	1835 ± 110	266 ± 21	86
Day 3	1772 ± 112	330 ± 13	81
Average	1812 ± 35	338 ± 76	81
Minimum	1648	243	75
Maximum	2040	466	86
WTP3			
Day 1	3305 ± 111	605 ± 35	82
Day 2	4179 ± 470	659 ± 23	84
Day 3	3331 ± 171	622 ± 41	81
Average	3605 ± 497	628 ± 28	83
Minimum	3123	562	78
Maximum	4464	684	85

Minimum and maximum – represent min and max sample value within the WTP and entire sampling period (data for single samples not shown).
Removal – portion of MPs removed based on the quotient of the number of MPs in treated water and the number of MPs in raw water.

3.2. Size and morphology

Microplastics were divided into five categories according to their size (1–5 μm; 5–10 μm; 10–50 μm; 50–100 μm; >100 μm) and into three groups depending on their shape (fibres, spherical and fragments). Examples of SEM images and representatives of fibres, spherical particles and fragments are depicted in Fig. 1. Generally, particles smaller than 10 μm significantly predominated in both raw and treated water at all treatment plants.

Among the categories of MP distribution in raw water (the MPs abundance in each size category is shown in Fig. 2a), microplastics of 1–5 μm prevailed in all the samples from any WTP, accounting for approximately 40–60% of the total MPs count, followed by the category 5–10 μm. A similar percentage (around 30–40%) of 5–10 μm microplastics was determined at all the plants. Particles bigger than 10 μm did not exceed a portion of 10% in any raw water sample, while the abundance of microplastics decreased with increasing size category and MPs > 100 μm were the least plentiful, comprising not more than 2% of total particle count. Interestingly, most of the existing studies that deal with plastics occurrence in waters analyse particles (recognized as microplastics) not smaller than 5 μm (Su et al., 2016; Schymanski et al., 2018) and even sampling sieves of mesh size ranging from dozens to hundreds of μm are often used (Andrary, 2011; Eerkes-Medrano et al., 2015; Mason et al., 2016; Su et al., 2016; Anderson et al., 2017; Di and Wang, 2018). Thus, unknown amounts of smaller particles are often likely not to be recorded. However, some of these studies indicate that the size distribution of MPs skews towards smaller sizes, probably because of the degradation of larger plastic debris (Zhao et al., 2014; Zhang et al., 2015).

Additionally, our study revealed also a substantial content of particles <1 μm in the raw water samples (111–2181 particles L^{-1}, depending on the WTP and the sampling day). Despite the fact that such small particles cannot be properly analysed for material composition and thus cannot be verified as microplastics, it could be expected that an unknown proportion of them might be of plastic origin. The limitations of available methods are a well-known hindrance in the determination of nano-sized particles in water (Koelmans et al., 2015; da Costa et al., 2016).

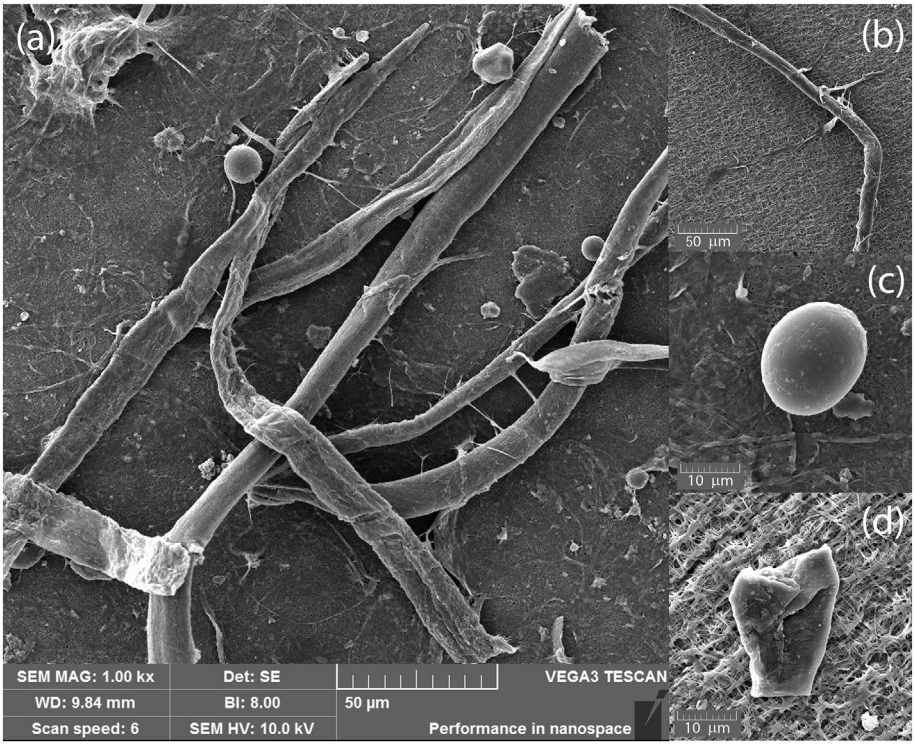

Fig. 1. Scanning electron microscopy (SEM) image of microplastics (a) and details of differently shaped microparticles: fibres (b), spherical particles (c), fragments (d).

When focused on the treated (drinking) water samples, our study revealed no microplastics bigger than 100 μm and only a minimum content of MPs ranging from 50 to 100 μm was observed. The prevailing size category was again 1–5 μm, comprising approximately 25–60% of the microplastics. The second most abundant size group was that of 5–10 μm (around 30–50% of MPs). The number of MPs in each size class is depicted in Fig. 2b.

Similar to the raw water samples, unidentified particles <1 μm occurred also in treated water, though their abundance was lower (27–230 particles L^{-1}, depending on the WTP and sampling day).

In general, the content of microplastics within different size categories was by 45–100% lower in the treated water samples than in the raw water samples. MPs > 50 μm seem to be almost completely removed from water at the treatment plants. The lowest difference in MPs abundance between raw and treated water (45–51%, depending on the sampling day) was observed at WTP2 (size class 10–50 μm) and it exceeded 60% in all the other cases.

Regarding the shape of microplastics, fragments were by far the most abundant morphotype in the raw water supplying WTP1 and WTP2 (fragments comprised 71–76%, depending on the WTP and sampling day). WTP3 raw water contained fragments in substantial amounts as well (42–48%), but the proportion of fibres was also important (37–61%). Shape distribution of MPs in raw water is depicted in Fig. 3a. Plastic fragments in water are expected to originate from a breakdown of various plastic products including e.g. packaging materials or from cosmetics and cleaning media (Zhang et al., 2015; Di and Wang, 2018). A source of plastic fibres in water environments is often discharge from washing machines, transported through sewage waters (Browne et al., 2011).

A similar trend in the predominant morphotype distribution as in raw water is observable also in the case of treated water, despite the

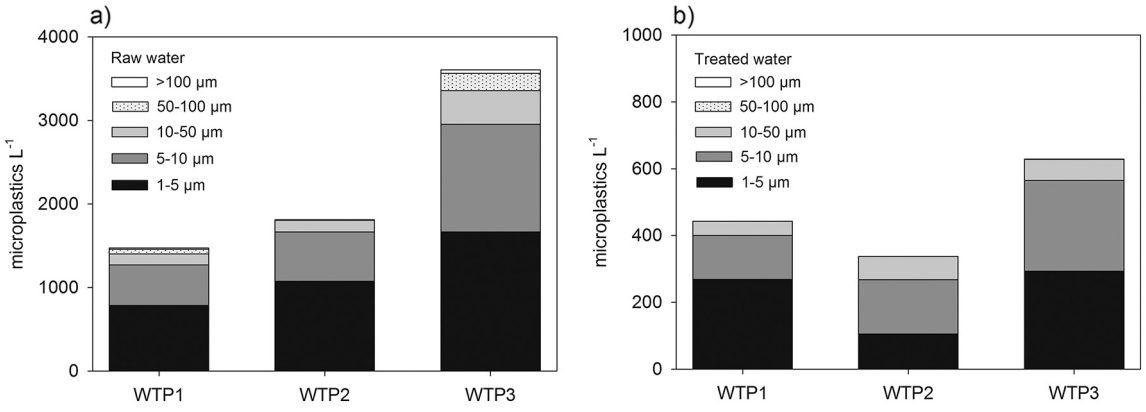

Fig. 2. Size distribution of microplastics detected in raw (a) and treated water (b) at water treatment plants 1 (WTP1), 2 (WTP2) and 3 (WTP3).

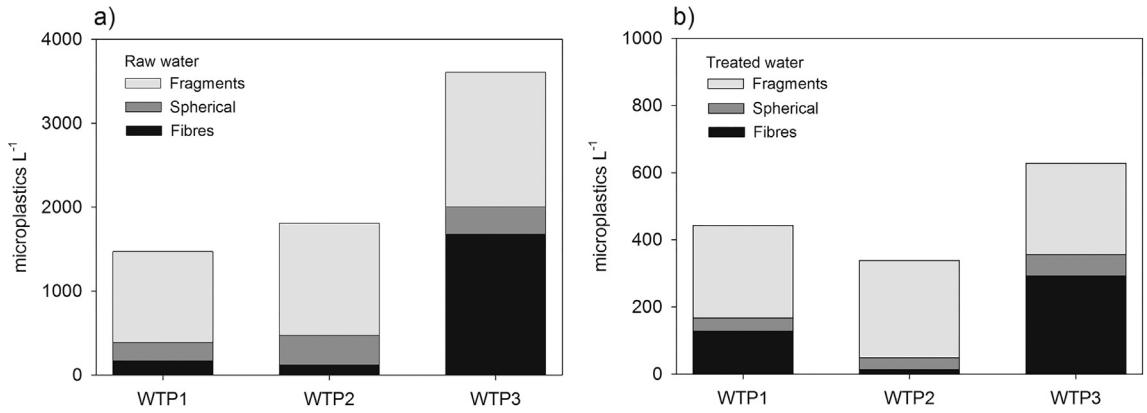

Fig. 3. Proportions of different microplastic shapes in raw (a) and treated water (b) at water treatment plants 1 (WTP1), 2 (WTP2) and 3 (WTP3).

total number of microplastics being much lower than in the raw water samples in all the cases (Fig. 3b). However, a relative increase in the proportion of fibres to the exclusion of fragments appeared in WTP1 treated water, possibly related to the low removal of fibres – only around 25% of them were eliminated at WTP1, compared to approximately 80–90% at both WTP2 and WTP3. These results suggest that there might be some relationship between the shape of microplastics and their removability by various water treatment technologies.

Finally, spherical particles were always the least abundant in both raw and treated water, comprising between 7 and 20% of total particle count.

3.3. Qualitative analysis

In general, 12 different plastic materials forming the MPs were identified by analysing the Al_2O_3 filters. The composition of microplastics found in the raw water samples is depicted in Fig. 4a. Polyethylene terephthalate (PET) particles were the most common in all the samples, comprising on average 60, 68 and 27% of MPs at WTP1, WTP2 and WTP3, respectively. Also polypropylene (PP) particles were rather abundant in water of all the treatment plants (16–26%). In case of WTP3, polyethylene (PE) comprised a substantial portion of MPs (24%), however, PE was not detected in WTP1 and WTP2 raw water. The presence of these plastics is attributable to their widespread usage. PET is utilized in clothing and also serves as a material for disposable beverage containers (Kuczenski and Geyer, 2010). PP also has a wide usage, including for example food packaging, automotive parts or pipes. PE serves as a material for food or cosmetics containers, various houseware, bags, toys, agricultural or food packaging films, etc. (PlasticsEurope, 2018). Further, some other plastic materials were found to be present in the raw water samples in smaller amounts (<10%). Within these, polystyrene (PS) and polyacrylamide (PAM) occurred at all the WTPs, polybutylacrylate (PBA) was detected at WTP2 and WTP3 and polyvinylchloride (PVC) at WTP1 and WTP2. Additionally, polyoxybenzylmethyleneglycolanhydride (recognized as Bakelite), poly(methyl methacrylate) (PMMA), *p* phenylene terephthalamide (PPTA) and polytrimethylene terephthalate (PTT) were determined in the samples from WTP3, accounting for 2, 6, 5 and 5%, respectively. Interestingly, di(2 ethylhexyl) phthalate (DEHP) was detected in the source water supplying WTP3. This substance (widely used as plasticizer) is known to be a reproductive and developmental toxicant in animals (Kavlock et al., 2002).

Within the treated water samples (Fig. 4b), PET was again the prevailing material, (accounting for 41, 62 and 26% of MPs at WTP1, WTP2 and WTP3, respectively), followed by PP (16–33%). Also PAM was detected in treated water of all three WTPs. It can be speculated that the obvious increase in PAM content in WTP1 treated water is associated to the usage of polyacrylamide containing coagulant. Nevertheless, it was beyond the scope of this study to exactly determine the origin of detected MPs. Next, small amounts (<5%) of

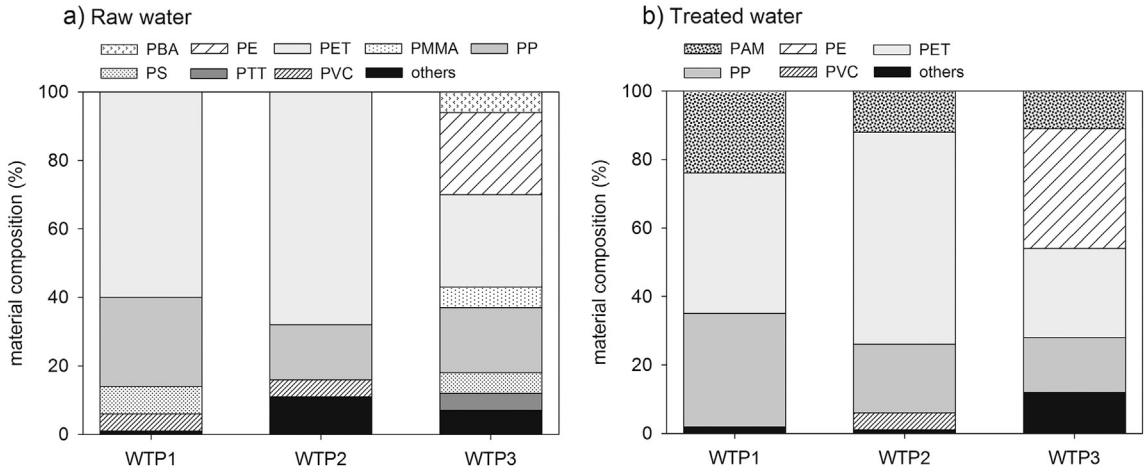

Fig. 4. Material composition of microplastic particles in raw (a) and treated (b) water at water treatment plants 1 (WTP1), 2 (WTP2) and 3 (WTP3); PAM – polyacrylamide, PBA – polybutylacrylate, PE – polyethylene, PET – polyethylene terephthalate, PMMA – poly(methyl methacrylate), PP – polypropylene, PS – polystyrene, PTT – polytrimethylene terephthalate, PVC – polyvinylchloride, others – other plastic materials individually comprising <5%.

Table 2
Comparison of our results on microplastic abundance with other studies.

Sample source	Size range of analysed particles	Microplastic abundance (particles L^{-1})		Reference
		Mean	Range	
Yangtze Estuary	>500 μm	4.165 ± 2.460	0.500–10.200	Zhao et al., 2014
Three Gorges Reservoir	48 μm–5 mm	4.703 ± 2.816	1.597–12.611	Di and Wang, 2018
Taihu Lake	5 μm–5 mm	–	3.4–25.8	Su et al., 2016
Amsterdam canal water	>10 μm	–	48–187	Leslie et al., 2017
Mineral water from returnable plastic bottles	>5 μm	118 ± 88	28–241	Schymanski et al., 2018
Mineral water from single-use bottles	>5 μm	14 ± 14	2–44	Schymanski et al., 2018
Mineral water from glass bottles	>5 μm	50 ± 52	4–156	Schymanski et al., 2018
Mineral water from beverage cartons	>5 μm	11 ± 8	5–20	Schymanski et al., 2018
Mineral water from single-use PET bottles	>1 μm	2649 ± 2857	90–9311	Oßmann et al., 2018
Mineral water from reusable PET bottles	>1 μm	4889 ± 5432	0–11,301	Oßmann et al., 2018
Mineral water from glass bottles	>1 μm	6292 ± 10,521	813–35,462	Oßmann et al., 2018
WTP1 raw water	>1 μm	1473 ± 34	1383–1575	This study
WTP1 treated water	>1 μm	443 ± 10	369–485	This study
WTP2 raw water	>1 μm	1812 ± 35	1648–2040	This study
WTP2 treated water	>1 μm	338 ± 76	243–466	This study
WTP3 raw water	>1 μm	3605 ± 497	3123–4464	This study
WTP3 treated water	>1 μm	628 ± 28	562–684	This study

WTP – water treatment plant.

PVC were found at WTP1 and WTP2 and of PBA at WTP2 and WTP3. Several other plastic materials occurred in WTP3 treated water, including PE (35%) and a small percentage (<5%) of PPTA, PTT and polyoxybenzylmethyleneglycolanhydride.

Examples of FTIR and Raman spectra of selected samples and their comparison to reference material spectra are shown in Fig. S3, Supplementary data. Additionally, elemental microanalysis of selected particles was performed to provide more information on their composition (see Supplementary data, Section S2, Figs. S4 and S5). While microplastics comprised predominantly of carbon and oxygen, sometimes with a contribution of fluorine or chlorine, significant content of other elements indicated non-plastic origin of the particles, such as silicon, aluminium, calcium and magnesium in case of glass fibres.

3.4. Comparison with other studies

Recently, the presence of microplastics in surface waters has gained considerable attention. However, the sampling methods significantly vary – while some authors quantify buoyant MPs from surface water layers as their number per km^2 (Free et al., 2014; Su et al., 2016; Anderson et al., 2017), others determine the content of particles per water volume (Su et al., 2016; Leslie et al., 2017; Di and Wang, 2018). Results of studies that deal with MPs in freshwater and quantify them in sample volume and are therefore to some extent comparable to our results are presented in Table 2. However, none of the studies dealing with natural waters analyse particles as small as in our study. As our results revealed that most of the particles are smaller than 10 μm, it is not surprising that MP content determined in our samples is much higher compared to the other studies (Zhao et al., 2014; Su et al., 2016; Di and Wang, 2018). By contrast, results in the same order of magnitude as in our raw water samples were obtained by Oßmann et al. (2018) who investigated MPs abundance in bottled mineral waters. It is likely due to the fact that they also determined microplastics down to the size of 1 μm. They reported the content of 2649 ± 2857 MPs L^{-1} in water from single use PET bottles, 4889 ± 5432 MPs L^{-1} in water from reusable PET bottles and 6292 ± 10,521 MPs L^{-1} in glass bottled water. Nevertheless, a possible release of MPs from the packaging materials might be responsible for an unknown proportion of the total MPs count ascertained by Oßmann et al. (2018), thus our results for treated drinking water are not well comparable. Schymanski et al. (2018) also measured the content of microplastics in packed mineral waters. They reported MPs abundance ranging from 11 ± 8 to 118 ± 88 L^{-1}, depending on the package material. Such lower numbers compared to the study by Oßmann et al. (2018) might be ascribed to the different size range of analysed particles. While Schymanski et al. (2018) determined MPs > 5 μm, Oßmann et al. (2018) measured MPs down to the size of 1 μm and reported that over 90% of the MPs were smaller than 5 μm. This corresponds with our finding that up to 95% of MPs were smaller than 10 μm and also points out to the difficult comparability of recent studies.

4. Conclusions

The content and characteristics of microplastics present in freshwaters supplying three different water treatment plants and in their treated water was determined. The average number of MPs in raw water ranged from 1473 ± 34 to 3605 ± 497 particles L^{-1}. Generally, the content of microplastics was significantly lower in treated compared to raw water (by 83% on average). However, the concentrations of MPs in treated water (from 338 ± 76 to 628 ± 28 L^{-1}) are not negligible and imply that the potable water might be an important source of microplastics to humans. Interestingly, most of the MPs (up to 95%) were within the size range of 1–10 μm, while such small MPs have been rarely quantified so far. Additionally, the smallest MPs were least removed at the treatment plants. Among the three morphotypes distinguished in our study, fragments predominated at WTP1 and WTP2, while fibres + fragments comprised majority of the MPs at WTP3. Most of the microplastics (>70%) composed of PET and PP in case of WTP1 and WTP2 and of PET, PP and PE at WTP3, while the main materials were the same in both raw and treated water. Further research should focus on the determination of small-sized MPs (<10 μm) in freshwater ecosystems in order to provide better insight into their sources and routes to potable water.

Acknowledgements

This work was supported by the Czech Science Foundation, Czech Republic [grant number GA18-14445S]; and by the institutional support of the Czech Academy of Sciences, Czech Republic [RVO: 67985874]. The authors acknowledge the financial assistance on this project.

Appendix A. Supplementary data

Supplementary data to this article can be found online at https://doi.org/10.1016/j.scitotenv.2018.08.102.

References

Anderson, P.J., Warrack, S., Langen, V., Challis, J.K., Hanson, M.L., Rennie, M.D., 2017. Microplastic contamination in Lake Winnipeg, Canada. Environ. Pollut. 225, 223–231. https://doi.org/10.1016/j.envpol.2017.02.072.

Andrary, A.L., 2011. Microplastics in the marine environment. Mar. Pollut. Bull. 62, 1596–1605. https://doi.org/10.1016/j.marpolbul.2011.05.030.
Browne, M.A., Crump, P., Niven, S.J., Teuten, E., Tonkin, A., Galloway, T., Thompson, R., 2011. Accumulation of microplastic on shorelines worldwide: sources and sinks. Environ. Sci. Technol. 45 (21), 9175–9179. https://doi.org/10.1021/es201811s.
Chae, Y., An, Y.-J., 2017. Effects of micro- and nanoplastics on aquatic ecosystems: current research trends and perspectives. Mar. Pollut. Bull. 124, 624–632. https://doi.org/10.1016/j.marpolbul.2017.01.070.
da Costa, J.P., Santos, P.S.M., Duarte, A.C., Rocha-Santos, T., 2016. (Nano)plastics in the environment – sources, fates and effects. Sci. Total Environ. 566–567, 15–26. https://doi.org/10.1016/j.scitotenv.2016.05.041.
Di, M., Wang, J., 2018. Microplastics in surface waters and sediments of the Three Gorges Reservoir, China. Sci. Total Environ. 616–617, 1620–1627. https://doi.org/10.1016/j.scitotenv.2017.10.150.
Eerkes-Medrano, D., Thompson, R.C., Aldridge, D.C., 2015. Microplastics in freshwater systems: a review of the emerging threats, identification of knowledge gaps and prioritisation of research needs. Water Res. 75, 63–82. https://doi.org/10.1016/j.watres.2015.02.012.
Free, C.M., Jensen, O.P., Mason, S.A., Eriksen, M., Williamson, N.J., Boldgiv, B., 2014. High-levels of microplastic pollution in a large, remote, mountain lake. Mar. Pollut. Bull. 85, 156–163. https://doi.org/10.1016/j.marpolbul.2014.06.001.
Hahladakis, J.N., Velis, C.A., Weber, R., Iacovidou, E., Purnell, P., 2018. An overview of chemical additives present in plastics: migration, release, fate and environmental impact during their use, disposal and recycling. J. Hazard. Mater. 344, 179–199. https://doi.org/10.1016/j.jhazmat.2017.10.014.
Kavlock, R., Boeckelheide, K., Chapin, R., Cunningham, M., Faustman, E., Foster, P., Golub, M., Henderson, R., Hingerg, I., Little, R., Seed, J., Shea, K., Tabacova, S., Tyl, R., Williams, P., Zacharewski, T., 2002. NTP Center for the Evaluation of Risks to Human Reproduction: phthalates expert panel report on the reproductive and developmental toxicity of di(2 ethylhexyl) phthalate. Reprod. Toxicol. 16, 529–653. https://doi.org/10.1016/S0890-6238(02)00033-3.
Koelmans, A.A., Besseling, E., Shim, W.J., 2015. Nanoplastics in the Aquatic Environment. Critical Review Marine Anthropogenic Litter. Springer International Publishing, pp. 325–340 https://doi.org/10.1007/978-3-319-16510-3_12.
Kuczenski, B., Geyer, R., 2010. Material flow analysis of polyethylene terephthalate in the US, 1996–2007. Resour. Conserv. Recycl. 54, 1161–1169. https://doi.org/10.1016/j.resconrec.2010.03.013.
Lei, L., Liu, M., Song, Y., Lu, S., Hu, J., Cao, C., Xie, B., Shi, H., He, D., 2018a. Polystyrene (nano)microplastics cause size-dependent neurotoxicity, oxidative damage and other adverse effects in *Caenorhabditis elegans*. Environ. Sci.: Nano https://doi.org/10.1039/C8EN00412A (in press).
Lei, L., Wu, S., Lu, S., Liu, M., Song, Y., Fu, Z., Shi, H., Raley-Susman, K.M., He, D., 2018b. Microplastic particles cause intestinal damage and other adverse effects in zebrafish *Danio rerio* and nematode *Caenorhabditis elegans*. Sci. Total Environ. 619-620, 1–8. https://doi.org/10.1016/j.scitotenv.2017.11.103.
Leslie, H.A., Brandsma, S.H., van Velzen, M.J.M., Vethaak, A.D., 2017. Microplastics en route: field measurements in the Dutch river delta and Amsterdam canals, wastewater treatment plants, North Sea sediments and biota. Environ. Int. 101, 133–142. https://doi.org/10.1016/j.envint.2017.01.018.
Liebezeit, G., Liebezeit, E., 2014. Synthetic particles as contaminants in German beers. Food Addit. Contam., Part A 31 (9), 1574–1578. https://doi.org/10.1080/19440049.2014.945099.
Mason, S.A., Garneau, D., Sutton, R., Chu, Y., Ehmann, K., Barnes, J., Fink, P., Papazissimos, D., Rogers, D.L., 2016. Microplastic pollution is widely detected in US municipal wastewater treatment plant effluent. Environ. Pollut. 218, 1045–1054. https://doi.org/10.1016/j.envpol.2016.08.056.
Mintenig, S.M., Int-Veen, I., Löder, M.G.J., Primpke, S., Gerdts, G., 2017. Identification of microplastic in effluents of waste water treatment plants using focal plane array-based micro-Fourier-transform infrared imaging. Water Res. 108, 365–372. https://doi.org/10.1016/j.watres.2016.11.015.
Morrison, D.F., 1990. Multivariate Statistical Methods. 3rd edition. McGraw-Hill Inc.
Oßmann, B.E., Sarau, G., Holtmannspötter, H., Pischetsrieder, M., Christiansen, S.H., Dicke, W., 2018. Small-sized microplastics and pigmented particles in bottled mineral water. Water Res. 141, 307–316. https://doi.org/10.1016/j.watres.2018.05.027.
PlasticsEurope, 2018. Plastics – the Facts 2017. An analysis of European plastics production, demand and waste data. www.plasticseurope.org.
Schymanski, D., Goldbeck, C., Humpf, H.-U., Fürst, P., 2018. Analysis of microplastic in water by micro-Raman spectroscopy: release of plastic particles from different packaging into mineral water. Water Res. 129, 154–162. https://doi.org/10.1016/j.watres.2017.11.011.
Su, L., Xue, Y., Li, L., Yang, D., Kolandhasamy, P., Li, D., Shi, H., 2016. Microplastics in Taihu Lake, China. Environ. Pollut. 216, 711–719. https://doi.org/10.1016/j.envpol.2016.06.036.
Talvitie, J., Mikola, A., Setälä, O., Heinonen, M., Koistinen, A., 2017. How well is microlitter purified from wastewater? – A detailed study on the stepwise removal of microlitter in a tertiary level wastewater treatment plant. Water Res. 109, 164–172. https://doi.org/10.1016/j.watres.2016.11.046.
Van Cauwenberghe, L., Jenssen, C.R., 2014. Microplastics in bivalves cultured for human consumption. Environ. Pollut. 193, 65–70. https://doi.org/10.1016/j.envpol.2014.06.010.
Yang, D., Shi, H., Li, L., Li, J., Jabeen, K., Kolandhasamy, P., 2015. Microplastic pollution in table salts from China. Environ. Sci. Technol. 49, 13622–13627. https://doi.org/10.1021/acs.est.5b03163.
Zhang, K., Gong, W., Lv, J., Xiong, X., Wu, C., 2015. Accumulation of floating microplastics behind the Three Gorges Dam. Environ. Pollut. 204, 117–123. https://doi.org/10.1016/j.envpol.2015.04.023.
Zhao, S., Zhu, L., Wang, T., Li, D., 2014. Suspended microplastics in the surface water of the Yangtze Estuary System, China: first observations on occurrence, distribution. Mar. Pollut. Bull. 86, 562–568. https://doi.org/10.1016/j.marpolbul.2014.06.032.

Supplementary Data for

Occurrence of microplastics in raw and treated drinking water

Martin Pivokonsky[a]*, Lenka Cermakova[a,b], Katerina Novotna[a,c], Petra Peer[a], Tomas Cajthaml[b], Vaclav Janda[c]

[a]*Institute of Hydrodynamics of the Czech Academy of Sciences, Pod Patankou 30/5, 16612 Prague 6, Czech Republic*

[b]*Institute for Environmental Studies, Faculty of Science, Charles University, Benatska 2, 12801 Prague 2, Czech Republic*

[c]*Department of Water Technology and Environmental Engineering, Faculty of Environmental Technology, University of Chemistry and Technology, Prague, Technicka 5, 16628 Prague 6, Czech Republic*

*Corresponding author:

Martin Pivokonsky

Tel.: +420 233 109 068; fax +420 233 324 361

E-mail: pivo@ih.cas.cz

This supplementary data contains the following sections, tables and figures:

Fig. S2 The average profiles of individual samples 1, 2 and 3 for raw (a) and treated (b) water for water treatment plant 3 (WTP3) at sampling day 1

Fig. S3 FTIR and Raman spectra of selected microplastic particles and a comparison to a reference library

Fig. S4 Elemental analysis of selected fibres derived from raw and treated water samples: plastic fibres (a,b) and a glass fibre (c); X axis: energy (keV); Y axis: counts per second per electronvolt (cps/eV)

Fig. S5 Elemental analysis of selected plastic particles derived from raw and treated water samples; X axis: energy (keV); Y axis: counts per second per electronvolt (cps/eV)

Fig. S6 SEM images of 0.2 μm (a) and 5 μm (b) PTFE filters

Fig. S7 Elemental analysis of PTFE filter; X axis: energy (keV); Y axis: counts per second per electronvolt (cps/eV)

Table S1 Quality parameters of raw and treated water at water treatment plants 1 (WTP1), 2 (WTP2) and 3 (WTP3) at sampling days within November 2017 – January 2018

	TOC (mg L^{-1})		**DOC (mg L^{-1})**		**COD_{Mn} (mg L^{-1})**		**Turbidity (NTU)**		**Microorganisms (count mL^{-1})**	
	Raw	**Treated**	**Raw**	**Treated**	**Raw**	**Treated**	**Raw**	**Treated**	**Raw**	**Treated**
WTP1										
Day 1	**5.2** ± 0.6	**3.3** ± 0.2	**4.7** ± 0.3	**2.9** ± 0.2	**2.3** ± 0.2	**1.0** ± 0.2	**0.5** ± 0.1	**0.2** ± 0.1	**240** ± 12	**0** ± 0
Day 2	**5.6** ± 0.6	**3.5** ± 0.5	**5.3** ± 0.5	**3.2** ± 0.3	**2.4** ± 0.1	**1.0** ± 0.2	**0.5** ± 0.1	**0.2** ± 0.1	**240** ± 21	**0** ± 0
Day 3	**4.7** ± 0.5	**3.0** ± 0.2	**4.3** ± 0.2	**2.7** ± 0.3	**2.3** ± 0.1	**1.2** ± 0.1	**0.4** ± 0.1	**0.2** ± 0.2	**250** ± 18	**2** ± 2
WTP2										
Day 1	**7.6** ± 0.6	**4.9** ± 0.3	**6.8** ± 0.4	**4.2** ± 0.1	**5.4** ± 0.4	**1.9** ± 0.2	**5.1** ± 0.2	**0.5** ± 0.2	**184** ± 24	**0** ± 0
Day 2	**7.8** ± 0.4	**5.2** ± 0.4	**6.9** ± 0.6	**4.1** ± 0.3	**5.7** ± 0.3	**1.8** ± 0.2	**4.6** ± 0.3	**0.5** ± 0.2	**220** ± 32	**0** ± 0
Day 3	**7.4** ± 0.4	**4.9** ± 0.3	**6.7** ± 0.5	**4.5** ± 0.4	**5.8** ± 0.5	**1.9** ± 0.1	**4.5** ± 0.3	**0.5** ± 0.2	**240** ± 15	**0** ± 0
WTP3										
Day 1	**5.1** ± 0.4	**3.6** ± 0.4	**4.7** ± 0.4	**3.5** ± 0.3	**3.7** ± 0.2	**0.5** ± 0.1	**7.9** ± 0.4	**0.3** ± 0.1	**2280** ± 61	**0** ± 0
Day 2	**5.5** ± 0.3	**2.1** ± 0.2	**4.8** ± 0.6	**2.0** ± 0.3	**6.1** ± 0.5	**1.0** ± 0.1	**36.9** ± 0.7	**1.4** ± 0.1	**2040** ± 48	**0** ± 0
Day 3	**4.9** ± 0.3	**3.4** ± 0.5	**4.5** ± 0.4	**3.2** ± 0.2	**4.2** ± 0.3	**1.1** ± 0.1	**8.2** ± 0.3	**0.8** ± 0.1	**2170** ± 73	**0** ± 0

TOC – Total Organic Carbon; DOC – Dissolved Organic Carbon; COD – Chemical Oxygen Demand

Table S2 Microplastic content in raw and treated water samples at water treatment plant 1 (WTP1, Day 1) based on individual cut-out data

WTP1, Day 1

FIBRES				SPHERICAL				FRAGMENTS			
		Microplastics L^{-1}				Microplastics L^{-1}				Microplastics L^{-1}	
Sample	Cut-out	Raw water > 1 µm	Treated water > 1 µm	Sample	Cut-out	Raw water > 1 µm	Treated water > 1 µm	Sample	Cut-out	Raw water > 1 µm	Treated water > 1 µm
	a	132	82		*a*	235	28		*a*	1116	277
1	*b*	118	73	1	*b*	217	33	1	*b*	1072	237
	c	157	118		*c*	258	33		*c*	967	226
cut-out average		**136 ± 18**	**91 ± 24**	**cut-out average**		**237 ± 21**	**31 ± 3**	**cut-out average**		**1052 ± 76**	**246 ± 29**
	a	174	139		*a*	218	55		*a*	859	296
2	*b*	158	132	2	*b*	171	46	2	*b*	1201	255
	c	216	174		*c*	213	28		*c*	938	293
cut-out average		**183 ± 30**	**148 ± 23**	**cut-out average**		**201 ± 26**	**43 ± 14**	**cut-out average**		**999 ± 179**	**381 ± 23**
	a	226	115		*a*	207	38		*a*	1082	279
3	*b*	178	142	3	*b*	207	34	3	*b*	1200	263
	c	156	164		*c*	210	42		*c*	1039	301
cut-out average		**187 ± 36**	**140 ± 25**	**cut-out average**		**208 ± 2**	**38 ± 4**	**cut-out average**		**1107 ± 83**	**281 ± 19**
sample average		**168 ± 35**	**126 ± 34**	**sample average**		**215 ± 23**	**37 ± 9**	**sample average**		**1053 ± 116**	**270 ± 26**

Table S3 Microplastic content in raw and treated water samples at water treatment plant 2 (WTP2, Day 1) based on individual cut-out data

WTP2, Day 1

FIBRES				SPHERICAL				FRAGMENTS			
		Microplastics L^{-1}				Microplastics L^{-1}				Microplastics L^{-1}	
Sample	Cut-out	Raw water > 1 µm	Treated water > 1 µm	Sample	Cut-out	Raw water > 1 µm	Treated water > 1 µm	Sample	Cut-out	Raw water > 1 µm	Treated water > 1 µm
	a	79	18		*a*	456	54		*a*	1405	330
1	*b*	62	11	1	*b*	499	37	1	*b*	1037	322
	c	65	7		*c*	324	44		*c*	1456	315
cut-out average		**69 ± 9**	**12 ± 6**	**cut-out average**		**426 ± 91**	**45 ± 9**	**cut-out average**		**1299 ± 229**	**322 ± 8**
	a	182	12		*a*	316	55		*a*	1725	351
2	*b*	169	15	2	*b*	319	45	2	*b*	1384	397
	c	172	24		*c*	391	52		*c*	1461	448
cut-out average		**174 ± 7**	**17 ± 6**	**cut-out average**		**342 ± 42**	**51 ± 5**	**cut-out average**		**1523 ± 179**	**399 ± 49**
	a	118	6		*a*	231	27		*a*	1318	329
3	*b*	68	6	3	*b*	205	34	3	*b*	1327	349
	c	88	12		*c*	329	42		*c*	1281	420
cut-out average		**91 ± 25**	**8 ± 3**	**cut-out average**		**255 ± 65**	**34 ± 8**	**cut-out average**		**1309 ± 24**	**366 ± 48**
sample average		**111 ± 50**	**12 ± 6**	**sample average**		**341 ± 95**	**43 ± 10**	**sample average**		**1377 ± 182**	**362 ± 48**

Table S4 Microplastic content in raw and treated water samples at water treatment plant 3 (WTP3, Day 1) based on individual cut-out data

WTP3, Day 1

FIBRES				SPHERICAL				FRAGMENTS			
		Microplastics L^{-1}				Microplastics L^{-1}				Microplastics L^{-1}	
Sample	Cut-out	Raw water > 1 µm	Treated water > 1 µm	Sample	Cut-out	Raw water > 1 µm	Treated water > 1 µm	Sample	Cut-out	Raw water > 1 µm	Treated water > 1 µm
	a	1340	345		*a*	211	115		*a*	1602	277
1	*b*	1264	328	1	*b*	240	98	1	*b*	1414	260
	c	1449	350		*c*	238	37		*c*	1613	217
cut-out average		**1351 ± 93**	**341 ± 12**	**cut-out average**		**229 ± 16**	**83 ± 41**	**cut-out average**		**1543 ± 112**	**251 ± 31**
	a	1281	274		*a*	242	62		*a*	1762	275
2	*b*	1491	278	2	*b*	319	44	2	*b*	1922	214
	c	1445	314		*c*	270	17		*c*	1787	208
cut-out average		**1405 ± 110**	**289 ± 22**	**cut-out average**		**277 ± 39**	**41 ± 22**	**cut-out average**		**1823 ± 86**	**332 ± 37**
	a	1127	276		*a*	216	69		*a*	2023	203
3	*b*	1232	226	3	*b*	263	60	3	*b*	1863	289
	c	1301	254		*c*	259	52		*c*	1576	306
cut-out average		**1220 ± 88**	**252 ± 25**	**cut-out average**		**246 ± 26**	**60 ± 9**	**cut-out average**		**1820 ± 226**	**266 ± 55**
sample average		**1325 ± 118**	**294 ± 42**	**sample average**		**251 ± 32**	**61 ± 30**	**sample average**		**1729 ± 193**	**250 ± 39**

S1. Statistical analysis

The homogeneity among samples from individual water treatment plants (WTPs) was assessed.

At first, a profile of each analysed cut-out was created, providing the information on microplastics abundance in distinct shape category (morphotype). An example is shown in Fig. S1 that depicts the profiles of three cut-outs representing one sample of raw water from WTP3. It can be seen that the number of microplastics per litre calculated based on single cut-outs do not differ considerably; the similar profiles demonstrate that the cut-outs sufficiently represent the sample as a whole. The same conclusion can be derived from analysis of all the other samples cut-outs from all the WTPs (data not shown).

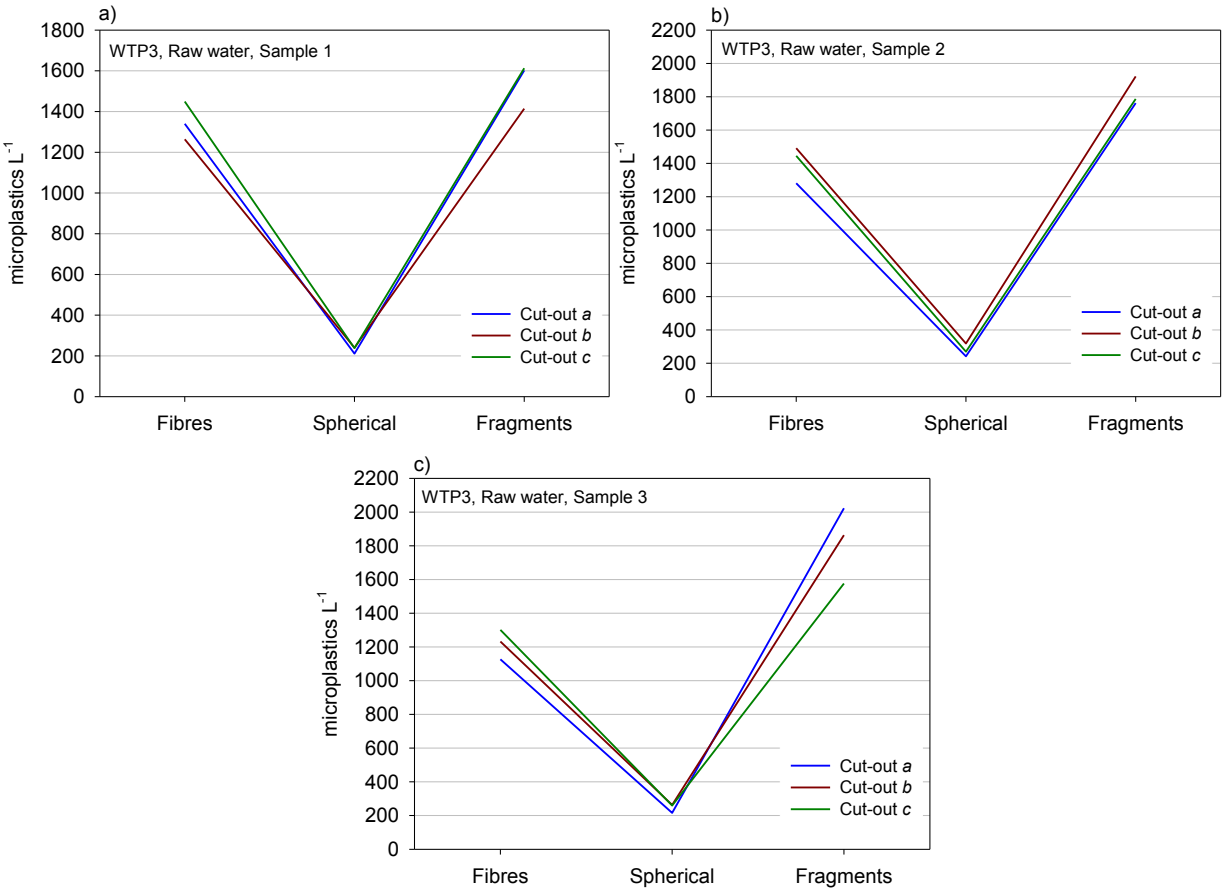

Fig. S1 The profiles of raw water cut-outs *a*, *b* and *c* from sample 1 (panel a), 2 (panel b) and 3 (panel c) for water treatment plant 3 (WTP3) at sampling day 1

Subsequently, the profiles from individual samples collected within one day were aggregated into datasets representing individual WTPs (separately for raw and treated water), an example is shown in Fig. S2. These datasets were used to test the homogeneity of samples applying the profile analysis (Morrison, 1990), while the profileR package from the programming language R was used for the testing. The profile analysis consisted of two steps. Firstly, the hypothesis of *parallel* sample profiles was tested, and secondly, the hypothesis of the *same level* of sample profiles was tested.

The hypothesis of parallel profiles was not rejected in any case (i.e. no *p-value* less than 0.05 was achieved). These results confirm that the shapes of profiles do not vary significantly between individual samples. The hypothesis of same levels was also not rejected in any case (again, no *p-value* less than 0.05 was achieved). Thus, it has shown that the differences between sample profiles for all the WTPs and all the sampling days were insignificant. It can be therefore concluded that the individual samples well represent the content and the distribution of microplastic particles in the water from a given water treatment plant.

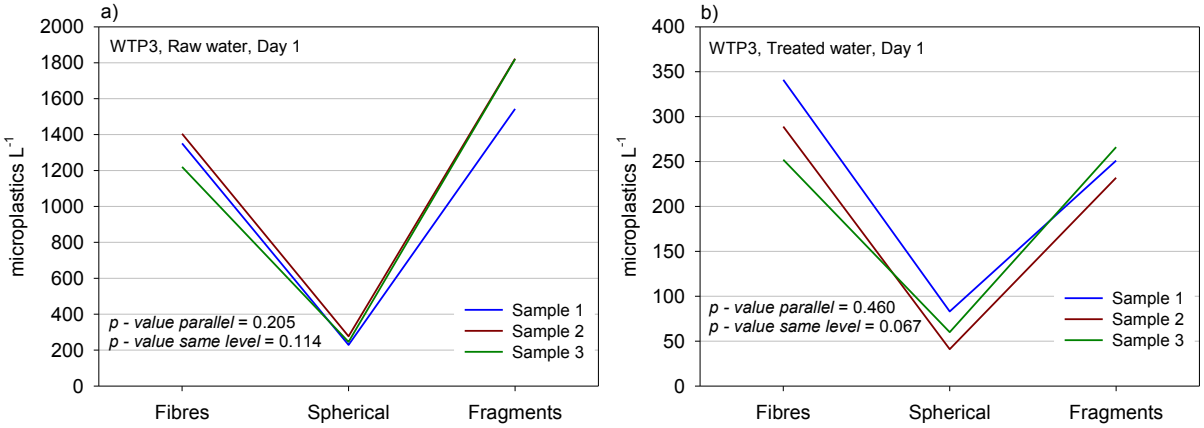

Fig. S2 The average profiles of individual samples 1, 2 and 3 for raw (a) and treated (b) water for water treatment plant 3 (WTP3) at sampling day 1

References:

Morrison, D.F., 1990. Multivariate Statistical Methods. 3rd Edition, McGraw-Hill Inc.

a)

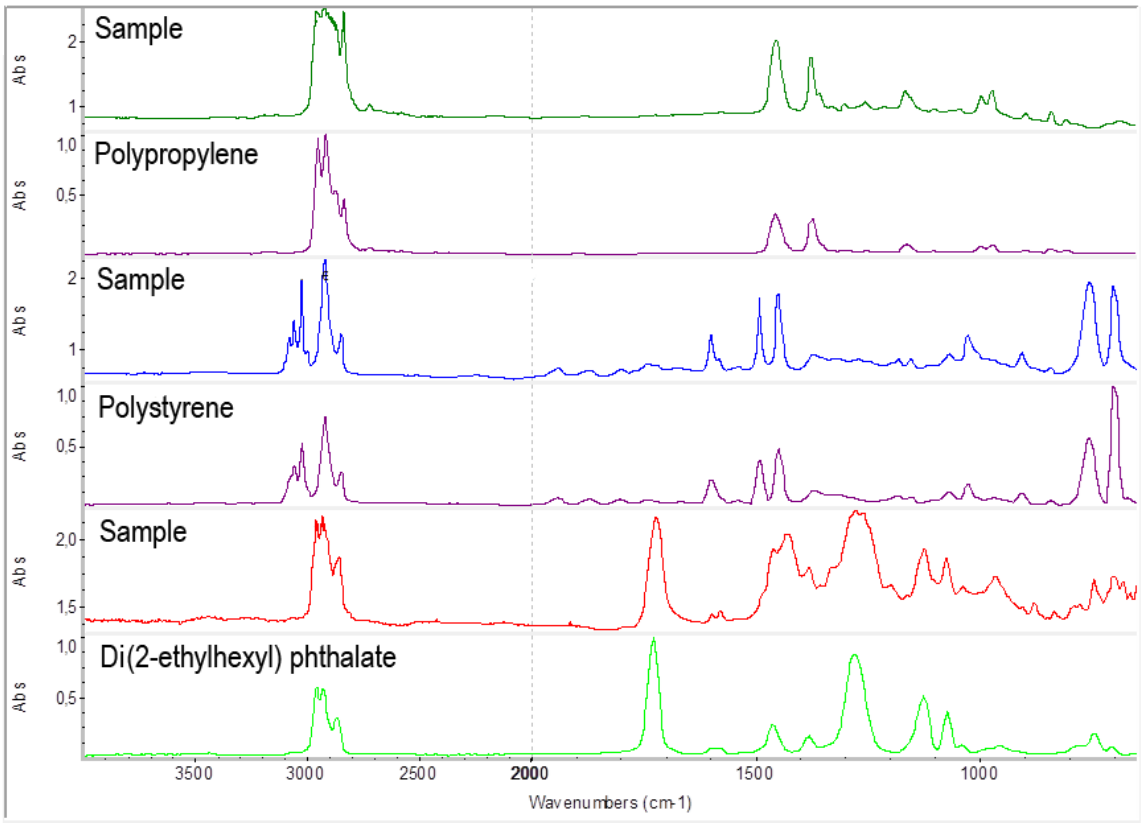
Sample
Polypropylene
Sample
Polystyrene
Sample
Di(2-ethylhexyl) phthalate
Abs
3500
3000
2500
2000
1500
1000
Wavenumbers (cm-1)

b)

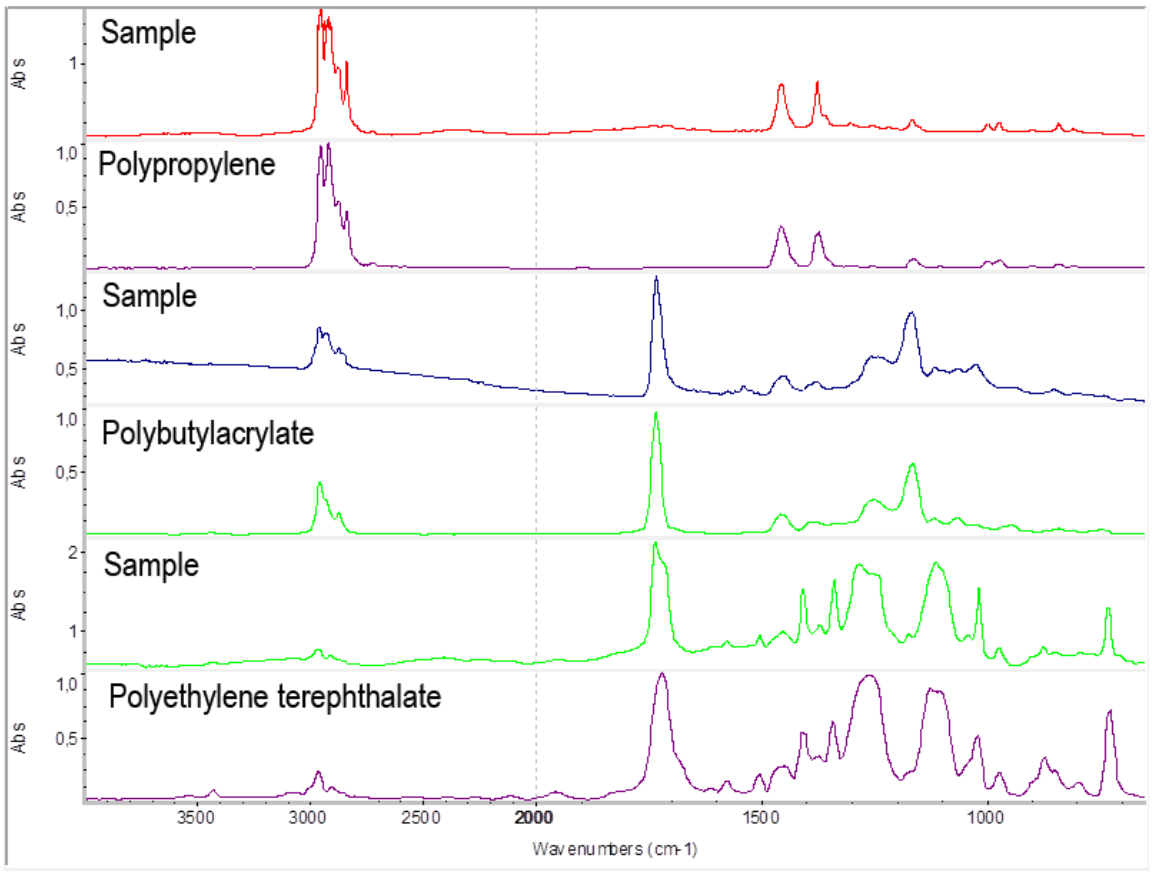
Sample
Polypropylene
Sample
Polybutylacrylate
Sample
Polyethylene terephthalate
Abs
3500
3000
2500
2000
1500
1000
Wavenumbers (cm-1)

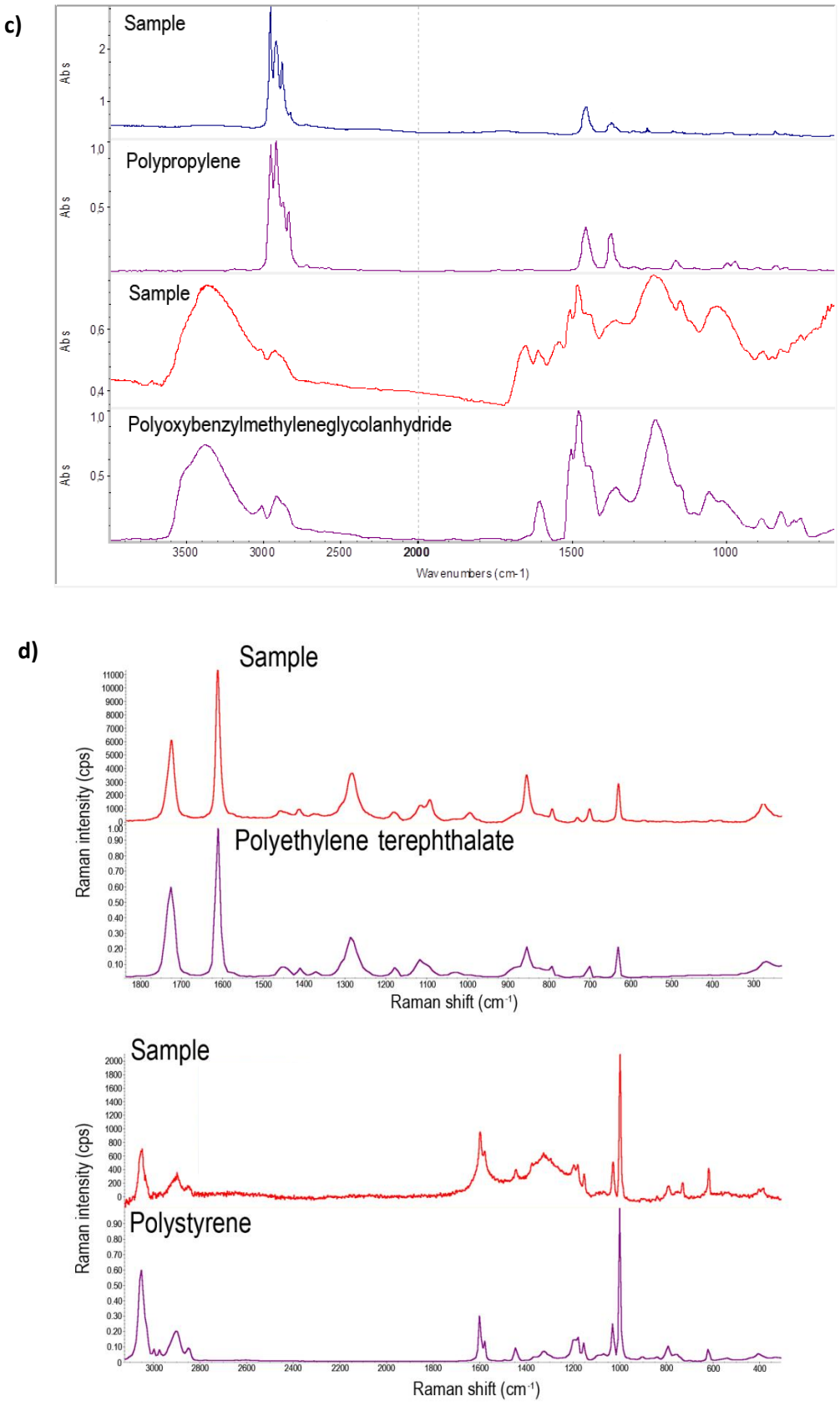

Fig. S3 FTIR and Raman spectra of selected microplastic particles and a comparison to a reference library (a-d)

S2. Elemental analysis of microparticles contained in raw and treated water samples

Elemental analysis of selected microparticles (approximately 30-50 particles from each filter) was conducted in order to provide additional information on their qualitative composition. Elemental microanalysis was performed by using Octane SDD EDX (energy dispersive X-ray) detector (AMETEK, Inc, USA) integrated into the NOVA NanoSEM 450 (FEI Company, USA) operated at 15 kV. Examples of the results are shown in Fig. S4 and Fig. S5. It should be noted that Au was detected in all the samples because gold is added during the analysis procedure.

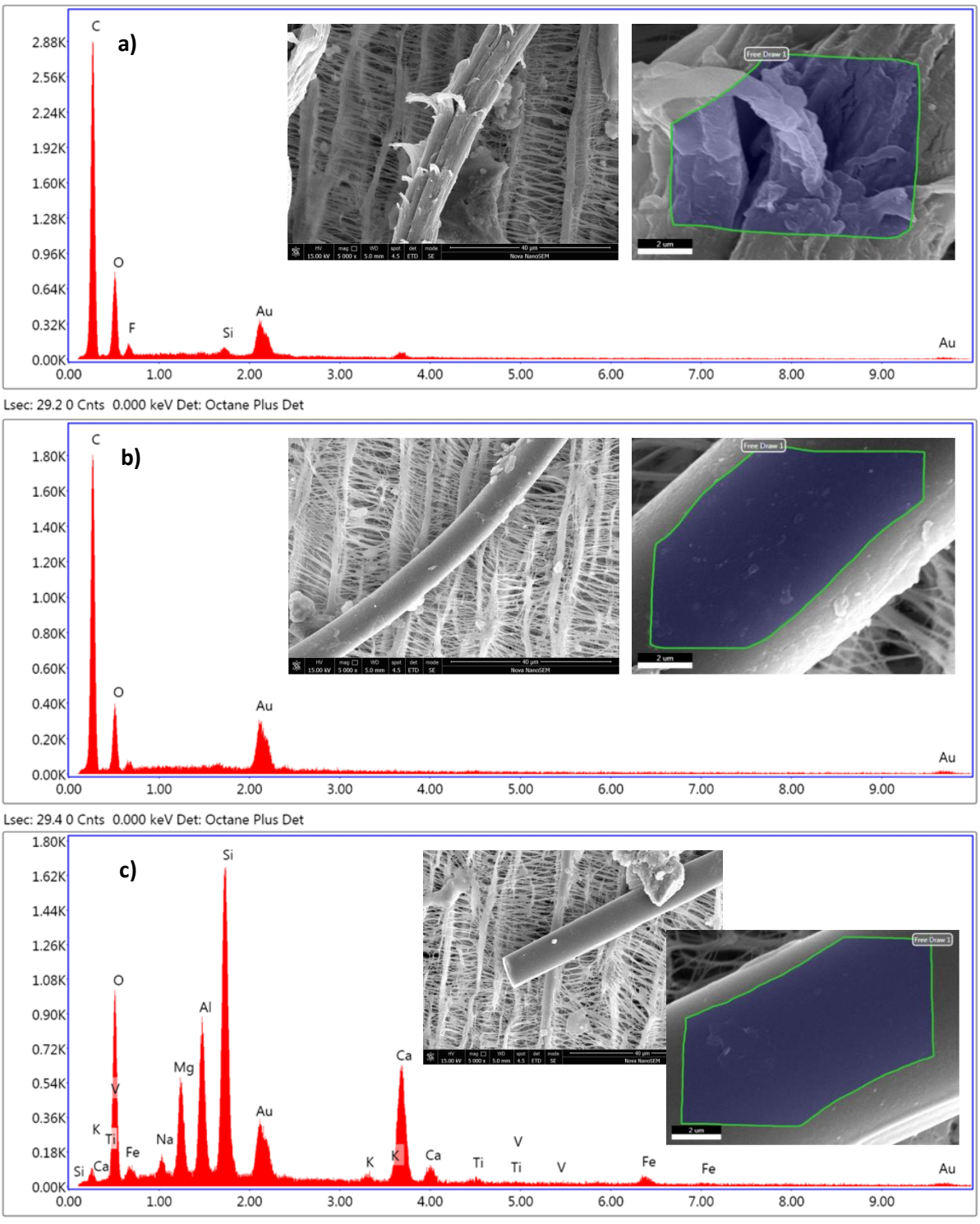

Fig. S4 Elemental analysis of selected fibres derived from raw and treated water samples: plastic fibres (a,b) and a glass fibre (c); X axis: energy (keV); Y axis: counts per second per electronvolt (cps/eV)

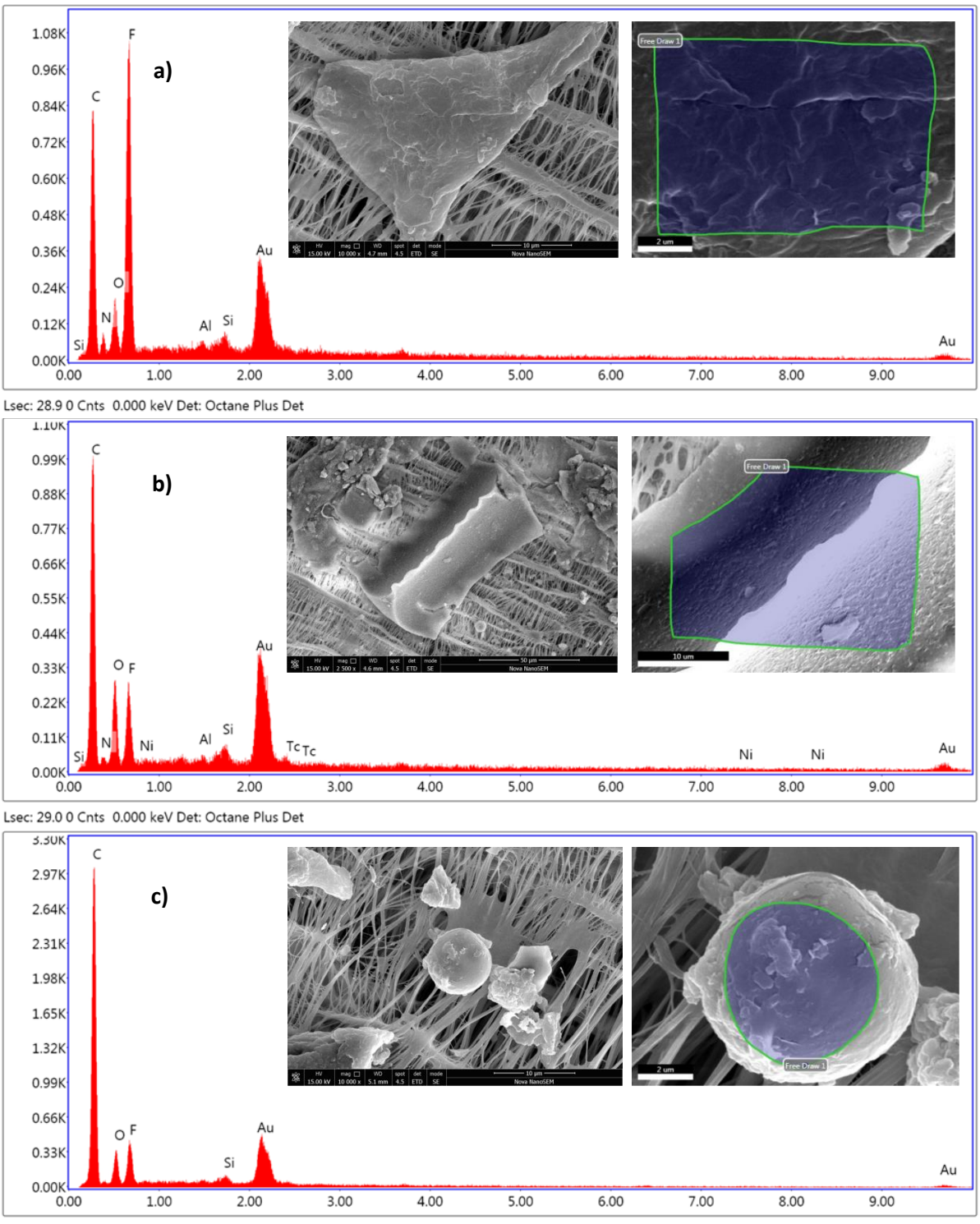

Fig. S5 Elemental analysis of selected plastic particles (a,b,c) derived from raw and treated water samples; X axis: energy (keV); Y axis: counts per second per electronvolt (cps/eV)

S3. Blank filters analysis

Table S5 Quantification of microplastics in blank samples

		Microplastics L^{-1}
Day 1	blank 1	8
	blank 2	6
	blank 3	3
Average Day 1		**6 ± 3**
Day 2	blank 1	10
	blank 2	10
	blank 3	5
Average Day 2		**8 ± 3**
Day 3	blank 1	10
	blank 2	5
	blank 3	13
Average Day 3		**9 ± 4**
Average Day 1, 2, 3		**8 ± 2**

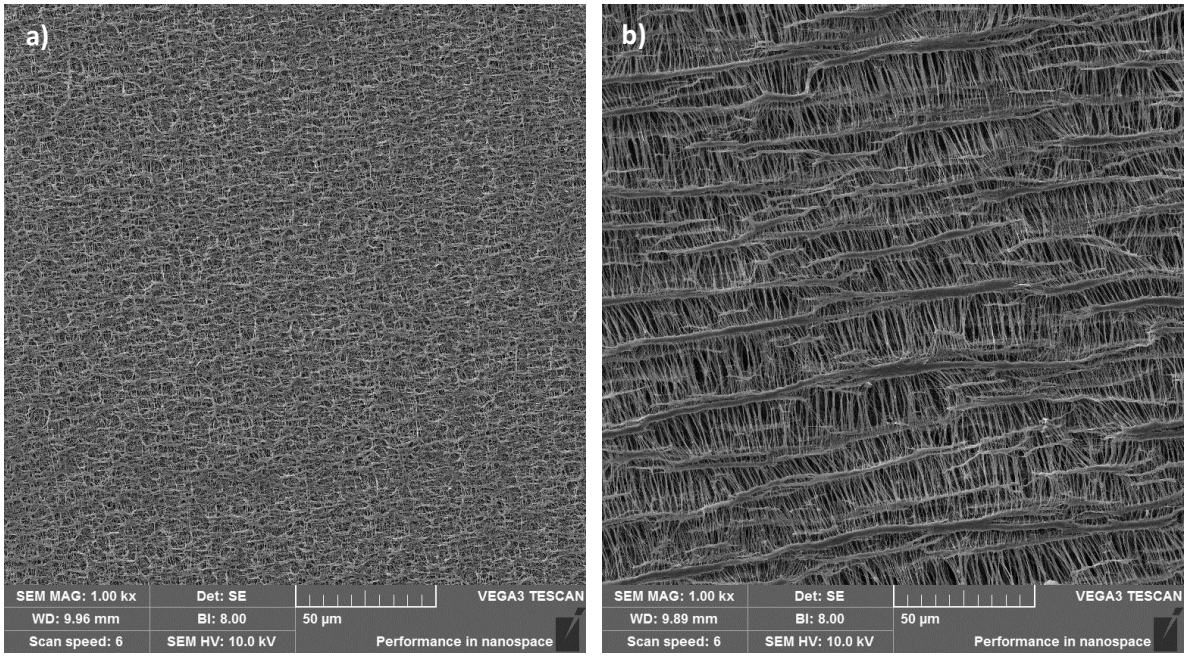

Fig. S6 SEM images of 0.2 µm (a) and 5 µm (b) PTFE filters

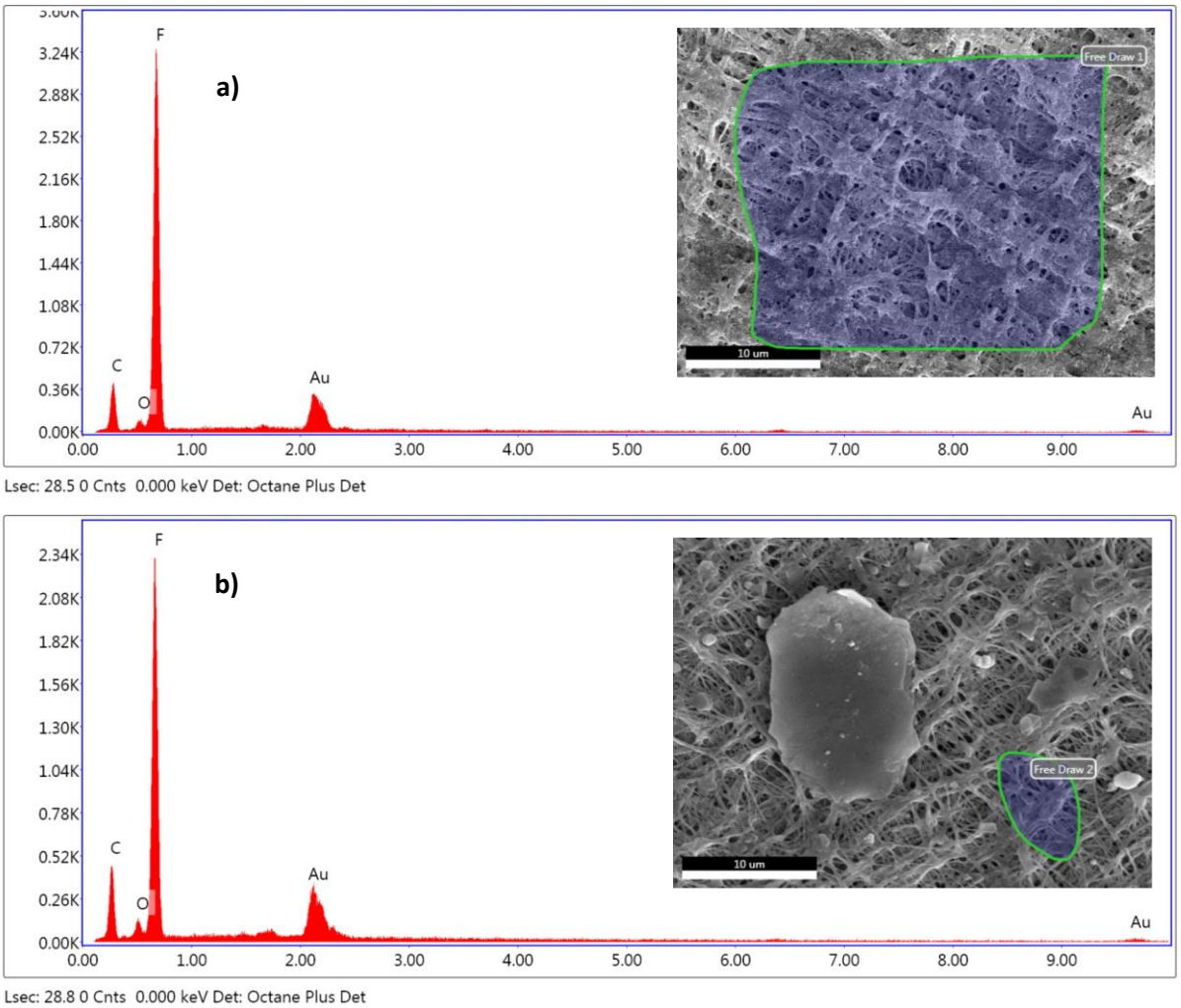

Fig. S7 Elemental analysis of PTFE filter (a,b); X axis: energy (keV); Y axis: counts per second per electronvolt (cps/eV)

PUBLIKACE 9

Microplastics in drinking water treatment – Current knowledge and research needs

Kateřina Novotná, **Lenka Čermáková**, Lenka Pivokonská, Tomáš Cajthaml a Martin Pivokonský

Science of the Total Environment 667 (2019) 730-740
DOI 10.1016/j.scitotenv.2019.02.431

Science of the Total Environment 667 (2019) 730–740

Contents lists available at ScienceDirect

Science of the Total Environment

journal homepage: www.elsevier.com/locate/scitotenv

Review

Microplastics in drinking water treatment – Current knowledge and research needs

Katerina Novotna [a,b], Lenka Cermakova [a,c], Lenka Pivokonska [a], Tomas Cajthaml [c,d], Martin Pivokonsky [a,*]

[a] Institute of Hydrodynamics of the Czech Academy of Sciences, Pod Patankou 30/5, 166 12 Prague 6, Czech Republic
[b] Department of Water Technology and Environmental Engineering, Faculty of Environmental Technology, University of Chemistry and Technology, Prague, Technicka 5, 166 28 Prague 6, Czech Republic
[c] Institute for Environmental Studies, Faculty of Science, Charles University, Benatska 2, 128 01 Prague 2, Czech Republic
[d] Institute of Microbiology of the Czech Academy of Sciences, Videnska 1083, 142 20 Prague 4, Czech Republic

HIGHLIGHTS

- Microplastics (MPs) are being detected in freshwaters and also in drinking water.
- Drinking water treatment plants pose a barrier for MPs to enter drinking water.
- Conventional treatment processes have a potential to remove a part of microplastics.
- Efficiency of distinct treatment steps versus MPs character should be understood.
- Regarding water treatment, special focus should be put on small-sized MPs (< 10 μm).

GRAPHICAL ABSTRACT

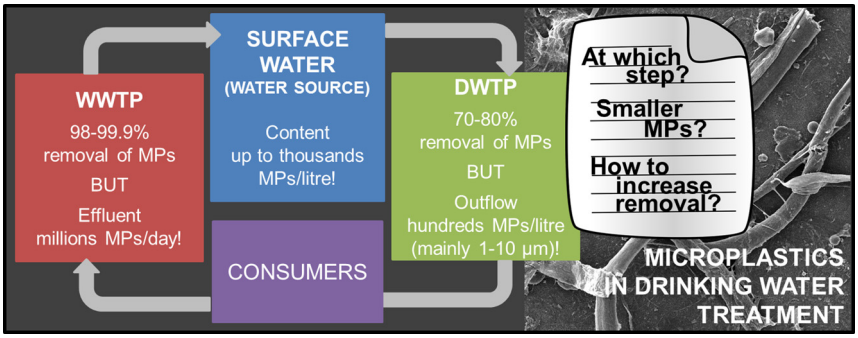

ARTICLE INFO

Article history:
Received 30 January 2019
Received in revised form 27 February 2019
Accepted 27 February 2019
Available online 28 February 2019

Editor: Damia Barcelo

Keywords:
Coagulation
Drinking water treatment
Microplastics
Potable water
Wastewater

ABSTRACT

Microplastics (MPs) have recently been detected in oceans, seas and freshwater bodies worldwide, yet few studies have revealed the occurrence of MPs in potable water. Although the potential toxicological effects of MPs are still largely unknown, their presence in water intended for human consumption deserves attention. Drinking water treatment plants (DWTPs) pose a barrier for MPs to enter drinking water; thus, the fate of MPs at DWTPs is of great interest. This review includes a summary of the available information on MPs in drinking water sources and in potable water, discusses the current knowledge on MP removal by different water treatment processes, and identifies the research needs regarding MP removal by DWTP technologies. A comparison of MPs with other common pollution agents is also provided. We concluded that special attention should be given to small-size MPs (in the range of several micrometres) and that the relationship between MP character and behaviour during distinct treatment processes should be explored.

* Corresponding author.
E-mail address: pivo@ih.cas.cz (M. Pivokonsky).

https://doi.org/10.1016/j.scitotenv.2019.02.431
0048-9697/

Contents

1. Introduction

Currently, microplastics (MPs) are emerging globally distributed pollutants that receive considerable attention, both from research communities and the public audience. MPs are defined as plastic particles not exceeding a 5 mm size limit (Andrary, 2011; Eerkes-Medrano et al., 2015; Koelmans et al., 2015), while the smallest size classes of plastic particles (<100 nm or <1000 nm, definition is unclear) are instead referred to as nanoplastics (NPs) (Koelmans et al., 2015; da Costa et al., 2016; Hahladakis et al., 2018). Contrary to NPs that thus far have been almost impossible to credibly identify in natural matrices, there are numerous studies on MP abundance in the environment. Regarding aquatic environments, much more effort has been put into investigating seas and oceans compared to freshwater, and despite significant abundance variations, MPs have been detected in marine waters worldwide (Cole et al., 2011; Auta et al., 2017). Nevertheless, freshwater bodies are the predominant drinking water sources for human consumption and are therefore suspect as potential sources of MPs to humans. Some raw water samples from selected drinking water treatment plants (DWTPs) have been already investigated for MPs and their presence was confirmed (Pivokonsky et al., 2018; Mintenig et al., 2019), with MPs reaching up to >4000 items per litre (Pivokonsky et al., 2018). MPs have also been reported as present in lakes, rivers and dams globally (Dris et al., 2015; Su et al., 2016; Anderson et al., 2017; Leslie et al., 2017; Di and Wang, 2018; Triebskorn et al., 2019), even in remote areas (Free et al., 2014; Waller et al., 2017; Green et al., 2018). Thus, DWTPs seemingly have to face the presence of a "new" polluting agent – MPs, at least in some areas.

Notably, the risk associated with toxicological effects of MPs (and NPs) is still not fully described. Numerous studies have investigated these pollutant effects on (predominantly aquatic) organisms and some negative impacts have been observed (de Sá et al., 2018; Triebskorn et al., 2019); however, the tested MP concentrations often greatly exceeded the values currently detected in nature, as reported by Triebskorn et al. (2019). Nonetheless, considering the growing production of plastics (Plastics Europe, 2018), increasing environmental concentrations of MPs may be expected. Recently, some sporadic studies on microplastic interactions with human cells have also been conducted. In vitro experiments by Schirinzi et al. (2017) revealed that MPs (mainly 10 μm polystyrene, accompanied by 40–250 nm NPs) induced oxidative stress to human cerebral and epithelial cells. Triebskorn et al. (2019) reported observing MPs (polystyrene, 0.25 ± 0.06 μm) taken up by human keratinocytes. Another concern may be a possible synergism with hydrophobic organic pollutants that tend to adsorb onto MPs and may be subsequently transferred to respective organs and tissues at elevated concentrations (F. Wang et al., 2018). Although the possible effects of chronical exposure to MPs on human health are still more of a subject of discussion (and future research) than a clearly defined issue (Barboza et al., 2018; Revel et al., 2018), the presence of MPs in potable water should not be neglected.

The aim of this review paper is (1) to summarize and discuss the available information on microplastics in drinking water sources, (2) to encapsulate the evidence regarding MPs in potable water and (3) to provide insight into a current overview of MP removal by water treatment processes, including comparison to other common pollutants. This research also leads us (4) to identify research gaps and needs in the field of microplastics versus drinking water sources and treatment.

2. MPs in sources of drinking water and freshwater bodies

To the best of our knowledge, raw water directly from the inlet of DWTPs has only been investigated by two studies (Pivokonsky et al., 2018; Mintenig et al., 2019), one of which dealt with surface water and the other with groundwater. By comparison, there are many more studies on MPs in freshwater bodies, but the research on MPs in groundwater is lacking. An overview of the MPs detected in the above-described water types (measured in bulk water samples) is provided in Table 1. The results of the different studies vary significantly, ranging from zero or very few (<10) to >4000 microplastic particles per litre (Wang et al., 2017; W. Wang et al., 2018; Pivokonsky et al., 2018; Su et al., 2018; Bordós et al., 2019; Luo et al., 2019; Mintenig et al., 2019). Naturally, the differences are related to spatial variations and thus strongly depend on the sampling location. Another reason may be the dissimilarities in sampling, sample preparation and analytical methods among the different studies, including the lower limit of MPs analysed, while the methodologies used for detection of MPs have been extensively discussed (Li et al., 2018a; Silva et al., 2018). The size ranges of microplastics analysed in the different studies are shown in Fig. 1. Since the sizes of MPs analysed and the size classifications varied considerably among studies, a straight comparison of MP abundance in detailed size ranges is impossible. However, the size distribution of MPs clearly skewed towards smaller sizes in some studies, e.g., 81–92% of MPs (>1 μm) were observed to be <10 μm (Pivokonsky et al., 2018), 96% of MPs (>4 μm) to be <20 μm (Triebskorn et al., 2019), 61% of MPs (>10 μm) to be <300 μm (Leslie et al., 2017), >80% of MPs (>50 μm) to be <2000 μm (Wang et al., 2017) or 73% of MPs (>50 μm) to be <500 μm (Yuan et al., 2019). By contrast, a majority of MPs within larger size classes have been observed in some other studies (W. Wang et al., 2018; Di et al., 2019; Luo et al., 2019). Based on these contradictory results, more research including the thorough size categorization of MPs should be performed, as this property may be of great importance with respect to water treatment technologies (Matilainen et al., 2010; Pivokonsky et al., 2011, 2016). Moreover, due to the very high numbers of MPs within the smallest size categories (<10 μm and <20 μm in studies by Pivokonsky et al. (2018) and Triebskorn et al. (2019), respectively) that were not covered by most other studies, more effort should be put into analysing such small particles. However, it is of note that due to the limited resolution of techniques applicable for MP detection, precise determination of MPs in micrometre range is

a big challenge and particular attention should be laid on providing reliable results.

In addition to the abundance and size categorization, most studies reported the different shapes of MPs. Again, the categories were not uniform; nevertheless, 10 of the 15 studies referenced in Table 1 distinguished fibres. The proportions of fibres (if known) are shown in Fig. 2. The contribution of fibres to the total MP count significantly varied within the samples from different studies, ranging from 7% to 99% (Pivokonsky et al., 2018; Di et al., 2019). This difference is likely due to the diverse origins of MPs. High amounts of plastic fibres are released when washing synthetic clothes, and their presence in surface water is therefore presumably caused by the inflow of sewage water (Browne et al., 2011; Napper and Thompson, 2016). The other shape categories distinguished in some studies include spherical particles, fragments, pellets, granules, films and styrofoam (Zhao et al., 2014; Su et al., 2016; Pivokonsky et al., 2018; W. Wang et al., 2018; Di et al., 2019; Luo et al., 2019; Yuan et al., 2019).

The material composition of MPs was reported by 11 of the 15 abovementioned studies. Polyethylene (PE) and polypropylene (PP) particles appeared in 10 studies, separately comprising up to >90% of MPs (Bordós et al., 2019; Triebskorn et al., 2019). These materials are both commonly used in various products, including, e.g., food and cosmetic packaging, houseware, toys, shopping bags, and food and agricultural packaging films in the case of PE and, e.g., food containers, pipes and automotive parts in the case of PP (Plastics Europe, 2018). However, the proportions of PE and PP significantly varied between the samples, as shown in Fig. 3a. In addition to PE and PP, surface freshwater contained polyethylene terephthalate (PET), polystyrene (PS), polyvinylchloride (PVC), polyester (PES), polyamide (PA), polyacrylate (PAC), polytetrafluorethylene (PTFE) or rayon (Wang et al., 2017; W. Wang et al., 2018; Di and Wang, 2018; Bordós et al., 2019; Di et al., 2019; Luo et al., 2019; Triebskorn et al., 2019; Yuan et al., 2019). In raw water for DWTPs, many other materials besides PE and PP were also identified, namely, PET, PS, PVC, polyacrylamide (PAM), polybutylacrylate (PBA), polymethyl methacrylate (PMMA), *p*-phenylene terephthalamide (PPTA), polytrimethylene terephthalate (PTT), di (2-ethylhexyl) phthalate (DEHP) and polyoxybenzylmethylenglycolanhydride (Bakelite) in raw water originating from surface waters (Pivokonsky et al., 2018) and PVC, PES and epoxy resin in raw water originating from groundwater (Mintenig

Table 1
The abundance and size distribution of microplastics in raw water for drinking water treatment plants and in freshwater (only studies that present MP numbers per water volume are included).

Type of water	Lower size limit of detected MPs (μm)	Microplastic abundance (L^{-1})		Size distribution of microplastics (μm)			Reference
		Mean	Range	<10	10–100	>100	
Raw water for DWTPs							
Raw water, DWTP referred to as "WTP1" supplied by a surface water reservoir, Czech Republic	1	1473	1384–1575	86%	13%	1%	Pivokonsky et al., 2018
Raw water, DWTP referred to as "WTP2" supplied by a surface water reservoir, Czech Republic	1	1812	1648–2040	92%	8%	0%	Pivokonsky et al., 2018
Raw water, DWTP referred to as "WTP3" supplied by a river, Czech Republic	1	3605	3123–4464	81%	17%	1%	Pivokonsky et al., 2018
Raw water, DWTP Nethen supplied by groundwater, Germany	20	<1	–	NA	100% (100% between 50–150 μm)		Mintenig et al., 2019
Raw water, DWTP Holdorf supplied by groundwater, Germany	20	<1	–	NA	100% (100% between 50–150 μm)		Mintenig et al., 2019
Raw water, DWTP Drossenkneten supplied by groundwater, Germany	20	0	–	NA	100% (100% between 50–150 μm)		Mintenig et al., 2019
Raw water, DWTP Sandelermoens supplied by groundwater, Germany	20	0	–	NA	100% (100% between 50–150 μm)		Mintenig et al., 2019
Raw water, DWTP Thuelsfelde supplied by groundwater, Germany	20	0	–	NA	100% (100% between 50–150 μm)		Mintenig et al., 2019
Freshwater bodies							
Yangtze Estuary, China	500	4.2	0.5–10.2	NA	NA	100%	Zhao et al., 2014
River Seine, France	100	30	3–106	NA	NA	100%	Dris et al., 2015
River Seine, France	330	0.4	0.3–0.5	NA	NA	100%	Dris et al., 2015
Taihu Lake, China	5	–	3.4–25.8	12%	88%		Su et al., 2016
Amsterdam canal water, Netherlands	10	–	48–187	NA	100% (61% 10–300 μm, 39% >300 μm)		Leslie et al., 2017
Wuhan water (urban lakes and rivers), China	50	–	1.6–8.9	NA	100% (>80% <2000 μm)		Wang et al., 2017
Three Gorges Reservoir, China	48	4.7	1.6–12.6	NA	100% (31–74% <500 μm)		Di and Wang, 2018
Yangtze River, China	20	–	0.5–3.1	NA	–	–	Su et al., 2018
Dongting Lake, China	50	–	<1–2.8	NA	100% (27% <330 μm)		W. Wang et al., 2018
Hong Lake, China	50	2.9	1.3–4.7	NA	100% (20% <330 μm)		W. Wang et al., 2018
Surface water (rivers and reservoirs), Carpathian basin, Hungary	100	<1	–	NA	NA	100%	Bordós et al., 2019
Danjiangkou Reservoir, China	48	2.6	0.5–15	NA	100% (6–44% <500 μm)		Di et al., 2019
Suzhou and Huangpu River, including creeks, China	20	–	1.8–2.4	NA	<15%	>75%	Luo et al., 2019
Groundwater wells, Holdorf, Germany	20	<1	–	NA	100% (100% between 50–150 μm)		Mintenig et al., 2019
Elbe River, Germany	4	–	100–900	100% (96% <20 μm)		0%	Triebskorn et al., 2019
Poyang Lake, China	50	–	5–34	NA	100% (73% < 500μm)		Yuan et al., 2019

Note: NA…MPs within this category were not measured. –… data not reported.

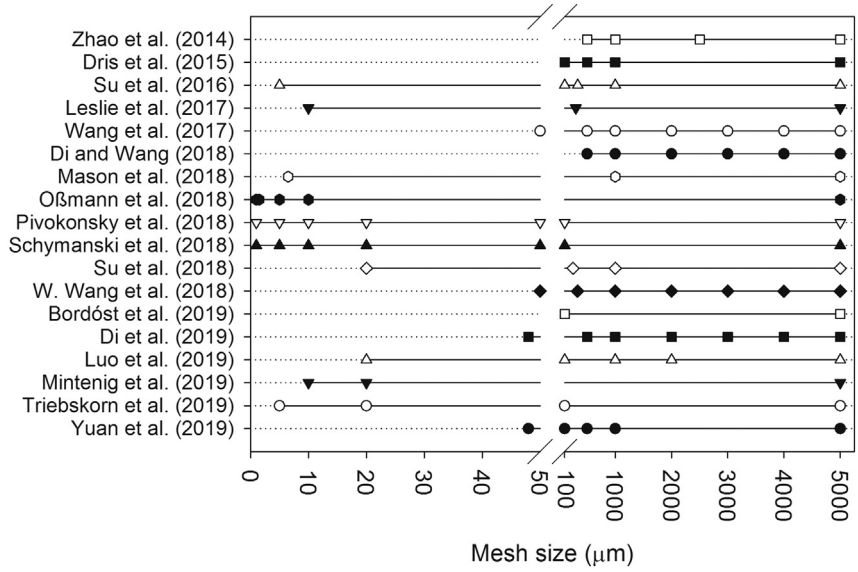

Fig. 1. Size ranges of microplastics analysed by different studies.

et al., 2019). Proportions of different materials are shown in Fig. 3a. Similar to the variation in shapes of MPs, material heterogeneity can be attributed to diverse MP origins.

3. MPs in potable water

Recently, studies on the presence of MPs in goods intended for human consumption have started to appear. MPs have already been detected in seafood (Van Cauwenberghe and Janssen, 2014; Cho et al., 2019; Teng et al., 2019), which is not very surprising with respect to the global presence of MPs in oceans and seas and the possible uptake of MPs by aquatic organisms (Cole et al., 2011; de Sá et al., 2018). However, MPs have also been detected in other edible consumer products, such as beer and salt (Liebezeit and Liebezeit, 2014; Yang et al., 2015).

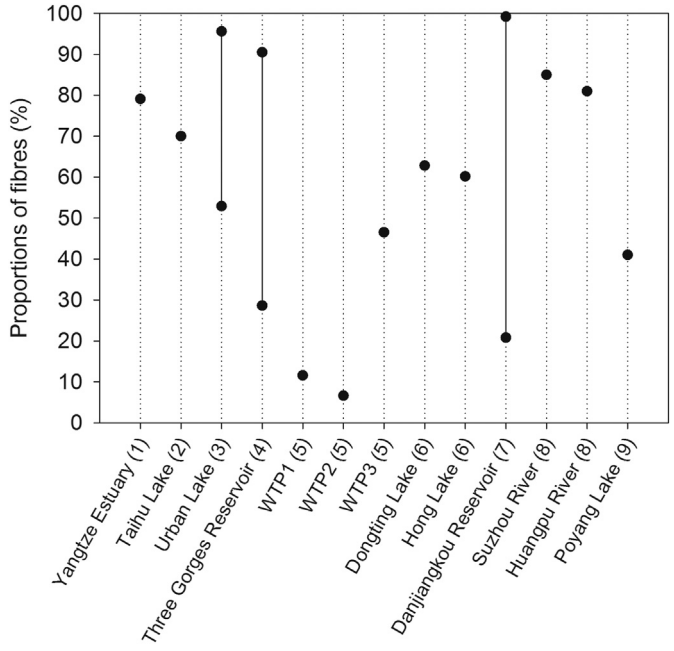

Fig. 2. Proportions of fibres expressed as a percentage in different raw water and freshwater samples. References: (1) Zhao et al. (2014); (2) Su et al. (2016); (3) Wang et al. (2017); (4) Di and Wang (2018); (5) Pivokonsky et al. (2018); (6) W. Wang et al. (2018); (7) Di et al. (2019); (8) Luo et al. (2019); (9) Yuan et al. (2019).

Considering the daily expected consumption, potable water might not be a negligible source of MPs to humans. Similar to research on MPs in freshwater bodies, the methodologies for determining MPs in potable water differ among studies, including the lower detection limits of MPs measured. However, studies dealing with potable water generally aim to determine MPs in smaller-size ranges compared to those dealing with freshwater. An overview of the results of studies published on MPs in potable water is provided in Table 2, which also includes information on MP size distribution.

To the best of our knowledge, only two peer-reviewed studies have been published thus far that offer some evidence of MP presence in public drinking water systems (Pivokonsky et al., 2018; Mintenig et al., 2019). In a study by Pivokonsky et al. (2018), the number and character of MPs (>1 μm) in treated water (sampled at the outflow of the DWTP for the treated water accumulation) was determined at three different plants (referred to as WTP1–3), supplied by surface water bodies (water reservoirs in the case of WTP1 and WTP2; a river in the case of WTP3) and located in the Czech Republic. MPs were detected in all samples, with average values of 443 ± 10 MPs L^{-1} at WTP1, 338 ± 76 MPs L^{-1} at WTP2 and 628 ± 28 MPs L^{-1} at WTP3. By contrast, in a study by Mintenig et al. (2019), <1 MP (>20 μm) per m^3 was found in treated water samples from five different DWTPs using groundwater managed by the Oldenburg-East-Frisian Water Board, Germany, and no MPs (>20 μm) were detected at the five investigated conventional household taps supplied by the DWTPs. The dissimilarity in the results of the two studies may be related to several factors, including the type of source (raw) water (groundwater versus surface water), location, applied treatment technologies, and to the lower size detection limit of particles. As shown in Table 2, the majority of MPs detected in treated water by Pivokonsky et al. (2018) were <10 μm, while Mintenig et al. (2019) detected only MPs >20 μm. There is definitely a need for more research aimed at MPs in public drinking water systems with a special focus on small-size MPs.

Another insight into the possible uptake of MPs via drinking water is provided by studies dealing with MPs in bottled water. It is of note that the packaging materials are often plastic, thus possible origin of MPs other than the water itself is pronounced. Anyway, substantial numbers of MPs (ranging from dozens to thousands per litre) were reported by all the studies, even including samples from glass bottles or beverage cartons (Mason et al., 2018; Oßmann et al., 2018; Schymanski et al., 2018). The overall highest numbers of MPs were reported in a study by Oßmann et al. (2018), ranging from 2649 ± 2857 MPs L^{-1} in

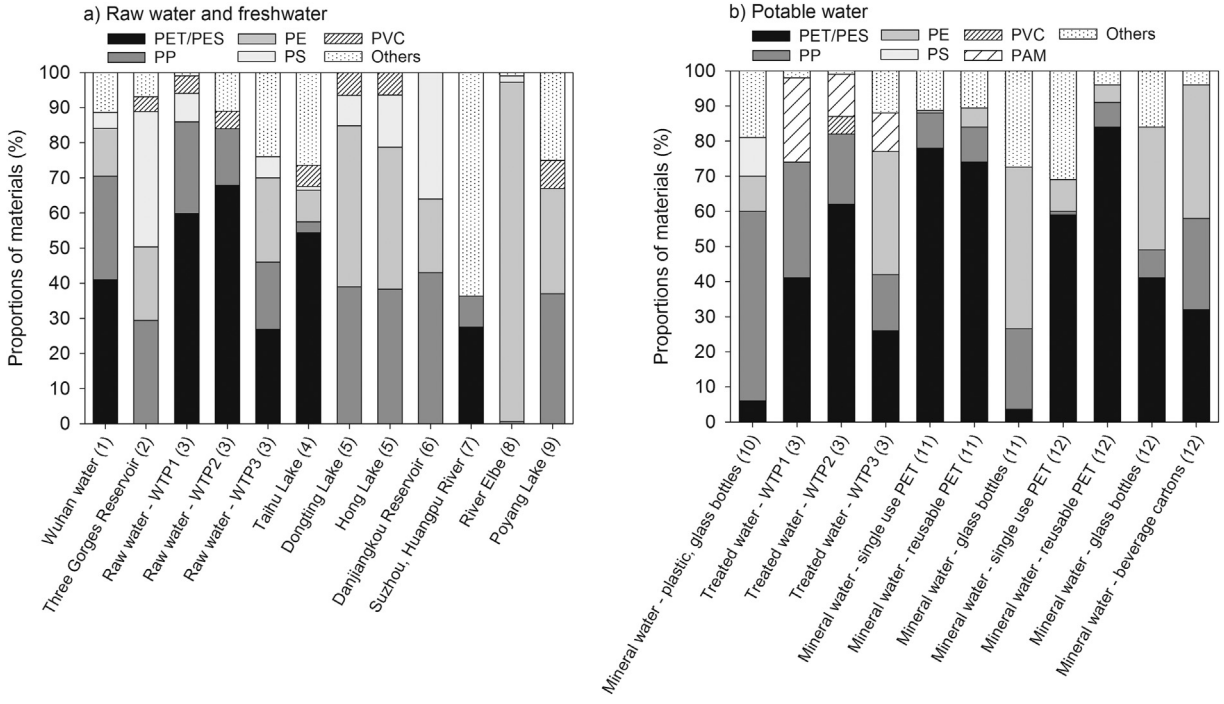

Fig. 3. Proportions of materials comprising MPs in different raw water and freshwater samples (a) and in potable water (b). References: (1) Wang et al. (2017); (2) Di and Wang (2018); (3) Pivokonsky et al. (2018); (4) Su et al. (2018); (5) W. Wang et al. (2018); (6) Di et al. (2019); (7) Luo et al. (2019); (8) Triebskorn et al. (2019); (9) Yuan et al. (2019), (10) Mason et al. (2018); (11) Oßmann et al. (2018); (12) Schymanski et al. (2018).

single-use plastic bottles to 6292 ± 10,521 MPs L^{-1} in glass bottles, and most of the MPs (78–98%) were within the 1–5 μm size range. Such small particles were not covered by the latter two studies (Mason et al., 2018; Schymanski et al., 2018). Detailed data are provided in Table 2. Conclusively, the size distribution of MPs detected in potable water clearly skews towards smaller sizes.

Table 2
The abundance and size distribution of microplastics in potable water.

Type of water	Microplastic abundance (L^{-1})						Reference
	1–5 μm	5[a]-10 μm	10–20 μm	20–50 μm	50–100 μm	>100 μm	
Public supply							
Treated water, DWTP referred to as "WTP1", Czech Republic	269	131		43	0	0	Pivokonsky et al., 2018
Treated water, DWTP referred to as "WTP2", Czech Republic	105	163		69	1	0	Pivokonsky et al., 2018
Treated water, DWTP referred to as "WTP3", Czech Republic	293	272		62	1	0	Pivokonsky et al., 2018
Drinking water[b], DWTP Nethen, Germany	NA	NA	NA	0	<1		Mintenig et al., 2019
Drinking water[b], DWTP Holdorf, Germany	NA	NA	NA	0	<1		Mintenig et al., 2019
Drinking water[b], DWTP Grossenkneten, Germany	NA	NA	NA	0	0		Mintenig et al., 2019
Drinking water[b], DWTP Sandelermoens, Germany	NA	NA	NA	0	<1		Mintenig et al., 2019
Drinking water[b], DWTP Thuelsfelde, Germany	NA	NA	NA	0	<1		Mintenig et al., 2019
Bottled water							
Plastic bottles, brand Aqua	NA			374		8	Mason et al., 2018
Plastic bottles, brand Aquafina	NA			200		13	Mason et al., 2018
Plastic bottles, brand Bisleri	NA			338		9	Mason et al., 2018
Plastic bottles, brand Dasani	NA			109		10	Mason et al., 2018
Plastic bottles, brand *E*-Pura	NA			238		10	Mason et al., 2018
Plastic bottles, brand Evian	NA			114		14	Mason et al., 2018
Plastic bottles, brand Gerolsteiner	NA			1396		15	Mason et al., 2018
Glass bottles, brand Gerolsteiner	NA			159		9	Mason et al., 2018
Plastic bottles, brand Minalba	NA			63		4	Mason et al., 2018
Plastic bottles, brand Nestle Pure Life	NA			912		20	Mason et al., 2018
Plastic bottles, brand San Pellegrino	NA			27		2	Mason et al., 2018
Plastic bottles, brand Wahaha	NA			90		6	Mason et al., 2018
Single use PET bottles	2604	45		0			Oßmann et al., 2018
Reusable PET bottles	4664	142		83			Oßmann et al., 2018
Glass bottles	4895	969		434			Oßmann et al., 2018
Single use plastic bottles	NA	6	4	3	2	0	Schymanski et al., 2018
Returnable plastic bottles	NA	66	34	14	2	1	Schymanski et al., 2018
Glass bottles	NA	26	16	7	4	2	Schymanski et al., 2018
Beverage cartons	NA	4	3	2	1	1	Schymanski et al., 2018

Note: NA…MPs within this category were not measured.
[a] The size class starts at 6.5 in case of results from Mason et al., 2018.
[b] Includes drinking water at plant outlet, at a water meter and at a household tap.

Contrary to the studies on MPs in freshwater, shape is not reported by most of the studies on MPs in drinking water. Only Pivokonsky et al. (2018) distinguished among three morphotypes, i.e., fibres, spherical particles and fragments. Fragments clearly prevailed in treated water at two investigated DWTPs, fibres together with fragments at one DWTP, and spherical particles were the least abundant.

By contrast, material composition of MPs was analysed by all the studies (Mason et al., 2018; Oßmann et al., 2018; Pivokonsky et al., 2018; Schymanski et al., 2018; Mintenig et al., 2019). Approximately 20 different materials forming MPs in potable water were identified, while some amounts of PET or PES were always reported. Next, PE and PP MPs were observed by 4 of the 5 studies. The other materials included, e.g., PVC, PAM, PBA, PPTA, PTT, PMMA or PA (Mason et al., 2018; Oßmann et al., 2018; Pivokonsky et al., 2018; Schymanski et al., 2018; Mintenig et al., 2019). Proportions of the different materials comprising MPs in drinking water are shown in Fig. 3b.

4. Removal of MPs by water treatment

Currently, there is neither any legislative limit for MP content in drinking water nor any treatment technology targeted directly at the removal of MPs. Nevertheless, DWTPs, generally intended to improve water quality so as to meet required legislative and consumer demands, mean a potential barrier for MP transfer from natural freshwater to drinking water for direct human consumption. On the other hand, it is the wastewater treatment plants (WWTPs) that have the capacity to retain MPs originating from households as a result of washing synthetic clothes (Browne et al., 2011; Napper and Thompson, 2016), using MP containing cleaners and cosmetics (Fendall and Sewell, 2009), etc. and to prevent MPs from entering natural aquatic environments. Thus, both of these types of facilities deserve attention with respect to MP removal.

There are two perspectives on how to evaluate MP removal: (1) measuring MPs at the inlet and outlet to the facility (DWTPs, WWTPs or after specific technological steps) and comparing the results, and (2) investigating MP removal efficiency by different processes in laboratory experiments under controlled conditions.

4.1. DWTPs

Pivokonsky et al. (2018) determined the MP content (>1 μm) at the inlet (raw water) and subsequently at the outlet (treated water) of three DWTPs. These plants are not named in the study (for confidentiality reasons) and are referred to as WTP1–3, but they are specified in terms of water source and technological steps. WTP1 is supplied by a large surface water reservoir and operates coagulation/flocculation and one-step separation (sand filtration); WTP2 is supplied by a small water reservoir and includes coagulation/flocculation, sedimentation, sand filtration and granular activated carbon (GAC) filtration; and WTP3 is supplied by a river and uses coagulation/flocculation, flotation, sand filtration and GAC filtration. All the plants are located in the Czech Republic. Much lower numbers of MPs (by approximately 70–80%) were detected in treated water compared to raw water in all samples from each DWTP. The average "removal" rate was lower at WTP1 (70%) compared to WTP2 and WTP3 (81 and 83%, respectively), and prospective connection to the separation steps applied at the distinct DWTPs was suggested. Additionally, as a relatively low fibre removal rate was observed at WTP1 (approximately 25% compared to over 80% for WTP2 and WTP3), a possible relationship between the shape of microplastics and their removal rate by various water treatment technologies was proposed Pivokonsky et al. (2018). However, the amount and character of MPs after each treatment step was not determined, so MP removal by single treatment steps is not known.

Mintenig et al. (2019) investigated the presence of MPs (>20 μm) at different stages in the drinking water supply chain, i.e., in groundwater extracted from three wells within one location (Oldenburg-East-Frisian Water Board, Germany, wells approximately 30 m deep), in raw water of five DWTPs supplied by water from the area (DWTPs Nethen, Holdorf, Grossenkneten, Sandelermoens and Thuelsfelde), in treated water from the five DWPTs and finally at a water metre and at a conventional water tap in one selected household in the distribution area of each DWTP. As very low numbers of MPs were found in the samples (0–7 MPs m^{-3}), it is difficult to observe any trends. However, at two DWTPs (Nethen and Holdorf), there were MPs in the raw water but none or less MPs in the treated water. By contrast, at DWTPs Sandelermoens and Thuelsfelde, there were no MPs in the raw water, but there were some in the treated water. Additionally, MPs were only detected in one of the investigated wells. Therefore, some MPs contamination may happen in the water supply chain. This idea is also supported by the material compositions of detected MPs that correspond to the polymer types used in the supply chain, but the very low numbers of MPs do not allow derivation of any clear conclusions. The possible undesirable addition of MPs during treatment is also mentioned in a study Pivokonsky et al. (2018), in which a relative increase of PAM was observed in treated water, while this polymer is rather commonly applied in water treatment.

Regarding investigation under laboratory conditions, two studies on the removal of MPs by coagulation and subsequent ultrafiltration were conducted by Ma et al. (2018, 2019). In general, coagulation/flocculation followed by the separation of the formed aggregates is an essential treatment step that is extensively employed at many DWTPs, mainly those that are supplied by surface water. If the process is effectively optimized, this method can potentially remove various polluting agents, including inorganic clay-like particles, humic substances, algal and cyanobacterial cells, algal organic matter, etc. (Packham, 1965; Jiang et al., 1993; Duan and Gregory, 2003; Sharp et al., 2006; Matilainen et al., 2010; Pivokonsky et al., 2016). Additionally, coagulation/flocculation was also employed at all the DWTPs investigated by Pivokonsky et al. (2018), at which approximately 70–80% removal of MPs was observed. It is therefore reasonable to expect some (at least limited) removal of MPs by using coagulation/flocculation, and this method definitely deserves substantial investigation.

In the studies by Ma et al. (2018) and Ma et al. (2019), polyethylene (PE) particles of different sizes (<0.5 mm, 0.5–1 mm, 1–2 mm, and 2–5 mm) were coagulated. However, the larger size classes exceeded the size of particles that are normally coagulated. In general, coagulation in water treatment is aimed at associating dissolved or colloidal compounds to create aggregates suitable for subsequent separation. Sedimentation or flotation is sometimes applied as an intermediate separation step; however, deep bed sand filtration is basically always used to remove the aggregates, and the required size is approximately in the range of dozens of micrometres (Ngo et al., 1995; Bai and Tien, 1997; Pivokonsky et al., 2011). Large aggregates are instead likely to be intercepted by the upper layer of a filter and cannot penetrate into the filter bed (Pivokonsky et al., 2011). Although Ma et al. (2018) and Ma et al. (2019) applied the sedimentation step, the need for coagulation of particles in the millimetre range is doubtful. Additionally, regarding the water sources for DWTPs, the presence of much smaller MPs is rather expected (based on MP size distributions shown in Table 2). We therefore further discuss only the results from Ma et al. (2018) and Ma et al. (2019) for PE particles <0.5 mm in this review.

Ma et al. (2018) coagulated the PE particles using $FeCl_3 \cdot 6H_2O$ and attained the best PE removal (17 ± 2%) at pH 8 at the coagulant dose of 2.0 mmol L^{-1}. It corresponds to approximately 112 mg L^{-1} Fe, which is much higher compared to doses commonly applied for coagulation of other impurities in drinking water treatment (<20 mg L^{-1}) (Henderson et al., 2008a; Safarikova et al., 2013; Gonzalez-Torres et al., 2014; Pivokonsky et al., 2015, 2016; Baresova et al., 2017). Ma et al. (2019) examined the performance of $FeCl_3 \cdot 6H_2O$ and $AlCl_3 \cdot 6H_2O$ and the Al-based coagulant appeared better – up to 37 ± 3% removal of PE particles was obtained (at pH 7). However, the required dose was extremely high – 15 mmol L^{-1}, which corresponds to 405 mg L^{-1} Al.

When using doses relevant at real conditions (e.g., 0.5 mmol L^{-1} or 13.5 mg L^{-1} Al), the PE removal was only 8 ± 1%. Additional application of flocculant polyacrylamide (PAM) to the coagulation of PE particles was also investigated. The combination of 2.0 mmol L^{-1} $FeCl_3 \cdot 6H_2O$ or 5 mmol L^{-1} $AlCl_3 \cdot 6H_2O$ with 3–15 mg L^{-1} anionic PAM (at pH 7) resulted in the PE removal of approximately 85–90% and 50–60%, respectively (Ma et al., 2018, 2019). However, the applied PAM concentrations greatly exceeded the maximum authorized dose of 1 mg L^{-1} (WHO, 2011a). Further, the influence of different levels of ionic strength (induced by NaCl), turbidity (generated by adding kaolin) and the presence of natural organic matter (specifically humic acids) on the coagulation of PE was examined, and no significant effects were observed (Ma et al., 2018, 2019).

Ultrafiltration of the above-described PE particles using a polyvinylidene fluoride (PVDF) membrane (nominal molecular weight cut-off of 100 kDa, corresponding to an average pore diameter of 30 nm) was also investigated, both with and without foregoing coagulation. PE particles were efficiently rejected by the membrane due to their much larger size compared to the membrane pores. More attention was therefore paid to membrane fouling. Only a minor influence was observed for non-coagulated PE particles, while slightly more pronounced fouling appeared after coagulation of PE by $FeCl_3 \cdot 6H_2O$ or $AlCl_3 \cdot 6H_2O$, especially at high doses (Ma et al., 2018, 2019).

To conclude, coagulation/flocculation and membrane filtration are promising technologies for MP removal and deserve further attention, but the experimental setup and conditions should better reflect conditions applicable in water treatment practices. Next, also possible interactions of MPs with other pollutants should be subjected to investigation. Interactions between some natural polluting agents (e.g., kaolinite and AOM, cyanobacterial cells and AOM, humic substances and AOM) have been observed, posing impacts on coagulation conditions and efficacy (Safarikova et al., 2013; Pivokonsky et al., 2015, 2016; Baresova et al., 2017). While Ma et al. (2018) and Ma et al. (2019) observed no effect of humic acid and kaolin presence on the coagulation of polyethylene MPs, S. Li et al. (2018) reported interactions between polystyrene MPs and HA. Although the latter study does not deal with water treatment, their suggestion that HA adsorbed on PS MPs could increase steric hindrance and electrostatic repulsion among the particles may have implications in processes such as coagulation/flocculation (S. Li et al., 2018).

4.2. WWTPs

Research has shown that significant numbers of MPs are entering WWTPs, up to several hundred per litre (Dris et al., 2015; Leslie et al., 2017; Simon et al., 2018). Compared to DWTPs, more attention has been paid to MP fate at WWTPs. However, the methodologies greatly differ among the studies. Only effluent samples were analysed in some studies that rather focused on the WWTPs as potential point sources of MPs (Mason et al., 2016; Wolff et al., 2019), while the MP content at the inlet and outflow of WWTPs was sometimes investigated (Leslie et al., 2017; Simon et al., 2018). In other cases, MPs were determined after distinct technological steps (Carr et al., 2016; Murphy et al., 2016; Talvitie et al., 2017a; Ziajahromi et al., 2017). In general, high removal rates were observed at several WWTPs, e.g., 98% removal of MPs >250 μm (Lares et al., 2018), 99.9% removal of MPs >100 μm (Carr et al., 2016), 98% removal of MPs >65 μm (Murphy et al., 2016), and 99% removal of MPs >10 μm (Simon et al., 2018). By contrast, Leslie et al. (2017) observed only 72% removal of MPs (>10 μm) and thus a quite lower removal rate compared to the abovementioned studies. Nevertheless, as the configuration of distinct WWTPs differs and the same treatment steps are not always applied, the results are difficult to compare. Moreover, dissimilar size classes of MPs were analysed by different studies, and no study covered very small MPs (<10 μm). Thus, the fate of MPs < 10 μm, possibly also present in wastewater, remains unexplored.

Some studies agree that significant portions of MPs were readily removed by first steps of the wastewater treatment chain, belonging to primary treatment aimed at removal of larger debris (Carr et al., 2016; Lares et al., 2018). However, this finding may be related to the relatively large size of MPs analysed (>100 μm by Carr et al. (2016), >250 μm by Lares et al. (2018)).

Ziajahromi et al. (2017) measured MPs (>25 μm) after primary, secondary and tertiary (if included) treatment steps at different WWTPs. A 66% decrease in MPs was observed between primary and secondary effluents at one WWTP, where the secondary step consisted of aeration, sedimentation and UV disinfection. An even higher removal of MPs (over 90%) was observed between the primary and final effluent at another WWTP that employed secondary and tertiary treatment, i.e., biological treatment, flocculation, disinfection/de-chlorination, ultrafiltration, reverse osmosis and de-carbonation (Ziajahromi et al., 2017).

Regarding the more advanced treatment in detail, Talvitie et al. (2017a) investigated removal of MPs (>20 μm) by a membrane bioreactor (MBR) (treating primary effluent) and three different tertiary treatment techniques, i.e., disc filter, rapid sand filter and dissolved air flotation (treating secondary effluent). The efficient removal of MPs (>95%) was attained by all the treatment technologies, suggesting they may be suitable for MP removal. Improvement in MP removal when using an MBR was also reported by Lares et al. (2018); by contrast, no effect of MBR was observed by Leslie et al. (2017). The contrary results may arise from differences in the character of both MPs monitored and in the employed MBRs. Further, Carr et al. (2016) investigated the removal of MPs (PE 10–300 μm) by a gravity filter (often included as tertiary treatment at WWTPs) at a bench scale and no breakthrough was observed, indicating that conventional filtering media (anthracite, sand, and gravel) may be useful in removing MPs. Mintenig et al. (2017) analysed wastewater from one WWTP before and after post-filtration (included as a tertiary treatment) using pile fabrics (nominal pore size of 10–15 μm) and observed 100% removal of MPs >500 μm and a decrease in MPs <500 μm.

Talvitie et al. (2017b) investigated removal of microlitter (ML) >20 μm (also partially including MPs) after distinct technological steps at one WWTP. Approximately 98% of the ML was already removed during pretreatment involving coarse screening, grit removal and chemically enhanced sedimentation. Further, 7–20% of the remaining ML was removed by the activated sludge process, and no further decrease in ML was observed after the biologically active filter (BAF). Furthermore, some relationships between the removal rates and the size and shape of ML were observed – pretreatment mainly removed larger size fractions of ML (>100 μm). Next, fibres comprised 70% of ML in the influent and only 30% of ML in the effluent (Talvitie et al., 2017b), which indicates the preferential removal of fibres. Better removal of fibres compared to other particles (99.1% and 89.8%, respectively) was also observed by Lares et al. (2018). These results imply that characterization of microlitter, including MPs, is important from the perspective of different treatment processes.

In general, up to 98–99.9% removal of MPs at WWTPs was reported (Carr et al., 2016; Murphy et al., 2016; Lares et al., 2018; Simon et al., 2018). However, despite the high removal efficiency, conventional WWTPs may still be a significant source of MPs given the large volumes of effluents discharged (Mason et al., 2016; Murphy et al., 2016; Leslie et al., 2017; Mintenig et al., 2017; Talvitie et al., 2017a, 2017b; Ziajahromi et al., 2017). Additionally, attention should also be paid to handling waste from WWTPs. If sludge that may contain substantial amounts of MPs is used, e.g., in agriculture, MPs can be transferred back to the environment (Zubris and Richards, 2005; Leslie et al., 2017; Talvitie et al., 2017b).

5. Comparison of MPs with other water polluting agents

Raw water usually contains a wide range of compounds – some of which are recognized as harmful (due to impacts on human health) or

are considered undesirable (e.g., because of deterioration of organoleptic properties), their content in treated water is regulated by legislation limits, and if such compounds are present, water treatment processes are aimed at their removal.

MPs with the size ranges observed in potable water cannot be detected by human senses, and their potential health effects are still largely unknown (Barboza et al., 2018; Revel et al., 2018). However, due to the worldwide occurrence of MPs in freshwater (Zhao et al., 2014; Dris et al., 2015; Su et al., 2016; Leslie et al., 2017; Wang et al., 2017; Di and Wang, 2018; Su et al., 2018; Triebskorn et al., 2019) and the increasing global production of plastic materials (Plastics Europe, 2018), MPs may become a target pollutant for drinking water treatment technologies. We therefore provide a comparison of MPs with some commonly observed water polluting agents, the removal of which is addressed with regard to conventional water treatment based on coagulation/flocculation and subsequent separation of formed aggregates.

As shown in Tables 1 and 2, the reported MP content in DWTPs raw water and freshwater bodies ranges from 0 to >4000 and from 0 to >6000 items per litre, respectively. However, it is very difficult to compare MP abundance with other pollutants, as these are usually expressed using different units, e.g. as weight per volume. A partial comparison can be provided by asbestos fibres that are usually reported in MFL (million fibres per litre), and asbestos content in drinking water has been extensively studied due to reasonable concerns about its detrimental impacts on human health. Very diverse asbestos concentrations ranging up to >10 MFL were reportedly present in various water supplies in Canada, Great Britain and the United States (Millette et al., 1983; Montizaan et al., 1989; WHO, 2003). These numbers are orders of magnitude higher compared to data published thus far on MP abundance (Table 2); however, asbestos is not solely a man-made material. Additionally, as the health hazards of asbestos are instead associated with inhalation of the fibres and as there is no consistent evidence of negative impacts if ingested, there is no health-based guideline value for asbestos in drinking water (WHO, 2011b). The median asbestos fibre lengths reported by the WHO (2003) (Canadian survey) were in the range of 0.5–0.8 μm and thus much smaller than MPs recently detected in potable water/aquatic environments (Tables 1, 2). The vast majority of the fibres in the US survey were <5 μm in length, with median lengths of 0.5 or 1 μm, depending on the location (Millette et al., 1983). Interestingly, in the Canadian survey, asbestos concentrations were higher in raw water compared to treated water, and the results indicated that coagulation with filtration was efficient in asbestos fibre removal (Toft et al., 1981). Lawrence et al. (1975) investigated asbestos fibre removal and revealed that of the methods tested, coagulation with subsequent sand filtration was the most effective, and 99.8% removal was attained (initial concentration $12.3 \cdot 10^6$ fibres L^{-1}, residual concentration below the detection limit of $2 \cdot 10^4$ fibres L^{-1}). The researchers used ferric chloride at a dose of 10 ppm and added 1 ppm of polyelectrolyte, and the pH was maintained at 7.5.

As mentioned above, coagulation is a traditional treatment commonly employed at DWTPs to remove different polluting agents, often for those of natural origin (algal or cyanobacterial cells, dissolved natural organic matter, and clay particles) (Packham, 1965; Jiang et al., 1993; Duan and Gregory, 2003; Sharp et al., 2006; Matilainen et al., 2010; Pivokonsky et al., 2016). Within the wide range of influential factors that govern coagulation efficacy, some distinct characteristics of the coagulated substances are most often pronounced, i.e., molecular weight (MW), charge properties and the degree of hydrophobicity. Table 3 provides a comparison of these properties between the named natural polluting agents and MPs. As shown in this table, the sizes of MPs recently observed as prevalent in raw water, i.e., 1–10 μm (Pivokonsky et al., 2018), are comparable to some natural polluting agents, e.g., cyanobacterial cells (Kim et al., 1997; Baresova et al., 2017) or clay particles (National Research Council, 1977) that can be efficiently coagulated (Safarikova et al., 2013; Gonzalez-Torres et al., 2014; Baresova et al., 2017). However, coagulation behaviour is also governed by other characteristics. Furthermore, the size, charge and hydrophobicity appear to also be essential in other common water treatment processes, such as membrane filtration (Domany et al., 2002; Matilainen et al., 2010; Pivokonsky et al., 2016) or activated carbon filtration (Newcombe and Drikas, 1997; Bjelopavlic et al., 1998; Pivokonsky et al., 2016). Interestingly, the size and surface charge are also the emphasized properties of MPs with regard to cellular uptake (Triebskorn et al., 2019).

6. Conclusions

Currently, microplastics are detected in different water samples, including in natural freshwater, WWTP influent and effluent, raw and treated water at DWTPs and in bottled water. However, the numbers of MPs vary significantly, from negligible to several thousand items per litre. In addition to the diversity of samples subjected to investigation, some differences may also result from variations in sampling, sample preparation and analytical methods. However, both WWTPs and DWTPs definitely have to face the presence of MPs, at least in some locations. Although the potential health impacts of MPs are still unknown, their occurrence in potable water should not be overlooked.

This review includes a summary of MP abundance and character in freshwater bodies and in potable water and discusses MP removal by water treatment processes, aiming to identify research needs with regard to drinking water treatment. Thus far, more attention has been paid to wastewater treatment plants, and research on MP removal by drinking water treatment processes is lacking. Therefore, the question remains as to whether appropriate adjustments of conventional treatment technologies can satisfactorily remove MPs or whether new techniques need to be developed. A significant decrease (by approximately 70–80%) in MP numbers between raw and treated water at different DWTPs was reported by one rare study; however, it is unclear which treatment step was responsible for the removal. Additionally, substantial numbers of MPs (hundreds per litre) still remained in the treated water. However, there is no legislative limit for MP content in drinking water, and it is not possible to assess the residual concentrations as too high or sufficiently low. Another study investigated the coagulation of microplastic (PE) particles, but their efficient removal was attained only at coagulant doses that are not usable in water treatment practices. Moreover, relatively large MPs were chosen for their experiments. By contrast, the current results of the reviewed literature imply that regarding potable water, a special focus should be placed on smaller MPs (in the micrometre range).

Anyway, more research is needed in the field of MPs in water treatment, i.e., (i) quantifying MPs (including particles as small as possible) and thorough MP characterization (in terms of size, shape, material composition and other properties related to water treatment) in drinking water sources and raw water at DWTPs, (ii) investigating MP removal by distinct treatment steps at DWTPs working under ordinary conditions and (iii) investigating possible water enrichment of MPs during the conventional treatment processes at DWTPs, next, if needed (iv), optimizing current treatment technologies or inventing new processes aimed at the removal of MPs or their problematic fractions that would remain in treated water after passing through an unaltered process. When working at the laboratory scale and/or preparing artificial MP samples, emphasis should be put on both environmentally relevant and practicable water treatment conditions. Further, also possible interactions of MPs with other polluting agents deserve particular attention. Finally, as microplastics are non-degradable persistent pollutants, their fate after removal from water should also be monitored.

Acknowledgements

This work was supported by the Czech Science Foundation, Czech Republic [grant number GA18-14445S]; and Czech Academy of

Table 3
Comparison of selected properties of some common surface water polluting agents and microplastics.

Polluting agent	Size/molecular weight (MW)	Charge	Hydrophilicity/hydrophobicity	Maximum removal efficacy attained by coagulation
Cyanobacterial cells	***Microcystis aeruginosa*** 2.6–5.4 μm in diameter [1] ***Merismopedia tenuissima*** <2 μm in diameter [2]	***M. aeruginosa*** negative at pH >2.2 [3] ***M. tenuissima*** negative within pH 3–9 [2]	–	≥99% (both *M. aeruginosa* and *M. tenuissima* cells) [2,4]
Algal organic matter – AOM (dissolved)	Several hundred Da – hundreds kDa [2,5,6]	Negative within pH 2–10 [5,6]	Hydrophilic content prevail (up to >80%) [6]	>50% [2,6]
Humic substances	**Fulvic acids** ≤2 kDa (60 nm average length, 2 nm average diameter of macromolecules) **Humic acids** 2–5 kDa [7]	Negative at pH >4 [8,9] (fulvic acids higher charge density than humic acids, measured at pH 7) [8]	Hydrophobic (humic acids more hydrophobic than fulvic acids) [7,9]	64–84% **Fulvic acids** 64% **Humic acids** 84% [8] **Humic substances** (fulvic + humic acids) 65% [10]
Clay mineral particles	<2 μm in diameter [11]	Negative at pH >3 [12,13]	Hydrophilic content prevail [14] Hydrophobic content prevail (only 25%, resp. 40% of kaolinite, resp. illite surface hydrophilic) [15]	>95% [12]
Microplastics	<5 mm [16,17,18] (MPs of 1–10 μm the most abundant in raw water originating from surface water) [19]	**PA** – negative at pH >6.52 [20] **PE** – negative at pH >4.30 [21] **PE** – negative at pH >6.63 [20] **PP** – negative at pH >4.26 [21] **PP** – negative at pH >6.76 [20] **PS** – negative at pH >2.7 [22] **PS** – negative at pH >3.96 [21] **PS** – negative at pH >6.69 [20] **PVC** – negative at pH >3.41 [22] **PVC** – negative at pH >6.65 [20]	Hydrophobic [24,25,26,27]	**PE** < 0.5 mm 7% ± 1% ($FeCl_3 \cdot 6H_2O \approx 0.2$ mmol L^{-1}, pH 8) 17% ± 2% ($FeCl_3 \cdot 6H_2O \approx 2$ mmol L^{-1}, pH 8) [28] 8% ± 1% $AlCl_3 \cdot 6H_2O \approx 0.5$ mmol L^{-1}, pH 7 12% ± 1% ($AlCl_3 \cdot 6H_2O \approx 5$ mmol L^{-1}, pH 7) [29] also described in chapter 4.1.

Note: Reference: [1] Kim et al. (1997); [2] Baresova et al. (2017); [3] Hadjoudja et al. (2010); [4] Gonzalez-Torres et al. (2014); [5] Henderson et al. (2008b); [6] Pivokonsky et al. (2016); [7] Domany et al. (2002); [8] Sharp et al. (2006); [9]Duan and Gregory (2003); [10] Pivokonsky et al. (2015); [11] National Research Council, 1977; [12] Safarikova et al. (2013); [13] Coles and Yong (2002); [14] Chen et al. (2019); [15] Saada et al. (1995); [16] Koelmans et al. (2015); [17] da Costa et al. (2016); [18] Hahladakis et al. (2018); [19] Pivokonsky et al. (2018); [20] Li et al. (2018b); [21] Xu et al. (2018); [22] S. Li et al. (2018); [23] Wu et al. (2019); [24] Mato et al. (2001); [25] Teuten et al. (2007); [26] Ma et al. (2016); [27] Rochman et al. (2013); [28] Ma et al. (2018); [29] Ma et al. (2019).

Sciences, Czech Republic [RVO 67985874]. The authors acknowledge the financial assistance on this project.

References

Anderson, P.J., Warrack, S., Langen, V., Challis, J.K., Hanson, M.L., Rennie, M.D., 2017. Microplastic contamination in Lake Winnipeg, Canada. Environ. Pollut. 225, 223–231. https://doi.org/10.1016/j.envpol.2017.02.072.

Andrary, A.L., 2011. Microplastics in the marine environment. Mar. Pollut. Bull. 62, 1596–1605. https://doi.org/10.1016/j.marpolbul.2011.05.030.

Auta, H.S., Emenike, C.U., Fauziah, S.H., 2017. Distribution and importance of microplastics in the marine environment: a review of the sources, fate, effects, and potential solutions. Environ. Int. 102, 165–176. https://doi.org/10.1016/j.envint.2017.02.013.

Bai, R., Tien, C., 1997. Particle detachment in deep bed filtration. J. Colloid Interface Sci. 186, 307–317. https://doi.org/10.1006/jcis.1996.4663.

Barboza, L.G.A., Vethaak, A.D., Laborante, R.R.B.O., Lundebye, A.-K., Guilhermino, L., 2018. Marine microplastics debris: an emerging issue for food security, food safety and human health. Mar. Pollut. Bull. 133, 336–348. https://doi.org/10.1016/j.marpolbul.2018.05.047.

Baresova, M., Pivokonsky, M., Novotna, K., Naceradska, J., Branyik, T., 2017. An application of cellular organic matter to coagulation of cyanobacterial cells (*Merismopedia tenuissima*). Water Res. 122, 70–77. https://doi.org/10.1016/j.watres.2017.05.070.

Bjelopavlic, M., Newcombe, G., Hayes, R., 1998. Adsorption of NOM onto activated carbon: effect of surface chargé. ionic strength and pore distribution. J. Colloid Interface Sci. 210, 271–280. https://doi.org/10.1006/jcis.1998.5975.

Bordós, G., Urbányi, B., Micsinai, A., Kriszt, B., Palotai, Z., Szábo, I., Hantosi, Z., Szoboszlay, S., 2019. Identification of microplastics in fish pond and natural freshwater environments of the Carpathian basin, Europe. Chemosphere 216, 110–116. https://doi.org/10.1016/j.chemosphere.2018.10.110.

Browne, M.A., Crump, P., Niven, S.J., Teuten, E., Tonkin, A., Galloway, T., Thompson, R., 2011. Accumulation of microplastic on shorelines worldwide: sources and sinks. Environ. Sci. Technol. 45, 9175–9179. https://doi.org/10.1021/es201811s.

Carr, S.A., Liu, J., Tesoro, A.G., 2016. Transport and fate of microplastic particles in wastewater treatment plants. Water Res. 91, 174–182. https://doi.org/10.1016/j.watres.2016.01.002.

Chen, J., Min, F., Liu, L., Liu, C., 2019. Mechanism research on surface hydration of kaolinite, insights from DFT and MD simulations. Appl. Surf. Sci. 476, 6–15. https://doi.org/10.1016/j.apsusc.2019.01.081.

Cho, Y., Shim, W.J., Jang, M., Han, G.M., Hong, S.H., 2019. Abundance and characteristics of microplastics in market bivalves from South Korea. Environ. Pollut. 245, 1107–1116. https://doi.org/10.1016/j.envpol.2018.11.091.

Cole, M., Lindeque, P., Halsband, C., Galloway, T.S., 2011. Microplastics as contaminants in the marine environment: a review. Mar. Pollut. Bull. 62, 2588–2597. https://doi.org/10.1016/j.marpolbul.2011.09.025.

Coles, C.A., Yong, N.Y., 2002. Aspects of kaolinite characterization and retention of Pb and Cd. Appl. Clay Sci. 22, 39–45. https://doi.org/10.1016/S0169-1317(02)00110-2.

da Costa, J.P., Santos, P.S.M., Duarte, A.C., Rocha-Santos, T., 2016. (Nano)plastics in the environment – sources, fates and effects. Sci. Total Environ. 566-567, 15–26. https://doi.org/10.1016/j.scitotenv.2016.05.041.

de Sá, L.C., Oliveira, M., Riberio, F., Rocha, T.L., Futter, M.N., 2018. Studies of the effects of microplastics on aquatic organisms. What do we know and where should we focus our efforts in the future? Sci. Total Environ. 645, 1029–1039. https://doi.org/10.1016/j.scitotenv.2018.07.207.

Di, M., Wang, J., 2018. Microplastics in surface waters and sediments of the Three Gorges Reservoir, China. Sci. Total Environ. 616-617, 1620–1627. https://doi.org/10.1016/j.scitotenv.2017.10.150.

Di, M., Liu, X., Wang, W., Wang, J., 2019. Pollution in drinking water source areas: microplastics in the Danjiangkou Reservoir. China. Environ. Toxicol. Pharmacol. 65, 82–89. https://doi.org/10.1016/j.etap.2018.12.009.

Domany, Z., Galambos, I., Vatai, G., Bekassy-Molnar, E., 2002. Humic substances removal from drinking water by membrane filtration. Desalination 145, 333–337. https://doi.org/10.1016/S0011-9164(02)00432-0.

Dris, R., Gasperi, J., Rocher, V., Saad, M., Renault, N., Tassin, B., 2015. Microplastic contamination in an urban area: a case study in Greater Paris. Environ. Chem. 12 (5). https://doi.org/10.1071/EN14167.

Duan, J., Gregory, J., 2003. Coagulation by hydrolysing metal salts. Adv. Colloid Interf. Sci. 100, 475–502. https://doi.org/10.1016/S0001-8686(02)00067-2.
Eerkes-Medrano, D., Thompson, R.C., Aldridge, D.C., 2015. Microplastics in freshwater systems: a review of the emerging threats, identification of knowledge gaps and prioritisation of research needs. Water Res. 75, 63–82. https://doi.org/10.1016/j.watres.2015.02.012.
Fendall, L.S., Sewell, M.A., 2009. Contributing to marine pollution by washing your face: microplastics in facial cleansers. Mar. Pollut. Bull. 58, 1225–1228. https://doi.org/10.1016/j.marpolbul.2009.04.025.
Free, C.M., Jensen, O.P., Mason, S.A., Eriksen, M., Williamson, M.J., Boldgiv, B., 2014. High-levels of microplastic pollution in a large, remote, mountain lake. Mar. Pollut. Bull. 85, 156–163. https://doi.org/10.1016/j.marpolbul.2014.06.001.
Gonzalez-Torres, A., Putnam, J., Jefferson, B., Stuetz, R.M., Henderson, R.K., 2014. Examination of the physical properties of *Microcystis aeruginosa* flocs produced on coagulation with metal salts. Water Res. 60, 197–209. https://doi.org/10.1016/j.watres.2014.04.046.
Green, D.S., Kregting, L., Boots, B., Blockley, D.J., Brickle, P., da Costa, M., Crowley, Q., 2018. A comparison of sampling methods for seawater microplastics and a first report of the microplastic litter in coastal waters of Ascension and Falkland Islands. Mar. Pollut. Bull. 137, 695–701. https://doi.org/10.1016/j.marpolbul.2018.11.004.
Hadjoudja, S., Deluchat, V., Baudu, M., 2010. Cell surface characterisation of *Microcystis aeruginosa* and *Chlorella vulgaris*. J. Colloid Interface Sci. 342, 293–299. https://doi.org/10.1016/j.jcis.2009.10.078.
Hahladakis, J.N., Velis, C.A., Weber, R., Iacovidou, E., Purnell, P., 2018. An overview of chemical additives present in plastics: migration, release, fate and environmental impact during their use, disposal and recycling. J. Hazard. Mater. 344, 179–199. https://doi.org/10.1016/j.jhazmat.2017.10.014.
Henderson, R.K., Parsons, S.A., Jefferson, B., 2008a. The impact of algal properties and pre-oxidation on solid-liquid separation of algae. Water Res. 42 (8–9), 1827–1845. https://doi.org/10.1016/j.watres.2007.11.039.
Henderson, R.K., Baker, A., Parsons, S.A., Jefferson, B., 2008b. Characterisation of algogenic organic matter extracted from cyanobacteria, green algae and diatoms. Water Res. 42 (13), 3435–3445. https://doi.org/10.1016/j.watres.2007.10.032.
Jiang, J.-Q., Graham. N.J.D., Harward, C., 1993. Comparison of polyferric sulphate with other coagulants for the removal of algae and algae-derived organic matter. Water Sci. Technol. 27 (11), 221–230. ISSN 02731223.
Kim, B.H., Choi, M.K., Chung, Y.T., Lee, J.B., Wui, I.S., 1997. Blue-Green alga *Microcystis aeruginosa* Kütz in natural medium. Bull. Environ. Contam. Toxicol. 59, 35–43. https://doi.org/10.1007/s001289900440.
Koelmans, A.A., Besseling, E., Shim, W.J., 2015. Nanoplastics in the Aquatic Environment. Critical Review Marine Anthropogenic Litter. Springer International Publishing, pp. 325–340 https://doi.org/10.1007/978-3-319-16510-3_12.
Lares, M., Ncibi, M.C., Sillanpää, M., Sillanpää, M., 2018. Occurrence, identification and removal of microplastic particles and fibers in conventional activated sludge process and advanced MBR technology. Water Res. 133, 236–246. https://doi.org/10.1016/j.watres.2018.01.049.
Lawrence, J., Tosine, H.M., Zimmermann, H.W., 1975. Removal of asbestos fibres from potable water by coagulation and filtration. Water Res. 9, 397–400. https://doi.org/10.1016/0043-1354(75)90184-0.
Leslie, H.A., Brandsma, S.H., van Velzen, M.J.M., Vethaak, A.D., 2017. Microplastics en route: field measurements in the Dutch river delta and Amsterdam canals, wastewater treatment plants, North Sea sediments and biota. Environ. Int. 101, 133–142. https://doi.org/10.1016/j.envint.2017.01.018.
Li, J., Liu, H., Chen, P., 2018a. Microplastics in freshwater systems: a review on occurrence, environmental effects, and methods for microplastics detection. Water Res. 137, 362–374. https://doi.org/10.1016/j.watres.2017.12.056.
Li, J., Zhang, K., Zhang, H., 2018b. Adsorption of antibiotics on microplastics. Environ. Pollut. 237 (2018), 460–467. https://doi.org/10.1016/j.envpol.2018.02.050.
Li, S., Liu, H., Gao, R., Abdurahman, A., Dai, J., Zeng, F., 2018. Aggregation kinetics of microplastics in aquatic environment: complex roles of electrolytes, pH, and natural organic matter. Environ. Pollut. 237, 126–132. https://doi.org/10.1016/j.envpol.2018.02.042.
Liebezeit, G., Liebezeit, E., 2014. Synthetic particles as contaminants in German beers. Food Addit. Contam.: Part A 31 (9), 1574–1578. https://doi.org/10.1080/19440049.2014.945099.
Luo, W., Su, L., Craig, N.J., Du, F., Wu, C., Shi, H., 2019. Comparison of microplastic pollution in different water bodies from urban creeks to coastal waters. Environ. Pollut. 246, 174–182. https://doi.org/10.1016/j.envpol.2018.11.081.
Ma, Y., Huang, A., Cao, S., Sun, F., Wang, L., Guo, H., Ji, R., 2016. Effects of nanoplastics and microplastics on toxicity, bioaccumulation, and environmental fate of phenanthrene in fresh water. Environ. Pollut. 219, 166–173. https://doi.org/10.1016/j.envpol.2016.10.061.
Ma, B., Xue, W., Ding, Y., Hu, C., Liu, H., Qu, J., 2018. Removal characteristics of microplastics by Fe-based coagulants during drinking water treatment. J. Environ. Sci. https://doi.org/10.1016/j.jes.2018.10.006 In press.
Ma, B., Xue, W., Hu, C., Liu, H., Qu, J., Li, F., 2019. Characteristics of microplastic removal via coagulation and ultrafiltration during drinking water treatment. Chem. Eng. J. 359, 159–167. https://doi.org/10.1016/j.cej.2018.11.155.
Mason, S.A., Garneau, D., Sutton, R., Chu, Y., Ehmann, K., Barnes, J., Fink, P., Papazissimos, D., Rogers, D.L., 2016. Microplastic pollution is widely detected in US municipal wastewater treatment plant effluent. Environ. Pollut. 218, 1045–1054. https://doi.org/10.1016/j.envpol.2016.08.056.
Mason, S.A., Welch, V.G., Neratko, J., 2018. Synthetic polymer contamination in bottled water. Front. Chem. 6, 1–11. https://doi.org/10.3389/fchem.2018.00407.
Matilainen, A., Vepsäläinen, M., Sillanpää, M., 2010. Natural organic matter removal by coagulation during drinking water treatment: a review. Adv. Colloid Interf. Sci. 159 (2), 189–197. https://doi.org/10.1016/j.cis.2010.06.007.
Mato, Y., Isobe, T., Takada, H., Kanehiro, H., Ohtake, C., Kaminuma, T., 2001. Plastic resin pellets as a transport medium for toxic chemicals in the marine environment. Environ. Sci. Technol. 35, 318–324. https://doi.org/10.1021/es0010498.
Millette, J.R., Clark, P.J., Stober, J., Rosenthal, M., 1983. Asbestos in water supplies of the United States. Environ. Health Perspect. 53, 45–48. https://doi.org/10.1289/ehp.835345.
Mintenig, S.M., Int-Veen, I., Löder, M.G.J., Primpke, S., Gerdts, G., 2017. Identification of microplastic in effluents of waste water treatment plants using focal plane array-based micro-Fourier-transform infrared imaging. Water Res. 108, 365–372. https://doi.org/10.1016/j.watres.2016.11.015.
Mintenig, S.M., Löder, M.G.J., Primpke, S., Gerdts, G., 2019. Low numbers of microplastics detected in drinking water from ground water sources. Sci. Total Environ. 648, 631–635. https://doi.org/10.1016/j.scitotenv.2018.08.178.
Montizaan, G.K., Knaap, A.G.A.C., Van der Heijden, C.A., 1989. Asbestos: toxicology and risk assessment for the general population in the Netherlands. Fd. Chem. Toxic. 27, 53–63. https://doi.org/10.1016/0278-6915(89)90093-8.
Murphy, F., Ewins, C., Carbonnier, F., Quinn, B., 2016. Wastewater treatment works (WwTW) as a source of microplastics in the aquatic environment. Environ. Sci. Technol. 50, 5800–5808. https://doi.org/10.1021/acs.est.5b05416.
Napper, I.E., Thompson, R.C., 2016. Release of synthetic microplastic plastic fibres from domestic washing machines: effects of fabric type and washing conditions. Mar. Pollut. Bull. 112, 39–45. https://doi.org/10.1016/j.marpolbul.2016.09.025.
National Research Council, 1977. Drinking Water and Health,: Volume 1. Washington, DC: The. National Academies Press https://doi.org/10.17226/1780.
Newcombe, G., Drikas, M., 1997. Adsorption of NOM onto activated carbon: electrostatic and nonelectrostatic effect. Carbon 35, 1239–1250. https://doi.org/10.1016/S0008-6223(97)00078-X.
Ngo, H.H., Vigneswaran, S., Dharmappa, H.B., 1995. Optimization of direct filtration: experiments and mathematical models. Environ. Technol. 16, 55–63. https://doi.org/10.1080/09593331608616245.
Oßmann, B.E., Sarau, G., Holtmannspötter, H., Pischetsrieder, M., Christiansen, S.H., Dicke, W., 2018. Small-sized microplastics and pigmented particles in bottled mineral water. Water Res. 141, 307–316. https://doi.org/10.1016/j.watres.2018.05.027.
Packham, F.F., 1965. Some studies of the coagulation of dispersed clays with hydrolyzing salts. J. Colloid Interface Sci. 20, 81–92. https://doi.org/10.1016/0095-8522(65)90094-2.
Pivokonsky, M., Bubakova, P., Pivokonska, L., Hnatukova, P., 2011. The effect of global velocity gradient on the character and filterability of aggregates formed during the coagulation/flocculation process. Environ. Technol. 32 (12), 1355–1366. https://doi.org/10.1080/09593330.2010.536786.
Pivokonsky, M., Naceradska, J., Brabenec, T., Novotna, K., Baresova, M., Janda, V., 2015. The impact of interactions between algal organic matter and humic substances on coagulation. Water Res. 84, 278–285. https://doi.org/10.1016/j.watres.2015.07.047.
Pivokonsky, M., Naceradska, J., Kopecka, I., Baresova, M., Jefferson, B., Li, X., Henderson, R.K., 2016. The impact of algogenic organic matter on water treatment plant operation and water quality: a review. Crit. Rev. Environ. Sci. Technol. 46 (4), 291–335. https://doi.org/10.1080/10643389.2015.1087369.
Pivokonsky, M., Cermakova, L., Novotna, K., Peer, P., Cajthaml, T., Janda, V., 2018. Occurrence of microplastics in raw and treated drinking water. Sci. Total Environ. 2018, 1644–1651. https://doi.org/10.1016/j.scitotenv.2018.08.102.
Plastic Europe, 2018. Plactics – the facts 2017. An analysis of european plastics production. Demand and Waste Data www.plasticseurope.org.
Revel, M., Châtel, A., Mouneyrac, C., 2018. Micro(nano)plastics: a threat to human health? Curr. Opin. Environ. Sci. Health 1, 17–23. https://doi.org/10.1016/j.coesh.2017.10.003.
Rochman, C.M., Hoh, E., Hentschel, B.T., Kaye, S., 2013. Long-term field measurement of sorption of organic contaminants to five types of plastic pellets: implications for plastic marine debris. Environ. Sci. Technol. 47, 1646–1654. https://doi.org/10.1021/es303700s.
Saada, A., Siffert, B., Papier, E., 1995. Comparison of the hydrophilicity/hydrophobicity of illites and kaolinites. J. Colloid Interface Sci. 174, 185–190. https://doi.org/10.1006/jcis.1995.1381.
Safarikova, J., Baresova, M., Pivokonsky, M., Kopecka, I., 2013. Influence of peptides and proteins produced by cyanobacterium *Microcystis aeruginosa* on the coagulation of turbid waters. Sep. Purif. Technol. 118, 49–57. https://doi.org/10.1016/j.seppur.2013.06.049.
Schirinzi, G.F., Pérez-Pomeda, I., Sanchís, J., Rossini, C., Farré, M., Barcelé, D., 2017. Cytotoxic effects of commonly used nanomaterials and microplastics on cerebral and epithelial human cells. Environ. Res. 159, 579–587. https://doi.org/10.1016/j.envres.2017.08.043.
Schymanski, D., Goldbeck, C., Humpf, H.-U., Fürst, P., 2018. Analysis of microplastics in water by micro-Raman spectroscopy: release of plastic particles from different packaging into mineral water. Water Res. 129, 154–162. https://doi.org/10.1016/j.watres.2017.11.011.
Sharp, E.L., Jarvis, P., Parsons, S.A., Jefferson, B., 2006. Impact of fractional character on the coagulation of NOM. Colloids Surf., A: Physicochem. Eng. Aspects 286, 104–111. https://doi.org/10.1016/j.colsurfa.2006.03.009.
Silva, A.B., Bastos, A.S., Justino, C.I.L., da Costa, J.P., Duarte, A.C., Rocha-Santos, T.A.P., 2018. Microplastics in the environment: challenges in analytical chemistry – a review. Anal. Chim. Acta 1017, 1–19. https://doi.org/10.1016/j.aca.2018.02.043.
Simon, M., van Alst, N., Vollertsen, J., 2018. Quantification of microplastic mass and removal rates at wastewater treatment plants applying Focal Plane Array (FPA)-based Fourier Transform Infrared (FT-IR) imaging. Water Res. 142, 1–9. https://doi.org/10.1016/j.watres.2018.05.019.

Su, L., Xue, Y., Li, L., Yang, D., Kolandhasamy, P., Li, D., Shi, H., 2016. Microplastics in Taihu Lake, China. Environ. Pollut. 216, 711–719. https://doi.org/10.1016/j.envpol.2016.06.036.

Su, L., Cai, H., Kolandhasamy, P., Wu, C., Rochman, C.M., Shi, H., 2018. Using the *Asian clam* as an indicator of microplastic pollution in freshwater ecosystems. Environ. Pollut. 234, 347–355. https://doi.org/10.1016/j.envpol.2017.11.075.

Talvitie, J., Mikola, A., Koistinen, A., Setälä, O., 2017a. Solutions to microplastic pollution – removal of microplastics from wastewater effluent with advanced wastewater treatment technologies. Water Res. 123, 401–407. https://doi.org/10.1016/j.watres.2017.07.005.

Talvitie, J., Mikola, A., Setälä, O., Heinonen, M., Koistinen, A., 2017b. How well is microliter purified from wastewater? – a detailed study on the stepwise removal of microliter in a tertiary level wastewater treatment plant. Water Res. 109, 164–172. https://doi.org/10.1016/j.watres.2016.11.046.

Teng, J., Wang, Q., Ran, W., Wu, D., Liu, Y., Sun, S., Liu, H., Cao, R., Zhao, J., 2019. Microplastic in cultured oysters from different coastal areas of China. Sci. Total Environ. 653, 1282–1292. https://doi.org/10.1016/j.scitotenv.2018.11.057.

Teuten, E.J., Rowland, S.J., Galloway, T.S., Thompson, R.C., 2007. Potential for plastic to transport hydrophobic contaminants. Environ. Sci. Technol. 41, 7759–7764. https://doi.org/10.1021/es071737s.

Toft, P., Wingle, D., Meranger, J.C., Mao, Y., 1981. Asbestos and drinking water in Canada. Sci. Total Environ. 18, 77–89. https://doi.org/10.1016/S0048-9697(81)80051-4.

Triebskorn, R., Braunbeck, T., Grummt, T., Hanslik, L., Huppertsberg, S., Jekel, M., Knepper, T.P., Krais, S., Müller, Y.K., Pittroff, M., Ruhl, A.S., Schmieg, H., Schür, C., Strobel, C., Wagner, M., Zumbülte, N., Köhler, H.-R., 2019. Relevance of nano- and microplastics for freshwater ecosystems: a critical review. Trends Anal. Chem. 110, 375–392. https://doi.org/10.1016/j.trac.2018.11.023.

Van Cauwenberghe, L., Janssen, C.R., 2014. Microplastics in bivalves cultured for human consumption. Environ. Pollut. 193, 65–70. https://doi.org/10.1016/j.envpol.2014.06.010.

Waller, C.L., Griffiths, H.J., Waluda, C.M., Thorpe, S.E., Loaiza, I., Moreno, B., Pacherres, C.O., Hughes, K.A., 2017. Microplastics in the Antarctic marine system: an emerging area of research. Sci. Total Environ. 598, 220–227. https://doi.org/10.1016/j.scitotenv.2017.03.283.

Wang, W., Wairimu Ndungu, A., Li, Z., Wang, J., 2017. Microplastics pollution in inland freshwaters of China: a case study in urban surface waters of Wuhan, China. Sci. Total Environ. 575, 1369–1374. https://doi.org/10.1016/j.scitotenv.2016.09.213.

Wang, F., Wong, C.S., Chen, D., Lu, X., Wang, F., Zeng, E.Y., 2018. Interaction of toxic chemicals with microplastics: a critical review. Water Res. 139, 208–219. https://doi.org/10.1016/j.watres.2018.04.003.

Wang, W., Yuan, W., Chen, Y., Wang, J., 2018. Microplastics in surface waters of Dongting Lake and Hong Lake, China. Sci. Total Environ. 633, 539–545. https://doi.org/10.1016/j.scitotenv.2018.03.211.

Wolff, S., Kerpen, J., Prediger, J., Barkmann, L., Müller, L., 2019. Determination of the microplastics emission in the effluent of a municipal waste water treatment plant using Raman microspectroscopy. Water Res. X 2, 100014. https://doi.org/10.1016/j.wroa.2018.100014.

World Health Organization, 2003. Asbestos in Drinking-Water, Background Document for Development of WHO Guidelines for Drinking-Water Quality.

World Health Organization, 2011a. Acrylamide in Drinking-Water (Background document for development of WHO Guidelines for Drinking-water Quality).

World Health Organization, 2011b. Guidelines for Drinking-Water Quality, Fourth Edition ISBN 978 92 4 154815 1.

Wu, P., Cai, Z., Jin, H., Tang, Y., 2019. Adsorption mechanisms of five bisphenol analogues on PVC microplastics. Sci. Total Environ. 650, 671–678. https://doi.org/10.1016/j.scitotenv.2018.09.049.

Xu, B., Liu, F., Brookes, P.C., Xu, J., 2018. Microplastics play a minor role in tetracycline sorption in the presence of dissolved organic matter. Environ. Pollut. 240, 87–94. https://doi.org/10.1016/j.envpol.2018.04.113.

Yang, D., Shi, H., Li, L., Li, J., Jabeen, K., Kolandhasamy, P., 2015. Mocriplastic pollution in table salts from China. Environ. Sci. Technol. 49, 13622–13627. https://doi.org/10.1021/acs.est.5b03163.

Yuan, W., Liu, X., Wang, W., Di, M., Wang, J., 2019. Microplastic abundance, distribution and composition in water, sediments, and wild fish from Poyang Lake, China. Ecotoxicol. Environ. Saf. 170, 180–187. https://doi.org/10.1016/j.ecoenv.2018.11.126.

Zhao, S., Zhu, L., Wang, T., Li, D., 2014. Suspended microplastics in the surface water of the Yangtze Estuary System, China: first observations on occurrence, distribution. Mar. Pollut. Bull. 86, 562–568. https://doi.org/10.1016/j.marpolbul.2014.06.032.

Ziajahromi, S., Neale, P.A., Rintoul, L., Leusch, F.D.L., 2017. Wastewater treatment plants as a pathway for microplastics: development of a new approach to sample wastewater-based microplatics. Water Res. 112, 93–99. https://doi.org/10.1016/j.watres.2017.01.042.

Zubris, K.A.V., Richards, B.K., 2005. Synthetic fibers as an indicator of land application of sludge. Environ. Pollut. 138, 201–211. https://doi.org/10.1016/j.envpol.2005.04.013.

6 SHRNUTÍ

Výzkum provedený v rámci disertační práce byl zaměřen na charakterizaci obtížně odstranitelných látek při úpravě vody a posouzení různých potenciálních metod jejich eliminace. V souvislosti s tím se práce konkrétně zabývala i) koagulací neproteinové složky AOM (Publikace 1), ii) vlivem předozonizace na odstraňování AOM koagulací (Publikace 2), iii) vlivem AOM na strukturu agregátů tvořených při koagulaci/flokulaci ostatních znečišťujících příměsí (Publikace 3), iv) možností využití adsorpce na aktivním uhlí při odstraňování nízkomolekulární složky AOM (Publikace 4, 5, 6 a 7) a v) kvantifikací a charakterizací mikroplastů v surové a pitné vodě (Publikace 8 a 9).

Výsledky výzkumu vyplývající ze stanovených cílů předkládané disertační práce lze shrnout do následujících bodů:

- Neproteinová složka AOM se i za optimalizovaných podmínek odstraňuje koagulací prostřednictvím síranu hlinitého a PACl nejvýše z 25 %. Důvodem je vysoký podíl zastoupení látek s nízkou molekulovou hmotností. Zatímco vysokomolekulární látky s nízkým povrchovým nábojem byly odstraněny s vysokou účinností, u látek s MH < 3 kDa a velkým nábojem k odstranění prakticky nedošlo. Jako optimální pH koagulace síranem hlinitým bylo zjištěno rozmezí pH 6,6-7,5, což odpovídá přibližně neutrální oblasti pH a u PACl se optimum pohybovalo spíše v zásaditější oblasti pH, konkrétně v rozmezí pH 7,5-9,0. Z toho lze usuzovat, že jako dominantní mechanismus koagulace AOM neproteinového charakteru se pravděpodobně uplatnila adsorpce na hydratované oxidy hliníku. Ve srovnání s předchozími studiemi zabývajícími se koagulací proteinové složky AOM vyžaduje ta neproteinová vyšší dávky koagulačního činidla a vykazuje nižší účinnost odstranění (25 % vs. 60-85 %). Zároveň dochází k odstraňování proteinové a neproteinové složky při různých hodnotách pH (kyselých vs. neutrálních/zásaditých), a to v důsledku uplatnění různých mechanismů koagulace. (Publikace 1)
- Předoxidace pomocí ozonizace obecně nevedla ke snížení koncentrace AOM, přičemž mírného poklesu bylo dosaženo pouze při vyšších dávkách ozónu a alkalickém ozonizačním pH (pH 9). Vlivem ozonizace došlo k rozkladu vysokomolekulárních látek na látky nízkomolekulární, a to zejména při vyšších dávkách ozónu a nízkém pH (pH 5). To se projevilo na celkovém snížení účinnosti koagulace COM sinice *M. aeruginosa*, přičemž účinnost klesala se zvyšující se

dávkou ozónu a snižujícím se ozonizačním pH a výrazněji byla ovlivněna v případě hlinitého koagulačního činidla v porovnání se železitým. Pozitivní účinek měla ozonizace na degradaci mikrocystinů, kdy i v přítomnosti COM došlo za vhodných podmínek k jejich téměř 100% odstranění. (Publikace 2)

- Při studiu vlivu AOM na strukturu agregátů bylo zjištěno, že při zvýšení gradientu rychlosti dochází ke zmenšení velikosti vloček (agregátů), a to v závislosti na charakteru znečišťujících příměsí a koagulačního činidla, kterými jsou vločky tvořeny. Průměrná velikost agregátů roste v pořadí kaolinit + Al < kaolinit + Fe < COM + Al < kaolinite + COM + Al < COM + Fe < kaolinite + COM + Fe, z čehož vyplývá, že COM zvyšuje velikost vloček a že koagulací prostřednictvím železitého činidla vznikají větší vločky než při použití činidla hlinitého. S narůstajícím gradientem rychlosti se přitom tyto rozdíly stírají, vzniká velikostně homogennější suspenze s kompaktnějšími a pravidelnějšími agregáty a vliv charakteru znečišťujících látek tvořících vločky klesá. Velkou roli při celém procesu hraje opět hodnota pH, která určuje protonizaci/deprotonizaci funkčních skupin v molekulách znečišťujících příměsí a tím jejich náboj a uplatňující se interakce mezi jednotlivými znečišťujícími příměsemi. (Publikace 3)
- Při posuzování účinnosti adsorpce aminokyselin, které jsou jednou ze skupin nízkomolekulárních látek produkovaných fytoplanktonem obtížně odstranitelných při koagulaci, na dvou druzích granulovaného aktivního uhlí bylo zjištěno, že tato účinnost je ovlivněna mnoha faktory jako je hodnota pH, iontová síla a teplota roztoku a zásadně se odvíjí od charakteru molekuly aminokyseliny. Dominantními mechanismy adsorpce jsou elektrostatické a hydrofobní interakce a vodíkové vazby a k jejich uplatnění dochází v závislost na výše uvedených faktorech. Arginin, aminokyselina zásaditého charakteru preferuje při adsorpci zásadité pH a hlavním mechanismem její sorpce jsou elektrostatické interakce. Vliv iontové síly a pH roztoku přitom účinnost adsorpce ovlivňuje více než teplota roztoku v porovnání s druhou posuzovanou aminokyselinou, fenylalaninem, a to zřejmě v souvislosti s převládajícím mechanismem adsorpce – elektrostatickými silami. Účinnost adsorpce *Phe* je pak ovlivněna teplotou roztoku mnohem více než *Arg* a to z toho důvodu, že při jeho adsorpci hrají pravděpodobně hlavní roli interakce hydrofobní, které jsou teplotou ovlivněny více než hodnotou pH. Třetí zkoumaná AMK, kyselina asparágová, se adsorbuje s velmi nízkou (v případě GAU FTL) a téměř

nulovou (v případě GAU PIC) účinností, a to pravděpodobně vzhledem jejímu silně hydrofobnímu charakteru. (Publikace 4, 5, 6 a 7)

- Při výzkumu přítomnosti mikroplastů ve zdrojích vody a ve vodě pitné bylo zjištěno, že tento druh mikropolutantu se u tří sledovaných úpraven vyskytuje jak ve zdrojích surové vody, a to v rozmezí od 1473 ± 34 do 3605 ± 497 částic na litr, tak ve vodě upravené, kde jejich počet dosahoval od 338 ± 76 do 628 ± 28 částic na litr. Většina mikroplastů se přitom pohybovala ve velikostním rozmezí 1-10 µm a tvarem převažovaly nepravidelné fragmenty. Z hlediska materiálového složení převažovaly mikroplasty z polyetylén tereftalátu, polypropylénu a polyetylénu. Důležitost problematiky výskytu mikroplastů ve vodních zdrojích pak vyplynula z provedené rozsáhlé rešerše (review), kde byly shrnuty dosavadní poznatky v oblasti jejich výskytu v povrchových vodách, ve zdrojích vody, v balených vodách a ve vodě pitné. (Publikace 8 a 9)

7 ZÁVĚR A PRAKTICKÝ VÝZNAM VÝSLEDKŮ PRÁCE

Disertační práce se zabývá charakterizací a odstraňováním problematických látek z vody při její úpravě na vodu pitnou. Mnohé dosažené výsledky přitom mají konkrétní dopad na samotný proces úpravy vody v praxi.

V rámci výzkumu koagulace organických látek produkovaných fytoplanktonem bylo zjištěno, že jejich neproteinová složka (konkrétně COM zelené řasy *Chlorella vulgaris*) se i při optimalizovaných podmínkách prakticky neodstraňuje, což může být při úpravě vody velice závažný problém. V EOM/COM některých druhů fytoplanktonu (zelené řasy, rozsivky atd.) totiž látky neproteinového charakteru významně převažují nad proteinovými, což následně zásadně ovlivní úpravu vody ze zdroje, kde tyto druhy nad ostatními dominují. Velmi zásadní a praktický dopad má také zjištění, že ačkoli je PACl všeobecně považován za účinnější koagulační činidlo aplikovatelné v širším rozsahu hodnot pH než tradiční síran hlinitý, v případě neproteinové složky AOM vykazuje vyšší účinnost naopak síran. Vezmeme-li pak v úvahu dosavadní výsledky týkající se koagulace proteinové složky, je více než zřejmé, že různé složky AOM jsou koagulací odstranitelné s různou účinností a při různých optimálních podmínkách. Z tohoto důvodu tedy lze ke koagulaci přistupovat jako k dvoustupňovému procesu, kdy nabitá proteinová složka bude odstraňována při pH v kyselé oblasti a neutrální neproteinová složka při neutrálních/alkalických hodnotách pH. Možnost využití takového dvoustupňového procesu by však měl posoudit další následující výzkum, který by přínos v podobě celkové zvýšené účinnosti odstranění AOM potvrdil, zhodnotil a ekonomicky zvážil. Stejně jako u proteinové složky, tak i v případě koagulace složky neproteinové, prakticky nedochází k odstraňování látek s nízkými molekulovými hmotnostmi. Tato skutečnost musí nutně vést ke snaze využívat další stupně úpravy vody, jako je membránová filtrace, adsorpce na aktivním uhlí a/nebo využití oxidačních metod.

Oxidace ozónem zařazená před proces koagulace/flokulace se však pro odstraňování COM sinice *Microcystis aeruginosa* ukázala jako zcela nevhodná. Bylo prokázáno, že vlivem účinku ozónu dochází k rozkladu vysokomolekulárních látek na látky nízkomolekulární, které koagulaci téměř nepodléhají. Tato skutečnost vedla k celkovému snížení účinnosti koagulace COM. Pozitivní vliv měla ale ozonizace na degradaci cynotoxinů, především mikrocystinů. Zdá se tedy, že v případě koagulace AOM by bylo mnohem vhodnější zařazení ozonizace až za koagulaci, čímž by došlo

k účinné koagulaci vzhledem k obsahu vysokomolekulárních látek a zároveň k degradaci mikrocystinů při následné ozonizaci.

Pro účinný průběh celého procesu úpravy vody je pak nutné brát v úvahu vlastnosti agregátů (vloček) tvořených při koagulaci a to s ohledem na předpokládaný způsob jejich separace. Vlastnosti vloček totiž zcela zásadně ovlivňují jejich separační účinnost a pro různé separační metody jsou vhodné agregáty různých vlastností. Z výzkumu provedeného v této oblasti bylo zjištěno, že pokud upravovaná voda obsahuje anorganické (kaolinit) a/nebo organické (COM) znečištění a jako koagulační činidlo je použit síran železitý či hlinitý, jsou při vyšším použitém gradientu rychlosti všechny vzniklé agregáty tvořené různými kombinacemi znečišťujících příměsí vhodné pro přímou filtraci, ovšem s výjimkou agregátů, které obsahují COM a vznikly při použití železitého koagulačního činidla. V takovém případě a také při použití nízkých gradientů rychlosti je nutná separace sedimentací.

Pro koagulací neodstranitelné nízkomolekulární látky se jako vhodný krok pro jejich eliminaci ukazuje technologie adsorpce na aktivním uhlí. Jde však o velmi komplexní proces ovlivněný mnoha faktory, a to jak vlastnostmi adsorbentu a adsorbátu, tak charakterem roztoku. Zásadní roli hraje při adsorpci hodnota pH, která řídí podobu (protonizaci/deprotonizaci) funkčních skupin na povrchu adsorbentu i adsorbátu, a ovlivňuje tak jejich vzájemné interakce, a tedy i adsorpční účinnost. Stejně jako v případě koagulace je nutné podmínky adsorpce optimalizovat, a to s ohledem na charakter látek, k odstraňování kterých je určena.

Z hlediska výskytu antropogenních mikropolutantů ve vodě byla ve zdrojích vody i ve vodě pitné prokázána přítomnost mikroplastů, a to až v řádech tisíců částic na litr v případě vody surové a až ve stovkách částic na litr ve vodě upravené, přičemž převažují částice nepravidelného tvaru a velikosti 1-10 μm. Výzkum byl však prováděn pouze na třech úpravnách vody, a je tedy velmi pravděpodobné, že s ohledem na různý charakter zdrojů surové vody (povrchová, podzemní voda), bude jejich výskyt značně kolísat. Z tohoto důvodu je nutné se problematice mikroplastů v rámci výzkumu v oblasti úpravy pitné vody i nadále věnovat. Toxicita těchto částic doposud nebyla spolehlivě potvrzena ani vyvrácena.

8 LITERATURA

Al Momani, F., Smith, D.W., Gamal El-Din, M., 2008. Degradation of cyanobacteria toxin by advanced oxidation processes. *Journal of Hazardous Materials* 150 (2), 238-249.

Amend, J.P., Helgeson, H.C., 1997. Solubilities of the common L-α-amino acids as a function of temperature and solution pH. *Pure and Applied Chemistry* 69 (5), 935-942.

Amy, G., 2008. Fundamental understanding of organic matter fouling of membranes. *Desalination* 231 (1-3), 44-51.

Anastopoulos, I., Kyzas, G.Z., 2016. Are the thermodynamic parameters correctly estimated in liquid-phase adsorption phenomena? *Journal of Molecular Liquids* 218, 174-185.

Anderson, P.J., Warrack, S., Langen, V., Challis, J.K., Hanson, M.L., Rennie, M.D., 2017. Microplastic contamination in Lake Winnipeg, Canada. *Environmental Pollution* 225, 223-231.

Andrary, A.L., 2011. Microplastics in the marine environment. *Marine Pollution Bulletin* 62, 1596-1605.

Ashraf, A., Dastgheib, S.A., Mensing, G., Shannon, M.A., 2013. Surface characteristics of selected carbon materials exposed to supercritical water. *The Journal of Supercritical Fluids* 76, 32-40.

Auta, H.S., Emenike, C.U., Fauziah, S.H., 2017. Distribution and importance of microplastics in the marine environment: A review of the sources, fate, effects, and potential solutions. *Environmental International* 102, 165-176.

Bansal, R.C., Goyal, M. Activated carbon adsorption. Boca Raton: Taylor & Francis, 2005, 497 s.

Barbosa, M.O, Moreira, N.F.F., Ribeiro, A.R., Pereira, M.F.R, Silva, A.M.T, 2016. Occurrence and removal of organic micropollutants: An overview ofthe watch list of EU Decision 2015/495. *Water Research* 94, 257-279.

Barešová, M., Pivokonský, M., Novotná, K., Načeradská, J., Brányik, T., 2017. An application of cellular organic matter to coagulation of cyanobacterial cells *(Merismopedia tenuissima*). *Water Research* 122, 70-77.

Bernhardt, H., Clasen, J., 1991. Flocculation of micro-organisms. *Journal of Water Supply: Research and Technology – AQUA* 40 (2), 76-87.

Bernhardt, H., Hoyer, O., Schell, H., Lüsse, B., 1985. Reaction mechanisms involved in the influence of algogenic organic matter on flocculation. *Zeitschrift für Wasser und Abwasserforschung* 18 (1), 18-30.

Bernhardt, H., Lüsse, B., Hoyer, O., 1986. The addition of calcium to reduce the impairment of flocculation by algogenic organic matter. *Zeitschrift für Wasser und Abwasserforschung* 19 (6), 219-228.

Bernhardt, H., Shell, H., Hoyer, O., Lüsse, B., 1991. Influence of algogenic organic substances on flocculation and filtration. *The Water Institute of South Africa* 1, 41-57.

Bertocchi, C., Navarini, L., Cesaro, A., 1990. Polysaccharides from Cyanobacteria. *Carbohydrate Polymers* 12, 127-153.

Bjelopavlic, M., Newcombe, G., Hayes, R., 1999. Adsorption of NOM onto activated carbon: effect of surface charge, ionic strength, and pore volume distribution. *Journal of Colloid and Interface Science* 210 (2), 271-280.

Bose, P., Reckhow, D.A., 2007. The effect of ozonation on natural organic matter removal by alum coagulation. *Water Research* 41, 1516-1524.

Bond, T., Goslan, E.H., Parsons, S.A., Jefferson, B., 2011. Treatment of disinfection by-product precursors. *Environmental Technology* 32 (1), 1-25.

Briley, D.S., Knappe, D.R.U., 2002. Optimizing ferric sulfate coagulation of algae with streaming current measurements. *Journal of American Water Works Association* 94 (2), 80-90.

Browne, M.A., Crump, P., Niven, S.J., Teuten, E., Tonkin, A., Galloway, T., Thompson, R., 2011. Accumulation of Microplastic on Shorelines Worldwide: Sources and Sinks. *Environmental Science and Technology* 45 (21), 9175-9179.

Brown, M.R., 1991. The amino-acid and sugar composition of 16 species of microalgae used in mariculture. *Journal of Experimental Marine Biology and Ecology* 145 (1), 79-99.

Bubáková, P., Pivokonský, M., 2012. The influence of velocity gradient on properties and filterability of suspension formed during water treatment. *Separation and Purification Technology* 92, 161-167.

Bubáková, P., Pivokonský, M., Filip, P., 2013. Effect of shear rate on aggregate size and structure in the process of aggregation and at steady state. *Powder Technology* 235, 540-549.

Bubáková, P., Pivokonský, M., Pivokonská, L., 2011. A method for evaluation of suspension quality easy applicable to practice: the effect of mixing on floc properties. *Journal of Hydrology and Hydromechanics* 59 (3), 184-195.

Campinas, M., Rosa, M.J., 2006. The ionic strength effect on microcystin and natural organic matter surrogate adsorption onto PAC. *Journal of Colloid and Interface Science* 299 (2), 520-529.

Campinas, M., Rosa, M.J., 2010. Assessing PAC contribution to the NOM fouling control in PAC/UF systems. *Water Research* 44 (5), 1636-1644.

Carmichael, W.W., 1992. Cyanobacteria secondary metabolites – the cyanotoxins. *Journal of Applied Bacteriology* 72, 445-459.

Clark, H.M., Alves, C.C.C., Franca, A.S., Oliveira, L.S., 2012. Evaluation of the performance of an agricultural residue-based activated carbon aiming at removal of phenylalanine from aqueous solution. *LWT-Food Science and Technology* 49, 155-161.

Cole, M., Lindeque, P., Halsband, C., Galloway, T.S., 2011. Microplastics as contaminants in the marine environment: A review. *Marine Pollution Bulletin* 62, 2588-2597.

Coral, L.A., Zamyadi, A., Barbeau, B., Bassetti, F.J., Lapolli, F.R., Prévost, M., 2013. Oxidation of *Microcystis aeruginosa* and *Anabaena flos-aquae* by ozone: Impacts on

cell integrity and chlorination by-product formation. *Water Research* 47 (9), 2983-2994.

Creighton, T.E., 1993. Proteins: Structures and Molecular Properties, second ed. W.H. Freeman and Company, New York, 507 pp.

Cui, X., Zhou, D., Fan, W., Huo, M., Crittenden, J. C., Yu, Z., Ju, P., Wang, Y., 2016. The effectiveness of coagulation for water reclamation from a wastewater treatment plant that has a long hydraulic and sludge retention times: A case study. *Chemosphere* 157, 224-231.

de Figueiredo, D.R., Azeiteiro, U.M., Esteves, S.M., Gonçalves, F.J.M., Pereira, M.J., 2004. Microcystin-producing blooms – a serious global public health issue. *Ecotoxicology and Environmental Safety* 59, 151-163.

Deblonde, T., Cossu-Leguille, C., Hartemann, P., 2011. Emerging pollutants in wastewater: A review of the literature. *International Journal of Hygiene and Environmental Health* 214, 442-448.

Delgado, L.F., Charles, P., Glucina, K., Morlay, C., 2012. The removal of endocrine disrupting compounds, pharmaceutically activated compounds and cyanobacterial toxins during drinking water preparation using activated carbon – A review. *Science of the Total Environment* 435-436, 509-525.

Destgheib, S.A., Karanfil, T., Cheng, W., 2004. Tailoring activated carbons enhanced removal of natural organic matter from natural waters. *Carbon* 42 (3), 547-557.

Di, M., Wang, J., 2018. Microplastics in surface waters and sediments of the Three Gorges Reservoir, China. *Science of the Total Environment* 616-617, 1620-1627.

Dixon, M.B., Falconet, C., Ho, L., Chow, C.W.K., O'Neill, B.K., Newcombe, G., 2010. Nanofiltration for the removal of algal metabolites and the effects of fouling. *Water Science and Technology* 61 (5), 1189-1199.

Dris, R., Gasperi, J., Rocher, V., Saad, M., Renault, N., Tassin, B., 2015. Microplastic contamination in an urban area: a case study in Greater Paris. *Environmental Chemistry* 12 (5), 2015.

Dyble, J., Fahnenstiel, G.L., Litaker, R.W., Millie, D.F., Tester, P.A., 2008. Microcystin concentrations and genetic diversity of *Microcystis* in the lower Great Lakes. *Environmental Toxicology* 23 (4), 507–516.

Ebie, K., Li, F., Azuma, Y., Yuasa, A., Hagashita, T., 2001. Pore distribution effect of activated carbon in adsorbing organic micropollutants from natural water. *Water Research* 35 (1), 167-179.

Edzwald, J.K., 1993. Coagulation in drinking water treatment: Particles, organics and coagulants. *Water Science and Technology* 27 (11), 21-35.

Edzwald, J.K., 1995. Principles and applications of dissolved air flotation. *Water Science and Technology* 31 (4), 1-23.

Edzwald, J.K., 2010. Dissolved air flotation and me. *Water Research* 44 (7), 2077-2106.

Edzwald, J.K., Haarhoff, J., 2011. Seawater pretreatment for reverse osmosis: Chemistry, contaminants, and coagulation. *Water Research* 45 (17), 5428-5440.

Eerkes-Medrano, D., Thompson, R.C., Aldridge, D.C., 2015. Microplastics in freshwater systems: A review of the emerging threats, identification of knowledge gaps and prioritisation of research needs. *Water Research* 75, 63-82.

Elsellami, L., Vocanson, F., Dappozze F., Puzenat E., Païsse, O., Houas, A., Guillard, C., 2010. Kinetic of adsorption and photocatalytic degradation of phenylalanine effect of pH and light intensity. *Applied Catalysis A: General* 380, 142-148.

Eschauzier, C., Beerendonk, E., Scholte-Veenendaal, P., De Voogt, P., 2012. Impact of Treatment Processes on the Removal of Perfluoroalkyl Acids from the Drinking Water Production Chain. *Environmental Science and Technology* 46 (3), 1708-1715.

Fan, J., Daly, R., Hobson, P., Ho, L., Brookes, J., 2013. Impact of potassium permanganate on cyanobacterial cell integrity and toxin release and degradation. *Chemosphere* 92, 529-534.

Fang, J., Yang, X., Ma, J., Shang, C., Zhao, Q., 2010. Characterization of algal organic matter and formation of DBPs from chlor(am)ination. *Water Research* 44 (20), 5897-5906.

Fogg, G.E., 1983. The ecological significance of extracellular products of phytoplankton photosynthesis. Botanica Marina 26, 3-14.

Free, C.M., Jensen, O.P., Mason, S.A., Eriksen, M., Williamson, N.J., Boldgiv, B., 2014. High-levels of microplastic pollution in a large, remote, mountain lake. *Marine Pollution Bulletin* 85, 156-163.

Freuze, I., Brosillon, S., Laplanche, A., Tozza, D., Cavard, J., 2005. Effect of chlorination on the formation of odorous disinfection byproducts. *Water Research* 39, 2636-2642.

Froese, K.L., Wolanski, A., Hrudey, S.E., 1999. Factors governing odorous aldehyde formation as disinfection by-products in drinking water. *Water Research* 33 (6), 1355-1364.

Gagnon, G.A., Slawson, R.M., Huck, P.M., 2000. Effect of easily biodegradable organic compounds on bacterial growth in a bench-scale drinking water distribution system. *Canadian Journal of Civil Engineering* 27 (3), 412-420.

Gao, Q., Xu, W., Xu, Y., Wu, D., Sun, Y., Deng, F., Shen, W., 2008. Amino acid adsorption on mesoporous materials: Influence of types of aminoacids, modification of mesoporous materials, and solution conditions. *The Journal of Physical Chemistry B* 112 (7), 2261-2267.

Garzon-Sanabria, A.J., Ramirez-Caballero, S.S., Moss, F.E.P., Nikolov, Z.L., 2013. Effect of algogenic organic matter (AOM) and sodium chloride on *Nannochloropsis salina* flocculation efficiency. *Bioresource Technology* 143, 231-237.

Ghernaout, B., Ghernaout, D., Saiba, A., 2010. Algae and cyanotoxins removal by coagulation/flocculation: A review. *Desalination and Water Treatment* 20 (1-3), 133-143.

Gibert, O., Lefevre, B., Fernandez, M., Bernat, X., Paraira, M., and Pons, M., 2013. Fractionation and removal of dissolved organic carbon in a full-scale granular activated carbon filter used for drinking water production. *Water Research* 47 (8), 2821-2829.

Gonzalez-Torres, A., Putnam, J., Jefferson, B., Stuetz, R. M., Henderson, R. K., 2014. Examination of the physical properties of *Microcystis aeruginos*a flocs produced on coagulation with metal salts. *Water Research,* 60 (1), 197-209.

Gonzalez-Torres, A., Rich A.M., Marjo, C.E., Henderson, R.K., 2017. Evaluation of biochemical algal floc properties using Reflectance Fourier-Transform Infrared Imaging. *Algal Research* 27, 345-355.

Goscianska, J., Olejnik, A., Pietrzak, R., 2013. Adsorption of L-phenylalanine onto mesoporous silica. *Material Chemistry and Physics* 142, 586-593.

Goscianska, J., Pietrzak, R., Olejnik, A., 2014. Adsorption of L-phenylalanine onto ordered mesoporous carbons prepared by hard template method. *Journal of the Taiwan Institute of Chemical Engineers* 45, 347-353.

Goslan, E.H., Seigle, C., Purcell, D., Henderson, R., Parsons, S.A., Jefferson, B., Judd, S.J., 2017. Carbonaceous and nitrogenous disinfection by-product formation from algal organic matter. *Chemosphere* 170, 1-9.

Grandjean, P., 2018. Delayed discovery, dissemination, and decisions on intervention in environmental health: a case study on immunotoxicity of perfluorinated alkylate substances. *Environmental Health* 17, 62.

Greiner, E., Kumar, K., Sumit, M., Giuffre, A., Zhao, W., Pedersen, J., Sahai, N., 2014. Adsorption of L-glutamic acid and L-aspartic acid to γ-Al_2O_3. *Geochimica et Cosmochimica Acta* 133, 142-155.

Guillossou, R., Le Roux, J., Brosillon, S., Mailler, R., Vulliet, E., Morlay, C., Nauleau, F., Rocher, V., Gaspéri, J., 2020. Benefits of ozonation before activated carbon adsorption for the removal of organic micropollutants from wastewater effluents. *Chemosphere* 245, 125530.

Gur-Reznik, S., Katz, I., Dosoretz, C.G., 2008. Removal of dissolved organic matter by granular-activated carbon adsorption as a pretreatment to reverse osmosis of membrane bioreactor effluents. *Water Research* 42 (6-7), 1595-1605.

Harada, K.I., 2004. Production of secondary metabolites by freshwater cyanobacteria. *Chemical and Pharmaceutical Bulletin* 52 (8), 889-899.

Health Canada, 2017. Guidelines for Canadian Drinking Water Quality: Guideline Technical Document — Cyanobacterial Toxins. Water and Air Quality Bureau, Healthy Environments and Consumer Safety Branch, Health Canada, Ottawa, Ontario. ISBN: 978-0-660-07494-8

Heberer, T., 2002. Occurrence, fate and removal of pharmaceutical residues inthe aquatic environment: a review of recent research data. *Toxicology Letters* 131, 5-17.

Hellebust, J.A., 1974. Extracellular products. In: Algal physiology and biochemistry (Stewart, W.D.P., Ed.), University of California Press, Berkeley, 989 p.

Henderson, R.K., Baker, A., Parsons, S.A., Jefferson, B., 2008a. Characterisation of algogenic organic matter extracted from cyanobacteria, green algae and diatoms. *Water Research* 42 (13), 3435-3445.

Henderson, R.K., Parsons, S.A., Jefferson, B., 2008b. The impact of algal properties and preoxidation on solid-liquid separation of algae. *Water Research* 42 (8-9), 1827-1845.

Henderson, R.K., Parsons, S.A., Jefferson, B., 2010. The impact of differing cell and algogenic organic matter (AOM) characteristics on the coagulation and flotation of algae. *Water Research* 44 (12), 3617-3624.

Henderson, R.K., Sharp, E., Jarvis, P., Jefferson, B., 2006. Identifying the linkage between particle characteristics and understanding coagulation performance. *Water Science and Technology* 6 (1), 31-38.

Her, N., Amy, G., Park, H.-R., Song, M., 2004. Characterizing algogenic organic matter (AOM) and evaluating associated NF membrane fouling. *Water Research* 38 (6), 1427-1438.

Hnaťuková, P., Kopecká, I., Pivokonský, M., 2011. Adsorption of cellular peptides of *Microcystis aeruginosa* and two herbicides onto activated carbon: Effect of surface charge and interactions. *Water Research* 45 (11), 3359-3368.

Ho, L., Lambling, P., Bustamante, H., Duker, P., Newcombe, G., 2011. Application of powdered activated carbon for the adsorption of cylindrospermopsin and microcystin toxins from drinking water supplies. *Water Research* 45 (9), 2954-2964.

Hölzer, J., Göen, T., Rauchfuss, K., Kraft, M., Angerer, J., Kleeschulte, P., Wilhelm, M., 2009. One-year follow-up of perfluorinated compounds in plasma of German residents from Arnsberg formerly exposed to PFOA-contaminated drinking water. *International Journal of Hygiene and Environmental Health* 212 (5), 499-504.

Hong, H.C., Wong, M.H., Liang, Y., 2009. Amino acids as precursors of trihalomethane and haloacetic acid formation during chlorination. *Archives of Environmental Contamination and Toxicology* 56 (4), 638-645.

Hoyer, O., Bernhardt, H., Lüsse, B., 1987. The effect of ozonation on the impairment of flocculation by algogenic organic matter. *Zeitschrift für Wasser und Abwasserforschung* 20, 123-131.

Hoyer, O., Lüsse, B., Bernhardt, H., 1985. Isolation and characterization of extracellular organic matter (EOM) from algae. *Zeitschrift für Wasser und Abwasserforschung* 18 (2), 76-90.

Huang, J., Graham, N., Templeton, M.R., Zhang, Y., Collins, C., Nieuwenhuijsen, M., 2009. A comparison of the role of two blue-green algae in THM and HAA formation. *Water Research* 43 (12), 3009-3018.

Huang, W., Chu, H., Dong, B., 2012. Characteristics of algogenic organic matter generated under different nutrient conditions and subsequent impact on microfiltration membrane fouling. *Desalination* 293, 104-111.

Huang, W.-J., Cheng, B.-L., Cheng, Y.-L., 2007a. Adsorption of microcystin-LR by three types of activated carbon. *Journal of Hazardous Materials* 141 (1), 115-122.

Huang, W.-J., Lai, C.-H., Cheng, Y.-L., 2007b. Evaluation of extracellular products and mutagenicity in cyanobacteria cultures separated from an eutrophic reservoir. *Science of the Total Environment* 377, 214-223.

Huang, Y., Li, H., Zhou, Q., Li, A., Shuang, C., Xian, Q., 2018. New phenolic halogenated disinfection byproducts in simulated chlorinated drinking water: Identification, decomposition, and control by ozone-activated carbon treatment. *Water Research* 146, 298-306.

Hureiki, L., Croue, J.P., Legube, B., 1994. Chlorination studies of free and combined amino acids. *Water Research* 28, 2521-2531.

Chekli, L., Corjon, E., Tabatabai, S.A.A., Naidu, G., Tamburic, B., Park, S. H., Shon, H.K., 2017. Performance of titanium salts compared to conventional $FeCl_3$ for the

removal of algal organic matter (AOM) in synthetic seawater: Coagulation performance, organic fraction removal and floc characteristics. *Journal of Environmental Management* 201, 28-36.

Chen, J.-J., Yeh, H.-H., 2005. The mechanisms of potassium permanganate on algae removal. *Water Research* 39 (18), 4420-4428.

Chen, J.-J., Yeh, H.-H., Tseng, I.-C., 2009. Effect of ozone and permanganate on algae coagulation removal – pilot and bench scale tests. *Chemosphere* 74, 840-846.

Chen, X., Xiao, B., Liu, J., Fang, T., Xu, X., 2005. Kinetics of the oxidation of MCRR by potassium permanganate. *Toxicon* 45, 911-917.

Cheng, W.P., Chi, F.H., 2003. Influence of eutrophication on the coagulation efficiency in reservoir water. *Chemosphere* 53 (7), 773-778.

Chow, C.W.K., Drikas, M., House, J., Burch, M.D., Velzeboer, R.M.A., 1999. The impact of conventional water treatment processes on cells of the cyanobacterium *Microcystis aeruginosa*. *Water Research* 33 (15), 3253-3262.

Chow, C.W.K., House, J., Velzeboer, R.M.A., Drikas, M., Burch, M.D., Steffensen, D.A. (1998): The effect of ferric chloride flocculation on cyanobacterial cells. *Water Research* 32 (3), 808-814.

Chronakis, I.S., 2001. Gelation of edible blue-green algae protein isolate (*Spirulina platensis* Strain Pacifica): thermal transitions, rheological properties, and molecular forces involved. *Journal of Agricultural and Food Chemistry* 49 (2), 888-898.

Chrost, R.H., Faust, M.A., 1983. Organic carbon release by phytoplankton: Its composition of dissolved utilisation by bacteriophytoplankton. *Journal of Plankton Research* 5 (4), 477-493.

Chu, W., Gao, N., Yin, D., Deng, Y., Templeton, M.R., (2012). Ozone–biological activated carbon integrated treatment for removal of precursors of halogenated nitrogenous disinfection by-products. *Chemosphere* 86, 1087-1091.

Ikhsan, J., Johnson, B.B., Wells J.D., Angove M.J., 2004. Adsorption of aspartic acid onto kaolinite. *Journal of Colloid and Interface Science* 273, 1-5.

Jiao, R., Xu, H., Xu, W., Yang, X., Wang, D., 2015. Influence of coagulation mechanisms on the residual aluminum-the roles of coagulant species and MW of organic matter. *Journal of Hazardous Materials* 290, 16-25.

Jugnia, L.B., Richardot, M., Debroas, D., De´vaux, J., 2006. Bacterial production in the recently flooded Sep Reservoir: diel changes in relation to dissolved carbohydrates and combined amino acids. *Hydrobiologia* 563, 421-430.

Kilduff, J.E., Karanfil, T., 2002. Trichlorethylene adsorption by activated carbon preloaded with humic substances: effets of solution chemistry. *Water Research* 36 (7), 1685-1698.

Kim, H.C., Yu, M.J., 2005. Characterization of natural organic matter in conventional water treatment processes for selection of treatment processes focused on DBPs control. *Water Research* 39 (19), 4779-4789.

Kim, M.-K, Zoh, K.-G., 2016. Occurrence and removals of micropollutants in water environment. *Environmental Engineering Research* 21 (4), 319-332.

Knappe, D.R.U., 2006. Surface chemistry effects in activated carbon adsorption of industrial pollutants. Interface science in drinking water treatment. Theory and

applications. Interface Science and technology – Vol. 10. Newcombe, G. a Dixon, D. (edit), Elsevier Ltd., 155-177.

Kodíček, M., Karpenko, V.: Biofysikální chemie. Academia, Praha, 2000, 337 s.

Koelmans, A.A., Besseling, E., Shim, W.J., 2015. Nanoplastics in the Aquatic Environment. *Critical Review Marine Anthropogenic Litter*. Springer International Publishing, pp. 325-340.

Kopecká, I., Pivokonský, M., Pivokonská, L., Hnaťuková, P., Šafaříková, J., 2014. Adsorption of peptides produced by cyanobacterium *Microcystis aeruginosa* onto granular activated carbon. *Carbon* 69, 595-608.

Kresak, M., Moreno, E.C., Zahradnik, R.T., Hay, D.I., 1977. Adsorption of amino acids onto hydroxyapatite. *Journal of Colloid an Interface Science* 59 (2), 283-292

Kristiana, I., Joll, C., Heitz, A., 2011. Powdered activated carbon coupled with enhanced coagulation for natural organic matter removal and disinfection by-product control: Application in a Western Australian water treatment plant. *Chemosphere* 83 (5), 661-667.

Laurens, L.M.L., Van Wychen, S., McAllister, J.P., Arrowsmith, S., Dempster, T.A., McGowen, J., Pienkos, P.T., 2014. Strain, biochemistry, and cultivation-dependent measurement variability of algal biomass composition. *Analytical Biochemistry* 452, 86-95.

Leloup, M., Nicolau, R., Pallier, V., Yéprémian, C., Feuillade-Cathalifaud, G., 2013. Organic matter produced by algae and cyanobacteria: Quantitative and qualitative characterization. *Journal of Environmental Sciences* 25 (6), 1089-1097.

Leslie, H.A., Brandsma, S.H., van Velzen, M.J.M., Vethaak, A.D., 2017. Microplastics en route: Field measurements in the Dutch river delta and Amsterdam canals, wastewater treatment plants, North Sea sediments and biota. *Environmental International* 101, 133-142.

Lewin, R.A, 1956. Extracellular polysaccharides of green algae. Canadian Journal of *Microbiology* 2 (7), 665-672.

Li, L., Gao, N., Deng, Y., Yao, J., Zhang, K., 2012. Characterization of intracellular & extracellular algae organic matters (AOM) of *Microcystis aeruginosa* and formation of AOM-associated disinfection byproducts and odor & taste compounds. *Water Research* 46 (4), 1233-1240.

Li, Q., Snoeyink, B.J., Campos, C., 2003a. Elucidating competitive adsorption mechanisms of atrazine and NOM using model compounds. Water Research 37, 773-784.

Li, Q., Snoeyink, B.J., Campos, C., 2003b. Pore blockage effect of NOM on atrazine adsorption kinetics of PAC: the roles of PAC pore size distribution and NOM molecular weight. Water Research 37, 4863-4872.

Liu, F.F., Fan, J.L., Wang, S.G., Ma, G.H., 2013. Adsorption of natural organic matter analogues by multi-walled carbon nanotubes: Comparison with powdered activated carbon. *Chemical Engineering Journal* 219, 450-458.

Liu, M., Huang, J., Deng, Y., 2007. Adsorption behaviors of L-arginin from aqueous solutions on a spherical cellulose adsorbent containing the sulfonic group. *Bioresource Technology* 98, 1144-1148.

Luo, Y., Guo, W., Ngo, H.H., Nghiem, L.D., Hai, F.I., Zhang, J., Liang, S., Wang, X.C., 2014. A review on the occurrence of micropollutants in the aquatic environment and their fate and removal during wastewater treatment. *Science of the Total Environment* 473-474, 619-641.

Ma, J., Liu, W., 2002. Effectiveness and mechanism of potassium ferrate(VI) preoxidation for algae removal by coagulation. *Water Research* 36 (4), 871-878.

Ma, M., Liu, R., Liu, H., Qu, J., 2012a. Effect of moderate pre-oxidation on the removal of *Microcystis aeruginosa* by $KMnO_4$-Fe(II) process: Significance of the *in-situ* formed Fe(III). *Water Research* 46 (1), 73-81.

Ma, M., Liu, R., Liu, H., Qu, J., Jefferson, W., 2012b. Effects and mechanisms of prechlorination on *Microcystis aeruginosa* removal by alum coagulation: Significance of the released intracellular organic matter. *Separation and Purification Technology* 86, 19-25.

Maksimova, I.V., Bratkovskaya, L.B., Plekhanov, S.E., 2004. Extracellular carbohydrates and polysaccharides of the algae *Chlorella pyrenoidosa* Chick S-39. *Biology Bulletin* 31 (2), 175-181.

Markou, G., Angelidaki, I., Georgakakis, D., 2012. Microalgal carbohydrates: an overview of the factors influencing carbohydrates production, and of main bioconversion technologies for production of biofuels. *Applied Microbiology and Biotechnology* 96, 631-645.

Mason, S.A., Garneau, D., Sutton, R., Chu, Y., Ehmann, K., Barnes, J., Fink, P., Papazissimos, D., Rogers, D.L., 2016. Microplastic pollution is widely detected in US municipal wastewater treatment plant effluent. *Environmental Pollution* 218, 1045-1054.

Matilainen, A., Gjessing, E.T., Lahtinen, T., Hed, L., Bhatnagar, A., Sillanpää, M., 2011. An overview of the methods used in the characterisation of natural organic matter (NOM) in relation to drinking water treatment. *Chemosphere* 83, 1431-1442

Matilainen, A., Vieno, N., Tuhkanen, T., 2006. Efficiency of the activated carbon filtration in the natural organic matter removal. *Environment International* 32, 324-331.

Matsui, Y., Yoshida, T., Nakao, S., Knappe, D.R.U., Matsushita, T., 2012. Characteristics of competitive adsorption between 2-methylisoborneol and natural organic matter on superfine and conventionally sized powdered activated carbons. *Water Research* 46 (15), 4741-4749.

Matsushita, T., Matsui, Y., Sawaoka, D., Ohno, K., 2008. Simultaneous removal of cyanobacteria and earthy odor compound by a combination of activated carbon, coagulation, and ceramic microfiltration. *Journal of Water Supply: Research and Technology – AQUA* 57 (7), 481-487.

Miao, H., Tao, W., 2009. The mechanisms of ozonation on cyanobacteria and its toxins removal. *Separation and Purification Technology* 66, 187-193.

Mintenig, S.M., Int-Veen, I., Löder, M.G.J., Primpke, S., Gerdts, G., 2017. Identification of microplastic in effluents of waste water treatment plants using focal plane array-based micro-Fourier-transform infrared imaging. *Water Research* 108, 365-372.

Moreno-Castilla, C., 2004. Adsorption of organic molecules from aqueous solutions on carbon materials. *Carbon* 42 (1), 83-94.

Myklestad, S., 1974. Production of carbohydrates by marine planktonic diatoms. I. Comparison of nine different species in culture. *Journal of Experimental Marine Biology and Ecology* 15 (3), 261-274.

Myklestad, S.M., 1995. Release of extracellular products by phytoplankton with special emphasis on polysaccharides. *Science of the Total Environment* 165, 155-164.

Načeradská, J., Pivokonský, M., Pivokonská, L., Barešová, M., Henderson, R.K., Zamyadi, A., Janda, V., 2017. The impact of pre-oxidation with potassium permanganate on cyanobacterial organic matter removal by coagulation. *Water Research* 114, 42-49.

Newcombe, G., 2006. Removal of natural organic material and algal metabolites using activated carbon. In: Newcombe G., Dixon D., editors. Interface Science in Drinking Water Treatment: Theory and Applications, Amsterdam; Elsevier Ltd., 133-153.

Newcombe, G., Drikas, M., 1997. Adsorption of NOM onto activated carbon: electrostatic and non-electrostatic effects. *Carbon* 35 (9), 1239-1250.

Ngo, H.H., Vigneswaran, S., Dharmappa, H.B., 1995. Optimization of direct filtration: Experiments and mathematical models. *Environmental Technology* 16 (1), 55-63.

Nguyen, M.-L., Westerhoff, P., Baker, L., Hu, Q., Esparza-Soto, M., Sommerfeld, M., 2005. Characteristics and reactivity of algae-produced dissolved organic carbon. *Journal of Environmental Engineering* 131 (11), 1574-1582.

Nicolaus, B., Panico, A., Lama, L., Romano, I., Manca, M. C., De Giulio, A., Gambacorta, A., 1999. Chemical composition and production of exopolysaccharides from representative members of heterocystous and non-heterocystous cyanobacteria. *Phytochemistry* 52, 639-647.

O'Connor, A.J., Hokura, A., Kisler, J.M., Shimazu, S., Stevens, G.W., Komatsu, Y., 2006. Amino acids adsorption onto mesoporous silica molecular sieves. *Separation and Purification Technology* 48, 197-201.

Ohio American Water Works Association and Ohio Environmental Protection Agency, 2015. White Paper on Algal Toxin Treatment.

Oloibiri, V., Ufomba, I., Chys, M., Audenaert, W.T.M., Demeestere, K., Van Hulle, S.W.H., 2015. A comparative study on the efficiency of ozonation and coagulation–flocculation as pretreatment to activated carbon adsorption of biologically stabilized landfill leachate. *Waste Management* 43, 335-342.

Oßmann, B.E., Sarau, G., Holtmannspötter, H., Pischetsrieder, M., Christiansen, S.H., Dicke, W., 2018. Small-sized microplastics and pigmented particles in bottled mineral water. *Water Research* 141, 307-316.

Ozawa, K., Fujioka, H., Muranaka, M., Yokoyama, A., Katagami, Y., Homma, T., Ishikawa, K., Tsujimura, S., Kumagai, M., Watanabe, M.F., Park H.-D., 2005. Spatial distribution and temporal variation of *Microcystis* species composition and microcystin concentration in Lake Biwa. *Environmental Toxicology* 20 (3), 270–276.

Paerl, H.W., Fulton, III, R.S., Moisander, P., Dyble, J., 2001. Harmful Freshwater Algal Blooms, With an Emphasis on Cyanobacteria. *The Scientific World* 1, 76-113.

Paralkar, A., Edzwald, J.K., 1996. Effect of ozone on EOM and coagulation. *Journal of the American Water Works Association* 88 (4), 143-154.

Parbhakar, A., Cuadros, J., Sephton, M.A., Dubbin, W., Coles, B.J., Weiss, D., 2007. Adsorption of l-lysine on montmorillonite. *Colloids and Surfaces A: Physicochem. Eng. Aspects* 307, 142-149

Pászti, Z., Guczi, L., 2009. Amino acid adsorption on hydrophilic TiO_2: A sum frequency generation vibrational spectroscopy study. *Vibrational Spectroscopy* 50, 48-56.

Pearson, L.A., Dittmann, E., Mazmouz, R., Ongley, S.E., D'Agostino, P.M., Neilan, B.A., 2016. The genetics, biosynthesis and regulation of toxic specialized metabolites of cyanobacteria. *Harmful Algae* 54, 98-111.

Pelekani, C., Snoeyink, V.L., 1999. Competitive adsorption in natural water: role of activated carbon pore size. *Water Research* 33 (5), 1209-1219.

Pendleton, P., Schumann, R., Wong, S.H., 2001. Microcystin-LR adsorption by activated carbon. *Journal of Colloid and Interface Science* 240 (1), 1-8.

Petruševski, B., van Breemen, A.N., Alaerts, G., 1996. Effect of permanganate pre treatment and coagulation with dual coagulants on algae removal in direct filtration. *Journal of Water Supply: Research and Technology – AQUA* 45 (6), 316-326.

Pietsch, J., Bornmann, K., Schmidt, W., 2002. Relevance of intra- and extracellular cyanotoxins for drinking water treatment. *Acta Hydrochimica et Hydrobiologica* 30 (1), 7-15.

Pivokonský, M., Bubáková, P., Pivokonská, L., Hnaťuková, P., 2011. The effect of global velocity gradient on the character and filterability of aggregates formed during the coagulation/flocculation process. *Environmental Technology* 32 (12), 1355-1366.

Pivokonský, M., Čermáková, L., Pivokonská, L., 2019. *Charakterizace organických látek surové a pitné vody na úpravně vody Želivka.* Praha: Želivská provozní, a. s. (Souhrnná výzkumná zpráva).

Pivokonský, M., Klouček, O., Pivokonská, L., 2006. Evaluation of the production, composition and aluminum and iron complexation of algogenic organic matter. *Water Research* 40 (16), 3045-3052.

Pivokonský, M., Načeradská, J., Brabenec, T., Novotná, K., Barešová, M., Janda, V., 2015. The impact of interactions between algal organic matter and humic substances on coagulation. *Water Research, 84*, 278-285.

Pivokonský, M., Načeradská, J., Kopecká, I., Barešova, M., Jefferson, B., Li, X., Henderson, R.K., 2016. The impact of algogenic organic matter on water treatment plant operation and water quality: A review. *Critical reviews in environmental science and technology* 46 (4), 291-335.

Pivokonský, M., Pivokonská, L., Baumeltová, J., Bubáková, P., 2009a. Vliv buněčných organických látek produkovaných sinicí *Microcystis aeruginosa* na úpravu vody (The effect of cellular organic matter produced by cyanobacteria *Microcystis aeruginosa* on water purification). *Journal of Hydrology and Hydromechanics* 57 (2), 121-129.

Pivokonský, M., Polášek, P., Pivokonská, L., Tomášková, H., 2009b. Optimized reaction conditions for removal of cellular organic matter of *Microcystis aeruginosa*

during the destabilization and aggregation process using ferric sulfate in water purification. *Water Environment Research* 81 (5), 514-522.

Pivokonský, M., Šafaříková, J., Barešová, M., Pivokonská, L., Kopecká, I., 2014. A comparison of the character of algal extracellular versus cellular organic matter produced by cyanobacterium, diatom and green alga. *Water Research* 51, 37-46.

Pivokonský, M., Šafaříková, J., Bubáková, P., Pivokonská, L., 2012. Coagulation of peptides and proteins produced by *Microcystis aeruginosa*: Interaction mechanisms and the effect of Fe-peptide/protein complexes formation. *Water Research* 46 (17), 5583-5590.

Plummer, J.D., Edzwald, J.K., 2002. Effects of chlorine and ozone on algal cell properties and removal of algae by coagulation. *Journal of Water Supply: Research and Technology – AQUA* 51 (6), 307-318.

Pranowo, R., Lee, D.J., Liu, J.C., Chang, J.S., 2013. Effect of O_3 and O_3/H_2O_2 on algae harvesting using chitosan. *Water Science and Technology* 67 (6), 1294-1301.

Qu, F., Liang, H., Tian, J., Yu, H., Chen, Z., and Li, G., 2012a. Ultrafiltration (UF) membrane fouling caused by cyanobateria: Fouling effects of cells and extracellular organics matter (EOM). *Desalination* 293, 30-37.

Qu, F., Liang, H., Wang, Z., Wang, H., Yu, H., Li, G., 2012b. Ultrafiltration membrane fouling by extracellular organic matters (EOM) of *Microcystis aeruginosa* in stationary phase: influences of interfacial characteristics of foulants and fouling mechanisms. *Water Research* 46 (5), 1490-1500.

Qi, J., Lan, H., Liu, H., Liu, R., Miao, S., Qu, J., 2016. Simultaneous surface-adsorbed organic matter desorption and cell integrity maintenance by moderate prechlorination to enhance *Microcystis aeruginosa* removal in $KMnO_4$-Fe(II) process. *Water Research* 105, 551-558.

Rabe, M., Verdes, D., Seeger, S., 2011. Understanding protein adsorption phenomena at solid surfaces. *Advances in colloid and interface science* 162 (1-2), 87-106.

Rahman, M.F., Peldszus, S., Anderson, W.B., 2014. Behaviour and fate of perfluoroalkyl and polyfluoroalkyl substances (PFASs) in drinking water treatment: A review. *Water Research* 50, 318-340.

Rositano, J., Newcombe, G., Nicholson, B., Sztajnbok, P., 2001. Ozonation of NOM and algal toxins in four treated waters. *Water Research* 35, 23-32.

Rositano, J., Nicholson, B.C., Pieronne, P., 1998. Destruction of cyanobacterial toxins by ozone. *Ozone Science and Engineering* 20, 223-238.

Rozas, O., Baeza, C., Núnez, Rossner, A., Urruita, R., Mansilla, H.D., 2017. Organic micropollutants (OMPs) oxidation by ozone: Effect of activated carbon on toxicity abatement. *Science of the Total Environment* 590-591, 430-439.

Schrader, M.E., 1975. Ultralight-vacuum techniques in measurement of contact angles. 4. Water on graphite (0001). *Journal of Physical Chemistry* 79 (23), 2508-2515.

Schreiber, B., Brinkmann, T., Schmalz, V., Worch, E., 2005. Adsorption of dissolved organic matter onto activated carbon — the influence of temperature, absorption wavelength, and molecular size. *Water Research* 39 (15), 3449-3456.

Schymanski, D., Goldbeck, C., Humpf, H.-U., Fürst, P., 2018. Analysis of microplastic in water by micro-Raman spectroscopy: Release of plastic particles from different packaging into mineral water. *Water Research* 129, 154-162.

Scully, F.E., Howell, G.D., Kravltz, R., Jewell, J.T., Hahn, V., Speed, M., 1988. Proteins in natural waters and their relation to the formation of chlorinated organics during water disinfection. *Environmental Science and Technology* 22, 537-542.

Shivakoti, B. R., Fujii, S., Nozoe, M., Tanaka, S., Kunacheva, C., 2010. Perfluorinated chemicals (PFCs) in water purification plants (WPPs) with advanced treatment processes. *Water Supply* 10 (1), 87-95.

Sillanpää, M., Ncibi, M.C., Matilainen, A., Vepsäläinen, M., 2018. Removal of natural organic matter in drinking water treatment by coagulation: A comprehensive review. *Chemosphere* 190, 54-71.

Sivonen, K., Jones, G.: Cyanobacterial toxins. In: Toxic cyanobacteria in water. A guide to their public health consequences, monitoring and management (Chorus, I., Bartram, J., Eds.), E & FN Spon Press, London, 1999, 416 s.

Su, L., Xue, Y., Li, L., Yang, D., Kolandhasamy, P., Li, D., Shi, H., 2016. Microplastics in Taihu Lake, China. *Environmental Pollution* 216, 711-719.

Sukenik, A., Teltch, B., Wachs, A.W., Shelef, G., Nir, I, Levanon, D., 1987. Effect of oxidants on microalgal flocculation. *Water Research* 21 (5), 533-539.

Szajdzinska-Pietek, E., Gebicki, J.L., 2000. Pulse radiolytic investigation of perfluorinated surfactants in aqueous solutions. *Research on Chemical Intermediates* 26 (9), 897-912.

Šafaříková, J., Barešová, M., Pivokonský, M., Kopecká, I., 2013. Influence of peptides and proteins produced by cyanobacterium *Microcystis aeruginosa* on the coagulation of turbid waters. *Separation and Purification Technology* 118, 49-57.

Takagi, S., Adachi, F., Miyano, K., Koizumi, Y., Tanaka, H., Watanabe, I., Tanabe, S., Kannan, K., 2011. Fate of Perfluorooctanesulfonate and perfluorooctanoate in drinking water treatment processes. Water Research 45 (13), 3925-3932.

Takaara, T., Sano, D., Konno, H., Omura, T., 2007. Cellular proteins of *Microcystis aeruginosa* inhibiting coagulation with polyaluminum chloride. *Water Research* 41 (8), 1653-1658.

Tan, I.A.W., Ahmad, A.L., Hameed, B.H., 2009. Adsorption isotherms, kinetics, thermodynamics and desorption studies of 2,4,6-trichlorophenol on oil palm empty fruit bunch-based activated carbon. *Journal of Hazardous Materials* 164 (2-3), 473-482.

Tang, X., Zheng, H., Gao, B., Zhao, C., Liu, B., Chen, W., Guo, J., 2017. Interactions of specific extracellular organic matter and polyaluminium chloride and their roles in the algae-polluted water. *Journal of Hazardous Materials* 332, 1-9.

Teixeira, M.R., Rosa, M.J., 2005. Microcystins removal by nanofiltration. *Separation and Purification Technology* 46 (3), 192-201.

Tentorio, A., Canova, L., 1989. Adsorption of α-amino acids on spherical TiO_2 Particles. *Colloids and Surfaces* 39, 311-319.

Terzyk, A.P., Rychlicki, G., Biniak, S., Łukaszewicz, J.P., 2003. New correlations between the composition of the surface layer of carbon and its physicochemical

properties exposed while paracetamol is adsorbed at different temperatures and pH. *Journal of Colloid and Interface Science* 257 (1), 13-30.

Thurman, E.M., 1985. Organic Geochemistry of Natural Waters. Martinus Nijhoff/Dr. W. Junk Publishers, Boston, p. 497.

Titus, E., Kalkar, A.K., Gaikar, V.G., 2003. Equilibrium studies of adsorption of amino acids on NaZSM-5 zeolite. *Colloids and Surfaces A: Physicochem. Eng. Aspects* 233, 55-61.

van der Westhuizen, A.J., Eloff, J.N., 1985. Effect of temperature and light on the toxicity and growth of the blue-green alga *Microcystis aeruginosa* (UV-006). *Planta* 163, 55-59.

Vandamme, D., Foubert, I., Fraeye, I., Muylaert, K., 2012. Influence of organic matter generated by *Chlorella vulgaris* on five different modes of flocculation. *Bioresource Technology* 124, 508-511.

Vandamme, D., Muylaert, K., Fraeye, I., Foubert, I., 2014. Floc characteristics of *Chlorella vulgaris*: Influence of flocculation mode and presence of organic matter. *Bioresource Technology* 151, 383-387.

Velten, S., Knappe, D.R.U., Traber, J., Kaiser, H.-P., von Guten, U., Boller, M., Meylan, S., 2011. Characterization of natural organic matter adsorption in granular activated carbon adsorbers. *Water Research* 45 (13), 3951-3959.

Villacorte, L.O., Ekowati, Y., Neu, T.R., Kleijn, J.M., Winters, H., Amy, G., Schippers, J.C., Kennedy, M.D., 2015. Characterisation of algal organic matter produced by bloom-forming marine and freshwater algae. *Water Research* 73, 216-230.

Vinu, A., Hossain, K.Z., Kumar, G.S., Ariga, K., 2006. Adsorption of L-histidine over mesoporous carbon molecular sieves. *Carbon* 44, 530-536.

Vlaški, A., van Breemen, A.N., Alaerts, G.J., 1996. Optimisation of coagulation conditions for the removal of cyanobacteria by dissolved air flotation or sedimentation. *Journal of Water Supply: Research and Technology – AQUA* 45 (5), 253-261.

Wang, L., Qiao, J., Hu, Y., Wang, L., Zhang, L., Zhou, Q., Gao, N., 2013. Pre-oxidation with $KMnO_4$ changes extra-cellular organic matter's secretion characteristics to improve algal removal by coagulation with a low dosage of polyaluminium chloride. *Journal of Environmental Sciences* 25 (3), 452-459.

Wei, D., Tao, Y., Zhang, Z., Zhang, X., 2016. Effect of pre-ozonation on mitigation of ceramic UF membrane fouling caused by algal extracellular organic matters. *Chemical Engineering Journal* 294, 157-166.

Wei, L., Zhao, Q., Xue, S., Jia, T., 2008. Removal and transformation of dissolved organic matter in secondary effluent during granular activated carbon treatment. *Journal of Zhejiang University SCIENCE A* 9 (7), 994-1003.

Wen, G., Zhu, H., Wei, Y., Huang, T., Ma, J., 2017. Formation of assimilable organic carbon during the oxidation of water containing *Microcystis aeruginosa* by ozone and an advanced oxidation process using ozone/hydrogen peroxide. *Chemical Engineering Journal* 307, 364-371.

Widrig, D.L., Gray, K.A., McAuliffe, K.S., 1996. Removal of algal-derived organic material by preozonation and coagulation: Monitoring changes in organic quality by pyrolysis-GC-MS. *Water Research* 30 (11), 2621-2632.

Whyte, J.N.C., 1987. Biochemical composition and energycontent of six species of phytoplankton used in mariculture of bivalves. *Aquaculture* 60 (3-4), 231-241.

Wu, Z., Zhu, Y., Huang, W., Zhang, C., Li, T., Zhang, Y., Li, A., 2012. Evaluation of flocculation induced by pH increase for harvesting microalgae and reuse of flocculated medium. *Bioresource Technology* 110, 496-502.

Xiao, F., Simcik, M.F., Gulliver, J.S., 2013. Mechanisms for removal of perfluorooctane sulfonate (PFOS) and perfluorooctanoate (PFOA) from drinking water by conventional and enhanced coagulation. *Water Research* 47 (1), 49-56.

Xie, P., Ma, J., Fang, J., Guan, Y., Yue, S., Li, X., Chen, L., 2013. Comparison of permanganate preoxidation and preozonation on algae containing water: Cell integrity, characteristics, and chlorinated disinfection byproduct formation. *Environmental Science and Technology* 47, 14051-14061.

Xie, P., Chen, Y., Ma, J., Zhang, X., Zou, J., Wang, Z., 2016. A mini review of preoxidation to improve coagulation. *Chemosphere* 155, 550-563.

Yang, Y., Ok, Y.S., Kim, K.-H., K, E.E., Tsang, Y.F., 2017. Occurrences and removal of pharmaceuticals and personal care products (PPCPs) in drinking water and water/sewage treatment plants: A review. *Science of the Total Environment* 596-597, 303-230.

Yoon, J.Y., Kim, J.H., Kim, W.-S., 1999. The relationship of interaction forces in the protein adsorption onto polymeric microspheres. *Colloids and Surfaces A* 153 (1-3), 413-419.

Zhang, K., Gao, N., Deng, Y., Shui, M., Tang, Y., 2011a. Granular activated carbon (GAC) adsorption of two algal odorants, dimethyl trisulfide and β−cyclocitral. *Desalination* 266 (1-3), 231-237.

Zhang, X., Amendola, P., Hewson, J.C., Sommerfeld, M., Hu, Q., 2012. Influence of growth phase onharvesting of *Chlorella zofingiensisby* dissolved air flotation. *Bioresource Technology* 116, 477-484.

Zhang, X., Fan, L., Roddick, F.A., 2013a. Influence of the characteristics of soluble algal organic matter released from *Microcystis aeruginosa* on the fouling of a ceramic microfiltration membrane. *Journal of Membrane Science* 425-426, 23-29.

Zhang, X., Fan, L., Roddick, F.A., 2013b. Understanding the fouling of a ceramic microfiltration membrane caused by algal organic matter released from *Microcystis aeruginosa*. *Journal of Membrane Science* 447, 362-368.

Zhang, X.-J., Chen, C., Ding, J.-Q., Hou, A., Li, Y., Niu, Z.-B., Su, X.-Y., Xu, Y.-J., Laws, E.A., 2010. The 2007 water crisis in Wuxi, China: Analysis of the origin. *Journal of Hazardous Materials* 182 (1-3), 130-135.

Zhang, Y., Tian, J., Nan, J., Gao, S., Liang, H., Wang, M., Li, G., 2011b. Effect of PAC addition on immersed ultrafiltration for the treatment of algal-rich water. *Journal of Hazardous Materials* 186 (2-3), 1415-1424.

Citace disertační práce:

Čermáková, L., 2020. Charakterizace a eliminace obtížně odstranitelných látek při úpravě vody. Disertační práce. Přírodovědecká fakulta, Univerzita Karlova, Česká republika.

cermakova@ih.cas.cz

Ústav pro hydrodynamiku AV ČR, v. v. i.
Akademie věd České republiky
Pod Paťankou 30/5
166 12 Praha 6
Česká republika
www.ih.cas.cz

Ústav pro životní prostředí
Přírodovědecká fakulta
Univerzita Karlova
Benátská 2
128 00 Praha 2
Česká republika
www.natur.cuni.cz